

Copyright  
by  
Amy Townsend-Small  
2006

**The Dissertation Committee for Amy Townsend-Small certifies that this is the  
approved version of the following dissertation:**

**Carbon and nitrogen cycling  
in the Peruvian Andean Amazon**

**Committee:**

---

Jay A. Brandes, Supervisor

---

Wayne S. Gardner, Co-Supervisor

---

Kenneth H. Dunton

---

Tamara K. Pease

---

Henrietta N. Edmonds

---

Michael E. McClain

**Carbon and nitrogen cycling  
in the Peruvian Andean Amazon**

**by**

**Amy Townsend-Small, B.A.**

**Dissertation**

Presented to the Faculty of the Graduate School of

The University of Texas at Austin

in Partial Fulfillment

of the Requirements

for the Degree of

**Doctor of Philosophy**

**The University of Texas at Austin**

**May, 2006**

## **Dedication**

This dissertation is dedicated to my parents, Richard Small and Donna Townsend, for their love, support, and DNA. I love you both. Thank you.

## **Acknowledgements**

This dissertation was an international collaboration and would not have been possible without the help of many, many colleagues. This work was first and foremost the product of my collaboration with the project supervisors, Dr. Jay Brandes of Skidaway Institute for Oceanography and Dr. Michael McClain of Florida International University. They allowed me freedom to pursue my research interests while remaining excellent guides and collaborators, and I'm grateful to both of them for the opportunities they've given me. The other person who deserves special recognition is Jorge Noguera of the Andean Amazon Research Station, who helped spark many of the ideas in this dissertation, and who provided much needed support in Peru.

I'd like to thank Dr. Hedy Edmonds, Dr. Tamara Pease, Dr. Ken Dunton and Dr. Wayne Gardner for being excellent teachers and providing support as members of my dissertation committee. Professor Carlos Llerena from the Universidad Nacional Agraria La Molina in Lima provided valuable international assistance and support. I would also like to thank Dick Chase Smith, Percy Summers, Edgardo Castro and Danny Pinedo of the Instituto del Bien Comun, Bill Anderson of Florida International University, and Tom Saunders of the University of Florida. Thanks to the following people from the Andean Amazon Research Station in Oxapampa, Peru: Bonnie Hall, Amalia Niura, Pilar Verde, Jossy Verde, Jaime Guerovich, Gino Arteaga, Carlos "Chamaco" Bondi, and others.

Lindsey Waggoner of Florida International University provided the land cover maps in Chapter 4. I also thank Jaime Haberer, Felicia Goulet-Miller and Patty Garlough at UTMSI, Heather Singler of FIU, Damien Catchpole of the University of Tasmania, and Patrick Kormos and Dr. Jim McNamara of Boise State University.

Tuition and stipends have been provided by the University of Texas Pre-Emptive Recruitment Fellowship, the University of Texas Research Internship, the University Continuing Fellowship, the National Science Foundation's GK-12 Fellowship and the University of Texas Marine Science Institute E.J. Lund Fellowship. Funding for research, equipment and travel was provided primarily by the Andrew Mellon Foundation, but also by smaller grants from the Geological Society of America, the American Alpine Club, the PEO International Foundation, and a Professional Development Award from the University of Texas Office of Graduate Studies. Field assistants were provided by the Earthwatch Institute and the National Science Foundation Research Experience for Teachers program. Radiocarbon analyses were generously donated by the Research Initiatives Program at the Woods Hole Oceanographic Institution's National Ocean Sciences Accelerator Mass Spectrometry Facility.

# **Carbon and nitrogen cycling in the Peruvian Andean Amazon**

Publication No. \_\_\_\_\_

Amy Townsend-Small, Ph.D.

The University of Texas at Austin, 2006

Supervisors: Jay A. Brandes and Wayne S. Gardner

This dissertation consists of several studies conducted at various spatial and temporal scales designed to identify the important processes that affect organic matter (OM) inputs from the Andes mountains to the Amazon headwaters, as well as carbon (C) and nitrogen (N) cycles in the rivers themselves. Andean rivers supplied approximately equal amounts of fine and coarse sediments to the Amazon, but most coarse sediments were retained in the Andean foreland while fine sediments continued downstream. Terrestrial plant  $\delta^{13}\text{C}$  increased with elevation, but terrestrial soil  $\delta^{13}\text{C}$  did not and was enriched by 1-3‰ over plants. Particulate organic matter (POM) concentrations were generally low, with periodic high concentrations during storms. There were significant differences in the isotopic composition of POM between seasons (wet vs. dry), reflecting changes in sediment source. During high flow, POM resembled terrestrial materials, but during drier periods there was evidence for a resuspended bottom sediment or algal source. During wet periods, OM content of soils and river POM decreased downstream, but the POM trend was complicated during drier months.  $\Delta^{14}\text{C}$  of POM decreased

downstream, suggesting that young, fresh OM introduced in small headwater streams was respired preferentially in rivers or diluted with older material downstream. Fine suspended POM was higher in  $\delta^{15}\text{N}$  and  $\delta^{13}\text{C}$  than coarse POM, indicating either greater degradation in the fine fraction or sorption of isotopically enriched dissolved OM. Deforestation is reflected in suspended POM in small headwaters, with enrichment in both  $^{13}\text{C}$  (due to introduced  $\text{C}_4$  grasses) and  $^{15}\text{N}$ . Epiphytic plants living in forest canopies were  $\delta^{15}\text{N}$ -deplete compared to rooted plants, and the biomass of these epiphytes was so high that their  $\delta^{15}\text{N}$  was reflected in stream POM. Precipitation was a major source of isotopically enriched dissolved organic N (DON) to cloudforests in the central Andes. Inorganic N export from these systems in streams was very low, but this seems to be the result of high demand for DIN by microbes and fine roots in riparian soils, not a high reactivity of dissolved inorganic N (DIN) in the stream. Low deposition of and demand for inorganic N in these forests appear to explain low ambient stream DIN concentrations.



## Table of Contents

List of Tables .....	xi
List of Figures .....	xiii
Chapter 1: Introduction and Overview.....	1
Chapter 2: Contributions of carbon and nitrogen from the Andes Mountains to the Amazon River: Evidence from an elevational gradient of soils, plants, and river material .....	6
Abstract.....	6
Introduction.....	7
Study area .....	10
Methods .....	10
Results .....	12
Discussion.....	15
Chapter 3: Stable and radioactive isotopic constraints on organic matter cycling in the Pachitea River Basin, Peruvian Andean Amazon .....	36
Abstract.....	36
Introduction.....	37
Materials and Methods .....	40
Results .....	42
Discussion.....	44
Conclusions.....	51
Chapter 4: A one-year time series study of carbon and nitrogen elemental and isotopic composition of riverine suspended sediments in the central Andean Amazon.....	66
Abstract.....	66
Introduction.....	67
Study Area .....	70
Methods .....	71

Results .....	74
Discussion.....	76
Conclusions.....	84
Chapter 5: Natural abundance isotopic indicators of carbon and nitrogen sources and cycling in old-growth and deforested cloudforest catchments of the Peruvian Andean Amazon.....	
Abstract.....	107
Introduction.....	108
Study Area .....	111
Results .....	114
Discussion.....	117
Conclusions.....	122
Chapter 6: Nitrogen transformations in soils and streams of the Amazon headwaters of Peru: Evidence from a series of <sup>15</sup> N tracer addition experiments .....	
Abstract.....	138
Introduction.....	139
Methods .....	141
Results .....	143
Discussion.....	146
Conclusions.....	152
References .....	165
VITA .....	180

## List of Tables

Table 2.1. Locations, names, and elevations of sampling sites in this study, with water characteristics as determined for each site.....	29
Table 3.1. Site names, sampling dates, locations, and radiocarbon content of soils and plants collected during this study. Radiocarbon content is presented as $\Delta^{14}\text{C}$ (in ‰) and below, in italics, as age in radiocarbon years (both as defined in Stuiver and Polach 1977). <i>mod</i> = modern (or formed after 1950). Also included are the reference numbers assigned to each sample from NOSAMS.....	53
Table 3.2. Stable isotopic composition ( $\delta^{13}\text{C}$ and $\delta^{15}\text{N}$ ) of various organic matter components sampled in this study. ....	54
Table 3.3. Concentration of organic C and N ( $\mu\text{g/L}$ ) in various size classes of organic matter sampled in this study.....	55
Table 3.4. Percent by weight of carbon and nitrogen in fine and coarse suspended sediments (FSS and CSS) sampled during this study. ....	56
Table 4.1. Physical and land cover characteristics of the three watersheds in this study. Data from Noguera (2006). ....	85
Table 4.2. Average, median, minimum, and maximum values of measured parameters for each of the four rivers in this study. ....	86

Table 4.3. Measured parameters for which there is a significant difference in means (at the 95% confidence interval) between the dry and wet seasons (April through September, and October through March, respectively). The difference between means was assessed using Tukey's honestly significant difference procedure. * : wet season is higher than dry season, ** : dry season is higher than wet season; blank = no seasonal difference.....	87
Table 4.4. Percent of total sediment and sedimentary OC and N in suspension in the Chorobamba River during five 2-day storm events. These calculations account for the entire period of the study from July 20, 2004 through July 21, 2005. ....	88
Table 4.5. Discharge, sediment load, and organic carbon and nitrogen losses in the study watersheds for the period November 10, 2004 through July 21, 2005. SOC = sedimentary organic carbon. SON = sedimentary organic nitrogen. ....	89
Table 5.1. Concentrations and $\delta^{15}\text{N}$ of total dissolved nitrogen (TDN) in rain and throughfall collected at the Parque Nacional Yanachaga-Chemillen. n/d = not determined. ....	125
Table 5.2. Average nitrogen and carbon stable isotopic and elemental composition of canopy plants and soils in the Wara catchment. Zones are as defined in Johansson (1974). Also shown is the number of each type of sample as well standard deviation of the $\delta^{15}\text{N}$ values for each type of sample (for identification of significant differences). ....	126
Table 5.3. $\delta^{15}\text{N}$ and $\delta^{13}\text{C}$ of various fractions in the pristine ("Wara") and deforested ("Killa") sites. n/a = not applicable. ....	127

## List of Figures

- Figure 1.1. Topographic map of the Amazon River Basin (yellow and black line). The Pachitea River Basin is shown in orange. Modified from Glauber (2001). The highest elevations in the basin are shown in dark brown, transitioning to white and then bright green as altitude decreases. ....5
- Figure 2.1. Map of the study area including areas of intense sampling (white triangles) and names of major rivers and towns. The dotted line indicates the position of the treeline. Large black triangle indicates the location of the highest mountain in the range (5879 masl). Inset shows location within northwestern South America.....30
- Figure 2.2. Elevational trends of A)  $\delta^{13}\text{C}$ , B)  $\delta^{15}\text{N}$ , C) %C, D) %N and E) molar C:N of plant leaves collected during this study. Each point represents an average value for all plants (riparian and upland) sampled at that station. ....31
- Figure 2.3. Elevational trends of A)  $\delta^{13}\text{C}$ , B)  $\delta^{15}\text{N}$ , C) %C, D) %N and E) molar C:N of soils collected during this study. Each point represents an average value for all soil horizons sampled at that station. Weight percent of carbon versus weight percent of nitrogen of soil samples is shown in panel (F). ....32
- Figure 2.4. Elevational trends of A)  $\delta^{13}\text{C}$ , B)  $\delta^{15}\text{N}$ , C) %C, D) %N and E) molar C:N of fine POM ( $> 0.2\ \mu\text{m}$ ,  $< 60\ \mu\text{m}$ ) collected from rivers on glass fiber filters during this study. Weight percent of carbon versus weight percent of nitrogen of fine particulate samples is shown in panel (F). ....33

Figure 2.5. Elevational trends of A) $\delta^{13}\text{C}$ , B) $\delta^{15}\text{N}$ , C) %C, D) %N and E) molar C:N of coarse POM ( $> 60\ \mu\text{m}$ ) collected from rivers on nylon filters during this study. Weight percent of carbon versus weight percent of nitrogen of coarse particulate samples is shown in panel (F). .....	34
Figure 2.6. Conceptual diagram of organic matter dynamics in the Peruvian Andean Amazon. Three major zones are depicted: A), the high-altitude <i>puna</i> , located above the treeline, or from about 3500 to 4500 masl; B), the montane cloud forest, situated between 2000 and 3500 masl; and C), the low jungle, or <i>selva baja</i> , which extends from 750 to 2000 masl, approximately. ....	35
Figure 3.1. Map of the Pachitea River watershed with sampling points for summer 2004 labeled on left. Position of the watershed within Peru and the western Amazon is shown on right. ....	57
Figure 3.2. Radiocarbon content (as $\Delta^{14}\text{C}$ ) of suspended POM samples in this study presented versus distance upstream from Iquitos (in kilometers). Individual $\Delta^{14}\text{C}$ values are shown. Corresponding altitudes of each sampling site are shown in Table 3.1. ....	58
Figure 3.3. $\Delta^{14}\text{C}$ (in ‰) of suspended POM and riparian soils collected in this study, presented versus distance upstream from Iquitos. ....	59
Figure 3.4. Carbon stable isotopic composition of various size classes of riverine organic matter collected during this study. DOC = dissolved organic carbon ( $< 0.2\ \mu\text{m}$ ); FPOM = fine particulate organic matter ( $> 0.7\ \mu\text{m}$ , $< 60\ \mu\text{m}$ ); CPOM = coarse particulate organic matter ( $> 60\ \mu\text{m}$ ). ....	60

Figure 3.5. Nitrogen stable isotopic composition of fine and coarse particulate organic matter (FPOM and CPOM) sampled during this study. FPOM = fine particulate organic matter ( $> 0.7 \mu\text{m}$ , $< 60 \mu\text{m}$ ); CPOM = coarse particulate organic matter ( $> 60 \mu\text{m}$ ). .....	61
Figure 3.6. Concentrations (in $\mu\text{g/L}$ ) of organic carbon in various size classes of river material sampled in this study. Note that the dissolved portion is plotted on a separate axis from the particulate portions. Dissolved: $< 0.2 \mu\text{m}$ ; fine: $> 0.7 \mu\text{m}$ , $< 60 \mu\text{m}$ ; coarse: $> 60 \mu\text{m}$ . .....	62
Figure 3.7. Concentrations of nitrogen (in $\mu\text{g/L}$ ) in coarse and fine river sediments collected during this study. Fine: $> 0.7 \mu\text{m}$ , $< 60 \mu\text{m}$ ; coarse: $> 60 \mu\text{m}$ . .....	63
Figure 3.8. Radiocarbon content of bulk river sediments presented versus carbon stable isotopic content of the same samples. The “low-order headwaters” category consists of the samples from the Llamaquizú, Esperanza, and Chontabamba Rivers. The other samples were classified as “higher-order rivers”. Also shown are the average $\delta^{13}\text{C}$ and $\Delta^{14}\text{C}$ values for each group of samples.....	64
Figure 3.9. Comparison of $\delta^{13}\text{C}$ of FPOM (A) and CPOM (A) in the study area for the sampling years 2002 and 2004. Data for 2002 is from Chapter 2 of this dissertation. ....	65
Figure 4.1. Map of the three watersheds and four rivers sampled during this study. Map on right shows the location of the study area within Peru. Map modified from Noguera (2006).....	90

Figure 4.2. Map of the three watersheds in this study delineated by black lines and categorized by land use. Land use data is derived from Noguera (2006). .....	91
Figure 4.3. Monthly rainfall amounts during the study period, as recorded at the Andean Amazon Research Station in Oxapampa.....	92
Figure 4.4. Total fine suspended sediment concentration (points) and river discharge (solid line) throughout the experiment, plotted versus time. A = Chorobamba, B = Esperanza, C = Llamaquizú, D = Chontabamba.	93
Figure 4.5. Total coarse suspended sediment concentration (points) and river discharge (lines) throughout the experiment, plotted versus time. A = Chorobamba, B = Esperanza, C = Llamaquizú, D = Chontabamba.	94
Figure 4.6. Coarse and fine POC concentrations plotted versus river discharge. A = Chorobamba, B = Esperanza, C = Llamaquizú, D = Chontabamba. Note log scale.....	95
Figure 4.7. Coarse and fine PON concentrations plotted versus river discharge. A = Chorobamba, B = Esperanza, C = Llamaquizú, D = Chontabamba. Note log scale.....	96
Figure 4.8. $\delta^{15}\text{N}$ of fine suspended sediments (FSS; points) and river discharge (lines) throughout the experiment, plotted versus time. A = Chorobamba, B = Esperanza, C = Llamaquizú, D = Chontabamba.	97
Figure 4.9. $\delta^{15}\text{N}$ of coarse suspended sediments (CSS; points) and river discharge (lines) throughout the experiment, plotted versus time. A = Chorobamba, B = Esperanza, C = Llamaquizú, D = Chontabamba.	98



- Figure 4.10.  $\delta^{13}\text{C}$  of fine suspended sediments (FSS; points) and river discharge (lines) throughout the experiment, plotted versus time. A = Chorobamba, B = Esperanza, C = Llamaquizú, D = Chontabamba. 99
- Figure 4.11.  $\delta^{13}\text{C}$  of coarse suspended sediments (CSS; points) and river discharge (lines) throughout the experiment, plotted versus time. A = Chorobamba, B = Esperanza, C = Llamaquizú, D = Chontabamba..... 100
- Figure 4.12. Weight percent of OC in fine suspended sediments (FSS; points) and river discharge (lines) throughout the experiment, plotted versus time. A = Chorobamba, B = Esperanza, C = Llamaquizú, D = Chontabamba. 101
- Figure 4.13. Weight percent of OC in coarse suspended sediments (CSS; points) and river discharge (lines) throughout the experiment, plotted versus time. A = Chorobamba, B = Esperanza, C = Llamaquizú, D = Chontabamba. 102
- Figure 4.14. Weight percent of N in fine suspended sediments (FSS; points) and river discharge (lines) throughout the experiment, plotted versus time. A = Chorobamba, B = Esperanza, C = Llamaquizú, D = Chontabamba. 103
- Figure 4.15. Weight percent of N in coarse suspended sediments (CSS; points) and river discharge (lines) throughout the experiment, plotted versus time. A = Chorobamba, B = Esperanza, C = Llamaquizú, D = Chontabamba. 104
- Figure 4.16. Percent organic carbon (OC) plotted versus the concentration of fine and coarse suspended sediments (FSS and CSS). Note the log scale for CSS and FSS concentration. .... 105
- Figure 4.17. Relationship of TSS (A) and river discharge (B) in the Chorobamba River with rainfall measured at the Andean Amazon Research Station. Note the log scale in the y-axis of (A). .... 106

Figure 5.1. Map of the study area. The location of the two study catchments (Wara and Killa) is shown within the San Alberto catchment, located in the Pachitea River Basin of the Peruvian Amazon.....	128
Figure 5.2. Canopy zonation scheme of Johansson (1974). ....	129
Figure 5.3. Concentration (in $\mu\text{M}$ ) and $\delta^{15}\text{N}$ (‰) of TDN in rain and throughfall collected in the Parque Nacional Yanachaga Chemillen. ....	130
Figure 5.4. Classification scheme of the epiphytes sampled in this study. ....	131
Figure 5.5. Results (as $p$ values) of two-tailed $t$ tests to determine significant differences in $\delta^{15}\text{N}$ between different categories of vascular epiphytes sampled in this study. Differences between classes are shown in (A), between families in (B), and between genera in (C). Values below $p = 0.05$ are highlighted in red.....	132
Figure 5.6. Carbon (A) and nitrogen (B) isotopic composition of soil horizons in 2 different plots each in the pristine (Wara) and deforested (Killa) sites. ....	133
Figure 5.7. Percent by weight of carbon (A) and nitrogen (B) of soil horizons in 2 different plots each in the pristine (Wara) and deforested (Killa) sites. ....	134
Figure 5.8. Mass of leaf litter – two different species in two treatments – remaining as a function of time in the leaf litter decomposition experiment. .	135
Figure 5.9. Carbon and nitrogen isotopic composition ( $\delta^{13}\text{C}$ and $\delta^{15}\text{N}$ ) of leaf litter as it decomposes. ....	136
Figure 5.10. Weight percent of OC and N as a function of time in leaf litter as it decomposes. ....	137
Figure 6.1. Molecular structure, formula, and weight of glycine. ....	154

Figure 6.2. Isotopic composition ( $\delta^{15}\text{N}$ ) of dissolved  $\text{NO}_3^-$  in stream water sampled during the  $^{15}\text{NH}_4^+$  tracer injection experiment. A:  $\delta^{15}\text{N}$  of  $\text{NO}_3^-$  for the entire experiment. Arrows represent the starting and stopping of the pump, and the box represents the time shown in (B). B:  $\delta^{15}\text{N}$  of  $\text{NO}_3^-$  observed only during the first day of the experiment. Arrow represents the time when the pump was turned on..... 155

Figure 6.3. Isotopic composition ( $\delta^{15}\text{N}$ ) of suspended POM in stream water sampled during the  $^{15}\text{NH}_4^+$  tracer injection experiment in January of 2003. A:  $\delta^{15}\text{N}$  of POM for the entire experiment. Arrows represent the starting and stopping of the pump, and the box represents the time shown in (B). B:  $\delta^{15}\text{N}$  of POM observed only during the first day of the experiment. Arrow represents the time when the pump was turned on..... 156

Figure 6.4. Isotopic composition ( $\delta^{15}\text{N}$ ) of  $\text{NO}_3^-$  in stream water sampled during the  $^{15}\text{NO}_3^-$  tracer injection experiment in July of 2004. A:  $\delta^{15}\text{N}$  of  $\text{NO}_3^-$  for the entire experiment. Arrows represent the starting and stopping of the pump, and the box represents the time shown in (B). B:  $\delta^{15}\text{N}$  of  $\text{NO}_3^-$  observed only when the pump was turned on. .... 157

Figure 6.5. Isotopic composition ( $\delta^{15}\text{N}$ ) of POM in stream water sampled during the  $^{15}\text{NO}_3^-$  tracer injection experiment in July of 2004. A:  $\delta^{15}\text{N}$  of POM for the entire experiment. Arrows represent the starting and stopping of the pump, and the box represents the time shown in (B). B:  $\delta^{15}\text{N}$  of POM observed only when the pump was turned on. .... 158

Figure 6.7. Isotopic composition ( $\delta^{15}\text{N}$ ) of  $\text{NO}_3^-$  in stream water sampled during the  $^{15}\text{N}$ -glycine tracer injection experiment in August of 2004. A:  $\delta^{15}\text{N}$  of  $\text{NO}_3^-$  for the entire experiment. Arrows represent the starting and stopping of the pump, and the box represents the time shown in (B). B:  $\delta^{15}\text{N}$  of  $\text{NO}_3^-$  observed only when the pump was turned on..... 159

Figure 6.8. Isotopic composition ( $\delta^{15}\text{N}$ ) of POM in stream water sampled during the  $^{15}\text{N}$ -glycine tracer injection experiment in August of 2004. A:  $\delta^{15}\text{N}$  of POM for the entire experiment. Arrows represent the starting and stopping of the pump, and the box represents the time shown in (B). B:  $\delta^{15}\text{N}$  of POM observed only when the pump was turned on. .... 160

Figure 6.9.  $\delta^{15}\text{N}$  of soil  $\text{NO}_3^-$ , soil OM, and fine roots during three different  $^{15}\text{N}$  tracer addition experiments in the Wara experimental forest. A =  $^{15}\text{NO}_3^-$  addition; B =  $^{15}\text{NH}_4^+$  addition; C =  $^{15}\text{N}$ -glycine addition..... 161

Figure 6.10  $\delta^{15}\text{N}$  of fine roots, soil OM, and soil  $\text{NO}_3^-$  observed for the first 30 minutes of the soil tracer experiments. A =  $^{15}\text{NO}_3^-$  addition experiment; B =  $^{15}\text{NH}_4^+$  addition experiment; C =  $^{15}\text{N}$ -glycine experiment. .... 162

Figure 6.11. Soil dissolved  $\text{NO}_3^-$  concentrations observed during the soil tracer experiments. Data from all three experimental plots are shown. A: Nitrate concentrations over the entire experiment. B: Initial and t = 30 min  $\text{NO}_3^-$  concentrations. .... 163

Figure 6.12. Nitrification rates calculated for specific time points in the stream  $^{15}\text{NH}_4^+$  addition experiment (A) and the  $^{15}\text{N}$ -glycine addition experiment (B). Values calculated using the equation of Mulholland et al. (2000). .... 164

## Chapter 1: Introduction and Overview

Rivers are the main means of transport of terrestrial organic carbon (C) and nitrogen (N) to the oceans, and they can be important biogeochemical reactors in and of themselves (Schlesinger 1997). The Amazon River is the world's largest river: it is the largest single source of fresh water and terrestrial organic C to the oceans (Richey et al. 1980). The Amazon has the world's largest watershed (Figure 1.1). The basin is bordered on the west by the Andes Mountains (Figure 1.1), which comprise about 12% of the total basin but are the source of most of the suspended solids and dissolved minerals in the Amazon (Gibbs 1967, Meade et al. 1995). The Andes are also thought to be a major source (~35%) of particulate organic C (POC) to the Amazon (Quay et al. 1992), but because of inaccessibility and political instability in many Andean countries during the late 20<sup>th</sup> century, few studies of C cycling have been conducted in the Andes (McClain et al. 1995, Hedges et al. 2000, Mayorga et al. 2005).

The western tropical Andes have levels of pollution, deforestation, urbanization, and other human impacts that are lower than many other areas of the world (Holland et al. 1999, Perakis and Hedin 2001, McClain and Naiman in prep). Studies of Andean rivers can provide baseline information about biogeochemistry of human-impacted rivers and streams, which can aid in predicting the responses of these systems to global change. Climate models predict that lowland deforestation will lead to decreased rainfall in the Andes (Avissar and Werth 2005, Chagnon and Bras 2005), which may lead to decreased river discharge and sediment loading due to reduced runoff. Also, local land use change due to increases in population and road building is expected to increase in the Andes this century (McClain and Naiman in prep). Thus, studies of baseline biogeochemical

functioning in the Andes, and natural experiments designed to test how rivers respond to changes in precipitation, discharge, and climate are important in evaluating how the Amazon headwaters will respond to global change. In particular, these studies will provide important baseline information useful in evaluating the effects of changes in climate and C cycling on Amazonian ecosystems.

The major question of this dissertation is: what are the important factors controlling the concentrations and sources of organic matter and nutrients in the Peruvian Amazon headwaters? Several different studies are presented here that attempt to constrain these factors from small to large size scales. All of these studies were conducted within the Pachitea River basin, located in central Peru (Figure 1.1). The Pachitea is an excellent representative of the range of ecosystems present in the Amazon headwaters: altitude in this watershed ranges from above 4500 to approximately 150 meters above sea level (masl). The Pachitea River joins the Ucayali River at the city of Pucallpa, Peru; the Ucayali subsequently joins the Amazon near the city of Iquitos, Peru.

Chapters 2 and 3 of this dissertation present information gathered during field campaigns along altitudinal gradients in the Pachitea Basin. Chapter 2 is built around samples gathered from the highest reaches of the Pachitea (above 4000 masl) and downstream to the lowlands around 700 masl. I present data on the stable isotopic ( $\delta^{13}\text{C}$  and  $\delta^{15}\text{N}$ ) and elemental (%C and %N) composition of terrestrial soils and plants as well as river materials that provide information on important sources of C and N to the Amazon headwaters and the processes that affect their transport downstream. This study is a detailed survey of C and N cycling in an Andean river. Chapter 3 is a similar altitudinal transect but is conducted on a smaller scale: samples of riverine organic matter were taken from about 2500 to 300 masl in the Pozuzo River, a sub-basin in the Pachitea. Here stable isotopic analyses were combined with radiocarbon measurements ( $\Delta^{14}\text{C}$ ) of

riverine POM to provide an indication of C sources to rivers and an indication of the time scale of C cycling in Andean headwater catchments. This chapter includes comparisons to the findings in Chapter 2, which was conducted during a much drier year than Chapter 3.

Small mountainous rivers have large dynamic ranges in both flow and suspended sediment content. Thus a shortcoming of “snapshot” studies like those presented in Chapters 2 and 3 is that they can miss “hot moments” that provide much of the flux of material out of the basin (McClain et al. 2003). Therefore, a comparison of riverine POM elemental composition and concentrations was conducted in a one-year time series study of three rivers with contrasting watershed physical characteristics and land uses, presented in Chapter 4. All of these rivers were located in Oxapampa, Peru, near the Andean Amazon Research Station at about 1800 masl. Because most of the annual precipitation occurs during the summer months in Peru (October through March), the study presented an opportunity to explore how the source of OM in rivers varies with river discharge and precipitation, which is an important indicator of how the Amazon headwaters might respond to climate change. This study also provides information about how land use change affects C and N transport from the landscape to rivers. In general, the detailed time series experiment presented in Chapter 4 provides information about sediment and OM dynamics in Andean rivers, which is needed to understand how these systems interact with precipitation, climate, and land use change.

In Chapters 5 and 6, the focus shifts to small catchment studies. Such catchments form the initial sources and filters of OM and nutrients entering Andean rivers. Chapter 5 presents an overview of C and N isotopic composition of various OM compartments in two adjacent watersheds in the tropical montane cloud forest region of the Peruvian Andes (~2400 masl). One of these watersheds was deforested three or four years before

the study began, and the other is covered by pristine old-growth forest. A comparison of C and N stocks and isotopic composition in these two watersheds provides information for predicting the effects of land use change on Andean OM exports to the Amazon lowlands. This information is also useful for determining the important factors controlling C and N cycles in these ecosystems, and the factors that control OM transport from the landscape to headwater streams. This study provides important information on how various C and N cycling processes affect the  $\delta^{13}\text{C}$  and  $\delta^{15}\text{N}$  of OM in this area.

The final chapter presents information gathered during a series of  $^{15}\text{N}$  tracer addition experiments conducted in the pristine watershed previously studied in Chapter 5. Labeled N compounds ( $^{15}\text{NO}_3^-$ ,  $^{15}\text{NH}_4^+$ , and  $^{15}\text{N}$ -glycine) were added to the stream and to riparian soils in order to estimate reactivity and fate of each compound. These techniques can show the relative importance of aquatic and terrestrial N reactions in controlling N retention and export in these systems. This knowledge is important for the Amazon headwaters because these streams have much lower inorganic N export than rivers in industrialized areas and because N export from headwater watersheds can impact OM dynamics downstream even in very large rivers such as the Amazon.



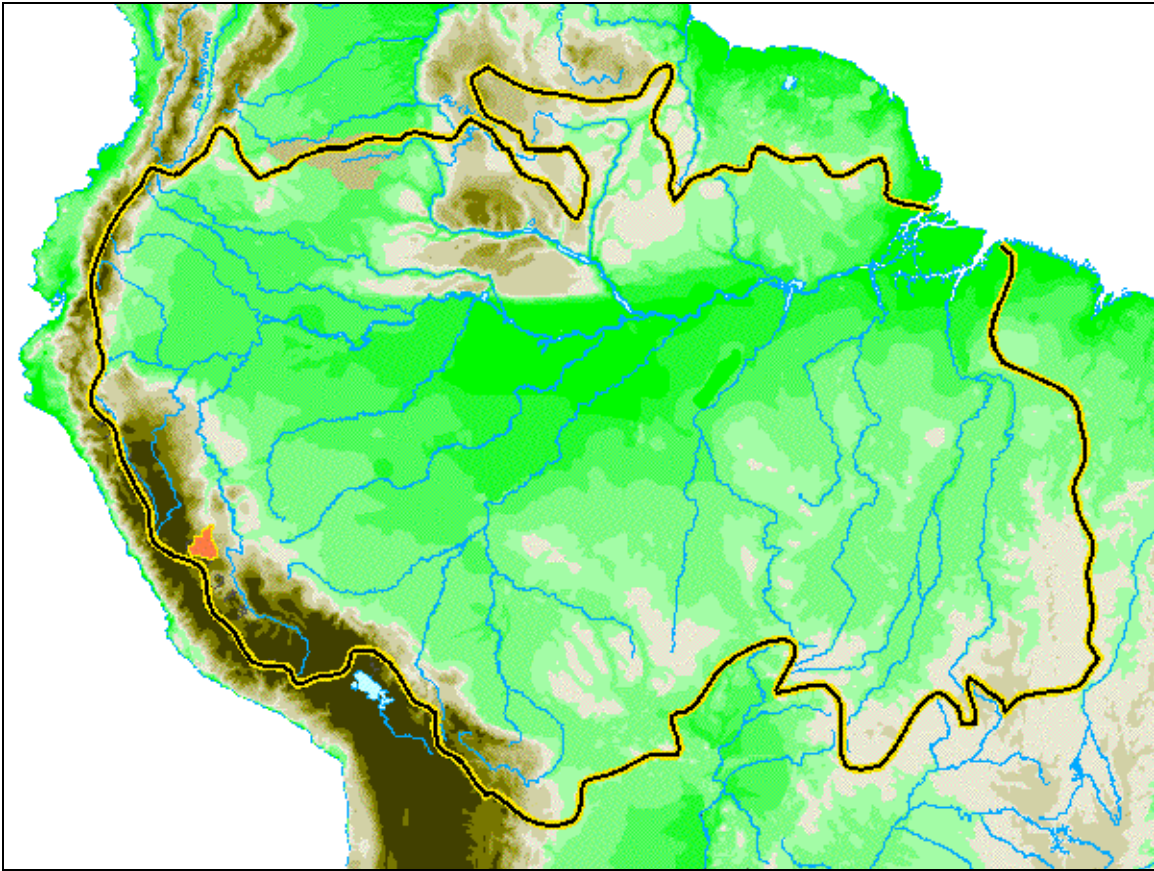


Figure 1.1. Topographic map of the Amazon River Basin (yellow and black line). The Pachitea River Basin is shown in orange. Modified from Glauber (2001). The highest elevations in the basin are shown in dark brown, transitioning to white and then bright green as altitude decreases.

## **Chapter 2: Contributions of carbon and nitrogen from the Andes Mountains to the Amazon River: Evidence from an elevational gradient of soils, plants, and river material<sup>1</sup>**

### **ABSTRACT**

We determined the carbon (C) and nitrogen (N) elemental and stable isotopic composition of riverine and terrestrial organic matter (OM), as well as the concentration of dissolved organic C (DOC),  $\delta^{15}\text{NO}_3^-$  and  $\delta^{18}\text{O}$  of river water along an altitudinal (4043 to 720 meters above sea level [masl]) transect in the Andes of Peru. Plant  $\delta^{13}\text{C}$  increased with increasing elevation, but unlike previous studies, foliar  $\delta^{13}\text{C}$  and %N were negatively correlated. Soil  $\delta^{13}\text{C}$  values did not exhibit similar trends and were enriched by 1-3‰ over plants. Isotopically, riverine fine particulate OM (FPOM, < 60  $\mu\text{m}$ ) resembled soils, and coarse particulate OM (CPOM, > 60  $\mu\text{m}$ ) resembled leaves. Both FPOM and CPOM exhibited OM levels beyond those attributable to sorption. Percent OC and N of soils and FPOM were positively correlated with altitude, and highlight a trend of sequential downstream dilution of OM with inorganic material. FPOM began to resemble plant OM isotopically at lower altitudes, perhaps due to increased plant and surface soil inputs to lower rivers. The compositional similarity of POM to terrestrial plants and soils indicates that the dominant processes affecting riverine OM are occurring on the landscape, not within the river. Dissolved OC (< 0.2  $\mu\text{m}$ ) concentration,  $\delta^{15}\text{NO}_3^-$ , and  $\delta^{18}\text{O}$  of  $\text{H}_2\text{O}$  are variable in high altitude tributaries but approach constant values downstream. Elemental and isotopic analyses of riverine OM suggest compositional differences between size fractions, similar to the lower Amazon; however, unlike previous studies, we have found significant within-stream changes with altitude in OM composition.

---

<sup>1</sup> Significant portions of this chapter have been previously published as Townsend-Small et al. (2005).

## INTRODUCTION

Rivers are the main means of transport of terrestrial organic carbon (OC) to the world's oceans, so an understanding of riverine C dynamics is critical to global C budgets. The Amazon River contributes about  $36 \times 10^9$  kg yr<sup>-1</sup> of OC to the oceans, of which about 62% is dissolved, 34% is fine particulate OC (FPOC, <63 µm) and 4% is coarse particulate OC (CPOC, >63 µm; Richey et al. 1990). Most of this flux is thought to be allochthonous (McClain and Richey 1996). Isotopic and biomarker OC studies in the lower Amazon have shown that coarse particulate organic matter (CPOM) is dominated by fresh plant material, and that fine particulate organic matter (FPOM) and dissolved organic matter (DOM) are more degraded (Hedges et al. 1986*a*, 2000). The organic composition of FPOM and DOM in the Amazon differs despite their presumed close interaction (Hedges et al. 1986*a*, 1994), implying different diagenetic histories. Biodegradation of fresh plant material leads to chemical alteration of OM into progressively smaller molecules, and isotopic, biochemical, and/or size fractionation of various molecules during degradation and transport is likely one control on OM distribution (Hedges et al. 2000).

The “regional chromatography model” was developed to explain the compositional differences in FPOM and DOM in the Amazon (Hedges et al. 1994, Devol and Hedges 2001). This model is based on observations that N-rich, hydrophobic organic molecules are more likely to be sorbed to terrestrial and riverine fine mineral particles than their N-poor, hydrophilic counterparts, which remain dissolved and are washed out of soils (Hedges et al. 1994). A laboratory study confirmed this partitioning of N during sorption (Aufdenkampe et al. 2001), and sorbed material is the majority of FPOM in the lower Amazon (Mayorga and Aufdenkampe 2002). Evidence for the regional chromatography model suggests spatial and temporal variability in OM distribution in the

Amazon, but sampling of the mainstem has failed to catch any major variations (Hedges et al. 2000, Devol and Hedges 2001). Past studies (Hedges et al. 1986a, 1994, 2000; Richey et al. 1980, 1990) have been modeled on the river continuum concept, which emphasizes longitudinal patterns in rivers from source to delta (Vannote et al. 1980). In contrast, small headwater streams often exhibit variable chemical characteristics because they reflect geomorphology and ecology in individual watersheds, consistent with a “river discontinuum” theory recognizing the uniqueness of small streams draining dramatically different catchments and gaps in downstream patterns that occur as tributaries merge (Poole 2002). Mountain rivers are especially likely to exhibit variable biogeochemical characteristics, when altitudinal changes in terrestrial ecosystems are reflected in streams.

It has been proposed that Andean headwater streams partially control OM distribution and composition in the Amazon (Hedges et al. 1994, 2000, Richey et al. 1990, Quay et al. 1992) although the Andes remain largely unstudied (McClain et al. 1995). Headwater streams may exert significant influence over C and N cycling in large rivers (Peterson et al. 2001). Consistent longitudinal patterns in mainstem OM led Hedges et al. (2000) to conclude that patterns were set in low-order headwater streams, whose variable chemical characteristics are integrated as water flows downstream. Andean tributaries are implicated as C, N, and phosphorus (P) sources because concentrations in the mainstem are often higher than in lowland tributaries (Devol and Hedges 2001). Enriched  $\delta^{13}\text{C}$  values of FPOM in the mainstem, relative to local sources, have been attributed to the Andes (Quay et al. 1992). The Andes are also implicated because they are the source of the vast majority of sediments to the Amazon (Meade et al. 1985), which may carry sorbed OM and nutrients (Aufdenkampe et al. 2001).

However, many questions remain about Andean river OM sources and factors influencing its transport and eventual deposition into the ocean, since no comprehensive study has been conducted to answer them. Cai et al. (1988) analyzed the  $\delta^{13}\text{C}$  of Andean river POM but not that of its potential sources. Guyot and Wasson (1994) studied DOC concentrations along an altitudinal gradient, but the highest samples were taken at 2500 meters above sea level (masl), well below the highest reaches of the Amazon. Hedges et al. (2000) studied C and N cycling in Bolivian tributaries of the Amazon, but only one high-altitude sample was taken at 3900 masl; the next highest sample was at 430 masl. These previous sampling efforts were insufficient to capture spatial or temporal variability in concentrations and compositions of OM size fractions, which is critical to understanding how OM is transported from headwater streams to the Amazon mainstem and eventually to the ocean.

Stable isotopes are natural indicators of geochemical and ecological processes and are useful in studies requiring small sample volumes and a time lapse between sampling and analysis. Carbon-13 ( $^{13}\text{C}$ ) shows an altitude effect in plants, with increasing  $\delta^{13}\text{C}$  values at higher altitudes (Körner et al. 1991). Plant  $^{13}\text{C}$  content also reflects its C source and its water-use efficiency; water stress increases  $\delta^{13}\text{C}$  values (Körner et al. 1991), and its photosynthetic pathway, either the Calvin cycle ( $\text{C}_3$ ), the Hatch-Slack cycle ( $\text{C}_4$ ), or Crassulacean acid metabolism (CAM; Lajtha and Marshall 1994). Nitrogen-15 ( $^{15}\text{N}$ ) has not been shown to vary with altitude, but the  $\delta^{15}\text{N}$  of soil OM does vary with precipitation and temperature (Amundson et al. 2003), both of which may vary with altitude.  $\delta^{15}\text{N}$  and  $\delta^{13}\text{C}$  can also be used to assess the diagenetic history of OM (Nadelhoffer and Fry 1988). In addition, oxygen-18 ( $^{18}\text{O}$ ) in river water generally becomes depleted at increasing altitude (Seigenthaler and Oeschger 1980).

In order to investigate these concepts, we conducted a field study of the Pachitea River basin in the Andean Amazon of Peru in July of 2002. The purpose of this study was to determine OM inputs into Andean streams, identify OM sources and factors controlling its transport, and survey trends in C and N concentrations and  $\delta^{13}\text{C}$  and  $\delta^{15}\text{N}$  of plants, soils, and suspended and dissolved OM. More specifically, this study addresses the question of how the composition and concentration of different OM reservoirs vary in the rivers of the Peruvian Amazon and whether these patterns are variable or conservative as streams flow into larger rivers downstream.

## **STUDY AREA**

All samples were collected during July 2002. Samples were taken in the Huancabamba, Chontabamba, and Santa Cruz River watersheds in the central Andes of Peru (Figure 2.1). Sampling began just east of the Huagaruncho range (5879 masl) in the Amazon drainage. Site elevations ranged from 4043 masl to 720 masl (Table 2.1). Highest elevation sampling was conducted above the treeline in the Santa Cruz and Huancabamba valleys. Samples were collected at mid-elevations on the Chontabamba River, and lowest elevation samples were taken from the Santa Cruz and Huancabamba Rivers near the town of Pozuzo (Figure 2.1).

## **METHODS**

***Sampling***—River water for particulate analysis was collected from the edge of the stream in a 1 liter polycarbonate bottle and filtered immediately, taking care to agitate the bottle before pouring to ensure particulate resuspension. Water for CPOM collection was filtered through preweighed, 47 mm diameter, 60  $\mu\text{m}$  pore size Millipore™ nylon filters. The filtrate was then filtered through precombusted, preweighed 50 mm diameter, 0.7  $\mu\text{m}$  pore size Whatman™ glass fiber filters using a hand-operated vacuum pump to isolate FPOM. Filters were kept in 50 mm diameter petri dishes. At the end of sampling, filters

were dried at 40°C at the Andean Amazon Research Station in Oxapampa (Figure 2.1). Unfiltered water for  $\delta^{18}\text{O}$  analysis was collected in 20 ml glass vials with polycarbonate cone tops. This water was carefully contained without headspace gas by filling and capping the bottles underwater. Water for DOC analysis was filtered on site through 0.2  $\mu\text{m}$  nylon syringe filters into precleaned, precombusted 20 ml glass vials containing 20  $\mu\text{l}$   $\text{H}_2\text{SO}_4$ . Water for  $\delta^{15}\text{NO}_3^-$  analysis was syringe filtered into precleaned, precombusted 40 ml amber borosilicate vials containing 40  $\mu\text{l}$  of  $\text{H}_2\text{SO}_4$ . The first 10 ml of all syringe-filtered water was discarded to prevent contamination from the syringe filter. All bottles were capped and sealed on the outside with Parafilm™.

Six soil samples were collected at each location, three at the riparian zone, not more than 1 m from the stream, and three about 100 m uphill, perpendicular to the stream. Soils were collected from three approximate depths: the surface below vegetation, 10 cm, and 20 cm. Soils were placed in precombusted 40 ml amber borosilicate vials. Leaves from the most abundant (by visual inspection) plants were also collected from each subsite at each sampling location. Small pieces of living, not visibly diseased or damaged leaves were removed and placed in precleaned, precombusted 40 ml amber borosilicate vials. Because most sampling sites were remote, it was impossible to dry all plants, soils and filters immediately, but all were kept dark and cool until arrival at the field station, when they were placed into an oven at 40°C.

***Sample analyses***—Dried particulate samples were analyzed for  $\delta^{13}\text{C}$  and  $\delta^{15}\text{N}$  and mass % C and N on a Carlo Erba NC 1500 elemental analyzer coupled to a Finnigan MAT DELTA plus continuous flow isotope ratio mass spectrometer. Carbonates were removed from soils and river particulates prior to  $\delta^{13}\text{C}$  analysis by vapor phase acidification with HCl for 24 hours followed by drying at 40°C for 24 hours (Hedges and Stern 1984). Inorganic C was, on average, 2.5% of soil C, based on %C measurements

before and after acidification. Neither particulate samples for  $\delta^{15}\text{N}$  analysis nor plants were acidified. Fine particulates on glass fiber filters were analyzed directly on the elemental analyzer; coarse particulates were washed onto glass filters. Glass fiber filter results were corrected for the filter blank.

Acidified water samples were neutralized with NaOH prior to  $\delta^{15}\text{NO}_3^-$  analysis with the “denitrifier” method (Sigman et al. 2001). Nitrous oxide produced by this method was analyzed on a Finnegan MAT DELTA<sup>plus</sup> with a ThermoFinnegan Trace GC and a PreCon interface. DOC was analyzed on a Shimadzu TOC Vesh analyzer. The  $\delta^{18}\text{O}$  of  $\text{H}_2\text{O}$  was measured by  $\text{CO}_2$  equilibration at the Jackson School of Geological Sciences at the University of Texas at Austin. C, N and O stable isotope ratios are reported as  $\delta^{13}\text{C}$ ,  $\delta^{15}\text{N}$ , and  $\delta^{18}\text{O}$  relative to the Vienna Pee Dee Belemnite, atmospheric  $\text{N}_2$ , and Vienna Standard Mean Ocean Water standards, respectively.

**Data analysis**—Location and elevation at each sampling location were recorded using hand-held GPS units. Results for plants and soils were averaged for each site; all trends shown are representative of the full data set. Plant data shown are for  $\text{C}_3$  plants only; plants whose  $\delta^{13}\text{C}$  indicated a  $\text{C}_4$  pathway ( $\sim -10\text{‰}$ ) were not included in our calculations.  $\text{C}_4$  plants were scarce (5 out of 68) and found only at sites below 2400 masl. Statistical significance of correlations was determined using critical values of  $r^2$ . A correlation was considered significant after a two-way regression analysis if the  $p$  value was 0.05 or below. Averages are expressed plus or minus the standard deviation ( $\pm$  SD).

## RESULTS

**Plants**—Plant  $\delta^{13}\text{C}$  values were positively correlated with altitude ( $r^2 = 0.3029$ ,  $p < 0.02$ ,  $n = 20$ ; Figure 2.2A); the average  $\delta^{13}\text{C}$  of leaves from all sites was  $-28.2\text{‰} \pm 1.8\text{‰}$ .  $\delta^{15}\text{N}$  of plants showed no significant trend with altitude ( $r^2 = 0.0007$ ), with an average  $\delta^{15}\text{N}$  of  $1.1\text{‰} \pm 2.1\text{‰}$  (Figure 2.2B). Percent N of leaves was negatively



correlated with altitude ( $r^2 = 0.4477$ ,  $p < 0.002$ ,  $n = 20$ ; Figure 2.2D). Percent C was not correlated with altitude ( $r^2 = 0.0007$ ; Figure 2.2C). C:N<sub>molar</sub> of plant leaves was negatively correlated with altitude ( $r^2 = 0.4568$ ,  $p < 0.002$ ,  $n = 20$ ; Figure 2.2E). Mean C:N<sub>molar</sub> of plants was  $24.7 \pm 8.7$ .

*Soils*—Stable isotope content of soils did not vary with altitude: neither  $\delta^{13}\text{C}$  ( $r^2 = 0.0581$ ) nor  $\delta^{15}\text{N}$  ( $r^2 = 0.0577$ ) of soils is correlated with altitude (Figure 2.3A and 2.3B). Soils were more enriched than plants in both  $^{13}\text{C}$  and  $^{15}\text{N}$ . The average  $\delta^{13}\text{C}$  of all soils sampled was  $-24.4\text{‰} \pm 1.9\text{‰}$  and the average  $\delta^{15}\text{N}$  was  $4.3\text{‰} \pm 1.6\text{‰}$ . Soils had greater OM content at higher altitudes. Percent C in soils was positively correlated with altitude ( $r^2 = 0.5477$ ,  $p < 0.001$ ,  $n = 20$ ), as was %N ( $r^2 = 0.3951$ ,  $p < 0.005$ ,  $n = 20$ ; Figure 2.3C and 2.3D). C:N<sub>molar</sub> was positively correlated with altitude ( $r^2 = 0.2616$ ,  $p < 0.05$ ,  $n = 20$ ; Figure 2.3E). C:N<sub>molar</sub> of soils was markedly different than that of aboveground biomass, averaging  $11.8 \pm 3.7$  (Figure 2.2E). Percent C and N in soils were well correlated to each other ( $r^2 = 0.8107$ ,  $p < 0.001$ ,  $n = 20$ ; Figure 2.3F), but with a positive y-intercept at 0.04 %N. The slope-derived C:N of soils was 15.3 (Figure 2.3F).

*Suspended particulates*— $\delta^{13}\text{C}$  and  $\delta^{15}\text{N}$  show that FPOM more closely resembled soils than plants. The  $\delta^{13}\text{C}$  of FPOM was positively correlated with altitude ( $r^2 = 0.2687$ ,  $p < 0.02$ ,  $n = 20$ ; Figure 2.4A), with the average for all sites being  $-25.3\text{‰} \pm 2.3\text{‰}$ .  $\delta^{15}\text{N}$  of FPOM was not correlated with altitude ( $r^2 = 0.1189$ ; Figure 2.4B), and the average was  $3.6\text{‰} \pm 0.9\text{‰}$ . Percent C of fine suspended sediments (FSS) was positively correlated with altitude ( $r^2 = 0.4017$ ,  $p < 0.01$ ,  $n = 17$ ; Figure 2.4C), as was %N ( $r^2 = 0.5585$ ,  $p < 0.001$ ,  $n = 18$ ; Figure 2.4D). There was no correlation of C:N<sub>molar</sub> of FPOM with altitude ( $r^2 = 0.0256$ ; Figure 2.4E), with an average value of  $10.6 \pm 5.7$ . %C and N of FSS were well correlated with each other ( $r^2 = 0.8127$ ,  $p < 0.001$ ,  $n = 17$ ; Figure 2.4F), but with a positive y-intercept at 0.12 %N. The slope derived C:N of FPOM was 12.5 (Figure

2.4F). There was a significant inverse logarithmic relationship (as initially expressed in Meybeck 1982) between %OC in fine sediments and the total fine sediment load ( $r^2 = 0.5962$ ,  $p < 0.02$ ,  $n = 15$ ).

On the other hand, the elemental and isotopic composition of CPOM more closely resembled that of fresh leaves than soils. Some trends are not statistically significant for CPOM because the sample number was reduced by a lab accident.  $\delta^{13}\text{C}$  of CPOM had a positive, although statistically insignificant, relationship with altitude ( $r^2 = 0.1191$ ), and the average was  $-26.6\text{‰} \pm 1.1\text{‰}$  (Figure 2.5A). The  $\delta^{15}\text{N}$  of CPOM is positively correlated with altitude ( $r^2 = 0.7548$ ,  $p < 0.05$ ,  $n = 6$ ), with an average value of  $1.9\text{‰} \pm 2.1\text{‰}$  (Figure 2.5B). Percent C of coarse suspended sediments (CSS) is positively correlated with altitude ( $r^2 = 0.4157$ ,  $p < 0.05$ ,  $n = 12$ ), although %N is not (Figure 2.5C and 2.5D).  $\text{C:N}_{\text{molar}}$  was not correlated with altitude. The average  $\text{C:N}_{\text{molar}}$  of CPOM was  $16.7 \pm 7.6$  (Figure 2.5E). Percent C and N of CSS were more poorly correlated ( $r^2 = 0.5485$ ) than those of soils and FSS. There was no significant logarithmic relationship between %OC in coarse particulates and total CSS ( $r^2 = 0.0933$ ), to be expected in a size class strongly influenced by plant litter, not mineral grains.

*Dissolved components*—Dissolved OC concentrations in rivers were not correlated with altitude ( $r^2 = 0.0124$ ; Table 2.1). The overall average DOC concentration was  $2.4 \text{ mg L}^{-1} \pm 1.4 \text{ mg L}^{-1}$ . DOC concentrations were more variable in streams above 3000 masl (average  $2.5 \pm 1.5 \text{ mg L}^{-1}$ ) and approached the average value in lower altitude rivers (average  $2.3 \pm 1.1 \text{ mg L}^{-1}$ ).  $\delta^{18}\text{O}$  of  $\text{H}_2\text{O}$  was negatively correlated with altitude ( $r^2 = 0.482$ ,  $p < 0.001$ ,  $n = 22$ ; Table 2.1). River  $\delta^{18}\text{O}$  was more scattered above 3000 masl (average  $-12.3\text{‰} \pm 1.2\text{‰}$ ) than below (average  $-10.9\text{‰} \pm 0.8\text{‰}$ ). The  $\delta^{15}\text{NO}_3^-$  varied between  $1.4\text{‰}$  and  $6.3\text{‰}$  and was not correlated with altitude ( $r^2 = 0.0007$ ; Table 2.1). The average  $\delta^{15}\text{NO}_3^-$  was  $3.8\text{‰} \pm 1.2\text{‰}$ , which was closer to that of FPOM ( $3.6\text{‰}$ ) and

soils (4.3‰) than plants (1.1‰).  $\delta^{15}\text{NO}_3^-$  was more scattered above 3000 masl (average  $3.7\text{‰} \pm 1.4\text{‰}$ ) than below (average  $4.1\text{‰} \pm 0.5\text{‰}$ ).

## DISCUSSION

Our results reveal distinct shifts in the biogeochemistry of riverine organic matter between 4000 and 700 masl, indicating that processes operating in this zone of the Andean Amazon are instrumental in determining the biogeochemistry of organic matter observed in lower reaches of the river system. The following discussion is divided into three sections. The first identifies and discusses downstream or altitudinal patterns in the data. The second considers whether these patterns are useful in tracing sources of organic matter to Andean rivers and, ultimately, to the Amazon River as a whole. These are pertinent questions to the study of the organic geochemistry of the Amazon, and in answering them this discussion incorporates patterns seen and questions raised in the past 40+ years of research in the Amazon. The final section attempts to place the results of this study within an appropriate conceptual framework.

*Altitudinal distributions*– Previous montane plant studies have shown increasing  $\delta^{13}\text{C}$  with increasing altitude, attributed to an increase in carboxylation efficiency at altitude that decreases the ratio of internal to atmospheric  $\text{CO}_2$  ( $p_i/p_a$ ) (Körner et al. 1991). Plants in this study follow this trend (Figure 2.2A). Several studies report a concurrent increase in leaf N with altitudinal  $\delta^{13}\text{C}$  increases (Morecroft et al. 1992, Sparks and Ehleringer 1997), attributed to an increase in N-rich, C-fixing enzymes such as ribulose 1,5-biphosphate carboxylase (RuBP carboxylase) at altitude (Hultine and Marshall 2000). However, the plant data in the current study do not have the same relationship (Figure 2.2D), and, in fact,  $\delta^{13}\text{C}$  of plants is significantly negatively correlated to leaf %N ( $r^2 = 0.4371$ ,  $p < 0.002$ ,  $n = 20$ ), suggesting that different processes may control plant C and N in this region.

Besides enzyme content, other factors may influence leaf %N, such as soil N availability and species composition. Venezuelan trees showed no change in %N with increasing altitude, attributed to lower N availability in upland soils (Diaz et al. 1996). Alternate explanations for the variation in  $\delta^{13}\text{C}$  of plants include water stress, variations in atmospheric  $\text{CO}_2$  content, and species composition. Water stress can increase  $\delta^{13}\text{C}$  (Körner et al. 1991), and precipitation decreases at altitude in the Andes (Mayorga and Aufdenkampe 2002). It is possible that ambient  $\text{CO}_2$  does not vary conservatively with atmospheric pressure because  $\text{CO}_2$  levels in forested areas are higher than in watersheds above the tree line; this may be an alternate explanation for our trend of increasing foliar  $\delta^{13}\text{C}$  with altitude. Furthermore, foliar  $\delta^{13}\text{C}$  does not always increase with altitude: Diaz et al. (1996) found that  $\text{C}_3$  trees in the Venezuelan Andes were not  $^{13}\text{C}$  enriched at altitude. Species composition can also affect  $\delta^{13}\text{C}$ : functional grouping of life forms is often a better predictor of altitudinal patterns of  $\delta^{13}\text{C}$  than  $p_i/p_a$  (Brooks et al. 1997). This is likely to be the case in this study, since a visible transition in plant ecosystems was observed down the mountain. If a change in plant functional groups, not an increase in RuBP carboxylase content, is the cause of the altitudinal  $\delta^{13}\text{C}$  trend, this may explain why leaf  $\delta^{13}\text{C}$  is negatively correlated with leaf N.

Neither  $\delta^{13}\text{C}$  nor  $\delta^{15}\text{N}$  of soils exhibited an altitudinal gradient (Figure 2.3A and 2.3B). Previous studies of altitudinal trends in soil  $\delta^{13}\text{C}$  have found patterns mirroring those of plants (Bird et al. 1994). In natural terrestrial ecosystems, soil OM typically is either derived from plants growing above or from root, microbial and/or fungal biomass growing in the soils (Ehleringer et al. 2000). Plant degradation, root inputs, and microbial growth can lead to  $^{13}\text{C}$  and  $^{15}\text{N}$ -enriched soils, and the dominant mechanism controlling soil isotope ratios is uncertain (Lehmann et al. 2002). Sorption can also influence the isotopic composition of POM (Aufdenkampe et al. 2001). Studies have

shown that fine roots are often enriched in  $^{13}\text{C}$  and  $^{15}\text{N}$  with respect to leaves (Kitayama and Iwamoto 2001, Hobbie et al. 2002), and preliminary data from another study site in the region confirm this (data not shown). Soils collected for this study are 1-3‰ more enriched in  $^{13}\text{C}$  and  $^{15}\text{N}$  than leaves. Also, the C:N of soils (11.3) indicates that they are a mixture of plant and microbial sources, since microbial biomass has a C:N from about 5-8 and plant material C:N is ~24. Unlike plant leaves, soil C:N decreased at lower altitudes (Figure 2.3E), possibly indicating a greater microbial component in low-altitude soils or faster decomposition rates at lower altitudes. Regardless of mechanism, the isotope shift between plants and soils is a potential indicator of riverine OM sources.

Past changes in plant populations and soil contributions from mass movement processes can potentially complicate the interpretation of soil patterns. Although soils are often derived from past plant populations, there is no evidence (isotopic or otherwise) that there has been a major shift in vegetation coverage in this area. Alluvial soil contributions are often important to riparian ecosystems, but no isotopic or elemental differences were found between riverbank soils and those located 100m away from the river. Belowground recycling of root biomass may also be a significant source of OM in these soils. Soil formation is also dependent on underlying geology. Rocks underlying the study area are mostly late Permian granites and granodiorites (Instituto Geologico, Minero y Metalurgico 1996). Old sedimentary rocks containing kerogen can be a source of OC in soil formation (Hedges and Oades 1997), but the igneous rocks found in this study area are unlikely to be a significant OC source. However, geology and sediment transport are very poorly studied in this area, and a better understanding of these processes will be necessary in the future to better constrain Andean sources of OM to the Amazon.

Unlike plants, %C and %N of soils sampled in this study are both significantly positively correlated with altitude (Figure 2.3C and 2.3D), indicating higher organic:mineral ratios with increasing altitude. Increases in soil OM degradation are usually accompanied by a decrease in %OC and %N (Nadelhoffer and Fry 1988). Soil stable isotope signatures also support this hypothesis. Our data indicate that soil OM at higher altitudes was closer in isotopic composition to plants and thus less degraded than soils at lower altitudes. Increasing dampness and lower temperatures at higher altitudes likely slow decomposition rates (Batjes 1996, Coûteaux et al. 2002). Peat soils (found at our highest altitude sites) are often OC-rich and minimally degraded (Batjes 1996). Thus, the combination of elemental and isotopic comparisons between soils and plant leaves supports the hypothesis of a soil decomposition gradient in the Peruvian Andean Amazon.

All the dissolved parameters measured in this study have more scattered distributions at higher altitudes and approach averages at lower altitudes, demonstrating the integrating effect of rivers and indicating that adjacent headwater streams can have dramatically different geochemical characteristics. The same trend can be seen in isotopic and elemental composition of FSS (Figure 2.4). Since high altitude samples represent smaller catchments, small differences in ecosystem C, N, and H<sub>2</sub>O cycling can lead to large differences in the chemical composition of exported water. Dissolved organic carbon concentrations in this study ranged from 0.7 to 6.1 mg L<sup>-1</sup> (Table 2.1). Previous studies found concentrations in the Andes to range from ~1 to 2 mg L<sup>-1</sup> (Guyot and Wasson 1994, Hedges et al. 2000), although one of these studies did not sample above 2500 masl (Guyot and Wasson 1994), and the other had only one sample above 450 masl, at 3900 masl (Hedges et al. 2000). And Guyot and Wasson (1994) found that DOC concentration increased at approximately 200 masl where the topography flattened and

wetlands appeared along the channels to a mainstem average of 5 mg L<sup>-1</sup> (Richey et al. 1980, 1990). In contrast, the current study shows no significant trend of downstream DOC enrichment (Table 2.1), and the highest concentrations are found in high-altitude streams draining peat soils. This is in sharp contrast to other high-mountain river studies, where DOC is usually among the lowest concentrations in the world (Meybeck 1982, Hedges et al. 2000), but most of these studies were conducted at higher latitudes where organic-rich peat soils do not occur at very high altitudes. Also, our high altitude samples were taken from small headwater streams, where the importance of stream order on riverine biogeochemistry is magnified during storm events, when runoff is generated rapidly in small streams but delayed in larger rivers (McGlynn and McDonnell 2003). DOC concentrations in this study were affected by the amount of precipitation (Table 2.1) as well as ecological and topographical differences between watersheds.

River water  $\delta^{18}\text{O}$  values become enriched downstream, as expected, except that isotopically heavy rains during sample collection weaken the correlation. In general, the highest  $\delta^{18}\text{O}$  values occurred when rainfall was heaviest, due to an enriched rain or runoff source. Stream  $\delta^{18}\text{O}$  is positively correlated (although insignificantly) to DOC concentration ( $r^2 = 0.1687$ ), raising the possibility that storm events contribute to loading of OC-rich, isotopically heavy soil waters, especially in small, low-order streams.

The average  $\delta^{15}\text{NO}_3^-$  in this study is  $3.8\text{‰} \pm 1.2\text{‰}$ , close to that measured in the Amazon mainstem at Manaus ( $4.1\text{‰} \pm 0.3\text{‰}$ , Brandes and Devol 2002). Nitrate concentrations in the mainstem are controlled by river-floodplain interactions and in-channel processes (Devol et al. 1995, McClain et al. 1997). However, mechanisms controlling  $\text{NO}_3^-$  concentrations in upstream tributaries are unknown. However, remineralization of organic N and uptake of DIN by heterotrophic microbes is likely significant; in fact, Brandes et al. (1996) found that in-stream remineralization of organic

N was the most likely source of  $\text{NO}_3^-$  to a small stream in the lower Amazon. Overall  $\delta^{15}\text{NO}_3^-$  values in this study are also consistent with a soil or POM (~ 4%) mineralization source, although values are not significantly correlated to each other ( $\delta^{15}\text{N}$  of FSS vs.  $\text{NO}_3^-$   $r^2 = 0.0077$ ;  $\delta^{15}\text{N}$  of soil N vs.  $\text{NO}_3^-$   $r^2 = 0.0367$ ). Nitrate may be isotopically lighter than POM at a site due to incomplete oxidation, a rainwater  $\text{NO}_3^-$  source, or the presence of  $\text{N}_2$  fixation, whereas an enriched  $\text{NO}_3^-$  pool may have been subjected to fractionation such as during denitrification or uptake (Brandes et al. 1996).

*Tracers of riverine OM sources*— $\delta^{13}\text{C}$ ,  $\delta^{15}\text{N}$  and  $\text{C:N}_{\text{molar}}$  of fine particulate organic matter (FPOM; Figure 2.4) are similar to those of soils (Figure 2.3), supporting the hypothesis that soils are the predominant source of C to these rivers. Phytoplankton growing in the Andean Amazon have an estimated  $\delta^{13}\text{C}$  of  $-33$  to  $-55\text{‰}$  (Cai et al. 1988), which, when compared to the average  $\delta^{13}\text{C}$  for both FPOM ( $-25.3\text{‰}$ ) and CPOM ( $-26.3\text{‰}$ ), indicate that algae is a minor component in these rivers. Also, undisturbed lowland Amazonian streams are thought to have virtually no in-situ photosynthesis (McClain and Elsenbeer 2001). FPOM  $\delta^{13}\text{C}$  and  $\delta^{15}\text{N}$  are more enriched than plants, but are similar to soils. Isotopic analyses as well as relatively high %C compositions at lower altitudes indicate that CPOM may be less degraded or altered from plant sources as compared to FPOM (Figure 2.5).  $\delta^{13}\text{C}$  values of CPOM are intermediate between plants and soils, and the low average  $\delta^{15}\text{N}$  of CPOM strongly resembles a plant source. In the lower Amazon, CPOM has chemical characteristics between those of plants and soils, and the original OM source is mainly leaves (Hedges et al. 1986a, 1986b, 2000). Previous studies of the Amazon using biochemical indicators of decomposition found that FPOM was more degraded than CPOM (Hedges et al. 1986a, 1994). In this study, FPOM is more enriched in  $\delta^{13}\text{C}$  and  $\delta^{15}\text{N}$  than CPOM, which may indicate that FPOM comes from a more degraded source than CPOM in the Andes as well as in the Amazon



mainstem. This study shows that sources of riverine fine and coarse particulate OM in the Andean Amazon are probably similar, at first approximation, to those determined for the lower Amazon, but, unlike the lower Amazon, chemical composition of those sources and fractions differs with altitude.

Despite their relatively distinct C and N isotopic signatures, elemental compositions of FSS and CSS exhibit similar patterns (Figure 2.4C, 2.4D, 2.5C, and 2.5D). Both FSS and CSS are enriched in OC with respect to soils (Figure 2.3C), with CSS more so and approaching plant values at high altitude (Figure 2.4C). FSS and CSS have similar N content as compared to plants (Figure 2.2C) but are slightly less N-rich than soils (Figure 2.3C). Both size classes of suspended sediment collected in this study are more enriched in OC than those found in the mainstem. FSS in the Amazon has from 0.9 to 1.5% OC by weight and CSS from 0.5 to 3.4% OC, with no downstream trend in %C of FSS (Richey et al. 1990). In contrast, OM contents of both FSS and CSS in the current study are positively correlated with altitude.

While  $\delta^{13}\text{C}$  and  $\delta^{15}\text{N}$  seem to indicate that FPOM is soil-derived, in general, OC and N are higher in FSS than in soils (Figure 2.3C, 2.3D, 2.4C, and 2.4D). In some cases, %C and N of FSS are nearly twice those of soils, indicating some type of in-stream process affecting the composition of FSS. Previously, Aufdenkampe et al. (2001) determined that sorption of DOM could increase the OM content of suspended kaolinite in simulated Amazonian rivers, but only from 0 to 3%. There are two possible reasons for the observed enrichment in OC and N in FPOM in this study over the probable soil source. The first possibility is that sorption of dissolved OM to riverine particles is greater than indicated by laboratory studies (Aufdenkampe et al. 2001), thus supporting the “regional chromatography model” of organic matter transport in the Amazon (Hedges et al. 1994, Devol and Hedges 2001). During a recent study of OM dynamics in the

Andean Amazon, Hedges et al. (2000) found a similar offset in N content of FSS and soils, and attributed it to the sorption of  $^{15}\text{N}$ -rich DOM to suspended soil minerals. The current study indicates a similar offset. Although the isotopic composition of DOM was not measured in this study, FPOM does have consistently lower  $\delta^{15}\text{N}$  values ( $\sim 0.5\text{‰}$ ) overall than soil OM (Figure 2.3B, 2.4B), indicating that sorbed DOM is isotopically light, consistent with a possible leaf leachate source. The second possibility is that FPOM in the Andes consists at least partially of small pieces of plant material and more OM-rich surface litter as opposed to deeper OM-poor soil minerals, which is supported by altitudinal trends in isotopic composition of FPOM (see further discussion below). These ideas will be further investigated in future studies using compound-specific analyses and/or radiocarbon measurements of soils and particulates.

Results from this study show a significant increase in  $\delta^{13}\text{C}$  of FPOM at higher altitudes (Figure 2.4A), consistent with Cai et al. (1988), whose highest  $\delta^{13}\text{C}$  values ( $-24.6\text{‰}$ ) in bulk POM were found in the high Andes. However, while Cai et al. (1988) attributed altitudinal patterns in POM  $\delta^{13}\text{C}$  values directly to changes in plant  $^{13}\text{C}$ , the results of this study indicate that FPOM is mainly soil, not plant, derived. We attribute elevational patterns in POM  $\delta^{13}\text{C}$  values to changes in the relative contribution of sources rather than to changes in  $\delta^{13}\text{C}$  of a single source. Decreasing POM  $\delta^{13}\text{C}$  values at lower altitudes support an increased contribution of plant material to FPOM at lower altitudes where riparian forests appear and litterfall inputs are greater (McClain and Richey 1996). At high altitudes ( $\sim 4000$  masl), cold temperatures and relatively low rainfall levels lead to the production of OM-rich soils, which are transported to the river by shallow runoff during rain events. On the other hand, OM inputs at lower altitudes are likely to be a mixture of fresh leaf litter and OM-poor soils added during frequent landslides or other disturbances as well as material exported from upstream. The OM-poor nature of lower

altitude soils will make any leaf litter contributions to rivers more important, as compared to higher altitudes where more OM-rich soils dominate riverine OM sources. These hypotheses are supported by elemental data (discussed below), as well as isotopic analyses: FPOM  $\delta^{13}\text{C}$  values approach those recorded for CPOM and plants at low altitude sampling sites (Figure 2.4A, 2.5A). There is no significant trend of  $\delta^{15}\text{N}$  of FPOM with altitude in this study (Figure 2.4B), consistent with both soils and plants (Figure 2.2B, 2.3B). Unlike the  $\delta^{13}\text{C}$  trend,  $\delta^{15}\text{N}$  of FPOM and CPOM seem to converge upstream, indicating that CPOM at sites above the tree line is derived from soils rather than plants, a logical conclusion for streams draining basins where more biomass is below ground than above. However, these hypotheses will need to be tested in other, more detailed studies.

Percent of C and N in FPOM and CPOM are positively correlated with altitude (Figure 2.4C, 2.4D, 2.5C, and 2.5D). This may be attributed to in-stream processing of POM, but as the same trend is apparent for soils (Figure 2.3C and 2.3D), the loss of C and N mass in particulates is a likely indicator of the downstream addition of low OM mineral soils. Previous river studies have shown that %OC of suspended particulates decreases when sediment load and discharge increase (Meybeck 1982), either because of dilution of suspended OM with mineral soils or because of differences in source and processing of OM at different locations along the river. In this study, %OC of FSS decreases with increasing total FSS load, but this relationship is not true for CSS, perhaps due to either low overall suspended sediment loads ( $< 10 \text{ mg L}^{-1}$ ) or low number of samples. Similarly, in the lower Amazon, TSS controls FPOM concentrations while CPOM concentrations are relatively independent of total CSS concentration (Hedges et al. 2000). However, unlike the present study, in the lower Amazon, FPOM concentrations increase as FSS increases (Hedges et al. 2000), because high-topography

Andean rivers are dominated by erosion as opposed to deposition and sorption. Because samples in this study were taken along a known altitudinal gradient, we can infer a decreased input of mineral soils at the highest altitudes.

The Andes have been proposed as a significant particulate inorganic N source to the Amazon based on C:N of FPOM and CPOM with positive N intercepts, indicating that an average of 50% of N was inorganic (Hedges et al. 2000). FPOM, CPOM, and soils (Figure 2.3F, 2.4F, and 2.5F) in the current study show evidence for only a small percentage at most (< 10% on average) of inorganic N in Andean particulates. In addition, unlike Hedges et al. (2000), we do not see a significant downstream increase in  $\delta^{15}\text{N}$  in any particulate fraction. Samples collected in this study were from higher altitudes than most of those in Hedges et al. (2000), and due to a combination of factors (different regions of the basin, different number of samples), our study indicates that the central Peruvian Andes are not a significant source of particulate inorganic N to lower altitude tributaries. In fact, the Andes are likely a greater source of dissolved than particulate inorganic N. Given an average FSS concentration of  $5.3 \text{ mg L}^{-1}$ , an average %N of FSS of 1.9%, and assuming that a maximum 10% of that N is inorganic, the approximate concentration of fine particulate inorganic N in these rivers is  $0.7 \text{ } \mu\text{mol L}^{-1}$ . This is more than an order of magnitude lower than the approximate maximum  $\text{NO}_3^-$  concentration of  $5 \text{ } \mu\text{mol L}^{-1}$ .

One goal of this and other studies has been to determine the extent to which Andean organic matter persists in the Amazon mainstem and estuary. Andean POM derived from high-altitude plants was thought to be the source of the enriched  $\delta^{13}\text{C}$  value of POM at Obidos (Quay et al. 1992). Quay et al. (1992) used the  $\delta^{13}\text{C}$  of POM from Cai et al. (1988) to calculate that approximately 65% of POC in the Amazon mainstem was Andean. More recently, this figure was revised based on other  $\delta^{13}\text{C}$  of FPOM data from

the Andes, to less than 40% (Hedges et al. 2000). Using the average  $\delta^{13}\text{C}$  of FPOM from all Andean rivers sampled in this study (-25.3‰) and the lowland endmember of -28.5‰ (Quay et al. 1992), 35% (by isotope balance) of FPOM in the Amazon mainstem at Obidos (-27.4‰, Hedges et al. 2000) is derived from Andean rivers above 700 masl. This is very close to the estimate of Andean FPOM loading by Hedges et al. (2000). This mass balance calculation for CPOM also yields the same results as Hedges et al. (2000): less than 40% of CPOM in the mainstem is derived from the Andes. Since the Andes supply ~85% of suspended sediment to the Amazon River (Meade et al. 1985), our results imply that OM transported with suspended particles is remineralized, replaced, and/or amended during transport through lowland portions of the river basin, in agreement with previous studies (Hedges et al. 2000). However, in contrast to previous work (e.g., Hedges et al. 2000), the present study shows that highly degraded soil C, as opposed to plant leaves, is the dominant source of POM in the Andes; indeed, if Andean riverine OC consisted of plants in the 1000 to 3000 masl region where most sediment loading occurs, it would be much lighter in  $\delta^{13}\text{C}$  and  $\delta^{15}\text{N}$  than what we find. Therefore, it seems that the dominant processes affecting OM composition in the Andean Amazon take place prior to entering the river, not within it.

The existing conceptual model of organic matter dynamics in the Amazon River system is the “regional chromatography model” (Hedges et al. 1986*b*, 1994, Devol and Hedges 2001), based on years of work in the mainstem Amazon. This model was developed to explain the different compositions and concentrations of various OM size classes. In the mainstem Amazon, leaves are the ultimate source of riverine organic matter. According to the regional chromatography model, leaf litter decays rapidly on the forest floor, where it is either exported as relatively intact CPOM or further decomposed into dissolved organic molecules. Depending on its hydrophobicity, this

DOM either remains dissolved or sorbs to soil minerals, producing FPOM. These patterns, as reflected in the chemical composition of these OM size classes, were found to be remarkably consistent along the entire ~1800 km of the Amazon mainstem. Although the current study does not include all the analytical techniques used to describe the above patterns, a preliminary comparison can be made between OM dynamics in the Peruvian Andes and those explained by regional chromatography. First of all, similar to the lowland Amazon, our data indicate that terrestrial plants are the ultimate source of riverine OM, although more specific evidence would strengthen this argument. In addition, stable isotopic evidence indicates that CPOM is derived from minimally degraded terrestrial plants, and that FPOM is more degraded, just as has been found in the mainstem. We also show preliminary evidence for sorption of dissolved organic N to FSS, but the levels of organic C and N in fine particulates are too high for sorption of DOM to be the main source of FPOM, as the regional chromatography model predicts (Hedges et al. 2000, Aufdenkampe et al. 2001), unless sorption is occurring at a much higher proportion in Andean rivers. We propose that soil OM consisting of highly degraded plant material, as opposed to mineral-sorbed DOM, is the primary source of FPOM in the Andean Amazon. As predicted by the regional chromatography concept, results presented here indicate that processes operating outside the river are the most important control on riverine organic matter composition, and downstream changes in in-stream compositional patterns are due to changes in terrestrial sources. However, important differences from the regional chromatography model are apparent in Andean riverine OM dynamics, namely, the much greater roles for altitude and climate-correlated soil diagenesis and erosion in the Andes.

Based on the results of this study we propose a preliminary conceptual model of OM dynamics in the Andean Amazon (Figure 2.6). At the highest reaches of the

Amazon (region A, Figure 2.6), above about 3000 masl, catchments and streams are small and rainfall is reduced. Low temperatures slow decomposition and soils accumulate particulate and dissolved OC. Erosion of mineral soils is low and erosion of surface (high OC) riparian soils dominates particulate loading to streams. Since streams and catchments are smaller,  $\delta^{15}\text{NO}_3^-$  and DOC concentrations are highly variable. Between about 3500 and 2000 masl (region B, Figure 2.6), greater rainfall leads to rapid, constant OC leaching and erosion of mineral rich, OC-poor soils. Soil OM is more degraded due to warmer temperatures and rapid flushing, and river FPOM reflects the input of soil OM from erosion. DOC is lower than in high altitude streams draining peat soils and  $\delta^{15}\text{NO}_3^-$  values are constant, reflecting the integrating nature of the larger rivers in this region. Finally, in the foothills of the Andes (2000 – 750 masl), where rainfall is at a maximum and topography is gentler, FPOM and CPOM begin to reflect the input of less degraded surface soil and leaf litter inputs (region C, Figure 2.6). DOC concentrations remain low and  $\delta^{15}\text{NO}_3^-$  values are consistent throughout the landscape. The assumptions of this model can be tested in future studies of the Andes, optimally including broader spatial coverage, identification of salient geomorphological features, river discharge, and more measurements of OM sources, transport, and residence times.

This study allows for several conclusions about carbon and nitrogen cycling in the Andean Amazon. Plants show a positive correlation of  $\delta^{13}\text{C}$  with altitude consistent with other studies, but the negative correlation of foliar N content with altitude indicates that nutrient limitation, water stress, or species composition are more important in determining foliar chemistry than internal  $\text{CO}_2$  levels. Soil OM is consistently degraded beyond the leaf litter stage, with a strong gradient in weight % OM with altitude. At all sites, riverine suspended FPOM is predominantly soil derived and becomes progressively enriched in  $\delta^{13}\text{C}$  at low altitudes, whereas CPOM compositionally resembles minimally

or partially degraded leaf litter. Overall, riverine FSS and CSS are enriched in OC and N over soils, indicating additional contributions from either sorption of DOM or C-rich POM sources such as leaf litter. Such leaf litter inputs may become an important source of FPOC to rivers at the lowest altitudes in our system. In general, riverine OM compositions are driven by erosion-dominated soil inputs, which are in turn controlled by physical factors such as rainfall, temperature, and topography. High altitude OM-rich soil inputs give way to OM-poor soil inputs at mid to low altitudes, resulting in a sharp gradient in riverine %OM with altitude. The high levels of degradation experienced by most Andean soils prior to transport to rivers and out to the main basin, as well as sorptive protection on mineral surfaces, may be primary reasons why this material survives in-river processing to provide a significant source of organic matter to the Amazon River. Delta  $^{15}\text{N}$  values indicate that riverine  $\text{NO}_3^-$  is derived from soils or POM. Dissolved OC concentrations observed at high altitudes (>2000 masl) were variable, but correlated to storm events, and decreased to relatively low values (1-2 mg L<sup>-1</sup>) in the lower basin. Indeed, all three solute parameters,  $\delta^{18}\text{O}$  of  $\text{H}_2\text{O}$ ,  $\delta^{15}\text{N}$  of  $\text{NO}_3^-$ , and DOC concentration, in headwater streams were highly variable. This illustrates the need to consider rivers, especially their mountain headwaters, within a longitudinal (e.g., Vannote et al. 1980) as well as a lateral framework embracing variability and abrupt geochemical transitions (e.g., Poole 2002). Perhaps the most important finding of this work is that soils are a more important source of riverine FPOM in Andean rivers as compared to rivers of the lower Amazon (Hedges et al. 1986a, 1986b, 1994, 2000). Moreover, in sharp contrast to the stable longitudinal biogeochemical patterns that characterize lowland rivers, the concentration and composition of various OM size classes, in plant and soil sources as well as riverine particulate exports, vary with altitude and downstream distance in the Andean Amazon.



Site	Altitude (masl)	Latitude (°S)	Longitude (°W)	DOC (mg L <sup>-1</sup> )	δ <sup>15</sup> N of NO <sub>3</sub> <sup>-</sup> (‰)	δ <sup>18</sup> O of H <sub>2</sub> O (‰)
Río Lecma, near lake source	4043	10° 27' 52.4"	76° 6' 39.4"	1.3	5.6	-14.2
Río Munapampa, lake source	4016	10° 30' 0.7"	76° 8' 1.6"	1.3	2.6	-13.7
Río Muñapampa 7/5/02	3797	10° 27' 52.4"	76° 9' 15.5"	1.6	5.1	-13.2
Río Muñapampa 7/9/02	★ 3797	10° 27' 52.4"	76° 9' 15.5"	2.6	2.4	-12.7
Río Lecma, high altitude	3780	10° 27' 37.0"	76° 9' 13.6"	1.3	6.3	-13.2
Río Galvez near source	★ 3749	10° 25' 59.1"	76° 11' 15.0"	4.7	n/d	-10.8
Río Lecma, mid-altitude	3562	10° 28' 6.2"	76° 11' 11.9"	3.2	3.8	-12.0
Río Ramos	★ 3500*	n/d	n/d	2.4	2.0	-11.3
Stream entering Río Ramos	★ 3488	10° 24' 15.2"	76° 10' 47.0"	1.3	4.4	-12.2
Bog draining into Río Galvez	★ 3433	10° 23' 54.7"	76° 11' 28.4"	0.7	3.6	-12.4
Río Galvez at treeline	★ 3433	10° 23' 54.7"	76° 11' 28.4"	2.8	2.9	-11.6
Confluence of Ríos Galvez and Ramos	3400*	n/d	n/d	2.8	1.4	-11.5
Río Galvez during storm	★ 3360	10° 23' 37.8"	76° 11' 10.5"	6.1	4.0	-10.6
Río Lecma, low altitude	★ 2760	10° 29' 39.9"	76° 14' 57.5"	3.8	3.6	-12.5
Río Muspes	★ 2422	10° 31' 6.1"	76° 16' 36.4"	3.8	4.3	-12.1
Río Llamaquizú	2394	10° 37' 26.3"	76° 42' 16.0"	4.6	n/d	-10.5
Río Huaylamayo	★ 2387	10° 30' 55.4"	76° 16' 49.3"	1.1	5.2	-12.0
Río Churumazu, high altitude	2200	10° 38' 11.8"	76° 32' 24.2"	n/d	n/d	-10.2
Río Churumazu, low altitude	1908	10° 36' 43.8"	76° 33' 4.2"	n/d	4.2	-9.7
Río San Alberto	1867	10° 34' 38.8"	76° 36' 27.8"	2.2	n/d	-10.8
Río Chontabamba, high altitude	1854	10° 36' 1.8"	76° 33' 25.5"	n/d	3.5	n/d
Río Chontabamba, mid altitude	1830	10° 34' 4.9"	76° 35' 12.4"	1.8	n/d	-10.5
Río Huancabamba upstream of Pozuzo	1756	n/d	n/d	n/d	3.8	-10.4
Río Chontabamba, low altitude	1752	10° 26' 1.4"	76° 28' 55.4"	1.9	4.7	-10.6
Río Huancabamba above Chontabamba	1715	10° 24' 0.5"	76° 26' 36.0"	1.4	n/d	-11.6
Río Huancabamba below Pozuzo	764	10° 6' 4.9"	76° 27' 28.7"	1.1	n/d	-10.3
Río Santa Cruz, above Huancabamba	720	10° 2' 32.0"	76° 27' 33.4"	n/d	3.8	-10.8

★ = sample was collected during a storm event

n/d = not determined

\* = estimated altitude, GPS not available

Table 2.1. Locations, names, and elevations of sampling sites in this study, with water characteristics as determined for each site.

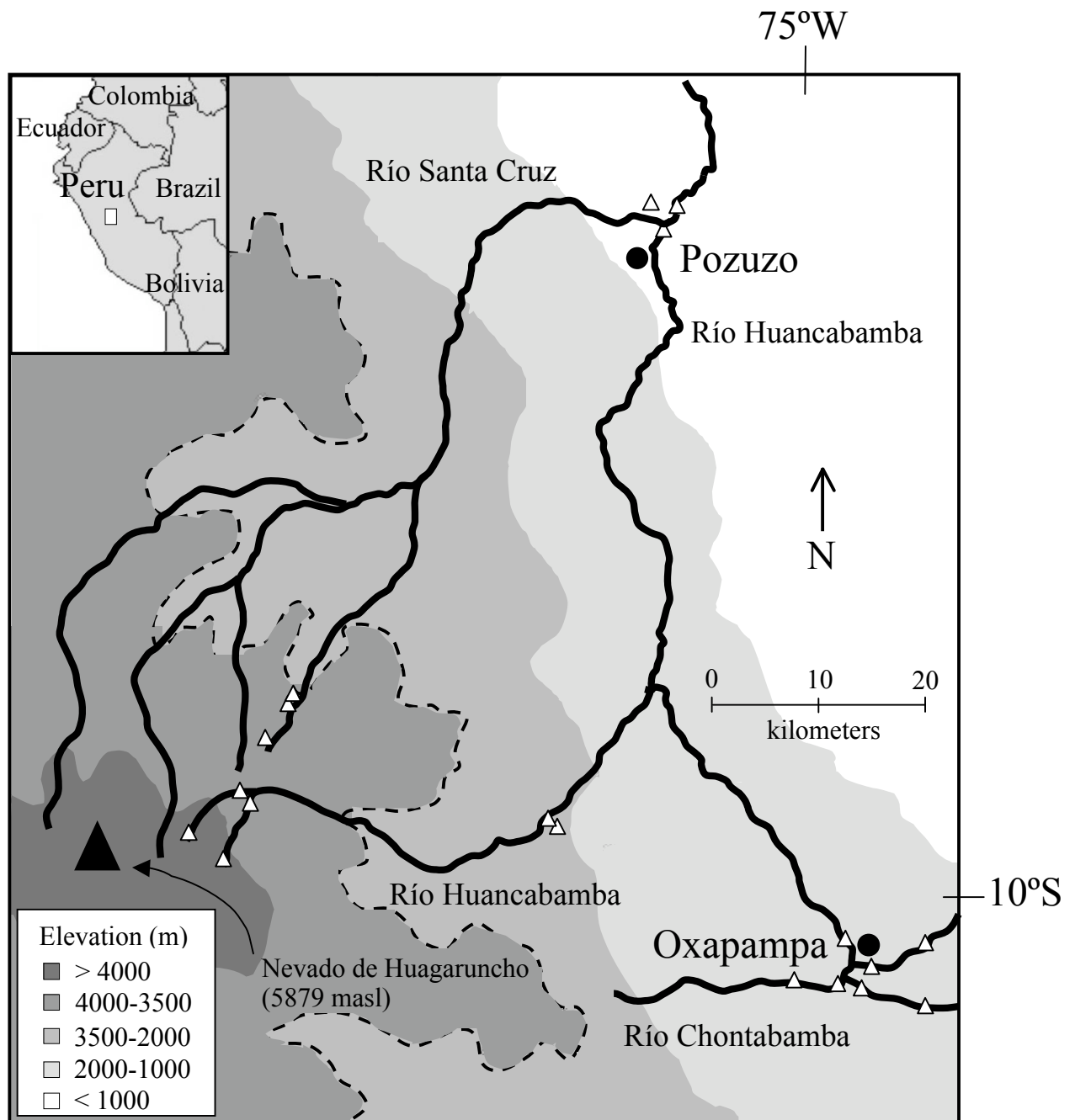


Figure 2.1. Map of the study area including areas of intense sampling (white triangles) and names of major rivers and towns. The dotted line indicates the position of the treeline. Large black triangle indicates the location of the highest mountain in the range (5879 masl). Inset shows location within northwestern South America.

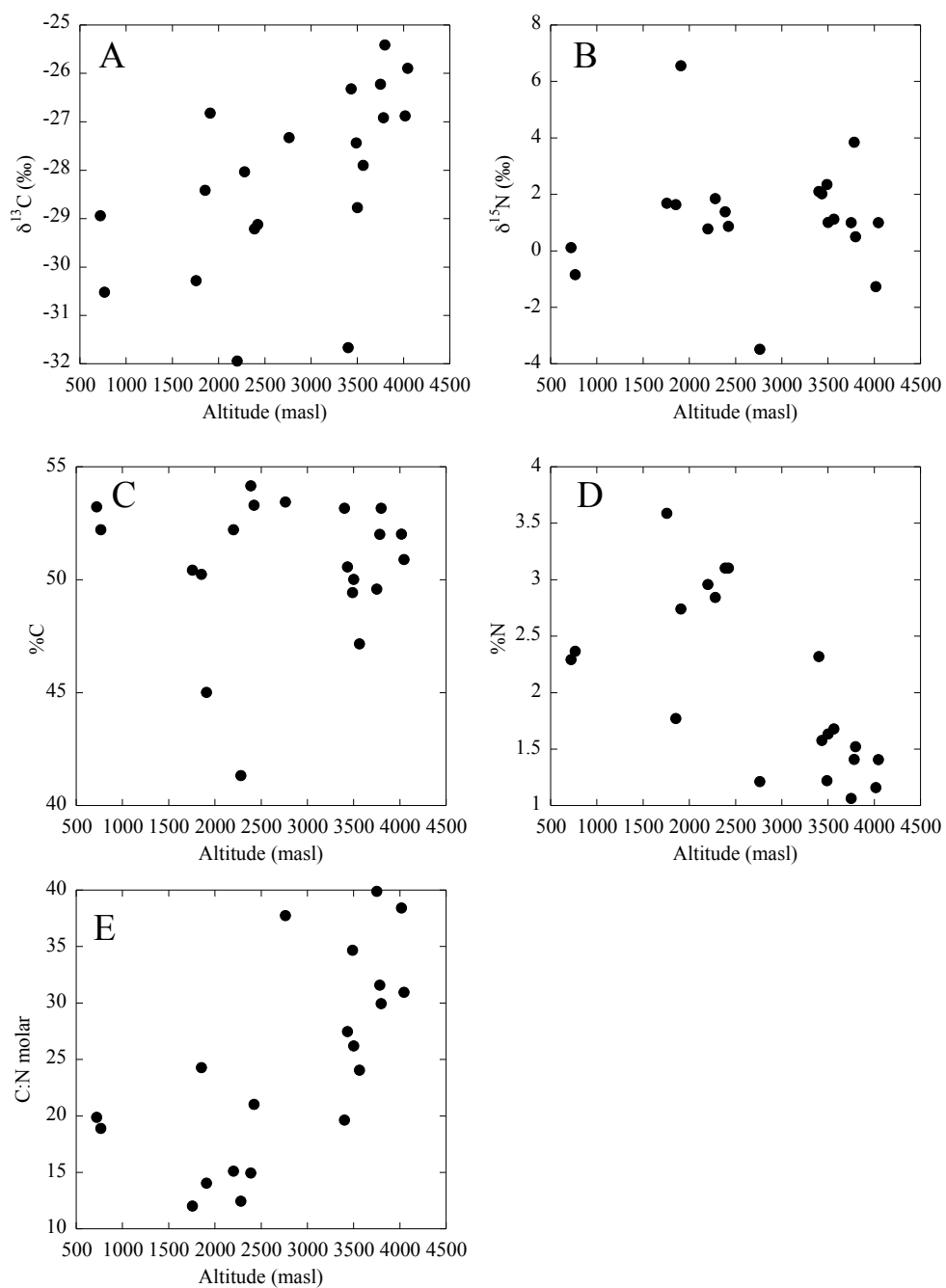


Figure 2.2. Elevational trends of A)  $\delta^{13}\text{C}$ , B)  $\delta^{15}\text{N}$ , C) %C, D) %N and E) molar C:N of plant leaves collected during this study. Each point represents an average value for all plants (riparian and upland) sampled at that station.

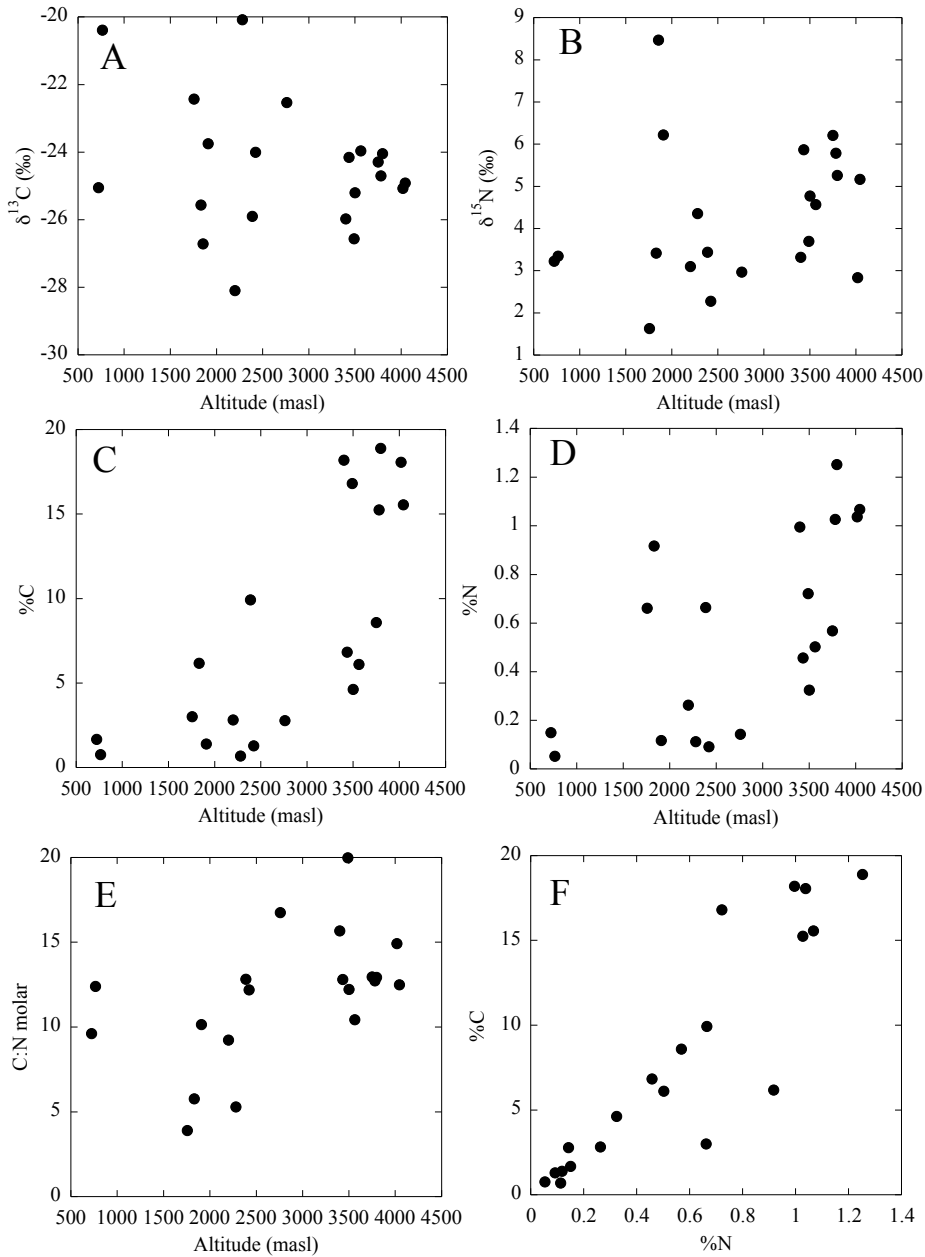


Figure 2.3. Elevational trends of A)  $\delta^{13}\text{C}$ , B)  $\delta^{15}\text{N}$ , C) %C, D) %N and E) molar C:N of soils collected during this study. Each point represents an average value for all soil horizons sampled at that station. Weight percent of carbon versus weight percent of nitrogen of soil samples is shown in panel (F).

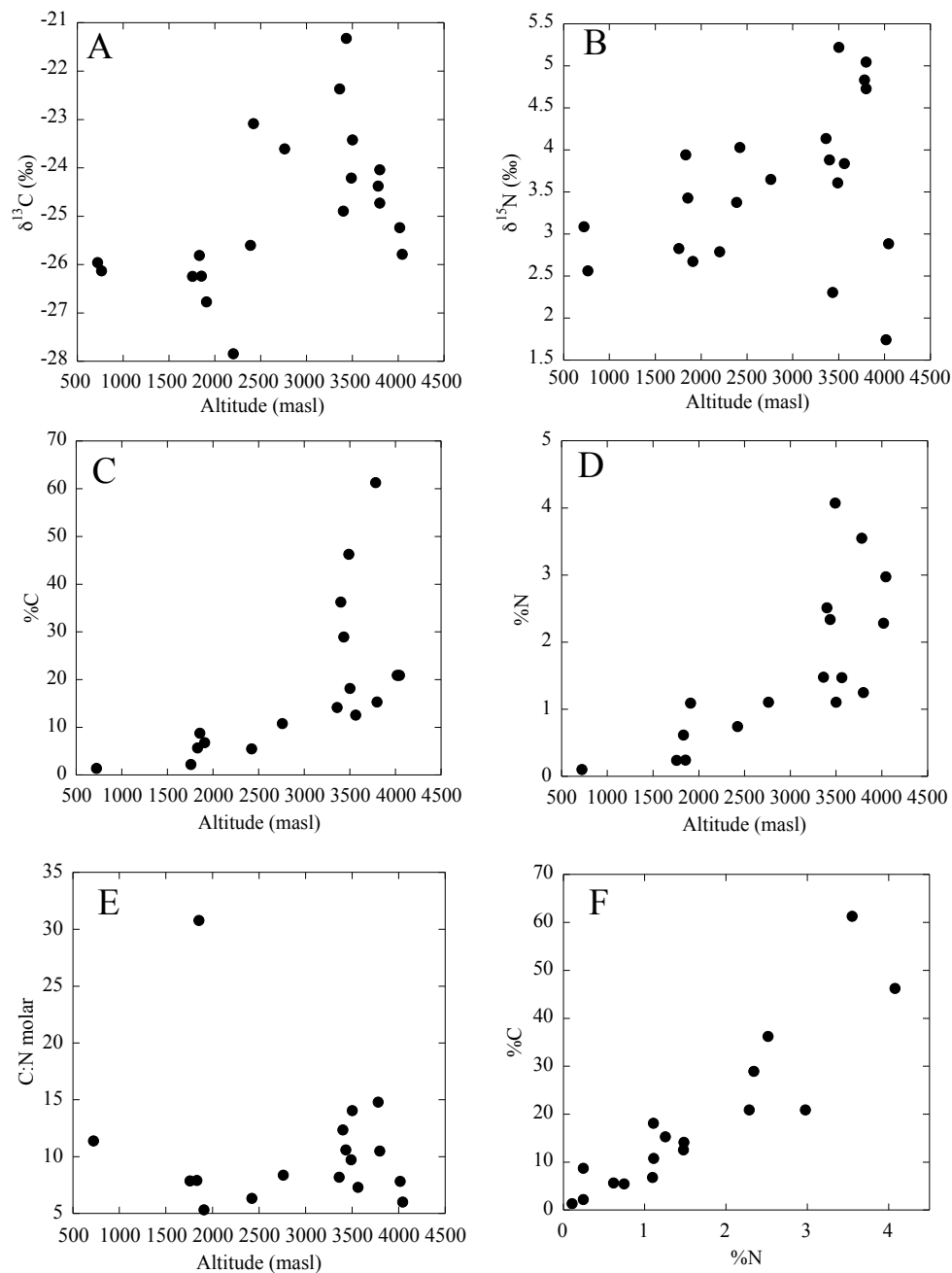


Figure 2.4. Elevational trends of A)  $\delta^{13}\text{C}$ , B)  $\delta^{15}\text{N}$ , C) %C, D) %N and E) molar C:N of fine POM ( $> 0.2 \mu\text{m}$ ,  $< 60 \mu\text{m}$ ) collected from rivers on glass fiber filters during this study. Weight percent of carbon versus weight percent of nitrogen of fine particulate samples is shown in panel (F).

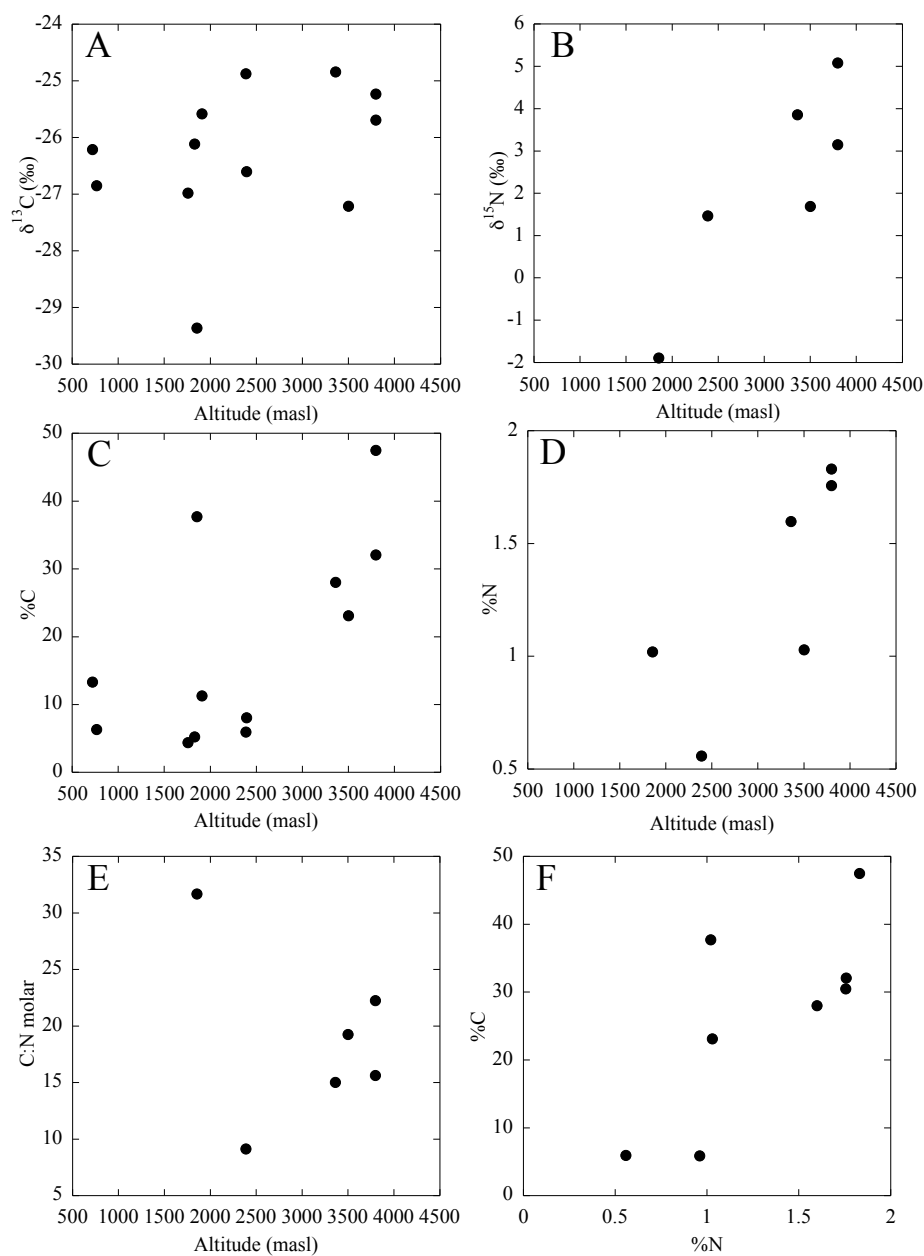


Figure 2.5. Elevational trends of A)  $\delta^{13}\text{C}$ , B)  $\delta^{15}\text{N}$ , C) %C, D) %N and E) molar C:N of coarse POM (> 60  $\mu\text{m}$ ) collected from rivers on nylon filters during this study. Weight percent of carbon versus weight percent of nitrogen of coarse particulate samples is shown in panel (F).

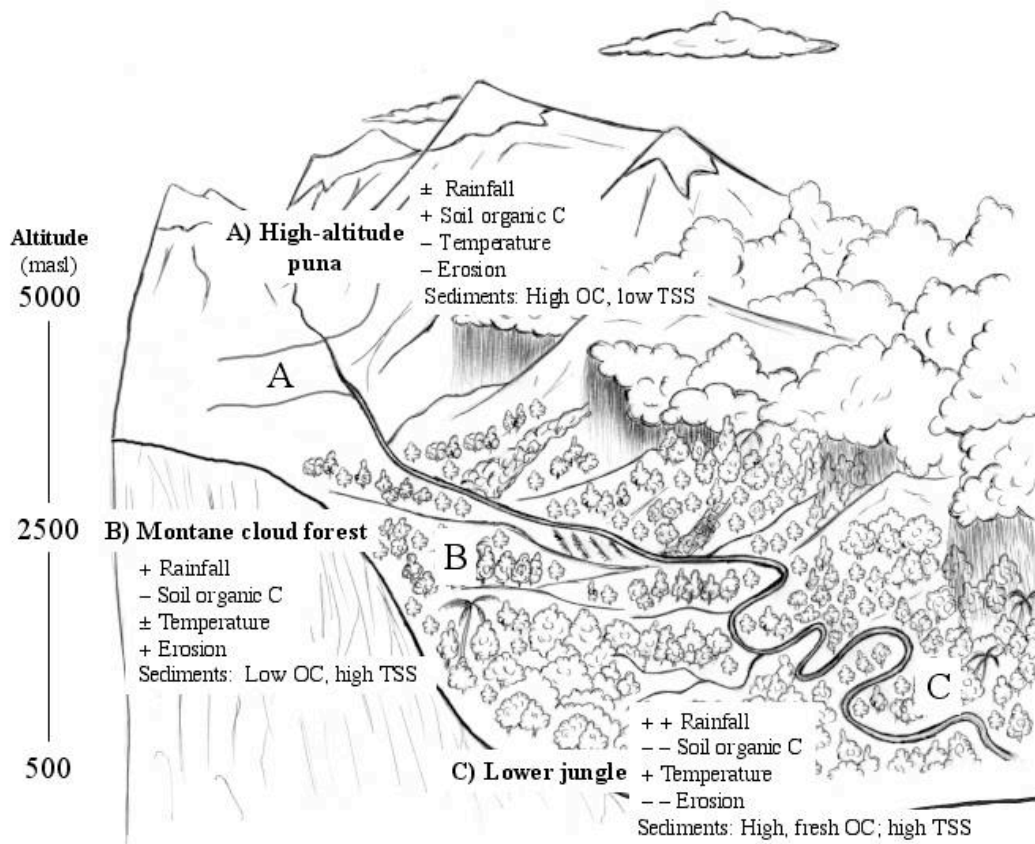


Figure 2.6. Conceptual diagram of organic matter dynamics in the Peruvian Andean Amazon. Three major zones are depicted: A), the high-altitude *puna*, located above the treeline, or from about 3500 to 4500 masl; B), the montane cloud forest, situated between 2000 and 3500 masl; and C), the low jungle, or *selva baja*, which extends from 750 to 2000 masl, approximately.

### **Chapter 3: Stable and radioactive isotopic constraints on organic matter cycling in the Pachitea River Basin, Peruvian Andean Amazon**

#### **ABSTRACT**

Rivers are critical links in the global carbon (C) cycle because they are the main means of transport of terrestrial organic C to the oceans. This study uses stable and radioactive isotopic tracers of organic C and nitrogen (N) cycling to determine the sources of organic matter to Andean rivers and the extent of their preservation and delivery downstream to the Amazon. We measured the  $\delta^{13}\text{C}$ ,  $\delta^{15}\text{N}$ , and  $\Delta^{14}\text{C}$  of organic matter in suspended sediments from the headwaters to below the lowland jungle in the Pozuzo River, a tributary of the Amazon River located in the Peruvian Andes. Particulate organic  $\Delta^{14}\text{C}$  decreases with downstream distance, suggesting that young, fresh organic matter introduced in small headwater streams is respired preferentially in rivers and older, more refractory material persists or is added downriver. Headwaters stream sediments were distinct isotopically from each other and from the mainstem samples, suggesting that differences in land use and other landscape processes in small catchments may impact the concentration and composition of organic C and N in streams. Unlike previous studies, the  $\delta^{13}\text{C}$  of POM was not correlated with altitude, indicating that in-stream processes such as photosynthesis or resuspension of degraded sediments might be more influential during dry conditions. Fine POM was higher in  $\delta^{15}\text{N}$  and  $\delta^{13}\text{C}$  than coarse POM, indicating either greater degradation in the fine fraction or sorption of enriched dissolved organic matter.



## INTRODUCTION

An understanding of carbon (C) cycling in rivers is vital to constraining the global C budget, because rivers are a critical biogeochemical link between the land and the oceans. Processes operating at the headwaters of rivers can influence water and element cycling downstream and at the mouths of rivers (e.g., Vannote et al. 1980, Peterson et al. 2001). The Peruvian Andes are a major source of water and sediments to the Amazon River, which is the largest single source of fresh water and terrestrial organic C to the oceans (Gibbs 1967, Sioli 1984). For many years, researchers have estimated that Andean rivers may provide a significant portion of organic C to the Amazon (Richey et al. 1990, Quay et al. 1992, Hedges et al. 1994, 2000), although very few studies have examined this hypothesis (McClain et al. 1995). Previous studies conducted in the Andes have concluded that the Andean headwaters may contribute about 35% of total particulate OC (POC) observed in the Amazon (Hedges et al. 2000, Chapter 2, this volume), but other studies have shown that the Andean C may not persist beyond the Andean foreland (Mayorga et al. 2005).

This study combines radioactive and stable isotopic tracers in order to determine sources and processing of organic C in rivers of the Peruvian Amazon. There are three natural C isotopes:  $^{12}\text{C}$  and  $^{13}\text{C}$  are both stable, and  $^{14}\text{C}$  is a cosmogenic radionuclide and decays with a half-life of 5370 years. Carbon-12 makes up the bulk of all C atoms on Earth, with  $^{13}\text{C}$  and  $^{14}\text{C}$  accounting for 1.11% and  $1 \times 10^{-10}\%$ , respectively (Faure 1986). Carbon-13 content (as  $\delta^{13}\text{C}$ ) is a useful tracer of organic C sources and diagenetic history for several reasons. Various photosynthetic pathways and the isotopic composition of inorganic C substrates can lead to differences in stable isotopic composition among terrestrial plants, aquatic plants and algae (Peterson and Fry 1987, Fogel and Cifuentes

1993). Also,  $\delta^{13}\text{C}$  signatures decrease during the process of degradation from fresh plants to leaf litter to soils (Wedin et al. 1995).

Radiocarbon, or  $^{14}\text{C}$ , is useful as a tracer of organic C (OC) sources in river basins as well as a dating tool (Hedges et al. 1986, Masiello and Druffel 2001, Raymond and Bauer 2001, Druffel et al. 2005). The atmospheric content of  $^{14}\text{C}$  increased during the middle of the 20<sup>th</sup> century due to above-ground nuclear weapons testing, and any fraction containing this so-called “bomb” radiocarbon is now defined as modern, or generated after 1950 (Stuiver and Polach 1977). Only a few studies have used radiocarbon as a tracer of organic matter cycling in the Amazon Basin. The  $\Delta^{14}\text{C}$  of dissolved and particulate OC was measured at several points along the Brazilian Amazon as part of the “Carbon in the Amazon River Experiment” (CAMREX) project (Hedges et al. 1986b). Their results showed a consistent offset in chemical composition of various size classes of organic matter, indicating their different sources and diagenetic histories, in line with other CAMREX tracers (Hedges et al. 1986b). All  $\Delta^{14}\text{C}$  values were positive, indicating that they contained “bomb”  $^{14}\text{C}$ . Most pertinent to the current study are the  $\Delta^{14}\text{C}$  values for fine (+19‰) and coarse (+227‰) particulate organic matter (POM) measured at Santo Antônio do Içá (Hedges et al. 1986b). This coarse POM (CPOM) sample was almost identical in  $^{14}\text{C}$  content to atmospheric  $\text{CO}_2$  at the time of sampling (234‰), indicating that it was derived from fresh terrestrial plant material. Fine POM (FPOM), the oldest fraction sampled, was considered to be derived from degraded terrestrial soils (Hedges et al. 1986b). The dissolved fractions (humic and fulvic acids) sampled in this study were also modern, and considerably younger than the fine POM, ranging from +141 to +344‰ (Hedges et al. 1986b).

The Hedges et al. (1986b) effort was the first to report radiocarbon abundances for Amazonian organic matter. Subsequent studies reported the chemical composition of

organic matter emerging from the Amazon into the Atlantic Ocean, a few of which included radiocarbon dates. Raymond and Bauer (2001) reported DOC and POC  $\Delta^{14}\text{C}$  for the Amazon mouth and several other rivers discharging into the Atlantic. As in the Hedges et al. (1986b) study, DOC was considerably younger than POC, but both fractions were older (28‰ and -145‰, for DOC and POC, respectively) than in the Hedges et al. (1986b) study (Raymond and Bauer 2001). The advanced age of the POC fraction was attributed in part to weathering of old sedimentary carbon in the Andean headwaters. A similar study of the Amazon mouth attributed the advanced age of the POC (with respect to the CAMREX results from the central Amazon) to a mixture of resuspended shelf sediments and POC from the river itself (Druffel et al. 2005). However, the CAMREX data represent a flux-weighted average of POC composition over several years in the inner Amazon, whereas both the Raymond and Bauer (2001) and Druffel et al. (2005) studies reported data for samples taken at a single time at the Amazon mouth during baseflow. Younger material may be transported more during high flow conditions when runoff and sediment load are greatest, whereas more aged or Andean carbon may be transported during baseflow. Radiocarbon content (as  $\Delta^{14}\text{C}$ ) of Amazonian soils decreases with depth from a maximum of about +150‰ in the organic layer to as low as about -750‰ in the lowest horizons (Telles et al. 2003), and upper soil horizons might be preferentially transported in runoff.

Recently, both radioactive and stable C isotopic composition of dissolved  $\text{CO}_2$  gas, DOC, and coarse and fine POC were studied in rivers throughout the Amazon basin, including some Andean headwaters (Mayorga et al. 2005). The  $\delta^{13}\text{C}$  of  $\text{CO}_2$  indicated that the youngest organic matter was preferentially respired, while the OM transported downstream can range in age from tens to thousands of years, in contrast to previous results (Hedges et al. 1986b). The  $\Delta^{14}\text{C}$  of  $\text{CO}_2$  increased and the  $\delta^{13}\text{C}$  of  $\text{CO}_2$  decreased

from the Peruvian Andes to the mainstem Amazon, indicating that dissolution of carbonate minerals and solid earth degassing are major sources of dissolved CO<sub>2</sub> in Andean rivers. The authors also suggest that the observed high CO<sub>2</sub> fluxes from Andean and Amazonian rivers indicate that little, if any, OC is transported from the Andes to the mainstem Amazon, although only a few samples were taken at high altitudes.

The Pachitea Basin is an excellent location to study carbon dynamics in riverine sediments because it encompasses such a wide range of ecotones, as was described in Chapter 2 of this dissertation. The Pachitea extends from the high-altitude *puna* ecosystems above 3500 meters above sea level (masl). This region has low sediment loading but high OC transfer from the landscape to rivers. From the *puna* the Pachitea headwaters descend through the Andean cloudforest, which is a region of both high sediment and terrestrial OC transfer due to rapid erosion rates, high rainfall, and frequent landslides. Finally, the lower parts of the basin are more traditional Amazonian jungles, which have less sediment and OC transfer to rivers due to decreased topography and lower soil OC content.

The main objectives of this study are to trace the relationship between soils and suspended particulates in rivers in the Peruvian Andean Amazon using stable and radioactive isotopes, and to provide information on in-stream processing of these materials. To address these issues, we studied the Pozuzo River basin, sampling from the high basin at about 2500 meters above sea level (masl) to the base of the Andes at 350 masl. These samples cover the cloudforest and jungle ecotones of the Pachitea Basin.

## **MATERIALS AND METHODS**

*Site description* – Samples were collected during July and August of 2004. Three headwater streams were sampled near their sources: the Río Esperanza, the Río Chontabamba, and the Río Llamaquizú (Figure 3.1). Several mainstem samples were

also taken, continuing down the Chorobamba/Huancabamba/Pozuzo River basin to Codo de Pozuzo, the “elbow” of the river, located at about 350 meters above sea level and below the high relief of the Andes. A total of nine sites were sampled (Figure 3.1). It is important to note that while the previous study (Chapter 2, this volume) started above the treeline in the Andean *puna*, this study starts below 3000 meters, well below the treeline in the Andean cloudforest. Altitudes and geographic coordinates at each site were determined using a hand-held global positioning system (GPS). Distance upstream from Iquitos (where the river begins to be called the Amazon) was determined using Arc View Geographic Information Systems software.

*Sample collection* – Water and suspended particulates were collected from each site. Water samples from Andean rivers were collected along the side of the river or stream. Whole water samples from these rivers were collected in site-rinsed 1-liter polyethylene bottles and filtered on site. Suspended sediments for  $\delta^{13}\text{C}$  analysis were first filtered through pre-weighed 60  $\mu\text{m}$  nylon net filters (Millipore Corporation) to retain coarse particulates and then through pre-weighed, pre-combusted 0.7  $\mu\text{m}$  glass fiber filters (Whatman GF/F) to retain fine particulates. Bulk suspended sediments for  $\Delta^{14}\text{C}$  analysis were collected on pre-weighed, pre-combusted quartz fiber filters (Whatman QMA), with an approximate pore size of 1  $\mu\text{m}$ . All filters were kept in tight-fitting Petri dishes and sealed on the outside with tape. Water samples were filtered in the field through 0.2  $\mu\text{m}$  nylon syringe filters into pre-combusted glass vials with Teflon lined lids, which were pre-cleaned and amended with 1  $\mu\text{l/ml}$  sample of  $\text{H}_2\text{SO}_4$ . Soil samples were taken from surface horizons near the banks of the rivers at the sampling sites. They were placed in combusted borosilicate vials and sealed tightly. All samples were kept cool or frozen until return to the field station in Oxapampa. There, water samples were refrigerated and soils and filters were dried at 40°C for 48 hours, then

stored in plastic Petri dishes in sealed Ziploc bags until analysis in the United States. All samples were handled carefully to minimize contamination.

*Sample Analysis* – All  $^{14}\text{C}$  samples were analyzed at the National Ocean Sciences Accelerator Mass Spectrometer Facility at the Woods Hole Oceanographic Institute. Inorganic C was removed from filter and soil samples prior to  $^{14}\text{C}$  analysis by vapor phase acidification with HCl. Nine suspended sediment samples and two soil samples were analyzed for  $^{14}\text{C}$  content. Radiocarbon content is reported here as both  $\Delta^{14}\text{C}$  and radiocarbon age, both as defined by Stuiver and Polach (1977).

Filters were analyzed for  $\delta^{13}\text{C}$  and  $\delta^{15}\text{N}$  of organic matter on a Carlo Erba NC 1500 elemental analyzer coupled to a Finnigan MAT DELTA plus continuous-flow isotope ratio mass spectrometer at the University of Texas Marine Science Institute. Carbonates were removed from soils and sediments prior to  $\delta^{13}\text{C}$  analysis by vapor-phase acidification with HCl for 24 hours, followed by drying at  $60^\circ\text{C}$  for 24 hours. Particulates on glass fiber filters were analyzed directly on the mass spectrometer; coarse particulates were first washed onto glass fiber filters. Isotopes and weight percent of OC and N were calibrated against a chitin standard. Stable isotopic ratios of OC and N are presented in delta notation versus the VPDB and air standards, respectively.

Dissolved organic carbon concentrations were determined by analysis on a Shimadzu Vcsh TOC analyzer. Carbon stable isotopic composition of dissolved organic matter was analyzed on the elemental analyzer – mass spectrometer according to the method of Gandhi et al. (2004).

## **RESULTS**

Physical parameters and radiocarbon content of various organic matter fractions are presented in Table 3.1. The three headwaters (Llamaquizú, Esperanza, and Chontabamba) have the youngest suspended POM. The one soil sample for which  $\Delta^{14}\text{C}$

was determined in the headwaters (Río Llamaquizú, 49‰) was also very young. Another soil sample taken in the middle of the altitudinal gradient in this study was even younger (Río Huancabamba,  $\Delta^{14}\text{C} = 68\%$ ). The radiocarbon content of bulk suspended sediments decreased downstream ( $r^2 = 0.6045$ ,  $n = 8$ ) (Figure 3.2). In the upper basin, riparian soils were more enriched in  $^{14}\text{C}$  (i.e., younger) than river sediments taken from the same locations. Downstream near the bottom of the Andes, however, riparian soils were older than suspended sediments in rivers (Figure 3.3), although there is only one sample from this region.

Stable isotopic compositions of C and N within various size classes of riverine organic matter are presented in Table 3.2. In contrast to previous studies (Chapter 2, this volume; Mayorga et al. 2005, Cai et al. 1988), we observed no trend of increasing  $\delta^{13}\text{C}$  of organic matter at high altitudes/upstream (Figure 3.4). In fact, FPOM and CPOM showed a slight increase in  $\delta^{13}\text{C}$  downstream, a trend driven by a few points in the uppermost basin. No trend in  $\delta^{13}\text{C}$  of DOC was observed with downstream distance. Nitrogen stable isotopic composition of both FPOM and CPOM were consistent throughout the study area (Figure 3.5). The  $\delta^{15}\text{N}$  of CPOM increased slightly with downstream distance, but there was no relationship between  $\delta^{15}\text{N}$  of FPOM and downstream distance (Figure 3.5). Consistent with previous studies (Townsend-Small et al. 2005), the  $\delta^{15}\text{N}$  and  $\delta^{13}\text{C}$  of FPOM were higher than that of CPOM. Fine POM was on average 0.6‰ more enriched in  $^{15}\text{N}$  and 1.0‰ more enriched in  $^{13}\text{C}$  than CPOM (Table 3.2).

The concentrations of OC and N in various size classes in this study are presented in Table 3.3. The concentration of DOC decreased downstream (Figure 3.6). On the other hand, FPOC and CPOC concentrations both increased as the river traveled downstream. Concentration of FPON also increased downstream, but the concentration

of CPON was not correlated with downstream distance (Figure 3.7). For reference, the weight percents of C and N in fine and coarse sediments are shown in Table 3.4. The weight % of C in fine sediments decreased downstream, while no trend of %C of coarse sediments with downstream distance was observed. The weight % of N in fine sediments decreased downstream, as did the %N of coarse sediments. These trends in weight percent of C and N in suspended sediments are similar to those observed previously (Chapter 2, this volume).

## DISCUSSION

My results indicate that the Andean cloudforests are a source of young, fresh particulate organic matter (high  $\Delta^{14}\text{C}$ , low  $\delta^{13}\text{C}$ ) to streams in the upper basin, but that this fresh POM is either replaced or remineralized in rivers in the lower basin where suspended POM is older and more degraded. There was a clear trend of aging organic matter as rivers travel downstream (Figure 3.2). Two explanations could account for this trend. The first possibility is that the youngest fraction of POM introduced to rivers in the Andean headwaters is remineralized rapidly and released as  $\text{CO}_2$ , leaving behind older, more recalcitrant C as the rivers move downstream (e.g., Mayorga et al. 2005). The other possibility is that POM becomes older as rivers travel downstream not because of biological activity in the river, but because of temporary sequestration of sediments along riverbanks. In fact, both processes are at work in all major rivers, which act as integrators of their watersheds, and where organic carbon is a mixture of upstream and local inputs that are subject to transport and reactive processes (Richey et al. 1991). The data presented in this chapter can help to determine the relative importance of these processes in the Amazon headwaters.

One interpretation of the results of this study is that young, fresh POM introduced in Andean headwaters is rapidly oxidized and respired, and that the older, more refractory



portion of POM persists downstream. In general, tropical rivers, including the Amazon, have high aquatic respiration rates supported by large inputs of terrestrial organic carbon. A study of the  $\delta^{18}\text{O}$  of dissolved oxygen indicated that the ratio of community respiration to gross photosynthesis (R:P) in Amazonian rivers ranges from 1.5 to 4 (Quay et al. 1995). Amazonian rivers and wetlands are also a large source of  $\text{CO}_2$  to the atmosphere due to respiration of organic C transported from upstream (Richey et al. 2002). Studies in tropical rivers in Puerto Rico also showed that respiration (R) was greater than photosynthesis (P) overall, and that both R and P increased from headwaters to mainstems (Ortiz-Zayas et al. 2005). Temperate rivers also have high respiration rates: studies in the Hudson River basin of New York, USA indicated that even ancient terrestrial organic carbon can be respired in rivers over very short time scales (Cole and Caraco 2001). This study did not include measurements of  $\Delta^{14}\text{C}$  of  $\text{CO}_2$  or respiration rate, but it is likely that at least some portion of POM in Andean Amazon rivers is consumed and respired as  $\text{CO}_2$ . However, because the concentration of suspended C and N remains the same as Andean rivers travel downstream, the young signature of POC in the headwaters may be dampened downstream by local erosion or resuspension of older materials.

The observed patterns in  $\Delta^{14}\text{C}$  and  $\delta^{13}\text{C}$  of POM in this study may be caused by the dilution of POM from the headwaters with older, more degraded material from local inputs downstream. Previous work (Chapter 2, this volume) showed that (1) POM in the Andean headwaters is composed mostly of OM-rich, minimally degraded surface soils, (2) that degraded OM, possibly associated with mineral soils, becomes a more important source of POM to rivers in the mid-Andes, and (3) gentler topography in the Andean foothills leads to a significant surface soil POM input. Young, but degraded, surface soils may be the main source of POM to the cloudforest headwaters of the Andes.

Downstream of the headwaters, the POM may be a mixture of upstream inputs and resuspended soils or floodplain sediments. Small headwaters, such as the ones sampled in this study, are coupled tightly to the landscape, so steady state POM composition resembles organic soils and plants, whereas in larger rivers OM composition is a balance between erosion of mineral soils and upstream sources, with some hydrodynamic sorting and in-stream processing. The dominance of soil erosion over leaf litter inputs has led to older POM in the Piracicaba River basin of Brazil than in the Amazon (Krusche et al. 2002). The sample taken at Codo de Pozuzo, located just below the Andean Cordillera, illustrates this trend. While this POM sample is the oldest observed in this study ( $-99\text{‰}$ , or 785 years old), the sediment sample collected from the riverbank is significantly older ( $-159\text{‰}$ , or 1320 years old). This sediment sample was collected from the floodplain area, so it may consist of river sediment deposited during the previous wet seasons up to 1000 years ago (Table 3.1) during flood stage and then aged in place.

The partitioning of POM sources can be estimated in the study river using an average  $^{14}\text{C}$  value for the headwater streams sampled in this study. A mass balance calculation using  $\Delta^{14}\text{C}$  indicates that 49% of suspended sediments in high-order Andean rivers (such as the Rio Pozuzo in this study, which had an average  $\Delta^{14}\text{C}$  of  $-72\text{‰}$ ) are derived from the headwaters (average  $\Delta^{14}\text{C} = 17.4\text{‰}$ ), and 51% from local soils or sediment resuspension (measured at  $-159\text{‰}$  at Codo de Pozuzo) (Figure 3.8). This may underestimate the amount of C that is conservatively transported from the headwaters, as sequestered sediments along the river may be younger than those observed at Codo de Pozuzo below the topography of the Andes. The validity of this mass balance would be improved by additional analyses, but the current information provides an initial constraint on the C budget of the system. This result has important implications for global C cycling, especially if these results are representative of other Andean rivers and POC in

rivers exiting the Andes is aged and recalcitrant. As much as 50% of these sediments in Andean rivers are sequestered in the Andean foreland (Aalto et al. 2003). If the Amazon headwaters are a source of refractory POC to the mainstem and eventually the ocean, it is likely that this POC is buried rather than remineralized to CO<sub>2</sub>.

In the mainstem Amazon in Brazil, the floodplain alternates between being a sediment and OM source and being a holding tank for these materials, depending on river stage (Junk 1985, Meade et al. 1985). Resuspension of floodplain particulates in rivers is a source of labile organic matter to the Amazon, and this fraction is oxidized rapidly in the river (Richey et al. 1991). In the lower Amazon, sediment deposition on the floodplain and sand bars is about 30% greater than local inputs due to erosion (Dunne et al. 1998), because the majority of suspended sediments in the Amazon are derived from upstream in the Andes (Gibbs 1967). However, the balance between erosion and sedimentation in organic matter cycling is unknown for the Andean headwaters. Because of the steep topography in the Peruvian headwaters, floodplain exchange may be less important than soil erosion in the Andes. This study indicates that there may be some exchange between the riverbanks and the channel itself, which is not surprising as these processes occur in all rivers. This study was conducted during the Amazonian dry season when resuspension is expected to dominate over sedimentation and storage (Meade et al. 1985). However, during low flow periods, heavier sediments (such as sand-sized particles in coarse suspended sediments) are deposited selectively on the streambed and then resuspended during higher flow velocities (Mayorga and Aufdenkampe 2002). In fact, most of the sediments on sand bars and riverbanks in Andean rivers are low-organic content sands (data not shown) not muds like those found on the Amazonian floodplain (Dunne et al. 1998). More studies are needed to determine the extent of sediment aging in Andean “floodplains” or riverbanks. However, the erosive nature of the Andes leads

to the initial assumption that few soils are alluvial in middle and upper Andean rivers. Eventual transport of more recalcitrant material from the Andes to the Amazon can be expected if sediment transport from the landscape to Andean rivers increases due to climate or land use change, especially if this increased sediment load is stored in floodplains and allowed to age.

Some of the oldest suspended POM ( $\sim 800\%$ ) sampled by Mayorga et al. (2005) in the Amazon basin were located high in the Andes Mountains, at much higher altitudes than the sampling sites of the current study, although both studies found that river POM was largely modern, and probably not of geologic origin. A gradient of increasing  $\Delta^{14}\text{C}$  and decreasing  $\delta^{13}\text{C}$  of dissolved  $\text{CO}_2$  and of suspended POM was observed as rivers traveled from the Andean headwaters to the Amazon mainstem (Mayorga et al. 2005). This pattern is exactly opposite of the one shown here for the Pachitea basin. However, the Mayorga et al. (2005) study had more samples than the current one, and included samples from higher altitudes in the Andes. On the other hand, the previous study did not sample the small headwater reaches of the Amazon, where the isotopic composition of POM differs most from previous findings (Mayorga et al. 2005) and from the rest of the samples in the current study. It may be that small headwater streams complicate the downstream trend in  $\Delta^{14}\text{C}$  because suspended POM is unusually fresh, while in general soil and river POM  $\Delta^{14}\text{C}$  increases at lower altitudes in the Amazon. The results from similar rivers and locations (Mayorga et al. 2005) are generally in line with the results of this chapter of the dissertation. Further sampling of headwaters above the Andean treeline is needed to complete the carbon cycling picture for the Pachitea basin, as many of these ecosystems are dominated by old but minimally degraded peats (Chapter 2, this volume).

Further information can be gleaned from a dual carbon isotope ( $^{13}\text{C}$  and  $^{14}\text{C}$ ) plot (Figure 3.8). The headwaters are isotopically distinct from each other and from the downstream samples, whereas the downstream waters are more homogeneous. This observation supports the idea that initial fresh, young OC is rapidly mineralized in streams while some older, more refractory component is transported downstream. The other possibility is that sediments are continually deposited and resuspended as they travel downstream, explaining the advanced age of samples taken at lower altitudes. This plot also shows that POM composition in headwater streams is more variable than in mainstems. The Mayorga et al. (2005) study concluded that very little, if any OC from the Andes is transported to the lower Amazon. The data presented here seem to indicate the opposite: the consistency of  $\Delta^{14}\text{C}$ ,  $\delta^{13}\text{C}$ , and concentration of POC along the mainstem of the Pozuzo River indicates that POC is transported somewhat conservatively in the larger rivers of the Andes, although the fate of this material in the Amazonian floodplain remains unknown.

One important difference between the results of this study and those of Chapter 2 (this volume) is that the  $^{13}\text{C}$  content of suspended sediments did not increase at high altitude (Figure 3.9). In fact, in 2004 the  $\delta^{13}\text{C}$  of both fine and coarse suspended sediments is lowest at the highest altitudes, while in 2002  $\delta^{13}\text{C}$  of both fractions increases with altitude. The average  $\delta^{13}\text{C}$  of FPOM for 2002 ( $-25.7\text{‰}$ ) was significantly lower than in 2004 ( $-24.5\text{‰}$ ;  $p = 0.06$ ), although there was no difference in the coarse fractions between years. Despite the sharp differences between  $\delta^{13}\text{C}$ , no difference in weight % of OC in either CPOM or FPOM was observed for the two years. One possible explanation for this result is that this study did not sample as high in the basin as the previous study, so that there may not be sufficient resolution to observe the same trend. Secondly, a high concentration of algae and/or phytoplankton in rivers could confound the terrestrial plant

signal. Little evidence of in-stream primary production has been found in previous studies of Andean rivers (Chapter 2, this volume; Cai et al. 1988), and light availability is thought to be too low to support photosynthesis in most Amazonian streams and rivers (McClain and Elsenbeer 2004). Phytoplankton in Andean rivers should have a  $\delta^{13}\text{C}$  from  $-33\text{‰}$  to  $-55\text{‰}$  (Cai et al. 1988). The  $\Delta^{14}\text{C}$  of algae is based on the  $^{14}\text{C}$  content of dissolved inorganic C and is therefore unknown at this point. Even a small increase in the algal contribution to POM could affect the  $^{13}\text{C}$  content of sediments overall. Interannual variation in climate may also affect the sediment composition in these rivers. The 2004 sampling period was much drier than in 2002, which may mean that more mineral soils were delivered to rivers as POM in 2002 as compared to 2004.

There is a consistent offset of  $\delta^{13}\text{C}$  and  $\delta^{15}\text{N}$  of FPOM and CPOM collected in this study, with FPOM enriched over CPOM (Figures 3.4 and 3.5). Previous studies have explained this enrichment either as a product of the higher degree of degradation of FPOM (Chapter 2, this volume; Hedges et al. 1986a, 2000), or as a product of sorption of enriched DOM to minerals (Aufdenkampe et al. 2001). With respect to sorption, in this study, the  $\delta^{13}\text{C}$  of DOM is not consistently enriched as compared to FPOM or CPOM, implying that another process may influence either the isotopic composition of sorbed DOM or the effects of sorption of that DOM to sediments, for example, if  $^{15}\text{N}$ -enriched DOM is preferentially sorbed. The trends in  $\delta^{15}\text{N}$  of FPOM and CPOM are different from those of  $\delta^{13}\text{C}$  (Figures 3.4 and 3.5). For  $\delta^{15}\text{N}$ , there is a consistent enrichment of FPOM over CPOM, but the patterns of  $\delta^{13}\text{C}$  for all the OM fractions do not indicate that sorption of DOM is responsible for the isotopic composition of FPOM. Clearly, the processes that control the  $^{15}\text{N}$  content of suspended sediments in these rivers are not the same as those that control the  $^{13}\text{C}$  content. Previous studies (Aufdenkampe et al. 2001, Hedges et al. 2000) have posited that sorption of N-rich DOM to minerals is the dominant

source of FPOM in the Amazon. This finding may explain why the  $\delta^{15}\text{N}$  of particles in this study does not vary with  $\delta^{13}\text{C}$ . However, the weight percents of organic C and N in FPOM samples from this study are higher than those attributable to sorption, either because of increased surface area of high-altitude weathered sediments (A.K. Aufdenkampe, personal communication; Lilienfein et al. 2004) or because sorption is not the only source of FPOM in Andean rivers. The isotopic composition of DOC from this study suggests the latter hypothesis. There is no clear relationship between the  $\delta^{13}\text{C}$  of DOC and that of either FPOM or CPOM. It appears that DOM cycling happens at a different scale or because of different processes than cycling of POM.

The concentrations of POC are lower in the headwaters than in the mainstem, but DOC concentrations are higher in the headwaters (Figure 3.6). This observation may indicate that POC is not being uniformly broken down into DOC, and that remineralization to  $\text{CO}_2$  or dilution of POC with lowland sediments are dominant processes in these rivers. Dissolved OC may be more labile than POC in Andean rivers, or it may be diluted by groundwater and runoff with lower DOC content in the lower basin. Dissolved OC may also be removed by sorption to suspended minerals. These results reinforce the idea that the rates and scales of POC and DOC cycling are quite different. Inputs of terrestrial OM to rivers in the Amazon basin are driven by rain and storm events (Chapter 2, this volume; Aalto et al., 2003). Perhaps storm events promote higher DOC concentrations in rivers, through increased groundwater flow, and add high concentrations of sediments with a very low percent of organic matter. These questions will be further addressed in Chapter 4 of this dissertation.

## CONCLUSIONS

Organic matter in suspended sediments in the Pachitea Basin exhibits a gradient of decreasing  $\Delta^{14}\text{C}$  as rivers travel down the Andes Mountains, indicating respiration or

other oxidation of younger, less degraded fraction of POM or dilution and replacement of young POM from the headwaters with older, more refractory material at downstream sites. This older material represents a potential source of refractory POC to the Amazon River. Stable isotopic patterns were different from previous observations, indicating significant large-scale controls on POM composition other than altitude or downstream distance. Comparisons with previous studies indicate that variability in climate and river discharge may affect the composition of dissolved and particulate OM in the Andean Amazon. Imminent land use and climate change could therefore have a significant impact on C cycling and transport in the Amazon River. More studies are needed to determine how suspended sediments are deposited, sequestered, and resuspended in Andean rivers, and how such sequestration might influence the lability of POM in Andean ecosystems.



Site	Date	Altitude (masl)	Distance upstream from Iquitos (km)	Latitude	Longitude	$\Delta^{14}\text{C}$ POM (‰) age (yrs)	$\Delta^{14}\text{C}$ soil (‰) age (yrs)	NOSAMS Accession Numbers
Río Llamaquizu	7/23/04	2474	1556	10° 37' 17"	-76° 37' 17"	-24 <i>140</i>	49 <i>mod</i>	OS-49051, OS-48366
Río Esperanza	8/6/04	2270	1551			13 <i>mod</i>		OS-49050
Río Chontabamba	7/24/04	2038	1560	10° 35' 45"	-76° 26' 56"	64 <i>mod</i>		OS-49088
Río Chorobamba	8/17/04	1814	1542	10° 35' 4"	-76° 26' 56"	-55 <i>400</i>		OS-48514
Río Huancabamba	8/14/04	1716	1520	10° 25' 56"	-76° 28' 38"	-45 <i>315</i>	68 <i>mod</i>	OS-48210 OS-49596
Cañon de Huancabamba	8/14/04	1426	1503	10° 16' 56"	-76° 27' 26"	-74 <i>565</i>		OS-49052
Río Pozuzo park edge	8/14/04	928	1488			-55 <i>400</i>		OS-48513
Pueblo de Pozuzo	8/8/04	802	1475	10° 4' 19"	-76° 27' 3"			
Codo de Pozuzo	8/7/04	355	1419	9° 34' 28"	-76° 34' 22"	-99 <i>785</i>	-157 <i>1320</i>	OS-48810, OS-48367

Table 3.1. Site names, sampling dates, locations, and radiocarbon content of soils and plants collected during this study. Radiocarbon content is presented as  $\Delta^{14}\text{C}$  (in ‰) and below, in italics, as age in radiocarbon years (both as defined in Stuiver and Polach 1977). *mod* = modern (or formed after 1950). Also included are the reference numbers assigned to each sample from NOSAMS.

<b>Site</b>	<b><math>\delta^{13}\text{C}</math> DOC (‰)</b>	<b><math>\delta^{13}\text{C}</math> FPOM (‰)</b>	<b><math>\delta^{13}\text{C}</math> CPOM (‰)</b>	<b><math>\delta^{15}\text{N}</math> FPOM (‰)</b>	<b><math>\delta^{15}\text{N}</math> CPOM (‰)</b>
Río Llamaquizu	-27.6	-27.6	-27.7	2.4	0.5
Río Esperanza	-26.6	-25.4	-26.8	1.8	3.2
Río Chontabamba	-27.6	-23.9	-25.8	1.8	0.6
Río Chorobamba	-24.8	-24.1	-25.6	3.2	1.0
Río Huancabamba	-25.9	-23.9	-24.4	3.6	2.3
Cañon de Huancabamba	-23.8	-23.8	-24.5	3.1	1.7
Río Pozuzo park edge	-28.0	-23.6	-24.6	2.6	3.8
Pueblo de Pozuzo	-23.6	-23.8		2.0	1.9
Codo de Pozuzo	-26.7	-24.4	-25.1	2.2	1.9

Table 3.2. Stable isotopic composition ( $\delta^{13}\text{C}$  and  $\delta^{15}\text{N}$ ) of various organic matter components sampled in this study.

<b>Site</b>	<b>DOC (µg/L)</b>	<b>FPOC (µg/L)</b>	<b>CPOC (µg/L)</b>	<b>FPON (µg/L)</b>	<b>CPON (µg/L)</b>
Río Llamaquizu	2928	180.9	15.6	12.2	3.0
Río Esperanza	1976	131.9	52.3	14.7	5.5
Río Chontabamba	4591	114.5	16.2	11.7	6.2
Río Chorobamba	2989	34.0	87.1	4.2	18.3
Río Huancabamba	1951	325.5	138.5	41.9	8.3
Cañon de Huancabamba	2123	243.5	84.6	35.8	8.6
Río Pozuzo park edge	1788	285.9	85.0	42.3	8.2
Pueblo de Pozuzo	2519	399.8		59.2	16.5
Codo de Pozuzo	1647	250.4	86.8	43.7	6.2

Table 3.3. Concentration of organic C and N (µg/L) in various size classes of organic matter sampled in this study.

<b>Site</b>	<b>%C FSS</b>	<b>%C CSS</b>	<b>%N FSS</b>	<b>%N CSS</b>
Río Llamaquizu	9.1	4.4	0.6	0.9
Río Esperanza	7.7	9.6	0.9	1.0
Río Chontabamba	18.5	7.8	1.9	3.0
Río Chorobamba	9.1	8.5	1.1	1.8
Río Huancabamba	7.3	10.5	0.9	0.6
Cañon de Huancabamba	7.2	8.4	1.1	0.9
Río Pozuzo park edge	5.3	8.4	0.8	0.8
Pueblo de Pozuzo	4.1		0.6	0.5
Codo de Pozuzo	3.5	7.4	0.6	0.5

Table 3.4. Percent by weight of carbon and nitrogen in fine and coarse suspended sediments (FSS and CSS) sampled during this study.

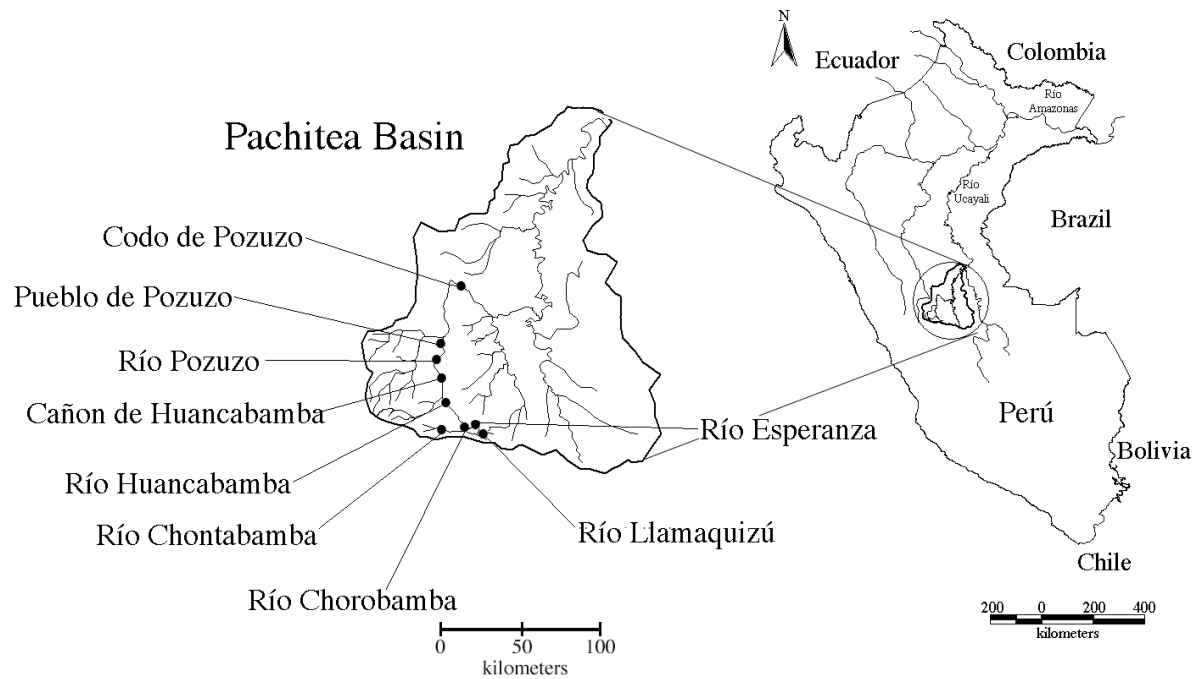


Figure 3.1. Map of the Pachitea River watershed with sampling points for summer 2004 labeled on left. Position of the watershed within Peru and the western Amazon is shown on right.

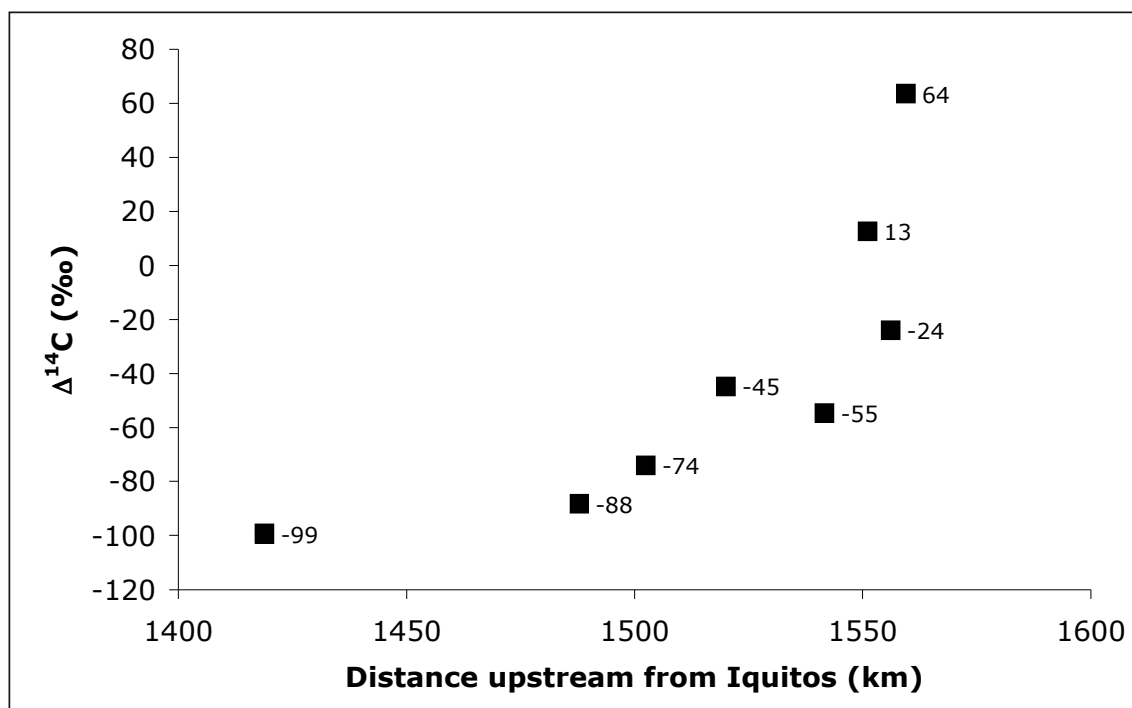


Figure 3.2. Radiocarbon content (as  $\Delta^{14}\text{C}$ ) of suspended POM samples in this study presented versus distance upstream from Iquitos (in kilometers). Individual  $\Delta^{14}\text{C}$  values are shown. Corresponding altitudes of each sampling site are shown in Table 3.1.

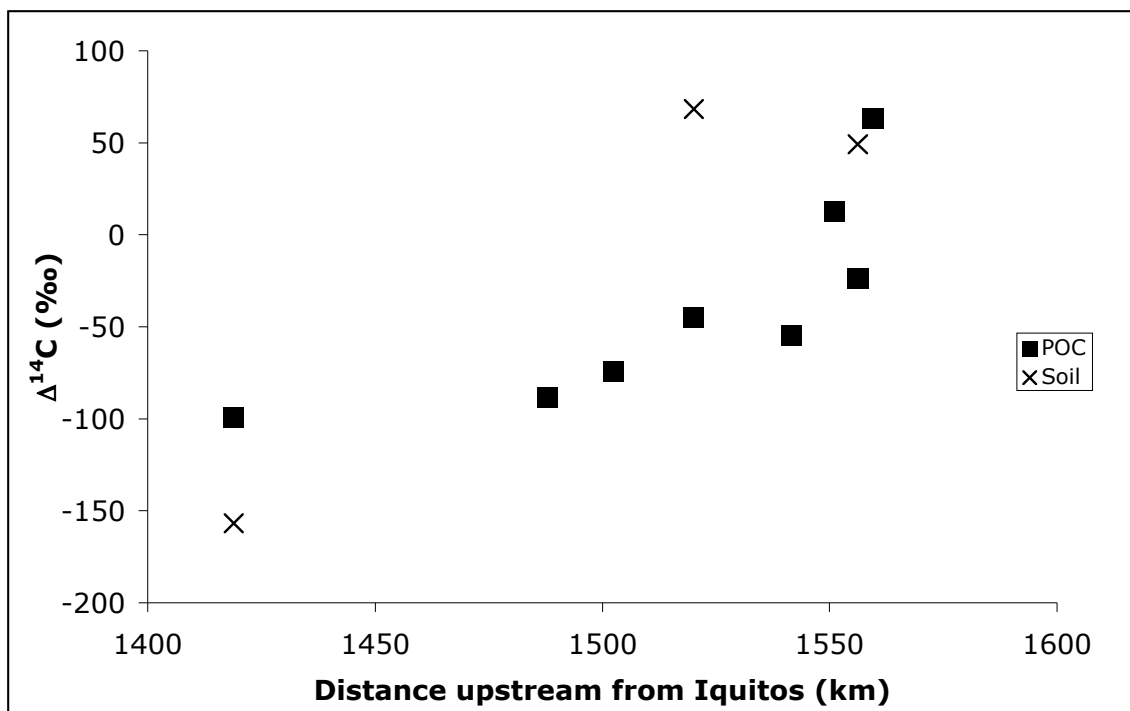


Figure 3.3.  $\Delta^{14}\text{C}$  (in ‰) of suspended POM and riparian soils collected in this study, presented versus distance upstream from Iquitos.

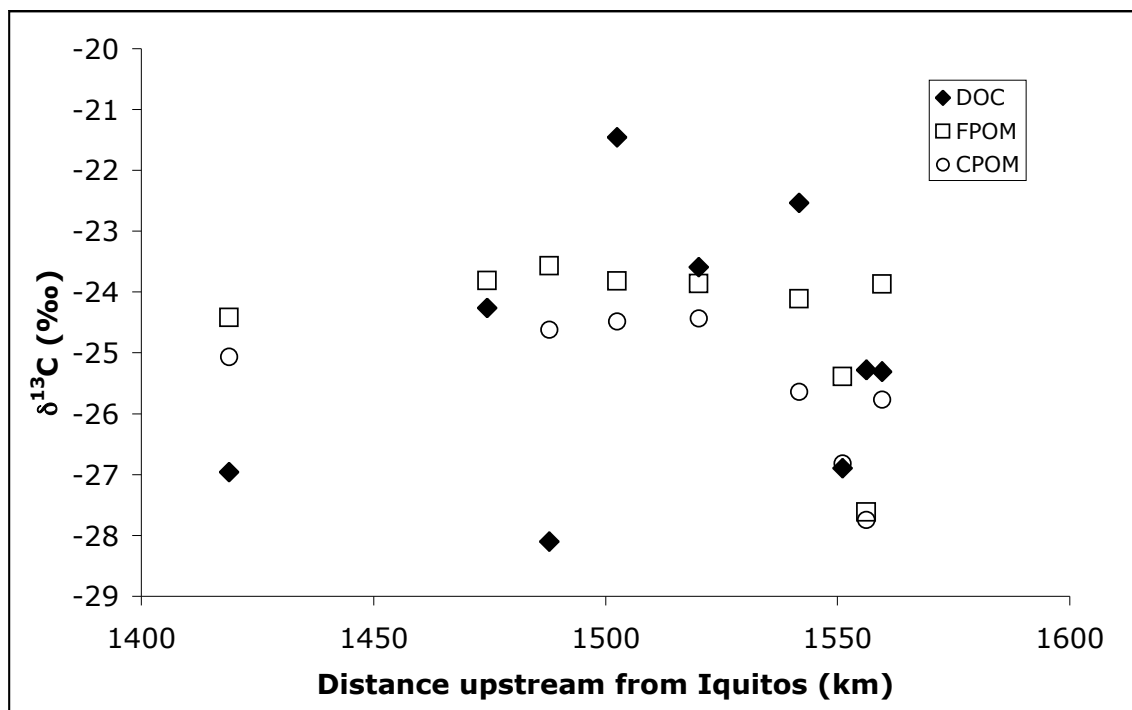


Figure 3.4. Carbon stable isotopic composition of various size classes of riverine organic matter collected during this study. DOC = dissolved organic carbon ( $< 0.2 \mu\text{m}$ ); FPOM = fine particulate organic matter ( $> 0.7 \mu\text{m}$ ,  $< 60 \mu\text{m}$ ); CPOM = coarse particulate organic matter ( $> 60 \mu\text{m}$ ).



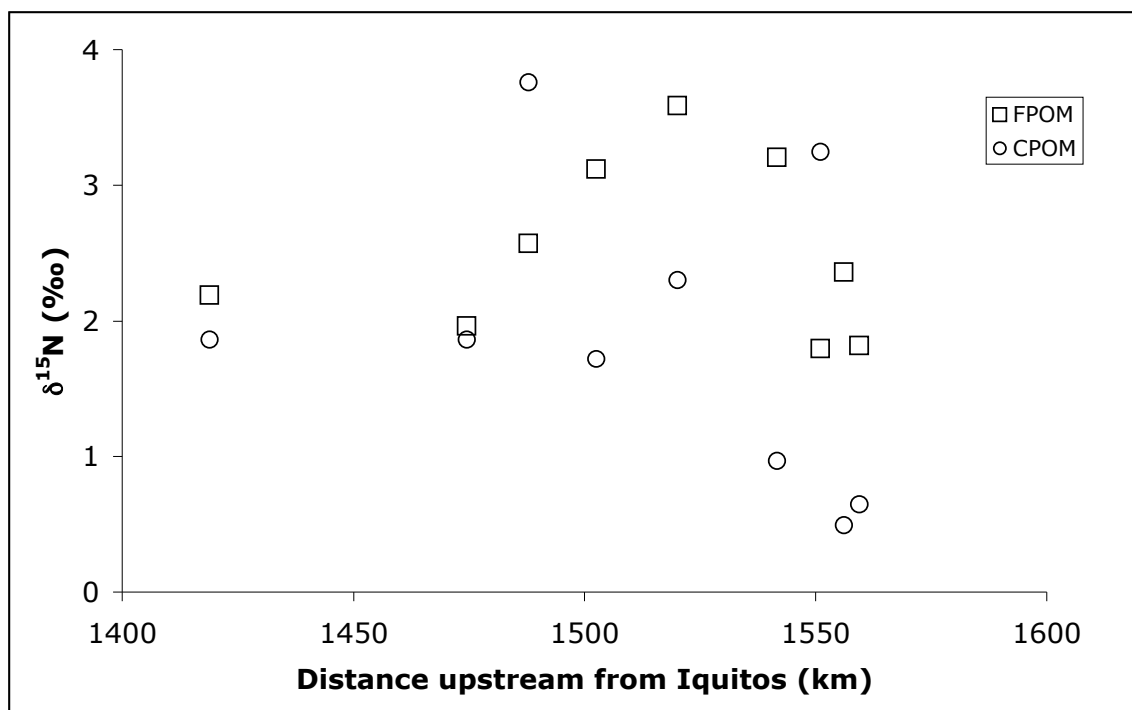


Figure 3.5. Nitrogen stable isotopic composition of fine and coarse particulate organic matter (FPOM and CPOM) sampled during this study. FPOM = fine particulate organic matter ( $> 0.7 \mu\text{m}$ ,  $< 60 \mu\text{m}$ ); CPOM = coarse particulate organic matter ( $> 60 \mu\text{m}$ ).

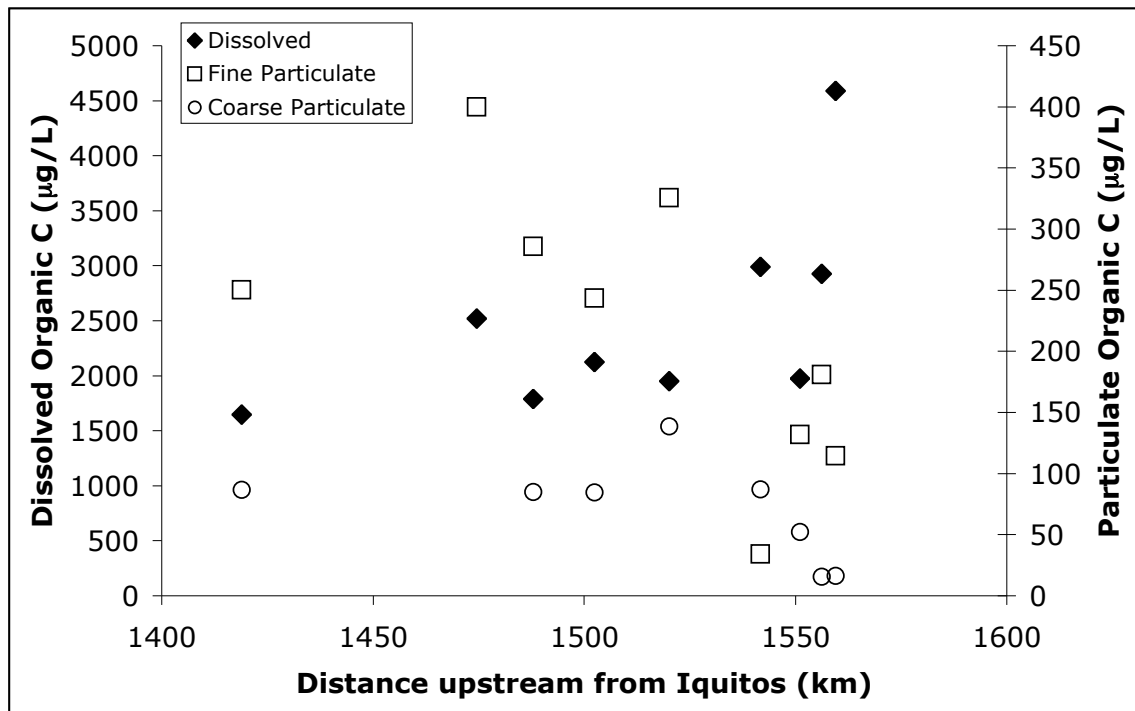


Figure 3.6. Concentrations (in µg/L) of organic carbon in various size classes of river material sampled in this study. Note that the dissolved portion is plotted on a separate axis from the particulate portions. Dissolved: < 0.2 µm; fine: > 0.7 µm, < 60 µm; coarse: > 60 µm.

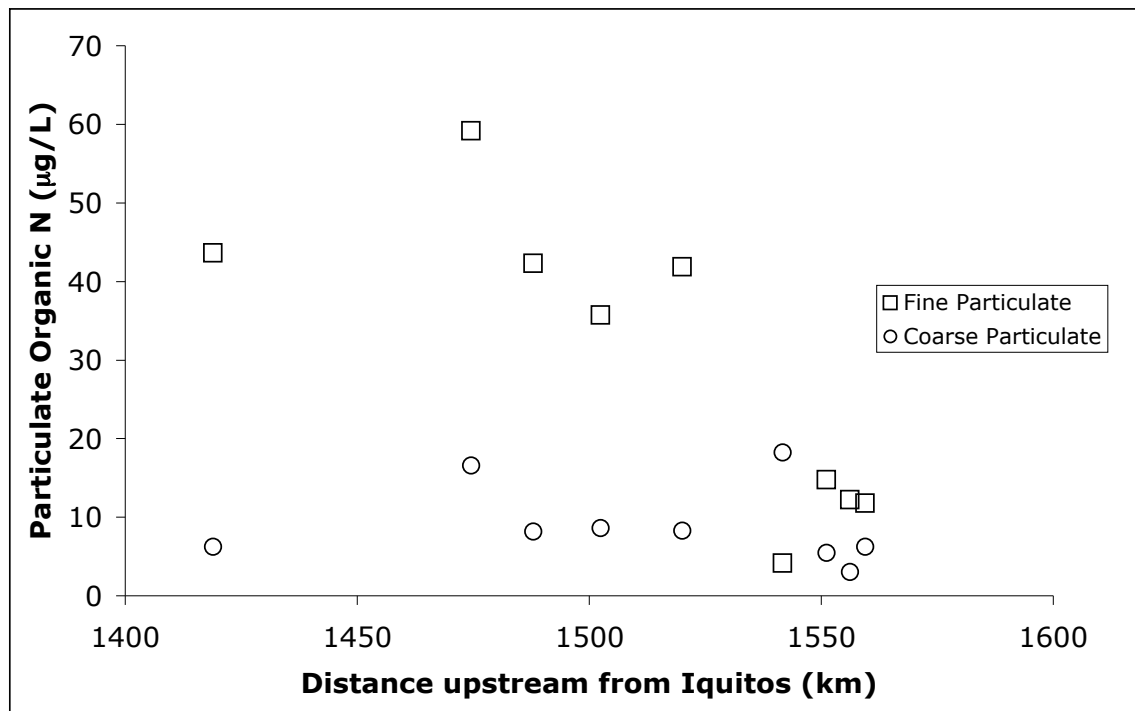


Figure 3.7. Concentrations of nitrogen (in µg/L) in coarse and fine river sediments collected during this study. Fine:  $> 0.7 \mu\text{m}$ ,  $< 60 \mu\text{m}$ ; coarse:  $> 60 \mu\text{m}$ .

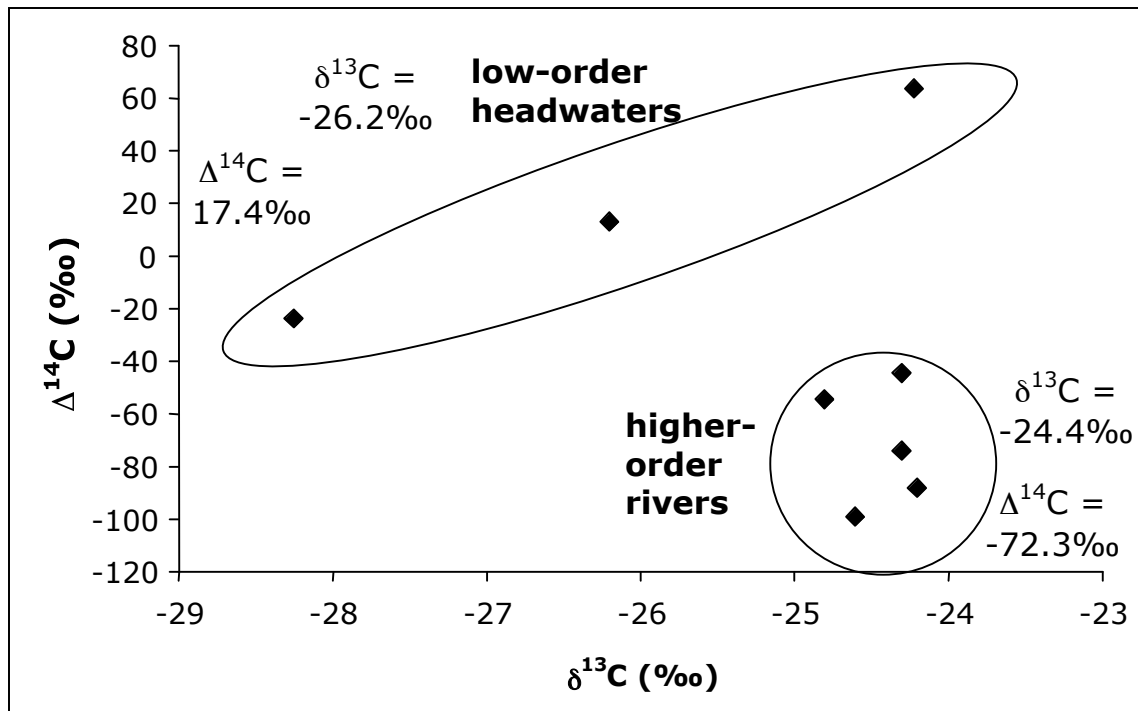


Figure 3.8. Radiocarbon content of bulk river sediments presented versus carbon stable isotopic content of the same samples. The “low-order headwaters” category consists of the samples from the Llamaquizú, Esperanza, and Chontabamba Rivers. The other samples were classified as “higher-order rivers”. Also shown are the average  $\delta^{13}\text{C}$  and  $\Delta^{14}\text{C}$  values for each group of samples.

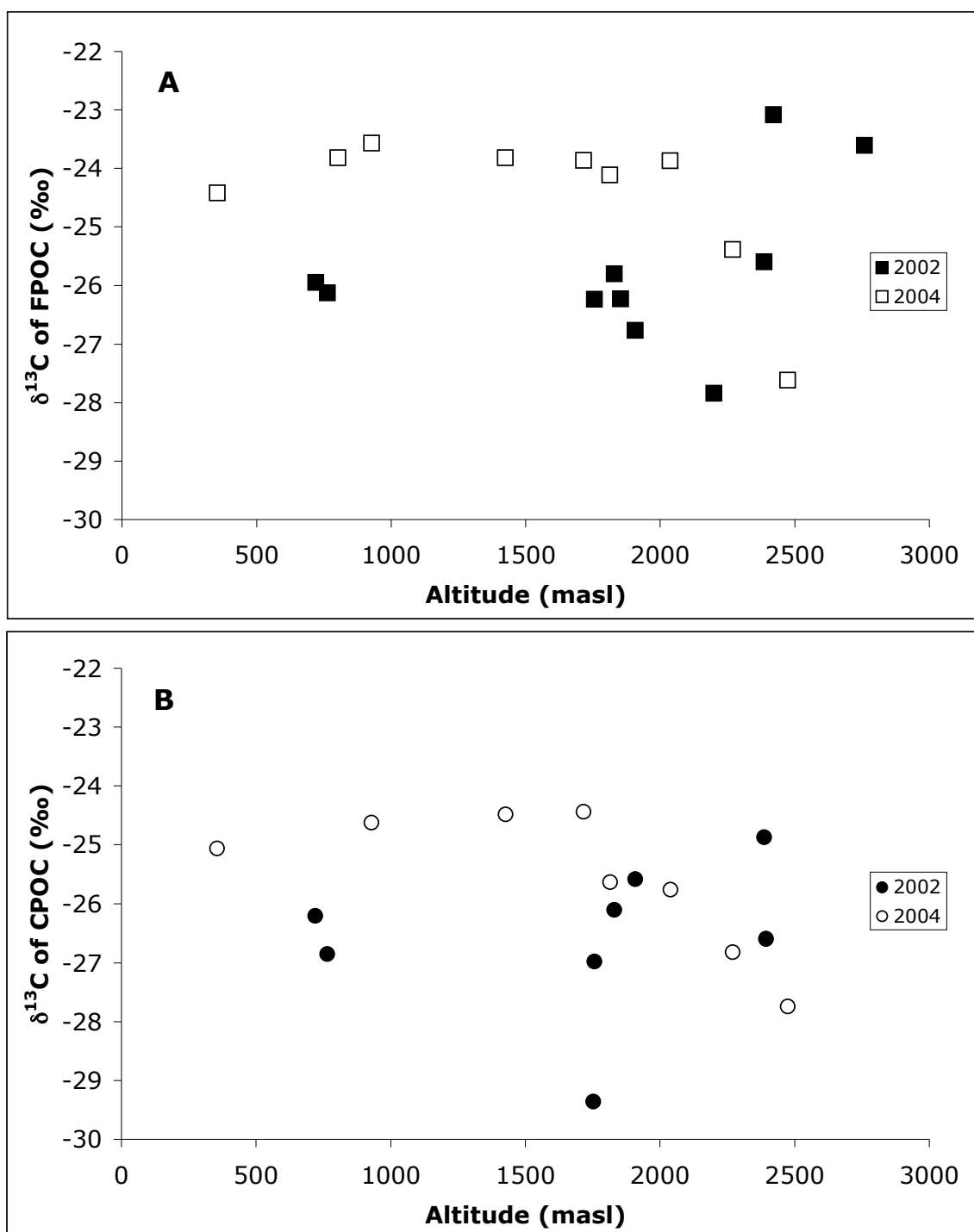


Figure 3.9. Comparison of  $\delta^{13}\text{C}$  of FPOM (A) and CPOM (A) in the study area for the sampling years 2002 and 2004. Data for 2002 is from Chapter 2 of this dissertation.

## **Chapter 4: A one-year time series study of carbon and nitrogen elemental and isotopic composition of riverine suspended sediments in the central Andean Amazon**

### **ABSTRACT**

Only a few studies have examined the dynamics of carbon (C) and nitrogen (N) and their export from small headwater basins in the Andes Mountains to the Amazon River. We measured river discharge as well as the concentration,  $\delta^{15}\text{N}$ ,  $\delta^{13}\text{C}$ , %N, and %OC of coarse and fine suspended sediments (CSS and FSS) in three tributary rivers and the mainstem of the Chorobamba River, located in the central Andean Amazon in Oxapampa, Peru. The three tributary rivers have watersheds of contrasting size and land use. Samples were taken at least once per week from each river over the course of a year, with additional sampling during major storm events. The time series data indicate that the Andes supply approximately equal amounts of fine and coarse sediments to the lower Amazon. Concentrations of POM were low in all of the study rivers, with periodic high concentrations during increased runoff due to storms. Increases in agricultural and pasture cover in watersheds are reflected in the isotopic composition of suspended particulate organic matter (POM), with enrichment in both  $^{13}\text{C}$  and  $^{15}\text{N}$  attributable to the removal of natural  $\text{C}_3$  and epiphytic plants. However, land use in the watersheds did not have an impact on the extent of soil erosion or OM loading to rivers. Significant differences occurred between seasons (wet and dry) for most measured parameters in all of the study rivers, reflecting seasonal changes in sediment sources. The vast majority of sediment and POM that travel from the Andes headwaters to the Amazon River are mobilized during short, infrequent storm events and landslides.

## INTRODUCTION

Riverine suspended sediments are the primary means of transfer of terrestrial organic carbon (OC) and nitrogen (N) to the oceans. Tributaries draining the Andes Mountains are the source of most sediments to the world's largest river, the Amazon (Gibbs 1967), and the Amazon is the third largest source of sediments to the ocean (Milliman and Meade 1983). Thus fluxes of organic matter (OM) from the Amazon River are critical to the global C cycle, since much of the terrestrial OM that persists to the ocean is refractory and eventually buried in marine sediments (Blair et al. 2004, Burdige 2005). Researchers have postulated that the Andes are a source of particulate organic carbon to the Amazon (Richey et al. 1990, Quay et al. 1992, Hedges et al. 1994, 2000), yet few detailed studies have been conducted in the headwaters (McClain et al. 1995). The Andes are tectonically active, so erosion rates are naturally high (Meade et al. 1985, Aalto et al. 2003). Land-use change from natural ecosystems to agriculture or pasture is progressing rapidly, which may accelerate erosion, altering stream biogeochemistry and ecology (Ludwig and Probst 1998) and making mountain soils a source of CO<sub>2</sub> rather than a sink (Bellanger et al. 2004).

Although a connection between sediment loading, organic carbon content of sediments, and storm events has been postulated for rivers in the Andean Amazon (Chapter 2, this volume), no explicit relationship has been shown because previous studies have been conducted at short time scales. Physical processes such as erosion occurring in montane watersheds exert significant control over POC composition and concentration (Blair et al. 2004). The percent of OC in suspended sediments decreases during high sediment loading events (Meybeck 1982, Devol and Hedges 2001, Mayorga and Aufdenkampe 2002, Bellanger et al. 2004, Coynel et al. 2005), because events such as storms or landslides change the relative amounts of soil minerals, organic matter, and

leaf litter delivered to rivers (Blair et al. 2004). In general, particulate OM is less dense than other suspended sediment fractions such as minerals, consequently OM may contribute a larger component of TSS during low flow (Mayorga and Aufdenkampe 2002).

Despite the decrease in %OC with increasing sediment concentration, in most mountainous rivers the bulk of C and N inputs from the landscape occur during floods, whether they are induced by storms or snowmelt. In the mountainous Santa Clara River basin (California USA), a major El Niño-derived storm resulted in increased suspended POC concentration derived from deep soil horizons and ancient bedrock, whereas during low flow, younger, fresher soils were transported preferentially (Masiello and Druffel 2001). In Puerto Rico, increases in discharge were associated with increases in suspended sediment, POC, DOC and PON concentrations (McDowell and Asbury 1994). However, the effects of storm or landslide events on particulate organic matter (POM) concentration or composition in Andean rivers have not been defined.

The land use and land cover of a watershed have several impacts on adjacent rivers. In the lower Amazon, conversion of forest to pasture resulted in a general decrease in water quality, with decreases in dissolved oxygen concentrations and increases in chlorophyll, TSS, POC, and PON concentrations (Thomas et al. 2004). Land use change can also affect the composition and concentration of suspended sediments in rivers. Agricultural practices such as farming and ranching can change plant coverage, which in turn affects soil composition and chemistry (Walling 1999). Also, clearing and tilling of land can increase soil erosion, which may result in higher suspended sediment levels and/or a change in the composition of suspended sediments as deeper soils are turned over and eroded (Walling 1999). Because of slope stability issues, mountainous watersheds are sensitive to changes in land use, and it is estimated that deforestation and



agriculture have more than doubled the suspended sediment load of mountainous rivers over the past ~2000 years (Milliman and Syvitski 1992).

While C and N content and C:N ratios have been used to examine basin–stream interactions (McClain et al. 1997, Saunders and McClain; in press) , stable isotopes can add another dimension of knowledge and are effective for studies of this nature. Agricultural cultivation of C<sub>4</sub> plants such as grasses or corn affects the carbon isotope ratio of soils and plants (and therefore, suspended sediments) because C<sub>4</sub> plants have higher levels of <sup>13</sup>C than the C<sub>3</sub> plants (Fogel and Cifuentes 1993) that make up most of the native vegetation in the Peruvian Andes. Thus suspended sediments from the more agricultural watersheds may have higher δ<sup>13</sup>C levels than do those from native forest watersheds. In the lowland Amazonian tributary of the Ji-Paraná River, land use change associated with deforestation and conversion to pasture was reflected in an increased δ<sup>13</sup>C of all riverine OC size fractions, but DOC and CPOC were more influenced by the presence of C<sub>4</sub> plants than FPOC (Bernardes et al. 2004). In the Venezuelan Andes, δ<sup>13</sup>C of riverine POM was higher in watersheds covered with maize than in those covered with coffee (Bellanger et al. 2004). Nitrogen isotopes are also useful indicators of OM cycling, as processes such as N fixation usually result in low <sup>15</sup>N content, whereas denitrification, degradation, and sewage inputs increase <sup>15</sup>N content of organic matter (Peterson and Fry, 1987, McClelland and Valiela 1998).

This study is driven by the following research questions. How do the concentration and composition of suspended sediments in the Andes change as a function of river discharge or season? Is there a connection between land use/land cover in watersheds and the source and composition of suspended sediments? We monitored river discharge and the concentration (fine and coarse suspended sediment [FSS and CSS]) and composition (δ<sup>13</sup>C, δ<sup>15</sup>N, %OC, %N) of suspended sediments over one year in four rivers

with contrasting land use and physical characteristics in the Peruvian Andean Amazon to address these questions.

## **STUDY AREA**

The study was conducted in the vicinity of Oxapampa, Peru (10.57 °S, 75.40 °W; 1800 meters above sea level), located in central Peru on the eastern flanks of the Andes in the Amazon headwaters. Four rivers were sampled (Figure 4.1): the mouths of three tributaries (Río Llamaquizú, Río Chontabamba, and Río Esperanza) and the union of these tributaries (Río Chorobamba). The Chorobamba point is located about 600 m downstream of the other sampling points, which are all located at the mouth of the river. All three rivers are located in the Pachitea River watershed, which combines with the Ucayali River just upstream of the city of Pucallpa, Peru. The study area and sampling points are shown in Figure 4.1. All sampling points are located in the town of Oxapampa.

Each of the three study watersheds has different physical and ecological characteristics that influence the concentration and composition of riverine suspended sediments. The Chontabamba watershed is the largest and has the greatest elevation range (Table 4.1), extending up to 3969 meters above sea level (masl), above the tree line in the puna ecosystem. The Chontabamba is also the least disturbed watershed, with 76% of the land cover existing in its natural state (Figure 4.2). The Esperanza watershed is the smallest of the three, but most of it is located in the Yanachaga-Chemillen National Park, so a great majority of the land in this watershed (72%) is also unaltered (Figure 4.2). The Llamaquizú watershed is the most impacted, with only 53% of land unaltered. The Llamaquizú is the most agricultural of the three watersheds (22%): corn, peppers, and pumpkins are the dominant crops. Seventeen percent of this watershed is devoted to

cattle grazing. The Chontabamba is the largest watershed by far, with an area of 221 km<sup>2</sup>. The Llamaquizú is the second largest with an area of 80 km<sup>2</sup>, and the Esperanza watershed has an area of 36 km<sup>2</sup> (Table 4.1). The watershed of the Chorobamba River at the sampling point in Figure 4.1 was considered to be the sum of the three headwaters (Table 4.1).

The climate in the Peruvian Andes is generally wet in the summer months (October through March) and dry in the winter (April through September) (Figure 4.3). Because of this seasonal fluctuation, river discharge is greatest in the summer and lowest in winter. The total rainfall over the study period was 1570 mm (Figure 4.3). The average monthly temperature, as recorded inside the Yanachaga-Chemillen National Park (2400 meters above sea level) ranges from 12.0°C in July to 14.4°C in January (D. Catchpole, personal communication).

## **METHODS**

Rivers at four sampling points were sampled every Wednesday for one year, from July 2004 until July 2005. Additional samples were collected from each river during major storm events to determine the effects of precipitation on riverine sediment concentration and composition. River water was collected in 1 L high-density polyethylene wide mouth Nalgene bottles. Water was transported back to the field station in Oxapampa and filtered immediately. A known volume of water was first passed through pre-weighed 60 µm nylon mesh filters (Millipore) to collect coarse suspended sediments (CSS). The filtrate was passed through pre-combusted, pre-weighed glass fiber filters (Whatman GF/F), with a pore size of about 0.7 µm: this fraction was defined as fine suspended sediments (FSS). Filters were dried for 48 hours

at 60°C and stored in tight-fitting plastic Petri dishes until they could be transported back to the University of Texas Marine Science Institute for analysis.

Carbon and N isotopic composition of suspended sediments was determined at the University of Texas Marine Science Institute stable isotope ecology laboratory, equipped with a Carlo Erba NC 1500 elemental analyzer coupled to a Finnegan MAT DELTA plus continuous-flow isotope ratio mass spectrometer. Carbonates were removed from soils and sediments prior to  $\delta^{13}\text{C}$  analysis by vapor-phase acidification with HCl for 24 hours, followed by drying at 60°C for 24 hours. Coarse particulates were transferred onto glass fiber filters prior to analysis. Coarse particulate OC and ON (CPOC and CPON) are defined as the percent of OC or N in the sample multiplied by the CSS concentration. Fine particulate OC and ON (FPOC and FPON) are calculated by multiplying the percent of OC and N in the sample by the FSS concentration.

During several months of the study (April through June of 2005), the Whatman GF/F filters used for collecting fine particulates were inadvertently replaced with non-combusted Millipore AP-15 prefilters. These filters have the same approximate pore size as Whatman GF/F filters, but are coated with an acrylic binding resin. Because this resin contained organic C and N, it was necessary to correct these isotope and weight percent values for the filter blank. Isotopic and elemental composition of the filter blank was determined by repeated analysis of unused filters obtained from the manufacturer. The blank values were replicable to better than the accuracy of the instrument (the instrument is accurate to within 0.2‰ for isotopes and 5% for weight percent) and were determined as follows:  $\delta^{13}\text{C}_{\text{filter}} = -33.88\text{‰}$ ,  $\delta^{15}\text{N}_{\text{filter}} = -0.09\text{‰}$ ,  $\% \text{OC}_{\text{filter}} = 2.53\%$ , and  $\% \text{N}_{\text{filter}} = 0.03\%$ .

Weight percent values were corrected as follows:

$$\begin{array}{l} \text{Corrected} \\ \% \text{OC of} \\ \text{sediment} \end{array} = \frac{(\text{mass}_{\text{filter} + \text{sediment}} * \% \text{OC}_{\text{filter} + \text{sediment}}) - (\text{mass}_{\text{filter}} * \% \text{OC}_{\text{filter}})}{\text{mass}_{\text{sediment}}}$$

The same calculation was performed for correcting %N values. Once a corrected weight percent value was obtained, delta values were then corrected as follows:

It proved impossible to correct  $\delta^{13}\text{C}$  values for samples on the resin-coated filters, perhaps due to a negative interaction between the resin and the hydrochloric acid treatment used to remove carbonates, so the  $\delta^{13}\text{C}$  values for FSS for the months of April,

$$\text{Corrected } \delta^{15}\text{N of sediment} = \frac{(\delta^{15}\text{N}_{\text{filter + sediment}} * \text{mg N}_{\text{filter + sediment}}) - (\delta^{15}\text{N}_{\text{filter}} * \text{mg N}_{\text{filter}})}{\text{mg N}_{\text{sediment}}}$$

May and June 2005 have been excluded. The correction for  $\delta^{15}\text{N}$  was simpler as the AP-15 filters contained only minor amounts of N.

River discharge measurements and rainfall amounts are from Noguera (2006). Briefly, river stage was measured daily at the Chorobamba River and converted to discharge by monthly calibration with a flow meter (Flowmeter Model 2030 Series). Rainfall was measured at the Andean Amazon Research Station in Oxapampa using a Rain-Wise™ digital rain gauge. Discharge was measured over the entire 12-month period of the experiment in the Chorobamba River, but staff gauges were installed after July 2004 in the other three rivers.

Land use in the three watersheds was calculated using ERDAS version 8.4 and mapped in Arc-View GIS software. The base map used was a LandSat 7 ETM+ from June 2001.

To calculate the importance of storm events on sediment and OC and N transport in this system, a storm is defined as when the river discharge increases by more than 25% in one day and a sediment sample was taken on the first day. Since the Chorobamba River is the only one for which a full record of discharge exists, it is the only river that could be modeled this way. During the study period (July 20, 2004 through July 21, 2005), a total of five of these storms occurred. For modeling purposes, storm sediment

concentrations were repeated for two days (one day after the event), and sediment concentrations measured during a normal day were repeated for seven days.

## RESULTS

Rainfall amounts for each month of the study are shown in Figure 4.3. As expected, rainfall was greater during the summer months (October through March). The winter of 2004 was much wetter than the winter of 2005. Two thousand five was the driest year in the Amazon Basin on record (J.L. Guyot, personal communication): the Amazon River reached the lowest river stage ever recorded, and some of the rivers being monitored for this project dropped below the lowest level of the staff gauges. The staff gauges were subsequently lowered and all of the reported values shown here have been corrected to the new, lower staff gauge heights.

A summary of all measured parameters (discharge, FSS, CSS, FPOC, CPOC, FPON, CPON,  $\delta^{15}\text{N}_{\text{FSS}}$ ,  $\delta^{15}\text{N}_{\text{CSS}}$ ,  $\delta^{13}\text{C}_{\text{FSS}}$ ,  $\delta^{13}\text{C}_{\text{CSS}}$ ,  $\%\text{OC}_{\text{FSS}}$ ,  $\%\text{OC}_{\text{CSS}}$ ,  $\%\text{N}_{\text{FSS}}$ , and  $\%\text{N}_{\text{CSS}}$ ) for each of the four study rivers is presented in Table 4.2. Time series of each of the sediment parameters are graphed along with discharge of each river in Figures 4.4, 4.5 and 4.8 through 4.15. Coarse and fine POC and PON concentrations are graphed versus river discharge for each of the study sites in Figures 4.6 and 4.7.

Suspended solid concentrations were low in all of the rivers, except for periodic high concentrations driven by storm or flood events. Figure 4.4 shows total fine suspended sediment (TFSS) concentrations over the course of the study in each of the four rivers, plotted with river discharge. The average TFSS load was generally low in each of the four rivers, but was variable based on high flow events (Table 4.2, Figure 4.4). Total coarse suspended sediment (TCSS) concentrations followed the same trend as FSS and were also related to discharge (Figure 4.5).

As with sediment concentration, the concentrations of fine particulate organic carbon (FPOC) also increased with discharge, but otherwise were low and constant throughout the year (Figure 4.6). Concentrations of coarse particulate organic carbon (CPOC) were similar to those observed for FPOC, and also increased during high discharge events (Figure 4.6).

Concentrations of fine particulate organic nitrogen (FPON) overall were lower than FPOC concentrations for the same sampling days, but followed the same pattern and relationship with discharge (Figure 4.7). Coarse particulate organic nitrogen (CPON) concentrations were similar to those of FPON, and had a similar distribution and relationship with discharge (Figure 4.7).

The  $\delta^{15}\text{N}$  of FSS in each of the study rivers is shown in Figure 4.8. The  $\delta^{15}\text{N}$  of FSS in the Chorobamba River was positively correlated with discharge ( $y = 0.0235x + 4.2855$ ,  $r^2 = 0.1489$ ), so that  $\delta^{15}\text{N}$  of fine sediments was lower in the drier months of the year (Figure 4.8A). The  $\delta^{15}\text{N}$  of FSS in the Llamaquizú River was significantly higher than that observed in the other three rivers ( $p < 0.001$ ). In all of the four study rivers, FSS was significantly enriched in  $^{15}\text{N}$  over CSS ( $p < 0.001$ ). The average  $\delta^{15}\text{N}$  of CSS is significantly higher in the Llamaquizú River than in each of the other study rivers ( $p < 0.001$ ).

The  $\delta^{13}\text{C}$  of FSS for the four study rivers is presented in Figure 4.12. The  $\delta^{13}\text{C}$  of FSS in the Llamaquizú River was significantly higher than that observed in each of the other study rivers ( $p < 0.001$ ). Coarse suspended sediment  $\delta^{13}\text{C}$  over the duration of the experiment is presented in Figure 4.11. The  $\delta^{13}\text{C}$  of CSS in the Llamaquizú River was significantly higher than that observed in all of the other rivers ( $p < 0.001$ ).

In this study, the majority of sediments are transported during infrequent storms (Table 4.4). Five events fit the characteristics defined above for storms: October 20,

2004; November 7, 2004; January 4, 2005; March 16, 2005; and May 25, 2005. Most of these events occurred during the wet season, with one or two occurring during the dry season. During these ten days (five storms), 81% of the sediment observed for the whole study period was in suspension in the Chorobamba River. These storms also accounted for 74% of SOC and 64% of SON for the entire year (Table 4.4).

Land use does not appear to have a major effect of sediment, OC, or N loss in these watersheds. Table 4.5 shows the relative amounts of sediment and sedimentary OM lost from each watershed. Because there is not a continuous discharge record for each of the study rivers, the three watersheds could only be compared for the period of November 10, 2004 through July 21, 2005. The most important factor in determining SOC and SON export from each of the three study watersheds appeared to be watershed size. That is, the Llamaquizú watershed did not contribute SOC or SON to the Chorobamba in an amount disproportionate to the size of its watershed (Table 4.5).

The percent of OC in sediments was inversely proportional to suspended sediment concentration (Figure 4.16), thus the relationship of %OC with TSS concentration is consistent with the accepted standard for rivers originally presented in Meybeck (1982); that is,

Total suspended sediment concentration in the Chorobamba River increased exponentially with increasing precipitation ( $p < 0.01$ ) (Figure 4.17A). Not surprisingly, river discharge also increased linearly with increasing rainfall ( $p < 0.01$ ) (Figure 4.17B).

## **DISCUSSION**

The discharge hydrographs observed for the Oxapampa rivers are quite unlike that observed in the Amazon mainstem (Devol et al. 1995), which is regular and dampened. This is not unexpected, as the Amazon integrates about 1 million Chorobamba-sized



streams. In Andean rivers, discharge is dominated by storm events, which increase discharge over short periods of time only, similar to other small mountainous rivers (e.g., Masiello and Druffel 2001, Dadson et al. 2005, Restrepo et al. 2006, and reviewed in Viviroli and Weingartner 2004). This characteristic has major implications for sediment and associated organic matter transport from the Andes to the Amazon. Because the Andes are a major source of sediments to the Amazon (Gibbs 1967), it was assumed that most of these sediments are transported during the rainy summer months (Devol et al. 1995). However, my results indicate that most of these sediments are transported during several discrete storm events rather than over the entire season: sediment concentration in our study rivers decreases rapidly following each storm event, and average sediment concentrations are similar between the dry and wet seasons (not including storms) (Noguera 2006). These Andean sediments may be stored on the Amazon floodplain and remobilized during high flow events. Whether or not the observed patterns for sediment concentration (i.e., high only for short periods of time) are the same for dissolved species such as alkalinity and major ions, which in the Amazon are also thought to be derived from the Andes, or for dissolved nutrients or OC, will be examined in a separate paper (McClain et al. in prep).

Unlike the mainstem Amazon, in Andean rivers neither FSS nor CSS show a regular seasonal concentration pattern (Devol et al. 1995), although there is a predictable pattern associated with discharge. Fine suspended sediment concentrations, on average, are much lower in Andean rivers than in the Amazon, although they can be much higher (above 1000 mg/L) during storms (Figure 4.4). This result indicates that there is not a consistent pattern of FSS loading from this region of the Andes to the Amazon, and that the regular pattern of FSS concentration observed in the Amazon (and attributed to the

Andes) must be regulated by sediment storage and resuspension occurring below the high relief of the Andes, consistent with Aalto et al. 2003.

In the Andean rivers studied here, patterns of CSS concentration are similar to those observed for FSS, and there is no difference between FSS and CSS concentrations in any of the study rivers (Chorobamba  $p = 0.8$ , Chontabamba  $p = 0.9$ , Esperanza  $p = 0.6$ , Llamaquizú  $p = 1.0$ ). This result contrasts those observed in the lower Amazon, where CSS concentrations are much lower than FSS (Devol et al. 1995). Similarly, in the lowland Ji-Paraná tributary, FSS concentrations ranged from 15-35 mg/L whereas CSS concentrations were almost always  $< 3$  mg/L (Bernardes et al. 2004). FSS was much higher than CSS in the Beni River and headwaters in Bolivia, but this river is much more turbid overall than the Pachitea (Hedges et al. 2000). Andean clear water rivers may supply just as much coarse sediment as fine sediment to the Amazon headwaters, but, when combined with the results of the previous study (Devol et al. 1995), our results indicate that fine sediments are preferentially transported downstream whereas coarse sediments are more or less permanently retained in the Andean foreland. This finding agrees with previous studies in the Bolivian Amazon, which indicated that about half of all sediments initially suspended in Andean rivers were retained in the lowland floodplains (Aalto et al. 2006), although previous research did not incorporate multiple size fractions of TSS. The floodplain in the lower Amazon has a dampening effect on sediment load, so TSS is more constant over the year (Meade et al. 1985). In the Andes, although sediment concentrations are higher on average during the wet season, there was no distinct seasonal pattern in sediment load. Sediment concentrations in Andean rivers are driven by storm events (Table 4.3), which raise sediment concentrations for short periods of time, and these events are more frequent and intense during the wet season.

This result is similar to those for other mountain river systems (Milliman and Syvitski 1992, Milliman 1995, Farnsworth and Milliman 2003).

The dependence of sediment load on precipitation (Figure 4.17) has implications for Amazon basin biogeochemistry in the face of global climate change. If local deforestation and global warming decrease rainfall in the Andean Amazon, as predicted by climate models (Avisar and Werth 2005, Chagnon and Bras 2005), sediment transfer from the Andes to the Amazon would decrease dramatically. In five years of river monitoring at the Andean Amazon Research Station in Oxapampa (2001-2005), annual rainfall has decreased each year (Noguera 2006). From 2003 to 2005, annual water discharge in the Chorobamba River decreased from  $762 \times 10^9 \text{ m}^3$  to  $517 \times 10^9 \text{ m}^3$  (a decrease of 32%), and sediment yield in the Chorobamba basin decreased, from  $626 \text{ t km}^{-2} \text{ yr}^{-1}$  to  $119 \text{ t km}^{-2} \text{ yr}^{-1}$  (a decrease of 81%) (Noguera 2006). For reference, the average sediment yield for the entire Amazon basin is  $203 \text{ t km}^{-2} \text{ yr}^{-1}$  (Ludwig and Probst 1998). If the Andean precipitation and river discharge continue to decrease, so will sediment and associated organic matter loading to the Amazon River. This is important because POM from upstream likely fuels Amazon food webs and provides substrate for soil formation in floodplain areas.

The low median concentrations of CSS and FSS presented here indicate that, overall, these Andean rivers fall into the category defined by Meybeck (1982) as “less turbid” ( $5 < \text{TSS} < 5000 \text{ mg/L}$ ). While sediment concentration in major rivers often displays low interannual variation, sediment loads in smaller rivers, especially mountainous ones, are often dependent on specific events (Farnsworth and Milliman 2003). My data agree with conclusions in the review of major rivers presented in Meybeck (1982) because as FSS and CSS concentrations increase, the percent by weight of OC decreases (Figure 4.16). In our study rivers, the majority of FPOC and CPOC in

suspension occur during storms (Table 4.4), as observed for other rivers in the world during storms (Masiello and Druffel 2001, and reviewed in Meybeck 1982 and Ittekkot 1988).

This study also provides insights into how land use change affects river biogeochemistry. The most impacted watershed in this study is the Llamaquizú, where nearly 50% of the natural vegetation has been replaced with secondary forests, pastures, and agriculture (Table 4.1). The land use of each watershed does not appear to affect overall sediment, C, or N losses: these parameters scaled nicely with watershed size in this study (Table 4.5). This implies that other parameters, such as regional precipitation, basin slope, and soil type, have greater impact on erosion rates than land cover. However, land cover does appear to be reflected in the isotopic composition of suspended sediments. Over the course of the study year, the average  $\delta^{13}\text{C}$  and  $\delta^{15}\text{N}$  of both FSS and CSS in the Llamaquizú River were significantly higher ( $p < 0.001$ ) than in the other three rivers. The average  $\delta^{13}\text{C}$  of FSS in the Llamaquizú was from 0.9 to 2.0‰ more enriched than the average for the other rivers (Figure 4.12), and the  $\delta^{13}\text{C}$  of CSS was from 1.7 to 2.2‰ more enriched than that found in the other rivers (Figure 4.13). The increase in  $\delta^{13}\text{C}$  can be explained by the replacement of natural  $\text{C}_3$  vegetation with  $\text{C}_4$  grasses and agriculture, especially corn. Similar occurrences have been observed in other rivers where forests have been converted to pastures. In general, the deforested Piracicaba River had higher  $\delta^{13}\text{C}$  of both CPOM and FPOM than the Amazon River (Krusche et al. 2002). Also in the Piracicaba, tributaries with more deforestation had dissolved and particulate OC more enriched in  $^{13}\text{C}$  than in forested catchments (Martinelli et al. 1999). The same patterns were observed for heavily deforested parts of the Amazon Basin, such as the Ji-Paraná (Bernardes et al. 2004). In many previous studies, DOM, thought to be the most rapidly cycling OC fraction, appeared to be most heavily influenced by the

presence of C<sub>4</sub> plants. Our study agrees with previous efforts showing that relatively recent changes in land cover (~50 years) can influence riverine biogeochemistry (Howarth et al. 1991, Neill et al. 2001, Thomas et al. 2004).

Fine and coarse sediments are also more enriched in <sup>15</sup>N in the Llamaquizú as compared to the other rivers. The average  $\delta^{15}\text{N}$  of FSS in the Llamaquizú River was from 1.1 to 1.7‰ more enriched than the average values for the three other rivers (Figure 4.10), and the average  $\delta^{15}\text{N}$  of CSS for the Llamaquizú was from 1.3 to 1.7‰ more enriched than average values in the other study rivers (Figure 4.11). Land conversion from forest to pasture is often associated with increases in  $\delta^{13}\text{C}$  (Mariotti et al. 1991, Martinelli et al. 1999, Krusche et al. 2002, Bernardes et al. 2004). There are several possible reasons for the observed enrichment of  $\delta^{15}\text{N}$  in sediments in the Llamaquizú River. Mobilization of deeper or more degraded soil horizons from agricultural or bare soils enriches the  $\delta^{13}\text{C}$  and  $\delta^{15}\text{N}$  of suspended OM in streams (Bellanger et al. 2004): the Llamaquizú has the highest proportion of agricultural and bare soils of any watershed in this study (Table 4.1). Also, the observed enrichment in <sup>15</sup>N could be anthropogenic, since the Llamaquizú watershed has the highest population density of humans and farm animals (Noguera pers. comm.). Human and animal waste has been known to enrich <sup>15</sup>N in aquatic systems (McClelland and Valiela 1998). There is also a large (approximately 1 million fish at any given time) commercial trout farm in the Llamaquizú watershed. Aquaculture facilities can cause <sup>15</sup>N enrichments in effluent (Lojen et al. 2005), although this particular farm is unstudied. The other possibility is deforestation may cause plants and other organic matter components in the Llamaquizú watershed to be more enriched in <sup>15</sup>N. Natural vegetation cover in this part of the world consists of montane cloud forests, of which a large portion of biomass is epiphytes such as lichens, bryophytes, and orchids. Epiphytes obtain nitrogen in one of two ways: through the atmosphere, via wet or dry

deposition or through  $N_2$  fixation; or via roots in canopy soils, which are usually derived from a mixture of host and epiphyte detritus (Coxson and Nadkarni 1995). Thus these epiphytes are depleted in  $^{15}N$  with respect to rooted plants and soils (Heitz et al. 2002). In fact, a study of epiphytes in the Esperanza watershed showed that they are less enriched in  $^{15}N$  than rooted plants, and a side-by-side comparison of two small watersheds in the Esperanza showed that deforestation could significantly increase  $^{15}N$  stocks over time scales of less than 10 years (Chapter 5, this volume).

A consistent offset between the  $\delta^{15}N$  of FSS and CSS was observed in this study: on average, FSS is significantly enriched over CSS in all four of the study rivers (Table 4.2, Figures 4.10 and 4.11). This finding appears to be consistent throughout the Amazon basin (Hedges et al. 1986a, 2000, Aufdenkampe et al. 2001, Chapter 2, this volume). Generally this enrichment is attributed either to a higher degree of degradation of fine particles (Hedges et al. 2000, Chapters 2 and 3, this volume), or to the sorption of  $^{15}N$ -enriched DOM to suspended minerals (Aufenkampe et al. 2001). Unlike the pattern observed for  $^{15}N$ , no consistent pattern was found between the  $\delta^{13}C$  of CSS and FSS in the study rivers. If a higher degree of degradation were responsible for the observed pattern in  $^{15}N$ , the same pattern would likely be observed for  $^{13}C$ . In other words, if FSS were derived from soils and CSS from plants in Andean rivers, as proposed in Chapter 2,  $^{13}C$  would be enriched in FSS as it is in soils as compared to plants (see also Chapter 5, this volume). More studies are needed to pinpoint the mechanisms responsible for the nitrogen isotopic composition of suspended OM in Andean and Amazonian rivers.

More information about the processes that influence the  $\delta^{13}C$  of suspended particles in Andean rivers can be gleaned from seasonal differences in concentrations and chemical composition of FSS and CSS. A significant difference (at the 95% confidence level) was observed between the wet and dry seasons (October through March and April

through September, respectively) for most of the measured parameters in all of the study rivers (Table 4.3). In almost all cases, the  $\delta^{13}\text{C}$  of both FPOM and CPOM is significantly higher in the dry season than in the wet season. In contrast, there is no consistent seasonal offset of  $^{15}\text{N}$  in either fraction. It is unlikely that there is a significant seasonal difference in  $^{13}\text{C}$  content of potential terrestrial sources such as plants or soils, although dry season POM may be more influenced by riparian than upland soils. If riparian soil  $\delta^{13}\text{C}$  is higher than that of upland soils, this may explain the observed seasonal pattern in  $\delta^{13}\text{C}$  of suspended sediments. However, no difference was shown in the isotopic composition of riparian versus upland soils (Chapter 2, this volume). The observed seasonal difference in  $\delta^{13}\text{C}$  of TSS may be due to the growth of phytoplankton or algae in streams during the dry season, when suspended sediment concentration is lower (Table 4.3) and light penetration is theoretically sufficient to sustain aquatic photosynthesis. Phytoplankton are assumed to be a negligible portion of suspended matter in Amazonian streams (Cai et al. 1988, McClain and Richey 1996, McClain and Elsenbeer 2001), but this speculation has not been verified. A small amount of algae enriched in  $^{13}\text{C}$  would be sufficient to alter the  $\delta^{13}\text{C}$  of TSS, and might also explain the increase in %OC and %N observed in TSS during low water (Table 4.3). The  $\delta^{13}\text{C}$  of phytoplankton in Andean rivers has not been measured, but it has been estimated to be depleted in  $^{13}\text{C}$  as compared to soils and terrestrial plants (Cai et al. 1988), not enriched. If there is an algal fraction of POM, it may not be transported conservatively downstream. If so, the Andean contribution of terrestrial and/or refractory OM to the Amazon has may have been overestimated. The other possibility for the seasonal patterns in  $\delta^{13}\text{C}$  of suspended sediments is that, during the dry season, suspended particles are composed of resuspended bottom sediments are more degraded, and thus more enriched in  $^{13}\text{C}$ . The

dominance of sorption may explain why there is no corresponding shift in  $\delta^{15}\text{N}$  of sediments during the dry season.

## CONCLUSIONS

This study represents a first step towards understanding seasonal variations in C and N cycling in rivers of the Amazon headwaters, and supplies some new information about mechanisms of sediment and associated OM transport from small basin rivers in the Andean Amazon. Sediment concentrations in Andean rivers depend on storm events; outside of these events TSS values are very low. Thus sediment transport to the lower Amazon is episodic. Concentrations of coarse and fine sediments and CPOC and FPOC are similar, indicating that the Andes are equal source of each size fraction to the lower basin, but that coarse sediments are probably retained preferentially in the Andean foreland. The connection between land use and riverine sediment concentration is less clear, but deforestation and increases in agriculture did significantly impact the isotopic composition of suspended sediments, if not the sediment or OM concentration. There was a clear difference in composition of sediments in the dry and wet seasons, indicating that there is a seasonal shift in the source of POC to Andean rivers. This study demonstrates that POC transport from the Andes to the Amazon is episodic, and that imminent land use and climate change may have significant impacts on the quantity and quality of OM transport downstream.



Watershed	Area (km <sup>2</sup> )	Elevation (masl)			Slope (°)			% Natural Ecosystem	% Secondary Forest	% Pasture	% Agriculture or Cleared
		min	max	mean	min	max	mean				
Chontabamba	221	1804	3969	2579	0	62.8	20.6	76%	8%	7%	8%
Esperanza	36	1807	3230	2419	0.1	49.0	20.4	72%	8%	13%	8%
Llamaquizú	80	1806	3204	2273	0	63.2	17.5	53%	8%	17%	22%

Table 4.1. Physical and land cover characteristics of the three watersheds in this study.  
Data from Noguera (2006).

	Chorobamba				Esperanza				Llamaquizú				Chontabamba			
	Avg	Med	Min	Max	Avg	Med	Min	Max	Avg	Med	Min	Max	Avg	Med	Min	Max
Discharge (m <sup>3</sup> /s)	17.9	14.8	6.5	113	1.7	1.6	0.5	6.8	2.5	1.2	0.3	13.7	15.3	12.8	5.2	85.8
FSS (mg/L)	50.0	160	2.0	891	57.1	5.6	1.7	1346	71.7	12.2	3.5	1593	31.0	4.7	1.6	723
CSS (mg/L)	42.6	3.2	0.9	901	83.7	3.8	0.8	2340	70.4	2.7	0.5	1617	27.4	3.3	0.9	654
FPOC (mg/L)	1.4	0.4	0.2	17.8	1.1	0.3	0.1	19.5	1.6	0.7	0.2	26.9	0.9	0.3	0.0	16.4
CPOC (mg/L)	1.9	0.3	0.0	34.8	3.7	0.3	0.0	116	1.1	0.2	0.1	16.0	1.0	0.2	0.0	23.3
FPON (mg/L)	0.1	0.0	0.0	1.5	0.2	0.0	0.0	1.8	0.2	0.1	0.0	2.7	0.1	0.0	0.0	1.8
CPON (mg/L)	0.1	0.0	0.0	1.1	0.1	0.0	0.0	1.5	0.1	0.0	0.0	1.6	0.0	0.0	0.0	0.3
$\delta^{15}\text{N}_{\text{FSS}}$ (‰)	4.8	4.7	2.3	7.2	4.5	4.5	1.1	6.8	5.9	5.9	3.6	8.2	4.2	4.1	1.4	6.7
$\delta^{15}\text{N}_{\text{CSS}}$ (‰)	3.4	3.6	-1.8	6.5	3.1	3.2	1.0	4.5	4.7	4.8	1.5	8.5	3.0	3.0	0.1	5.6
$\delta^{13}\text{C}_{\text{FSS}}$ (‰)	-25.3	-25.4	-26.6	-25.4	-24.9	-25.1	-26.6	-22.8	-24.0	-24.0	-25.6	-22.2	-26.0	-26.1	-24.2	-26.1
$\delta^{13}\text{C}_{\text{CSS}}$ (‰)	-25.9	-26.1	-30.2	-21.4	-25.7	-25.8	-29.1	-21.6	-24.0	-24.1	-26.2	-17.9	-26.2	-26.4	-33.6	-22.9
%OC <sub>FSS</sub>	6.7	6.3	1.9	20.7	6.7	6.2	1.3	19.7	5.8	4.9	1.3	15.3	8.5	6.9	2.0	20.4
%OC <sub>CSS</sub>	7.9	7.2	1.8	15.8	7.0	7.5	0.5	14.8	8.0	7.8	0.6	17.0	9.3	9.8	1.6	16.0
%N <sub>FSS</sub>	0.7	0.6	0.2	1.9	0.8	0.7	0.1	3.4	0.6	0.5	0.2	1.8	0.9	0.7	0.2	3.7
%N <sub>CSS</sub>	0.6	0.4	0.1	2.3	0.5	0.5	0.1	2.2	0.5	0.5	0.1	1.1	0.7	0.6	0.1	1.7

Table 4.2. Average, median, minimum, and maximum values of measured parameters for each of the four rivers in this study.

	<b>Chorobamba</b>	<b>Chontabamba</b>	<b>Esperanza</b>	<b>Llamaquizú</b>
<b>Discharge</b>	*	*	*	
<b>CSS</b>	*	*	*	*
<b>FSS</b>	*	*	*	*
$\delta^{15}\text{N}_{\text{CSS}}$		*		
$\% \text{N}_{\text{CSS}}$	**	**		**
$\delta^{13}\text{C}_{\text{CSS}}$	**	**	**	**
$\% \text{OC}_{\text{CSS}}$	**	**		**
$\delta^{15}\text{N}_{\text{FSS}}$		*	*	
$\% \text{N}_{\text{FSS}}$	**	**	**	**
$\delta^{13}\text{C}_{\text{FSS}}$	**		**	**
$\% \text{OC}_{\text{FSS}}$	**	**	**	**

Table 4.3. Measured parameters for which there is a significant difference in means (at the 95% confidence interval) between the dry and wet seasons (April through September, and October through March, respectively). The difference between means was assessed using Tukey's honestly significant difference procedure. \* : wet season is higher than dry season, \*\* : dry season is higher than wet season; blank = no seasonal difference.

	Percent during storm events
Total sediment	81
Coarse sediment	85
Fine sediment	78
POC	74
CPOC	83
FPOC	62
PON	64
CPON	68
FPON	61

Table 4.4. Percent of total sediment and sedimentary OC and N in suspension in the Chorobamba River during five 2-day storm events. These calculations account for the entire period of the study from July 20, 2004 through July 21, 2005.

	<b>Chontabamba</b>	<b>Llamaquizu</b>	<b>Esperanza</b>	<b>Total of tributaries</b>	<b>Chorobamba</b>
<b>SOC (tons)</b>	484.5	120.3	44.0	648.1	749.5
<b>SON (tons)</b>	44	9.6	4.9	58.5	59.2
<b>Total discharge (L)</b>	$3.3 \times 10^{11}$	$5.5 \times 10^{10}$	$3.3 \times 10^{10}$	$4.2 \times 10^{11}$	$4.2 \times 10^{11}$
<b>TSS (tons)</b>	14789	4540	1411	20740	20381
<b>Watershed size (km<sup>2</sup>)</b>	221	80	36	337	
<b>% of total</b>	66	24	11		
<b>% of total: TSS</b>	73	22	7		
<b>% of total: SOC</b>	75	19	7		
<b>% of total: SON</b>	75	16	8		
<b>SOC tons/km<sup>2</sup></b>	2.2	1.5	1.2		
<b>SON tons/km<sup>2</sup></b>	0.20	0.12	0.14		

Table 4.5. Discharge, sediment load, and organic carbon and nitrogen losses in the study watersheds for the period November 10, 2004 through July 21, 2005. SOC = sedimentary organic carbon. SON = sedimentary organic nitrogen.

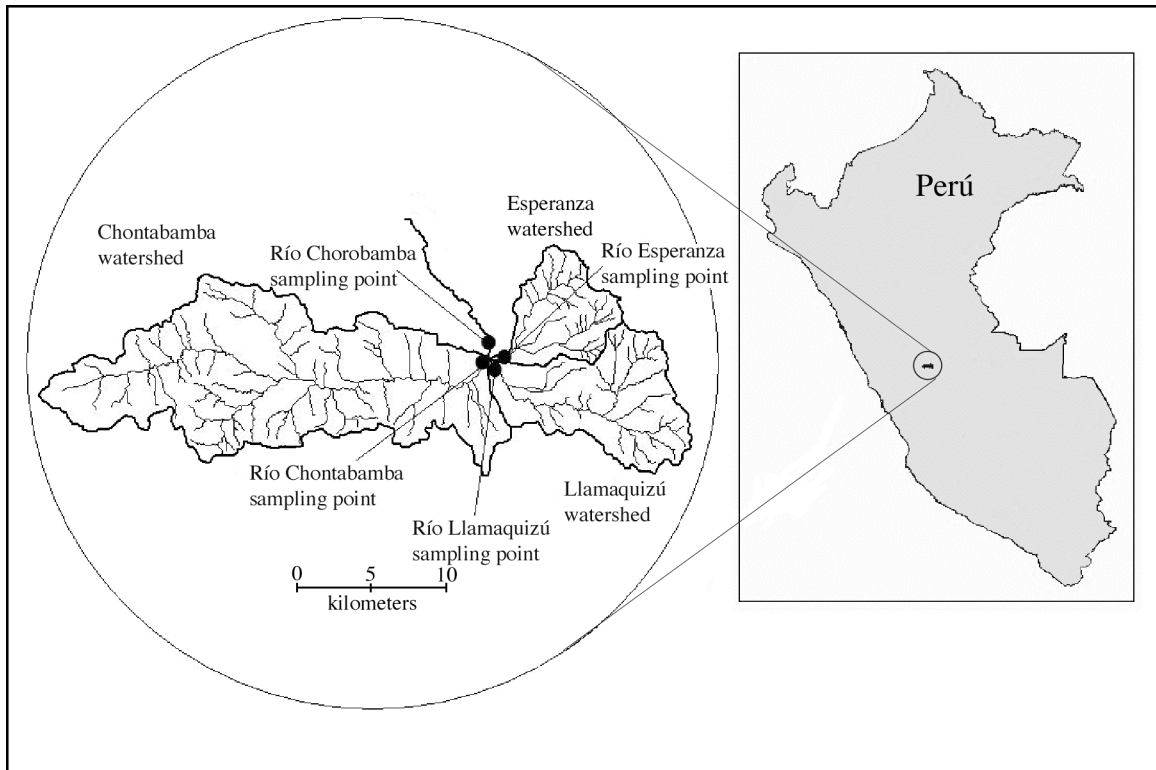


Figure 4.1. Map of the three watersheds and four rivers sampled during this study. Map on right shows the location of the study area within Peru. Map modified from Noguera (2006).

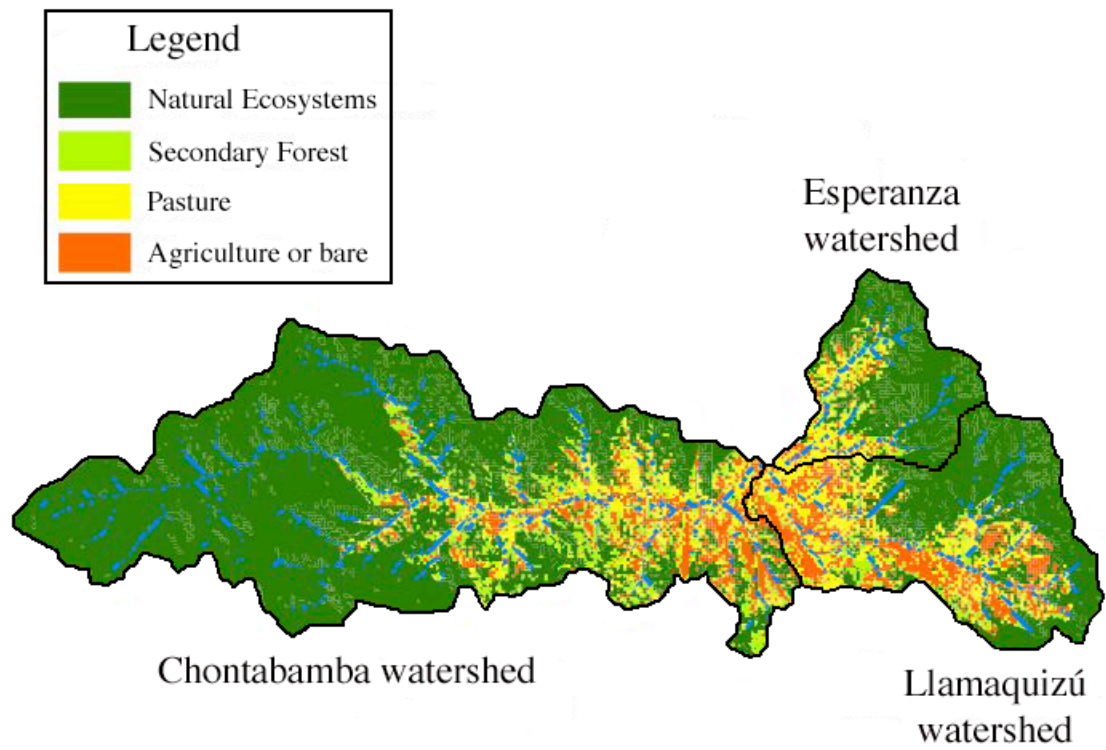


Figure 4.2. Map of the three watersheds in this study delineated by black lines and categorized by land use. Land use data is derived from Noguera (2006).

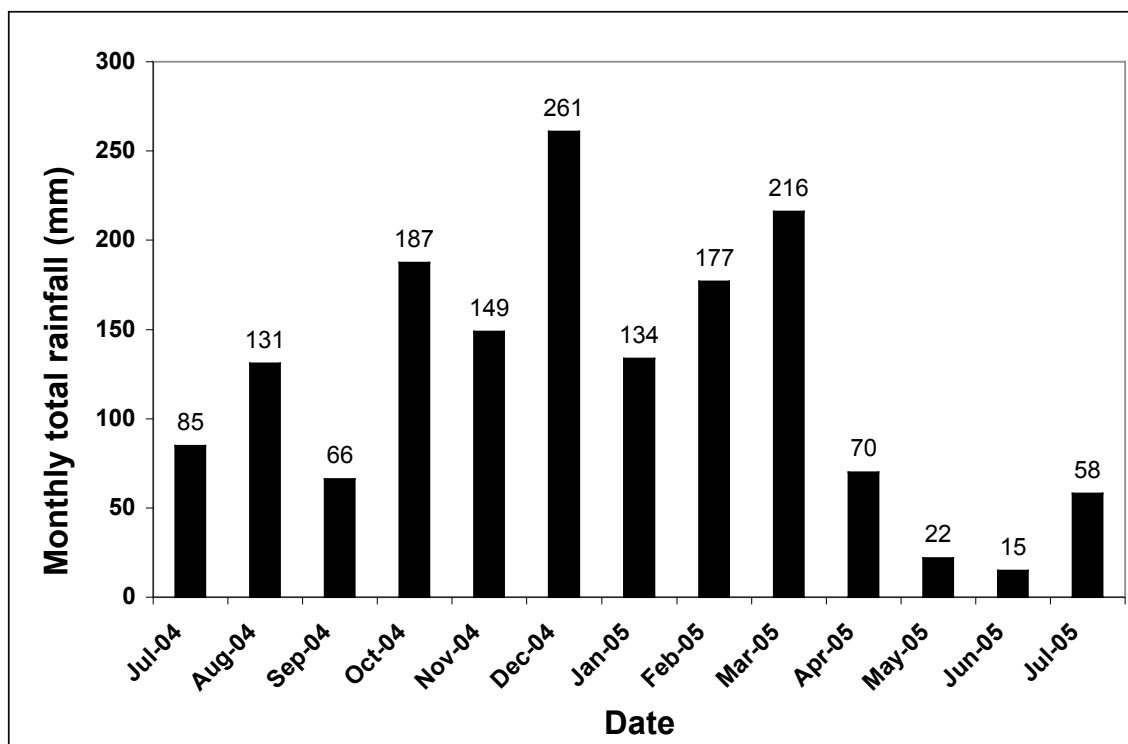


Figure 4.3. Monthly rainfall amounts during the study period, as recorded at the Andean Amazon Research Station in Oxapampa.



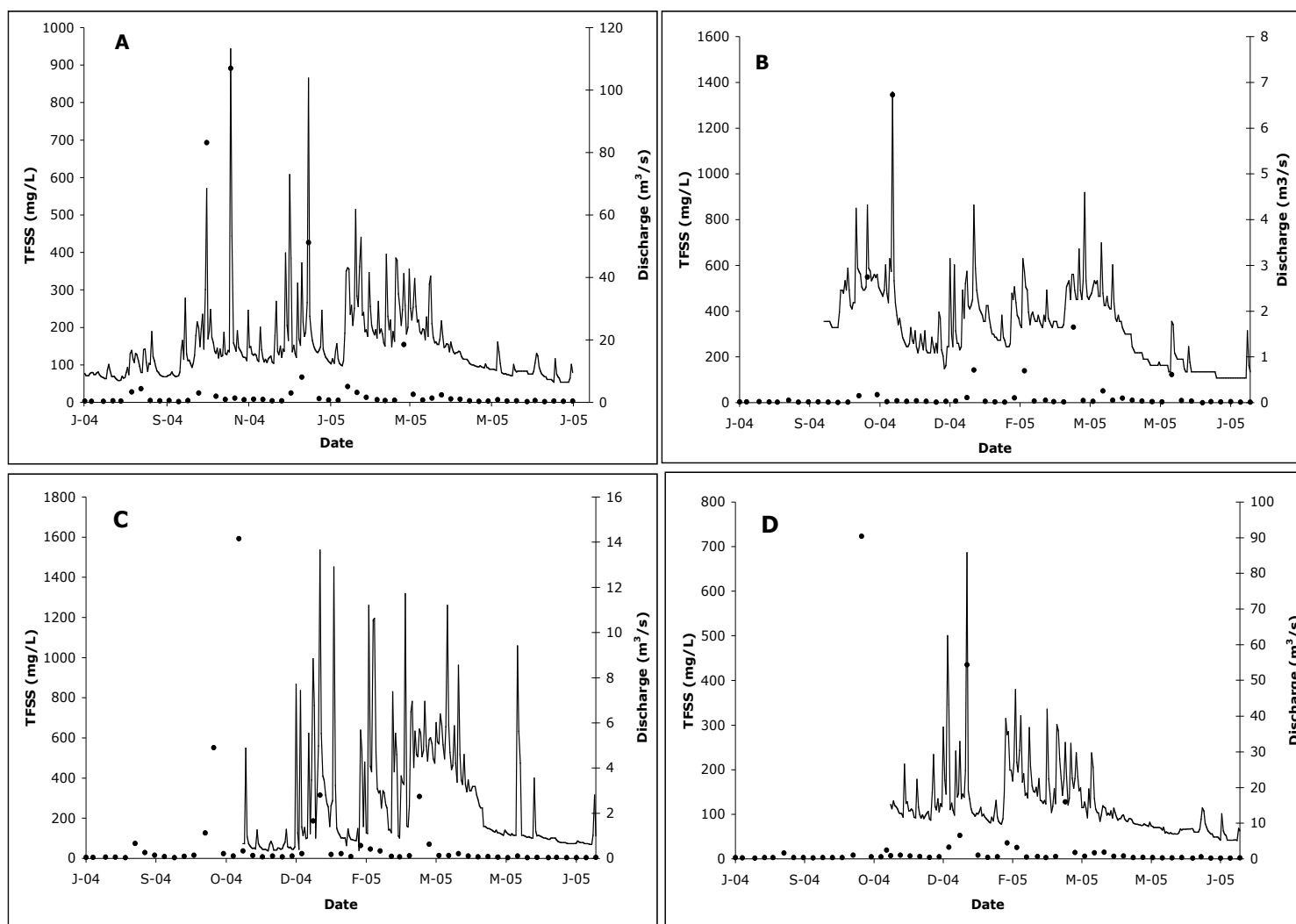


Figure 4.4. Total fine suspended sediment concentration (points) and river discharge (solid line) throughout the experiment, plotted versus time. A = Chorobamba, B = Esperanza, C = Llamaquizú, D = Chontabamba.

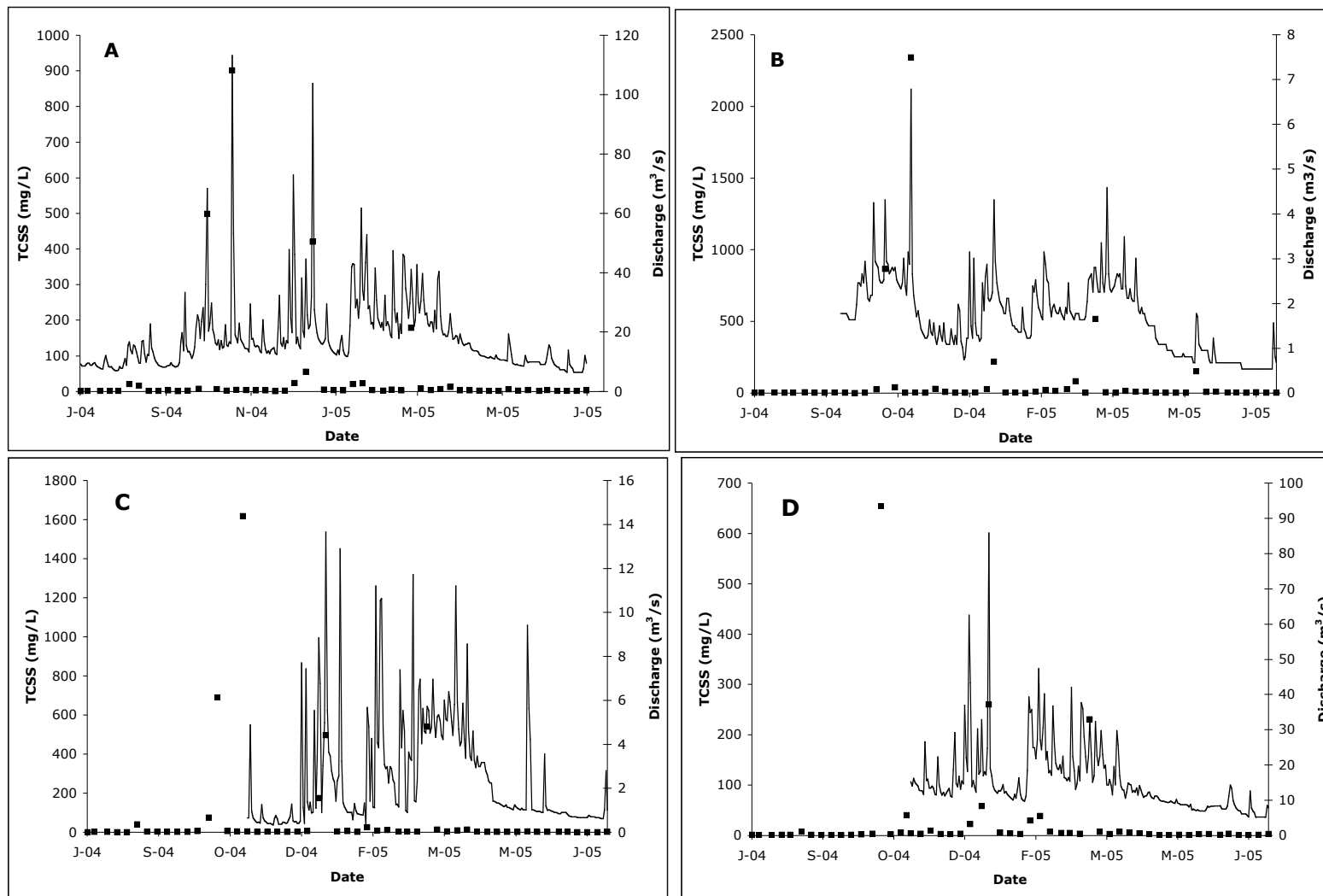


Figure 4.5. Total coarse suspended sediment concentration (points) and river discharge (lines) throughout the experiment, plotted versus time. A = Chorobamba, B = Esperanza, C = Llamaquizú, D = Chontabamba.

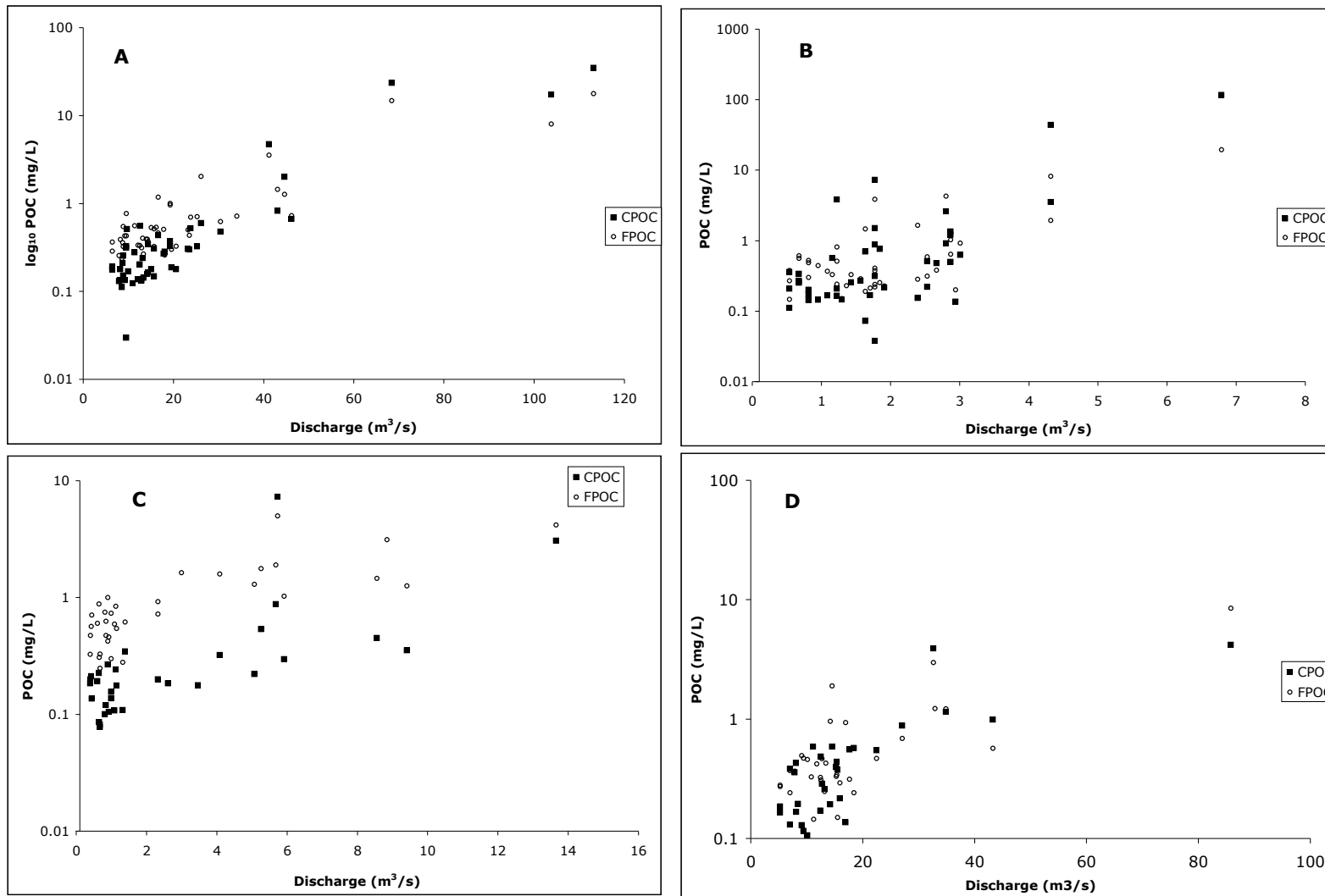


Figure 4.6. Coarse and fine POC concentrations plotted versus river discharge. A = Chorobamba, B = Esperanza, C = Llamaquizú, D = Chontabamba. Note log scale.

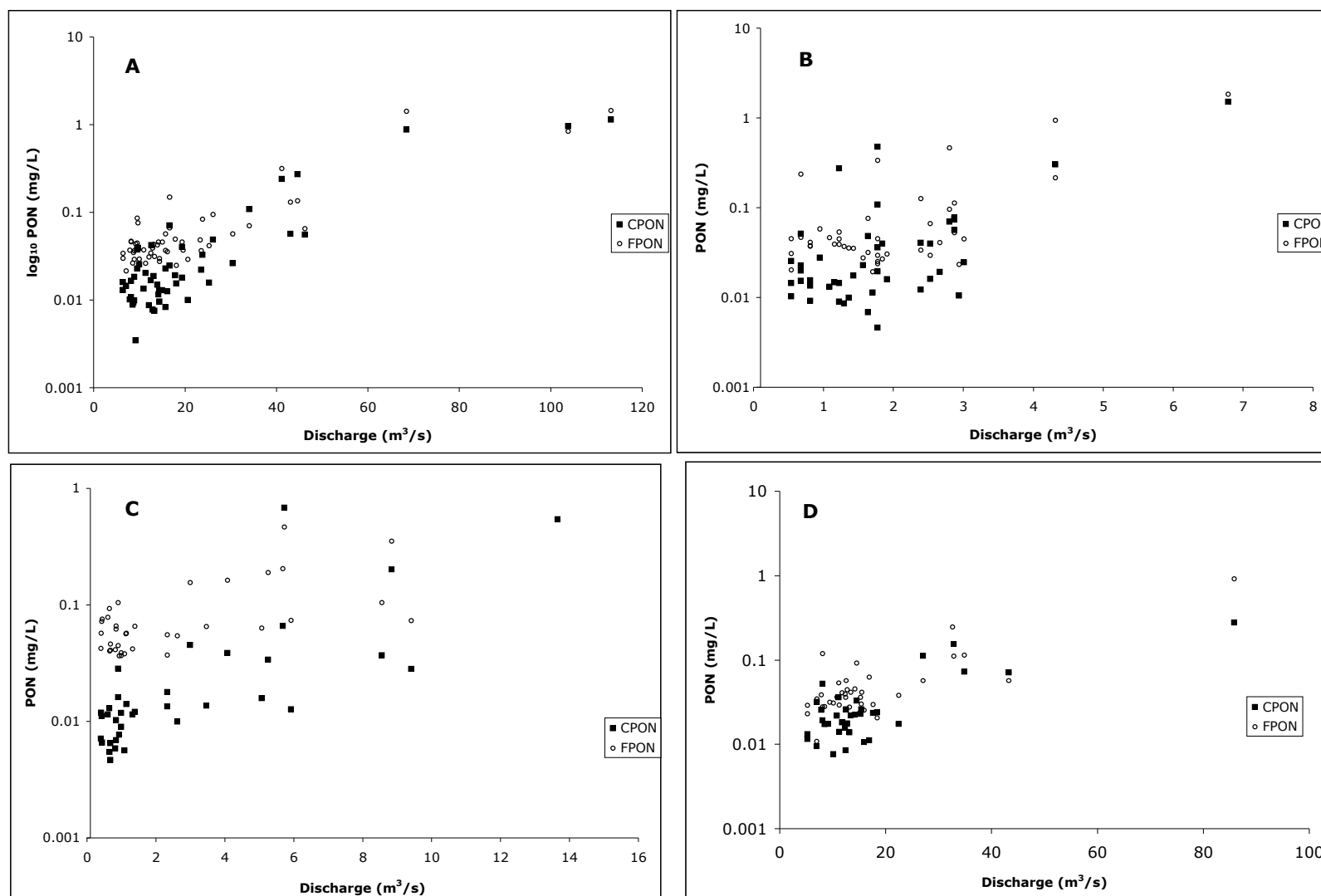


Figure 4.7. Coarse and fine PON concentrations plotted versus river discharge. A = Chorobamba, B = Esperanza, C = Llamaquizú, D = Chontabamba. Note log scale.

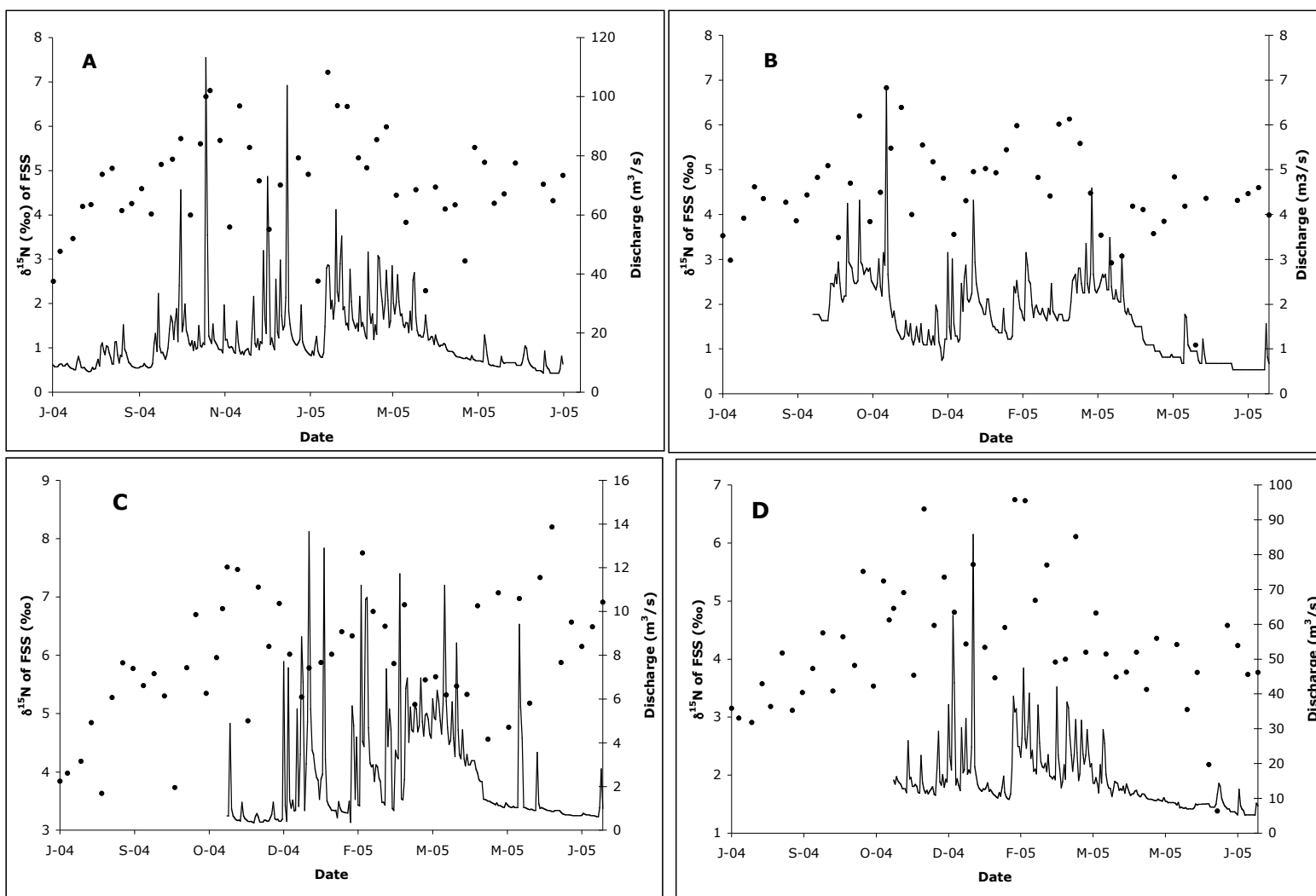


Figure 4.8.  $\delta^{15}\text{N}$  of fine suspended sediments (FSS; points) and river discharge (lines) throughout the experiment, plotted versus time. A = Chorobamba, B = Esperanza, C = Llamaquizú, D = Chontabamba

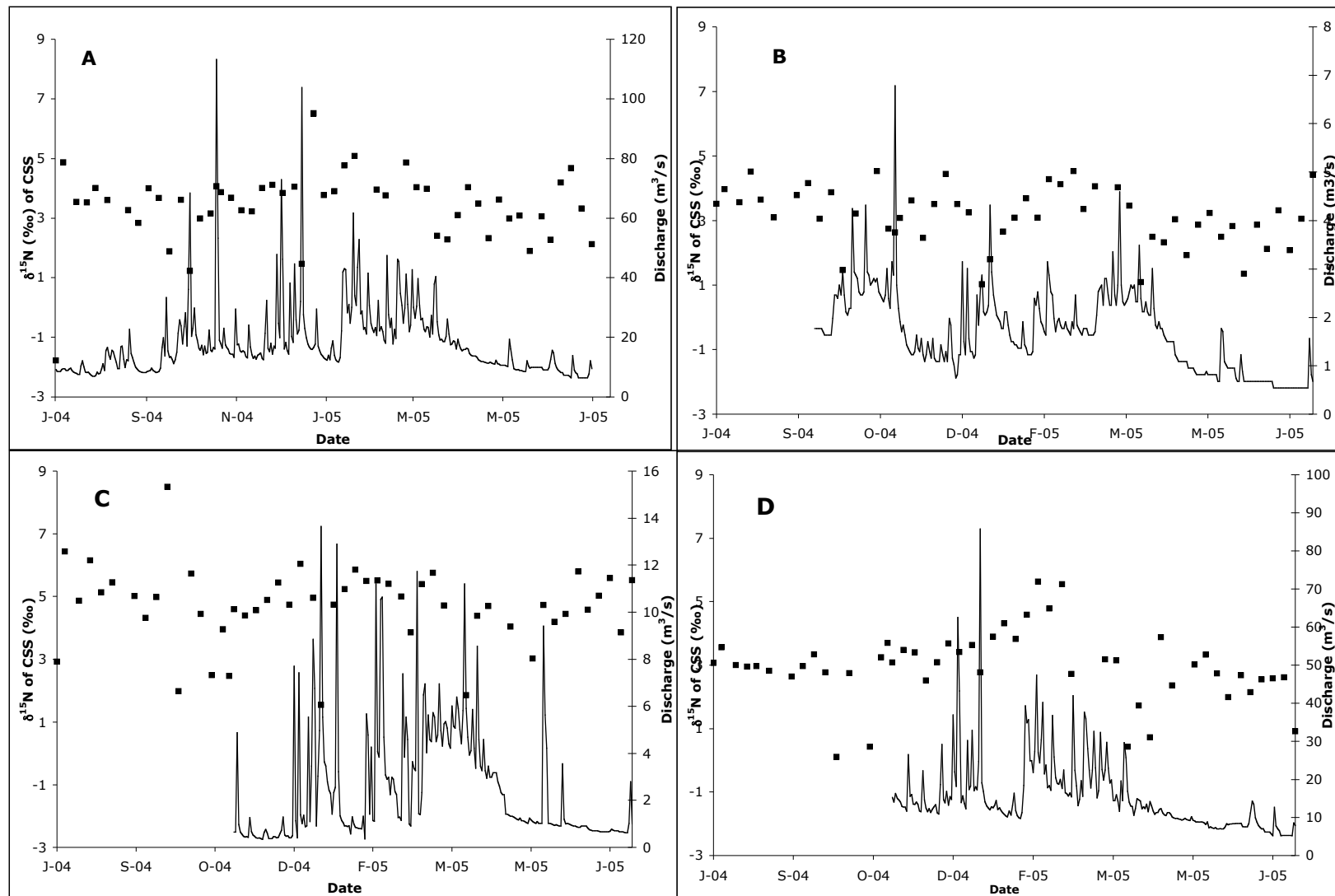


Figure 4.9.  $\delta^{15}\text{N}$  of coarse suspended sediments (CSS; points) and river discharge (lines) throughout the experiment, plotted versus time. A = Chorobamba, B = Esperanza, C = Llamaquizú, D = Chontabamba.

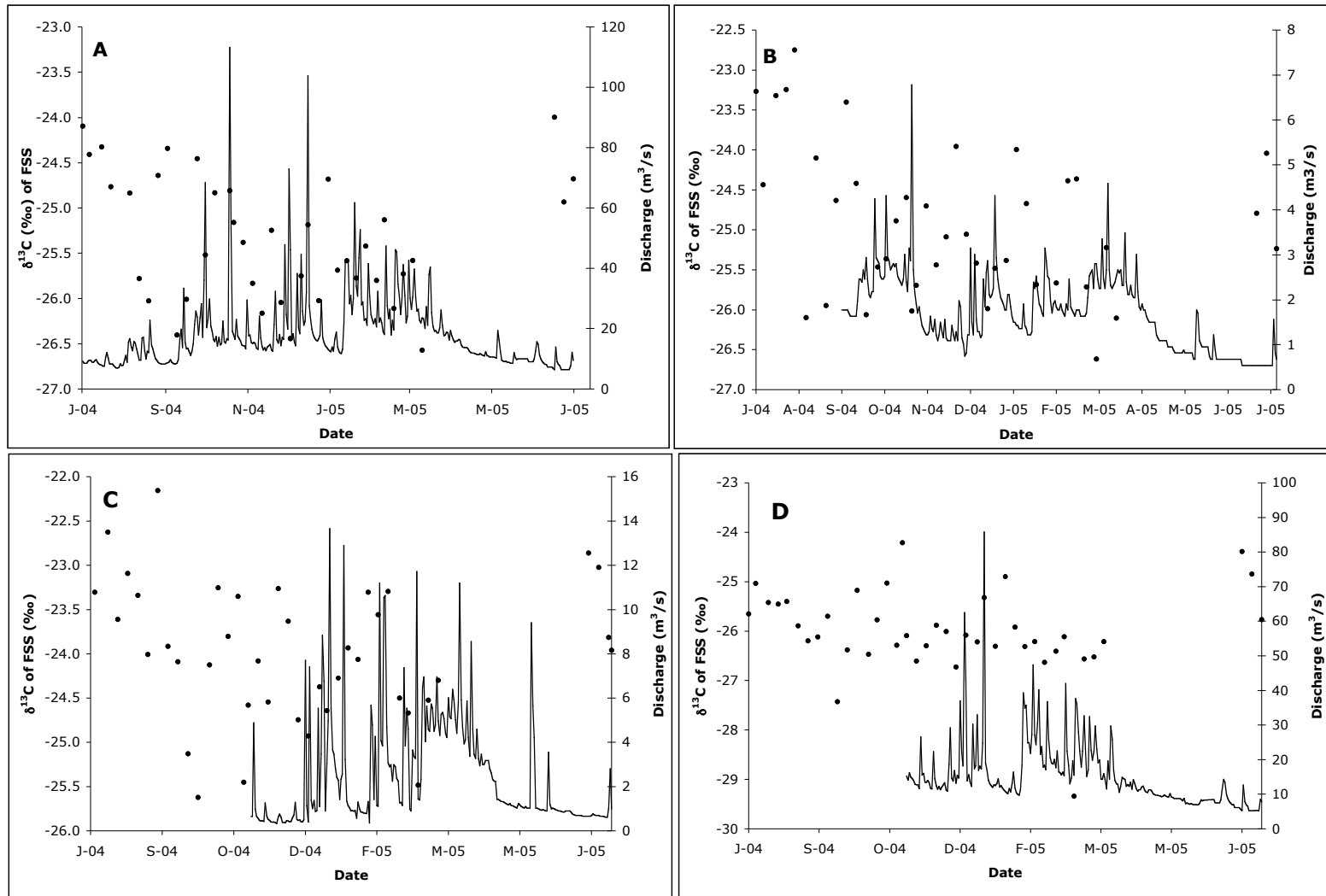


Figure 4.10.  $\delta^{13}\text{C}$  of fine suspended sediments (FSS; points) and river discharge (lines) throughout the experiment, plotted versus time. A = Chorobamba, B = Esperanza, C = Llamaquizú, D = Chontabamba.

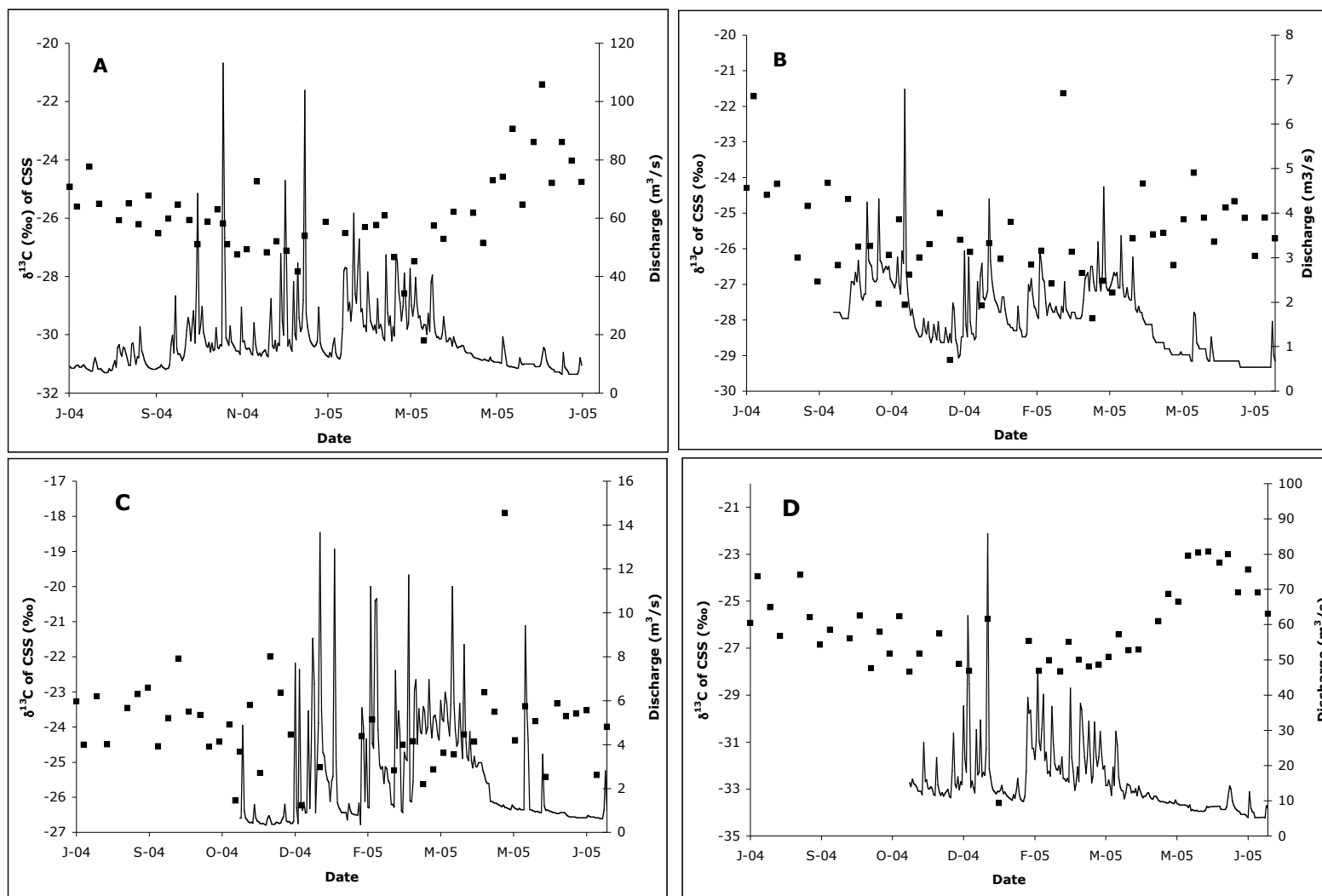


Figure 4.11.  $\delta^{13}\text{C}$  of coarse suspended sediments (CSS; points) and river discharge (lines) throughout the experiment, plotted versus time. A = Chorobamba, B = Esperanza, C = Llamaquíz, D = Chontabamba.



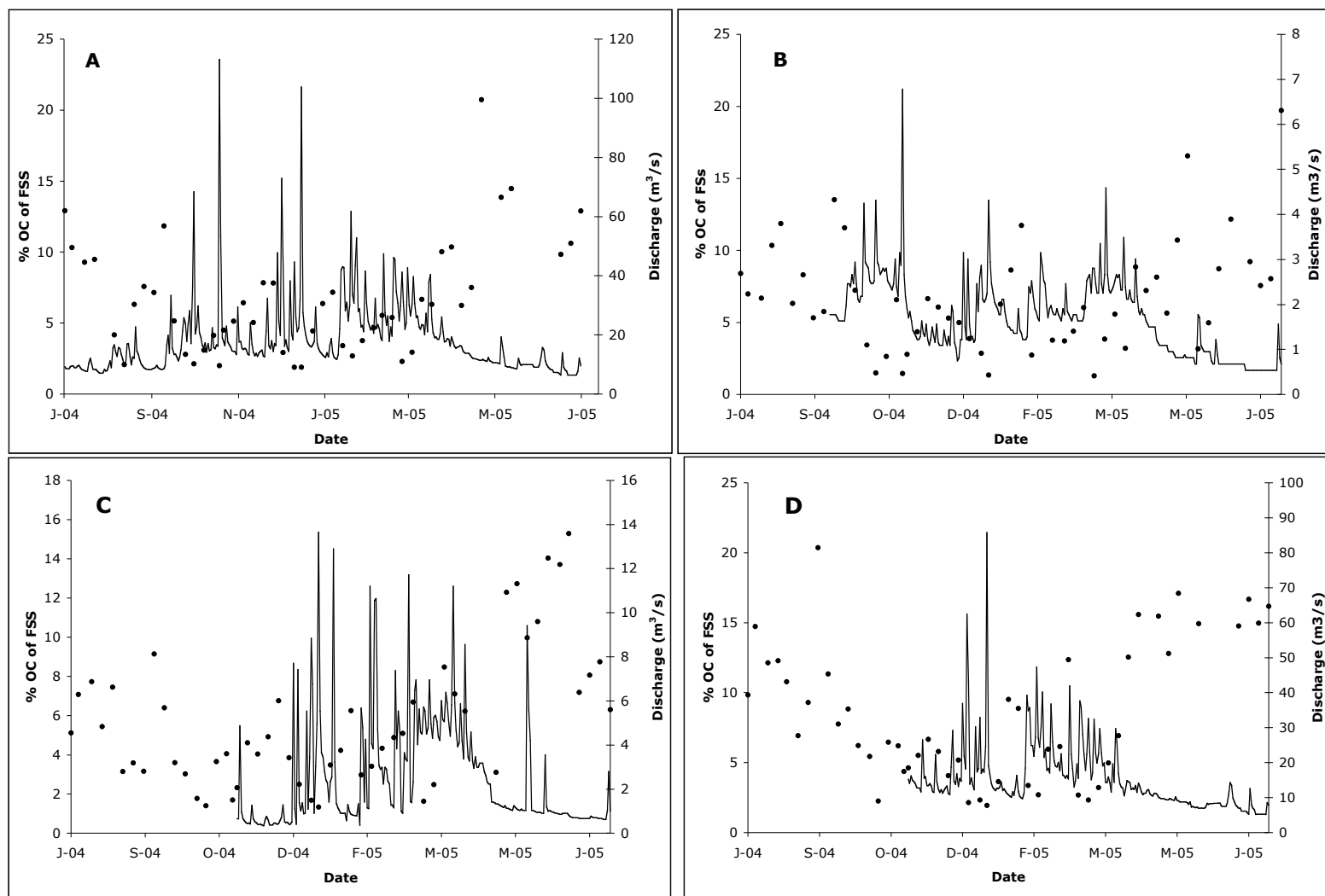


Figure 4.12. Weight percent of OC in fine suspended sediments (FSS; points) and river discharge (lines) throughout the experiment, plotted versus time. A = Chorobamba, B = Esperanza, C = Llamaquizú, D = Chontabamba.

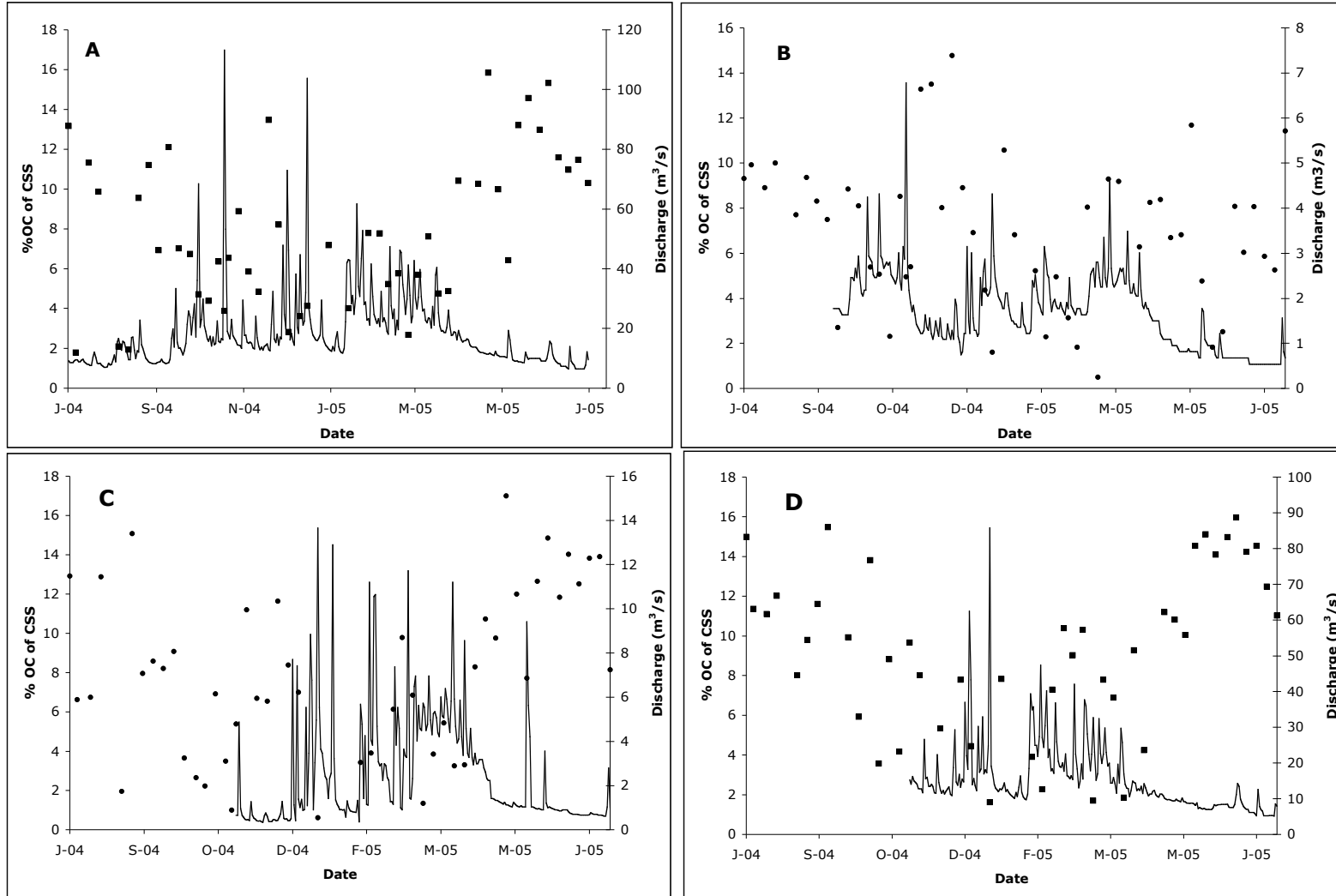


Figure 4.13. Weight percent of OC in coarse suspended sediments (CSS; points) and river discharge (lines) throughout the experiment, plotted versus time. A = Chorobamba, B = Esperanza, C = Llamaquizú, D = Chontabamba.

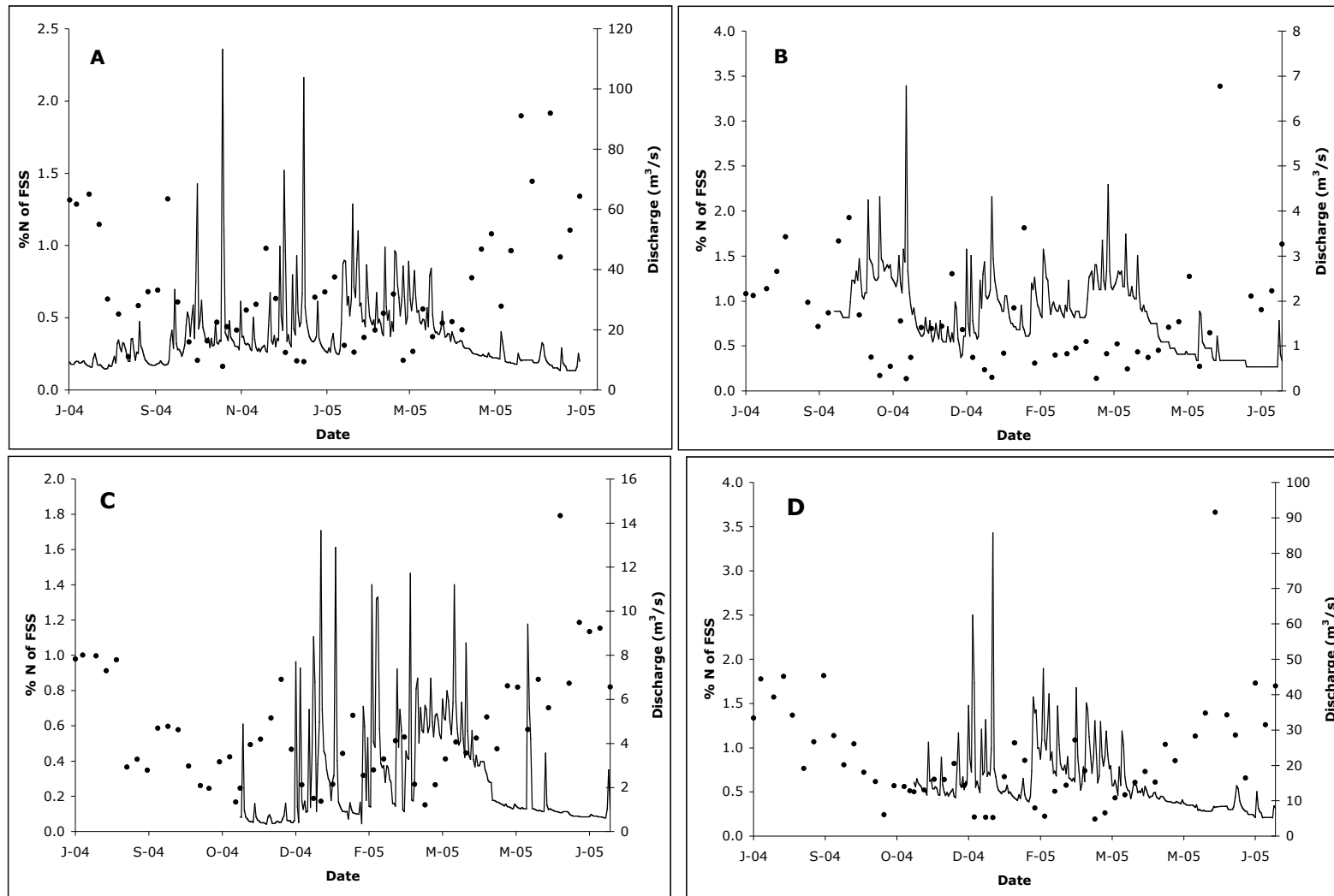


Figure 4.14. Weight percent of N in fine suspended sediments (FSS; points) and river discharge (lines) throughout the experiment, plotted versus time. A = Chorobamba, B = Esperanza, C = Llamaquizú, D = Chontabamba.

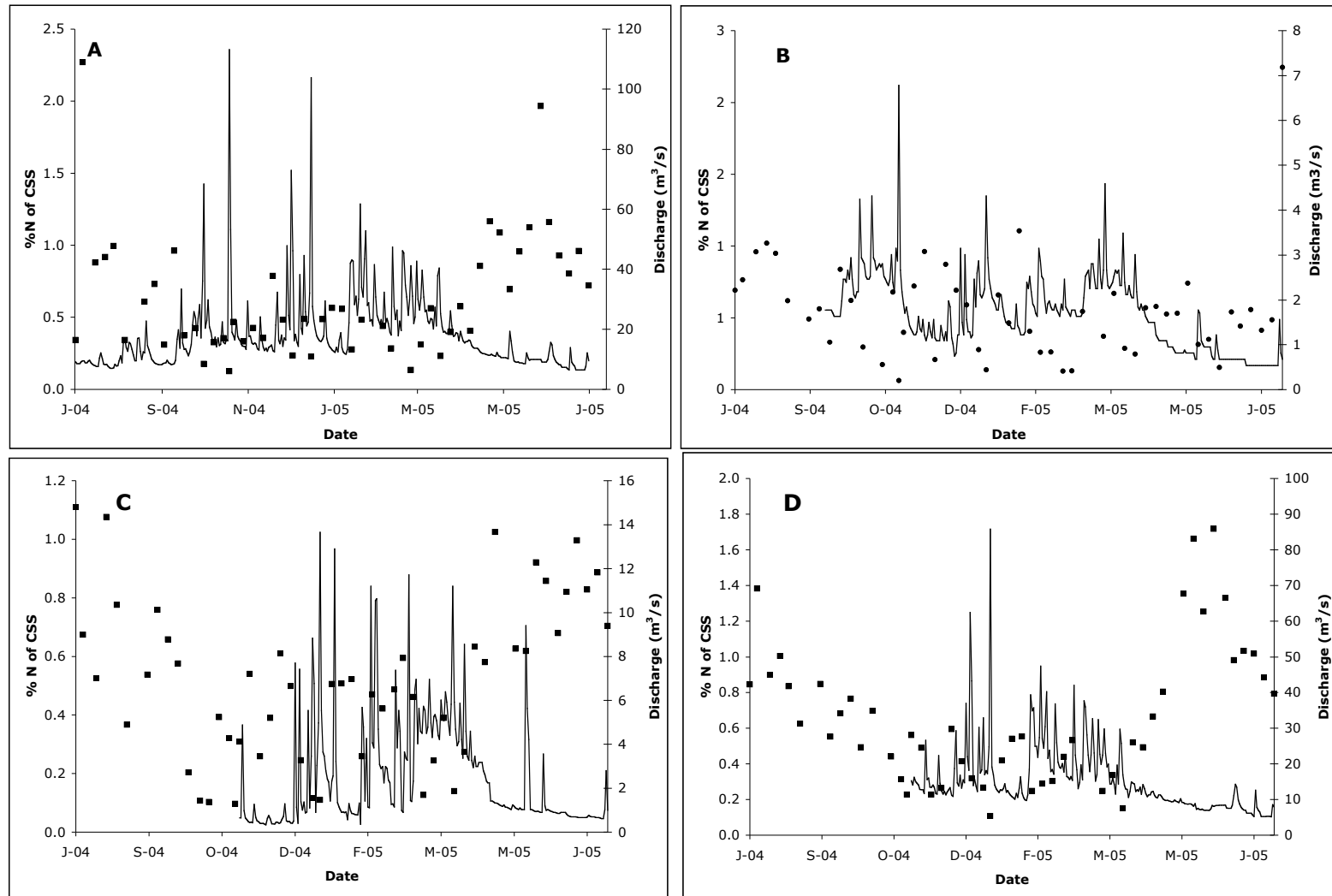


Figure 4.15. Weight percent of N in coarse suspended sediments (CSS; points) and river discharge (lines) throughout the experiment, plotted versus time. A = Chorobamba, B = Esperanza, C = Llamaquizú, D = Chontabamba.

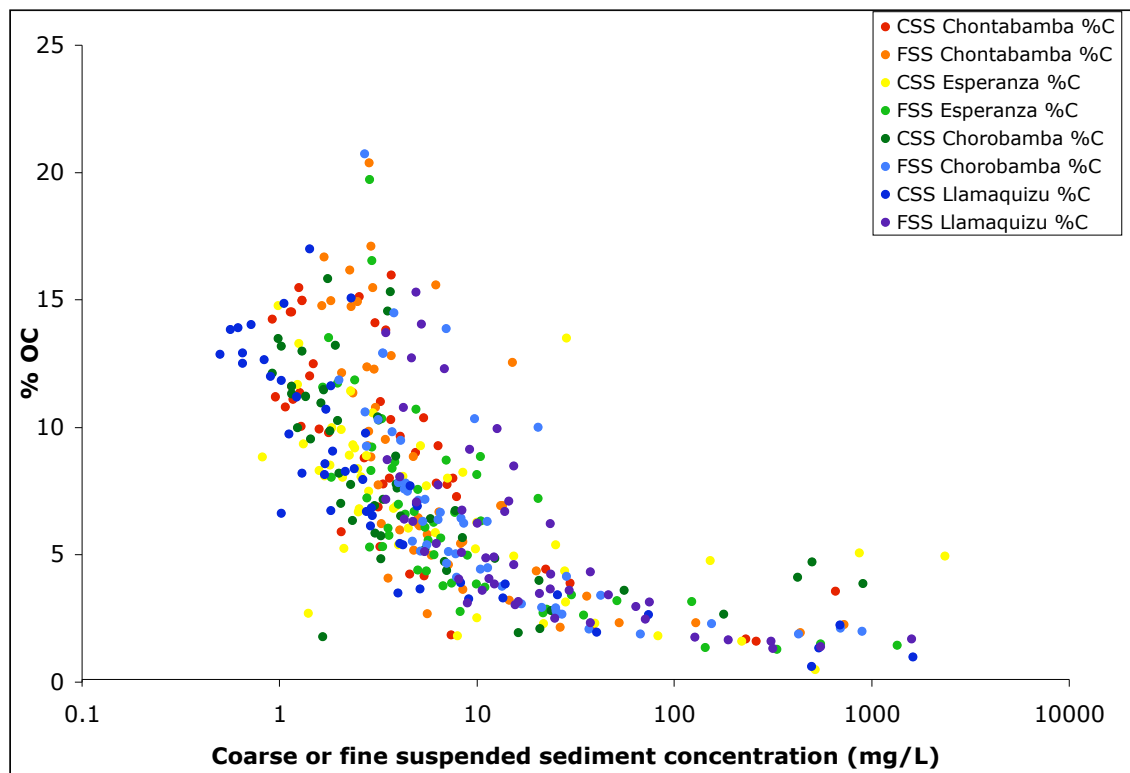


Figure 4.16. Percent organic carbon (OC) plotted versus the concentration of fine and coarse suspended sediments (FSS and CSS). Note the log scale for CSS and FSS concentration.

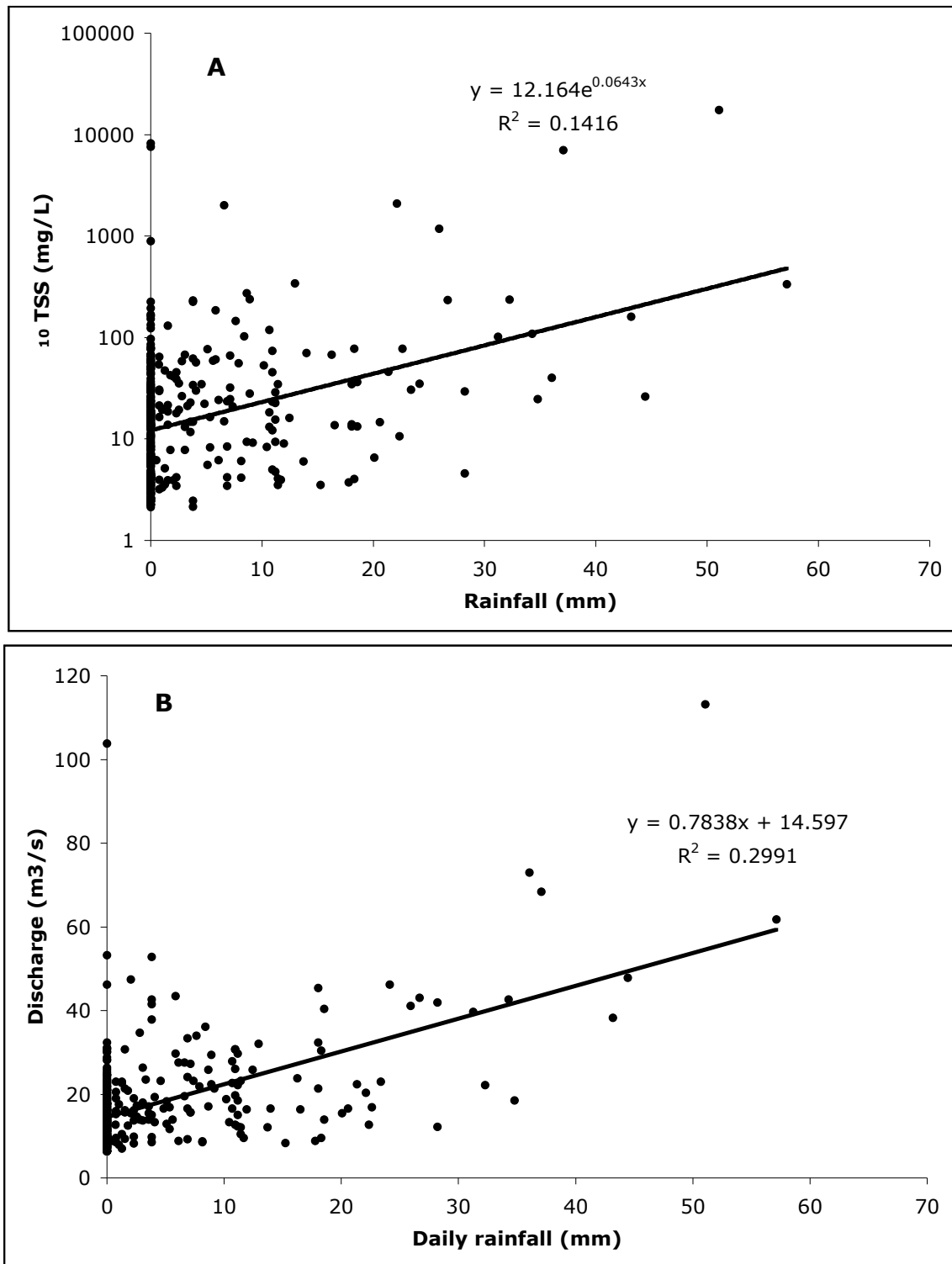


Figure 4.17. Relationship of TSS (A) and river discharge (B) in the Chorobamba River with rainfall measured at the Andean Amazon Research Station. Note the log scale in the y-axis of (A).

## **Chapter 5: Natural abundance isotopic indicators of carbon and nitrogen sources and cycling in old-growth and deforested cloudforest catchments of the Peruvian Andean Amazon**

### **ABSTRACT**

Stable isotopes are useful indicators of large-scale transport of organic matter from terrestrial to aquatic ecosystems, but small-scale studies are needed to confirm hypotheses about sources and diagenetic history. In this study I analyzed carbon (C) and nitrogen (N) stable isotopic and elemental ratios in organic matter (OM) in two small (~5 ha) catchments in the Amazon headwaters of Peru: one recently deforested and one old-growth forest. Precipitation was a major source of enriched dissolved organic N (DON) to both catchments, although DON concentrations were higher in throughfall (rain that passes through the forest canopy) than in rain falling in a clearings. Epiphytic plants living in the canopy of the old-growth site have more depleted  $\delta^{15}\text{N}$  signatures than rooted plants in either catchment. Leaf litter decomposition and soil OM formation complicate the isotopic composition of residual OM, indicating that  $\delta^{13}\text{C}$  and  $\delta^{15}\text{N}$  may not be appropriate indicators of diagenetic history in this system. This research suggests that observed N cycling differences between pristine and impacted ecosystems may be due to a disruption of canopy nutrient cycles during deforestation, representing a significant loss of sequestered C and N in deforested regions. This study supports the idea that ecosystems unaffected by anthropogenic N deposition have very little inorganic N storage or export.

## INTRODUCTION

The cloudforests of the Andean Amazon (located from about 3500 to 1500 meters above sea level in the Andes Mountains) are minimally impacted by atmospheric pollution (such as N deposition) and other human impacts such as deforestation, urbanization, and agriculture. These environments have different biogeochemical characteristics than similar ecosystems located in industrialized areas, such as the dominance of dissolved organic over inorganic N losses in pristine forest streams (Perakis and Hedin 2001, 2002). Studying unimpacted areas provides baseline information needed to determine how nitrogen cycling in aquatic and riparian systems has been altered anthropogenically, and provide an opportunity to evaluate the influence of human impacts on biogeochemical theory (Hedin et al. 1995). In other words, studies such as these can help to identify how ecosystems function without additional anthropogenic reactive N (Galloway et al. 2003). Studies of small headwater streams are particularly important, as these systems exert disproportionate control on the nitrogen cycle in large river basins (Peterson et al. 2001).

The Peruvian Andes are under tremendous pressure for conversion into farmland or urban areas (McClain and Naiman in prep): by studying how whole-catchment biogeochemistry changes with deforestation, one can predict the large-scale impacts of deforestation on the ecology of the Amazon headwaters and other regions. The cloud forests of the Amazon basin are a major source of sediments and associated organic matter to upland Amazonian tributaries (Chapter 2, this volume). Deforestation has a complicated impact on river hydrology and biogeochemistry in this area (Chapter 4, this volume), but erosion is often greater in deforested montane catchments than in pristine ones, and deforestation can lead to an increased dominance of runoff over baseflow in streams (Ludwig and Probst 1998, Walling 1999).



Dissolved organic N (DON) dominates N losses from South American old-growth forests (Hedin et al. 1995, Perakis and Hedin 2001), as opposed to streams in industrialized areas where nitrate ( $\text{NO}_3^-$ ) losses dominate (Perakis and Hedin 2002). For an ecosystem at equilibrium, dissolved nitrogen export is balanced by inputs of new nitrogen such as  $\text{N}_2$  fixation, natural atmospheric deposition, or erosion and weathering of geological nitrogen (Perakis and Hedin 2002, Holloway et al. 1998). In particular, fog and clouds can be a significant source of water and nutrients to tropical montane cloud forests (Asbury et al. 1994, Clark et al. 1998b, Chang et al. 2002). In this study we analyze the inputs of N into high altitude cloudforest ecosystems by measuring N content and composition in rain and throughfall, in plants and soils in the forest canopy, and in stream N exports.

Epiphytes are an often-overlooked portion of biomass in tropical forests (Clark et al. 1998a, Nadkarni et al. 2004). They may represent completely separate biogeochemical cycles that are disconnected or minimally connected to the traditional soil-root-leaf N cycle because they live exclusively in the forest canopy. However, when these epiphytes die or fall to the ground, or release organic and inorganic N, they represent a new N source to forest floor communities. Deforestation and regrowth of secondary forests abruptly halts N cycling in canopy communities, and may cause large-scale disruptions in N cycling to the forest or to the watershed as a whole (Benzing 1998). The implications of deforestation and the subsequent loss of epiphytic N on terrestrial ecosystems are broad and understudied. Epiphytes obtain N in one of two ways: through the atmosphere, via wet or dry deposition or through  $\text{N}_2$  fixation; or via roots in canopy soils, which are usually derived from a mixture of host and epiphyte detritus (Coxson and Nadkarni 1995). Thus, canopy communities can represent both a sink for atmospheric fixed N (Clark et al. 2005) and a source of N to communities

growing on the forest floor (Coxson 1991, Vera et al. 1999). Litter from the host tree can be intercepted by canopy ecosystems and incorporated into canopy soils (Nadkarni and Matelson 1991). Stable isotopic analysis is a convenient tool to identify epiphytic N and C sources (Heitz et al. 2002). Because epiphytes growing in forest canopies lack access to soil nutrients available to rooted plants, their  $\delta^{15}\text{N}$  values often differ from those of host plants. Concurrent analysis of weight percents of C and N with stable isotopes in epiphyte leaves contributes to determination of chemical budgets in these systems.

The isotopic and elemental effects of leaf litter decomposition and soil organic matter formation are well studied but vary significantly depending on climate, amount of precipitation, and litter quality (Aber and Melillo 1991, Krull et al. 2003). In addition, the mechanisms of changes in stable isotopic content during the decomposition process are hotly debated (Ehleringer et al. 2000, Lehmann et al. 2004). Small scale studies of isotopic patterns in whole ecosystems are necessary to validate studies that attempt to use stable isotopes as tracers of organic matter processing in larger basins, such as the studies presented previously in this dissertation (Chapters 2, 3, and 4; this volume).

Only a few studies have addressed the biogeochemistry of cloud forest ecosystems, and several questions still remain. What are the sources of N to cloudforest headwater catchments? What can natural stable isotopic signatures tell us about C and N cycling in natural and impacted forest systems? How will land use change, specifically deforestation, change C and N dynamics and export in forested headwaters of the Amazon River? To answer these questions, we performed a series of experiments in two small headwater catchments in the Peruvian Andean Amazon, located at about 2500 meters above sea level (masl). One catchment was pristine forest; the other was completely deforested in 1999.

## STUDY AREA

This study was conducted in the Parque Nacional Yanachaga-Chemillen, located on the eastern flank of the Peruvian Andes in the Amazon headwaters (Figure 5.1). This area is characterized by lower montane tropical cloud forests. We sampled two adjacent headwater stream catchments in the park. One stream basin (“Wara”) is located within Yanachaga-Chemillen National Park and the other (“Killa”) is just outside the park border. The two catchments are about 500 m apart and are both located at approximately 2400 meters above sea level. Killa was completely deforested and burned for experimental purposes in 1999, while Wara is classified as a primary forest. Wara is approximately 4.5 ha in area, and Killa is about 3.8 ha. The sites are approximately 4 km away from the Andean Amazon Research Station in Oxapampa. The average annual temperature at the field station is 15°C and the average annual rainfall is 2302 mm. The average annual rainfall in the park is approximately the same, but the temperature is about 1° lower (Catchpole 2004). It rains frequently in the park and the forest canopy is almost always in constant contact with clouds and mist. Epiphyte biomass is extensive in the pristine sections of the forest (Catchpole 2004).

## Methods

*Sample collection*—Rain and throughfall were collected weekly from the Parque Nacional Yanachaga-Chemillen from February to July 2004 (Gomez 2005). Rain collectors were located near the Wara stream. Rain was collected in a small (1000 m<sup>2</sup>) clearing near the weather station. Throughfall was collected below a large tree in an old-growth section of the forest. Sample collection protocol was as follows: acid washed and rinsed plastic bottles were placed on the rain collectors, and the following day any rain or throughfall was transferred to pre-cleaned, pre-combusted amber borosilicate vials, then

immediately transported to the field station in Oxapampa, where they were frozen (Keene et al. 2002) until analysis in Texas.

Epiphytes and canopy soils were collected in 2003 from a mature *Ficus* tree located in the Wara catchment. Vascular epiphytes (bryophytes and orchids) were collected according to the zonation scheme of Johansson (1974), shown in Figure 5.2. Epiphytes were only found in zones 3, 4, and 5. Zone 3 is located on the upper trunk of the tree, zone 4 is the innermost part of the canopy, and zone 5 is the middle of the canopy. Epiphytes were collected using rope access and traditional arborist techniques (Catchpole 2004), which allow for epiphyte sampling without removing branches and with minimal disturbance.

The isotopic and elemental effects of leaf litter decomposition were analyzed in a 10 month litter bag study. The leaves of two species of very common trees in the Wara catchment (Gomez 2001), one from the upper canopy (species A) and one from the lower canopy (Species B) were selected for the experiment. Fresh leaves were dried at 60° C to constant mass at the field station in Oxapampa. The leaves were broken into 500 mg pieces and placed in litter bags made from 1 mm mesh nylon plankton net. A set of 12 bags for each species were placed on the soil and nailed down to approximate the fate of leaves that fall to the forest floor. Two more sets were placed in the stream and anchored in place to the datalogger near the weir. One of each type of bag for each treatment was removed approximately every 30 days. The bags were returned to the field station where they were dried at 60°C for 48 hours, then removed from the oven and stored in a cool (~ 15° C) dark place in sealed plastic bags until the end of the experiment, when the leaves were removed and weighed, then taken back to the laboratory in Texas for C and N elemental and isotopic analysis. Transport from the park to the field station was

controlled for: samples from the first time point were brought to and from the park on the first day of the experiment.

Samples for comparison of the pristine and deforested catchments were collected from 2000 to 2004. Stream suspended particulates were filtered in the field from water sampled at the mouth of both watersheds (Figure 5.1) onto pre-combusted glass fiber filters (Whatman GF/F). Plants and soil horizons were collected in pre-cleaned, pre-combusted glass vials. Soils were collected in the summer of 2004. Two soil pits were dug in each watershed, within 5 meters of each other and of the weir at the mouth of each watershed. Soils in this area are very thin (less than 6 inches), and samples were taken from the organic (O) horizon, the A horizon, and the mineral layer (mostly carbonates). All solid samples were dried at 60°C at the Andean Amazon Research Station in Oxapampa for 48 hours and then tightly sealed until they could be analyzed at the University of Texas Marine Science Institute. Stream dissolved N samples were filtered in the field through 0.2 µm nylon syringe filters into 40 ml pre-cleaned, pre-combusted amber borosilicate vials containing 40 µl of concentrated H<sub>2</sub>SO<sub>4</sub> as a preservative. These were kept in a cool, dark place until they could be transported back to the USA.

*Sample analysis*—Particulate (soils, sediments, plants) samples were analyzed for δ<sup>15</sup>N, δ<sup>13</sup>C, %N by weight, and %C by weight on a Carlo Erba elemental analyzer interfaced with a Finnigan MAT Delta PLUS isotope ratio mass spectrometer at the University of Texas Marine Science Institute. Inorganic C was removed from soil and suspended particulate samples prior to organic C analysis by vapor phase acidification with HCl for 24 hours (Hedges and Stern 1984), followed by drying at 60° for 24 hours. Samples for nitrogen analysis were not acidified.

Nitrogen isotopic composition of NO<sub>3</sub><sup>-</sup> was determined using a bacterial method (Sigman et al. 2001). Total dissolved N (TDN) concentrations were analyzed after

persulfate oxidation (Valderrama 1981, Bronk et al. 2000). Nitrogen isotopic composition of TDN was analyzed by converting TDN to  $\text{NO}_3^-$  by persulfate oxidation (Valderrama 1981, Bronk et al. 2000), then converting  $\text{NO}_3^-$  to  $\text{NO}_2^-$  (Jones et al. 1984), and finally by converting  $\text{NO}_2^-$  to  $\text{N}_2\text{O}$  using a modification of the azide method (McIlvin and Altabet 2005). The azide method was modified to allow for smaller sample volumes and  $\text{NO}_3^-$  concentrations. The procedure is similar to the method presented in Knapp et al. (2005), except that we used the azide reaction as opposed to denitrifying bacteria to convert  $\text{NO}_2^-$  to  $\text{N}_2\text{O}$ . Nitrous oxide was analyzed for  $\delta^{15}\text{N}$  using a ThermoFinnegan Trace GC gas chromatograph with an in-line preconcentrator unit coupled to the isotope ratio mass spectrometer at UTMSI.

## RESULTS

Nitrate concentrations in both rain and throughfall were negligible. The concentrations and  $\delta^{15}\text{N}$  of TDN in rain and throughfall throughout the study period are presented in Table 5.1 and Figure 5.3. The average concentration of TDN in throughfall was significantly higher than the average concentration in rain ( $p < 0.001$ , Figure 5.3A), but there was no difference in  $\delta^{15}\text{N}$  of rain and throughfall (Figure 5.3B).

Vascular epiphytes were depleted in  $^{15}\text{N}$  with respect to the atmosphere (Table 5.2). The  $\delta^{15}\text{N}$  of epiphyte leaves decreased with distance into the canopy. Epiphytes in zone 3 were more enriched in  $^{15}\text{N}$  than those in zone 4 ( $p = 0.02$ ) and zone 5 ( $p = 0.001$ ), and zone 4 was more enriched than zone 5 ( $p = 0.04$ ). The average values of  $\delta^{15}\text{N}$ , %N,  $\delta^{13}\text{C}$ , and %C for each species of epiphyte sampled are also shown in Table 5.2. The classification scheme for these vascular orchids is shown in Figure 5.4. Three classes are represented: Monocotyledonia, Pteridophyta, and Dicotyledonia. Two families of Monocotyledonia were represented: Orchidaceae and Bromeliaceae, with five and two

different species, respectively. There was one family (Lomariopsidaceae) and two species of Pteridophyta. One family (Ericaceae) and two species represented Class Dicotyledonia. In general, monocots were more enriched in  $^{15}\text{N}$  (average  $\delta^{15}\text{N} = -2.9 \pm 1.2\text{‰}$ ) and significantly different than dicots and pteridophytes (average  $\delta^{15}\text{N} -5.7 \pm 1.0$  and  $-6.2 \pm 1.9\text{‰}$ , respectively), which were not significantly different from each other (Figure 5.5A). The average  $\delta^{15}\text{N}$  of each family were significantly different from each other, except that the  $\delta^{15}\text{N}$  of Lomariopsidaceae and Ericaceae were the same (Figure 5.5B). On the genus level, many species had significantly different  $\delta^{15}\text{N}$  signatures regardless of zone. Most notably, the *Vriesia* samples (the bromeliads) had a significantly higher  $\delta^{15}\text{N}$  than any other species (Figure 5.5C). On the other hand, the *Disterigma* and *Elaphoglossum* species had significantly lower  $\delta^{15}\text{N}$  than almost all of the other species sampled (Figure 5.5C).

The  $\delta^{13}\text{C}$  and  $\delta^{15}\text{N}$  of soil horizons in the forested and deforested plots are shown in Figure 5.6. In most cases, the  $\delta^{13}\text{C}$  of soil organic matter increases with depth in the soil profile, but this trend is not evident in all of the soil sampling locations (Figure 5.6A), despite the fact that soil samples were taken very close to each other for each watershed. There was a more defined trend for  $\delta^{15}\text{N}$  (Figure 5.6B), and the  $\delta^{15}\text{N}$  values were more similar to each other than the  $\delta^{13}\text{C}$  values. There was one soil sampling site (Wara B) where there was no trend in  $\delta^{13}\text{C}$  and  $\delta^{15}\text{N}$  with soil depth. The profiles of %OC and %N are much more clear for these soils. In all cases, the %OC and %N was much higher in the organic layer (mostly composed of leaf litter), decreased sharply in the A horizon, and then stayed about the same in the mineral horizon (Figure 5.7). Soils on the forest floor had much less C and N by weight than canopy soils (Table 5.2).

Leaf litter mass decreased predictably with decomposition time (Figure 5.8). By the end of ten months, almost no leaf of either species remained in either treatment. The

samples in the stream decayed more slowly, or at least they had greater mass remaining, than the samples decomposing on the forest floor. However, by the end of the experiment the soil treatment samples were larger in mass than those in the stream (Figure 5.8). Unlike the leaf mass, there was not a predictable relationship between decomposition time and either  $\delta^{13}\text{C}$  or  $\delta^{15}\text{N}$  of the remaining leaf material (Figure 5.9). For species A, in both treatments  $\delta^{13}\text{C}$  was periodically elevated up to 5‰ over the initial substrate. Species B  $\delta^{13}\text{C}$  was more consistent, although still somewhat variable, throughout the experiment.  $\delta^{13}\text{C}$  was never much lower than initial values in any of the treatments (Figure 5.9).  $\delta^{15}\text{N}$ , on the other hand, decreased initially in both soil treatments. In species A, the  $\delta^{15}\text{N}$  was always lower in the soil treatment than the initial observation. In both stream treatments,  $\delta^{15}\text{N}$  fluctuated throughout the experiment and to an eventual value that was slightly higher than the initial observation (Figure 5.9B). Percent of OC and N by weight did not decrease with decreasing leaf mass (Figure 5.10 A and B). Percent OC decreased gradually in the samples decomposing in the stream, but appeared to increase slightly in the samples stored on the forest floor, at least initially (Figure 5.10A). Percent N of species A in both treatments remained more or less constant throughout the experiment, which %N of species B increased throughout the experiment in both treatments (Figure 5.10B).

An overview of isotopic differences between Wara and Killa is presented in Table 5.3. In most cases, the  $\delta^{15}\text{N}$  of a given compartment in Wara is lower than in Killa, with the exception of dissolved  $\text{NO}_3^-$  in the streams and TDN in the stream and in precipitation (Table 5.3). The dissolved  $\delta^{15}\text{N}$  values were not statistically distinguishable from site to site. In Wara, the epiphyte leaves were more depleted in  $^{15}\text{N}$  than tree leaves. Dissolved parameters, in general, were more enriched in  $^{15}\text{N}$  than plants, and the  $\delta^{15}\text{N}$  of dissolved  $\text{NO}_3^-$  and TDN in the stream was similar to those observed for riparian soils. The



concentrations of stream TDN were not significantly different between sites (Wara average =  $15.7 \pm 6.8 \mu\text{M}$ ; Killa average =  $13.5 \pm 6.6 \mu\text{M}$ ). The  $\delta^{15}\text{N}$  of TDN was the same for both rain and throughfall, and they were more enriched than any other canopy fraction. There was no consistent difference in  $\delta^{13}\text{C}$  between Wara and Killa. Several plants with non- $\text{C}_3$  photosynthetic pathways were found in the Killa catchment, explaining the variability of  $\delta^{13}\text{C}$  of shrubs and soil in this site.

## DISCUSSION

*Nitrogen budget*– The eastern flank of the Andes experiences very little dissolved inorganic N (DIN) deposition (Holland et al. 1999), and we were not able to measure any  $\text{NO}_3^-$  in either rain or throughfall in this study. In contrast, DON is a minimal portion of total dissolved N deposition in most systems in the United States and Europe (Keene et al. 2002). Dissolved ON ranges from 11 to 41% of TDN in rainwater in studies conducted all over the world (Cornell et al. 2003). However, in more remote sites DON can be a larger percentage of total N in cloud and rain water (Weathers et al. 2000). The exact source of DON in precipitation is unknown, but may be derived from one of three types of atmospheric organic N (AON): 1, organic nitrates derived from reactions of atmospheric  $\text{NO}_3^-$  with hydrocarbons; 2, aerosol amines or urea derived from marine or agricultural systems; and 3, terrestrial organic compounds such as pollen or volatile organic molecules (Neff et al. 2002). In a study on the Chilean Pacific coast, DON in cloudwater was thought to be marine in origin (Weathers et al. 2000). Since atmospheric  $\text{NO}_3^-$  is minimal in my study area, fossil fuel combustion and marine aerosols probably have a minor effect on atmospheric composition. The most likely source of DON to precipitation in this system is emission of volatile organic compounds (VOCs) from the forest itself (Greenberg et al. 2004, Guenther 1997). I conclude that both fractions have

the same source of organic N because the  $\delta^{15}\text{N}$  in rain was not statistically different from that in throughfall. VOCs emitted from the canopy are likely absorbed in clouds and then released with rain because clouds are in constant contact with vegetation. Throughfall has a higher average TDN concentration than rain, perhaps because precipitation makes physical contact with plants in the canopy as it falls.

As DON appears to dominate atmospheric N in unpolluted systems, it also dominates dissolved N exports in streams (Perakis and Hedin 2002). Approximately 80% of stream dissolved N export in this study site is organic (Saunders and McClain, in press). The similarity of  $\delta^{15}\text{N}$  in precipitation at each site may also explain why dissolved N (both  $\text{NO}_3^-$  and TDN) in the pristine and deforested streams had the same isotopic composition. Unpolluted streams may export DON because the majority of N introduced through precipitation is organic. Systems unaffected by anthropogenic alterations in N cycling have a tendency to store N in organic forms (van Breemen 2002), and our study supports this hypothesis.

The results of this study and the previous study (Saunders and McClain in press) allow comparison of dissolved N import and export in this system. Given an average throughfall TDN concentration of  $30\ \mu\text{M}$ , a rainfall amount of about 2000 mm per year, and a watershed size (Wara) of 4.5 ha, throughfall provides approximately 37.8 kg of DON to the watershed per year. Assuming an average stream DON concentration of  $8\ \mu\text{M}$  and an approximate streamflow rate of 1.5 L/sec (Saunders and McClain in press), about 1.2 kg of DON are exported annually from the watershed via the stream. This calculation indicates that approximately 85% of DON introduced to the watershed in throughfall is recycled, while 14% is exported downstream. It explains why not all N introduced in throughfall is retained, if the TDN observed in rain (average  $9\ \mu\text{M}$ , or 30% of TDN in throughfall) represents N derived from outside the catchment. Alternatively,

all deposited DON could be retained and cycled, and a different fraction of DON could be exported, which may explain why TDN in the stream has a heavier  $\delta^{15}\text{N}$  than TDN in rain and throughfall (Table 5.3).

*Epiphytes and N cycling*– Vascular epiphytes in the forest canopy are depleted in  $^{15}\text{N}$  with respect to the atmosphere, vs observed in other montane forest ecosystems (Heitz et al. 2002, Wania et al. 2002, Santiago et al. 2005, Stewart et al. 1995). Epiphytes obtain N from the atmosphere ( $\text{N}_2$  fixation or fixed N deposition) or from mineralization of canopy soils (Reynolds and Hunter 2004). Epiphytes sampled in this study were more enriched in the upper canopy than in the lower canopy (Table 5.2), similar to results from other tropical rainforest canopies (Wania et al. 2002). However, in the current study there was no significant difference in  $\delta^{15}\text{N}$  or N content of canopy soils between zones, and the  $\delta^{15}\text{N}$  of canopy soils was higher than that of plants. This result indicates that if canopy soils are a source of N to epiphytes, the relative proportion of N from soils and atmospheric N changes within the canopy. Inorganic N availability may be greater at the outer canopy than inside it: Lovett (1994) found that forest edges have more N deposition than the inner forest. However, since inorganic N deposition is minimal in this system, it may be that epiphytes in outer zones of the canopy are getting more N from  $\text{N}_2$  fixation and that inner canopy specimens may rely on throughfall DON and bacterial remineralization.

Epiphyte species also has an impact on  $\delta^{15}\text{N}$ . Bryophytes and orchids (class Monocotyledonia) had significantly higher  $\delta^{15}\text{N}$  than the ferns (class Pteridophyta) or the dicotyledonous flowers (class Dicotyledonia), which were not significantly different from each other (Table 5.2, Figures 5.3 and 5.4). Epiphytes with higher  $\delta^{15}\text{N}$  obtained more of their N from soils or from atmospheric  $\text{N}_2$  fixation, while plants with lower  $\delta^{15}\text{N}$  had more fixed N from cloudwater DIN, which in that study was depleted in  $^{15}\text{N}$  with respect

to atmospheric  $N_2$  (Wania et al. 2002). In fact, orchids are the only epiphytic species known to associate with microrrhizae (Lesica and Antibus 1990). I was not able to detect inorganic N (the most likely source of fixed N to canopy plants) in rain or throughfall – either due to a lack of pollution or to high uptake rates of canopy plants – so we cannot attribute a lower  $\delta^{15}N$  to a greater uptake of atmospheric fixed N. Also, I could not measure N concentrations or isotopes in clouds or fog water, which may be a significant source of water and N to canopy communities (Asbury et al. 1994, Clark et al. 1998b, Chang et al. 2002). I did not measure the  $\delta^{15}N$  or concentration of canopy soil dissolved N, nor do we have any information on N remineralization rates in canopy microbial communities. Measurements of atmospheric  $NH_4^+$  and other sources of dissolved N to the canopy are needed to definitively capture the sources of N to canopy plants in these communities, since reduced DIN is often more prevalent than  $NO_3^-$  in rain and fog, and N concentrations are often higher in cloudwater than in rain or throughfall (Asbury et al. 1994). The nutrient uptake mechanisms of epiphytes are poorly understood, and may depend on many different climatic and environmental factors (Zotz and Hietz 2001).

For the purposes of this study, epiphytes are most important as drivers of C and N cycling in old-growth forests. We observed a persistent difference in the  $\delta^{15}N$  of particulate organic matter between the pristine and deforested sample sites in this study (Table 5.3), with Wara (the old-growth site) consistently lower than Killa. On average, POM in Wara (not including dissolved N) was 1.8‰ lower in  $\delta^{15}N$  than Killa (Table 5.3). This difference indicates that epiphyte and other canopy biomass have a major impact on N stocks and cycling in old-growth forests. Canopy soils are very high in organic matter, with almost as much OC by weight as the epiphytes they support, and more than twice as much N by weight as canopy plants (Table 5.2). The persistent difference in  $\delta^{15}N$  between the two catchments provides further evidence that canopy epiphytes are fixing

atmospheric N<sub>2</sub>. If epiphytes were simply taking up some labile, isotopically depleted N from precipitation or clouds, that fraction should have been picked up by another fraction in the deforested site. Epiphytes in the forest canopy may draw on a N source unavailable to other kinds of organisms.

The high biomass of epiphytes (Catchpole 2004) and canopy detritus and leaf litter are major components of N stocks in these old-growth cloudforest systems. Vascular epiphytes comprise up to 50% of all plant biomass in the tropical Andes (Kelly et al. 1994, Bussmann 2001), and are persistent throughout the Andes from 1500 to 3000 meters above sea level (Catchpole 2004). This fraction represents about 9% of the Amazon Basin, or about 550,000 km<sup>2</sup>. Vascular epiphytes such as orchids and bromeliads in Andean cloudforests alone may represent around 5% of total biomass in the Amazon basin, and thus they represent a significant source of N for the basin due to atmospheric uptake and N<sub>2</sub> fixation.

*Isotopic effects of OM decomposition*—Soils in both catchments did not have a predictable relationship with depth of either  $\delta^{13}\text{C}$  or  $\delta^{15}\text{N}$  (Figure 5.5). Previous studies have shown that  $\delta^{13}\text{C}$ , in particular, and to some extent  $\delta^{15}\text{N}$  increases with depth in soil profiles, either due to differential degradation of organic molecules, microbial fractionation, or shifts in the relative fractions of microbial and plant OM as degradation increases (Peterson and Fry 1987, Wedin et al. 1995, Ehleringer et al. 2000). In my study,  $\delta^{13}\text{C}$  and  $\delta^{15}\text{N}$  decreased with depth in some places, but stayed the same or even increased in others. Landslides are thought to turn over soils in this area about once every 100 years (Glauber 2001). As a result, soils are very thin (~10 - 15 cm) and consist mostly of a thick organic layer with much smaller A and mineral horizons. The inconsistent trend in isotopic composition of soils may be due to frequent disturbance.

Also, due to the steep grade of these forests, landslides can result in total removal of organic matter to downstream areas.

The leaf litter decomposition experiment indicates that decomposition does not predictably change the isotopic composition of organic matter in this system. Decomposition caused almost no net change in  $\delta^{13}\text{C}$  or  $\delta^{15}\text{N}$  of decomposing leaves, even though significant variability occurred in both parameters during the experiment (Figure 5.9). This result indicates that incorporation of microbial biomass (with variable isotopic signatures) is significant during litter decomposition in this system (Wedin et al. 1995). This conclusion is supported by data on %OC and %N by weight during the decomposition process (Figure 5.10). Although mass of remaining litter decreased throughout the experiment, very little net change in the proportion of either C or N was observed. This result contrasted with those of most other studies tracking nutrient composition during litter decay (Aber and Melillo 1991), where C was lost exponentially and N initially increased then began to decrease. The current experiment shows that the organic layer in soils in this region consisted of large pieces of litter and a significant amount of microbial biomass rather than a homogeneous mixture of OM and minerals as it is traditionally defined (Aber and Melillo 1991).

## CONCLUSIONS

These findings on soil OM composition and the effects of litter decomposition have important implications for our studies of organic matter dynamics in the Andes and transport to the Amazon River. In Chapter 2 of this volume, we hypothesized that POM in high altitude headwater streams consisted of small pieces of leaf litter, not minerals with sorbed DOM as has been observed in lower-altitude tropical rivers (Aufdenkampe et al. 2001). This study supports this hypothesis. Traditional soil organic matter sorbed to

minerals appears to be transported only during landslides and other very high flow events. In small Andean headwaters such as the ones studied here, stream suspended POM is composed of leaf litter that may have a significant portion of microbial biomass. This trend is evident in the POM composition of the pristine and deforested sites. The  $\delta^{15}\text{N}$  of stream POM in the deforested site was characteristic of fresher leaf litter, not deeper horizons, and was offset in the deforested site due to the lack of epiphytic biomass.

This study has implications for our study of  $^{14}\text{C}$  content of POM in the Andean headwaters (Chapter 3, this volume). The three highest altitude streams sampled in that study were very similar to the ones studied here. If POM in these systems is a mixture of leaf litter and microbial biomass, this result could explain the extreme variability in radiocarbon content of POM in these systems. While leaf litter likely has a modern  $^{14}\text{C}$  signature, microbial biomass  $\Delta^{14}\text{C}$  depends on the substrate, which appears to vary over the timescale of hundreds of years (Chapter 3, this volume). As material from these small headwaters travels downstream, the fresh litter and less refractory microbial components of POM are consumed and minerals are a larger portion of POM (Chapter 4, this volume), so overall POM has lower  $\%C$  and more consistent isotopic signatures, due to the influence and more consistent nature of sorption of DOM to minerals (Aufdenkampe et al. 2001).

I conclude that land use change may alter standing stocks of organic C and N in Andean cloudforests, and that these changes can be reflected in the composition of stream POM. This conclusion is important in systems with extensive epiphytic biomass such as Yanachaga-Chemillen. Dissolved constituents of precipitation and streams seem to be independent of land use or land cover, or else they are controlled by forces larger than the watershed scale or on longer time scales than the one studied here ( $\sim 5$  years). More

information on the amount of canopy biomass is necessary to estimate of the effects of deforestation on local and global C and N budgets. Exactly where epiphytes in this system obtain their nutrients remains unclear. More studies on smaller scales, and including cloudwater samples, are needed to pinpoint N sources to canopy ecosystems in the Peruvian Andes.



	Throughfall		Rain	
Date collected	TDN concentration ( $\mu\text{M}$ )	$\delta^{15}\text{N}$ of TDN (‰)	TDN concentration ( $\mu\text{M}$ )	$\delta^{15}\text{N}$ of TDN (‰)
2/10/04	32.4	n/d	0.7	0.1
2/17/04	10.0	2.2	1.4	1.8
2/24/04	20.5	0.5	n/d	n/d
3/2/04	33.3	1.4	26.4	-5.9
3/9/04	19.3	1.7	6.0	8.3
3/16/04	44.4	2.1	1.4	2.0
3/23/04	9.9	0.9	1.4	4.5
3/30/04	12.9	2.2	0.0	6.5
4/7/04	49.9	-1.2	1.5	5.6
4/13/04	n/d	n/d	22.6	1.4
4/20/04	75.6	2.9	3.2	0.3
4/27/04	59.2	3.0	10.9	6.4
5/4/04	28.5	-1.1	9.7	-1.8
5/11/04	11.8	3.1	3.2	-0.9
5/18/04	76.1	3.7	7.1	3.9
5/25/04	21.8	0.3	4.9	-3.8
6/1/04	n/d	n/d	31.7	3.1
6/8/04	n/d	n/d	3.6	2.7
6/15/04	34.0	2.3	2.2	7.9
6/22/04	18.5	0.9	52.9	3.2
6/29/04	n/d	n/d	6.5	-3.8
7/6/04	4.1	1.8	0.0	0.3
7/13/04	32.4	4.2	1.9	6.0
Average	31.3	1.7	9.1	2.2
Std. Deviation	21.3	1.5	13.2	3.9

Table 5.1. Concentrations and  $\delta^{15}\text{N}$  of total dissolved nitrogen (TDN) in rain and throughfall collected at the Parque Nacional Yanachaga-Chemillen. n/d = not determined.

	<b>n</b>	<b><math>\delta^{15}\text{N}</math></b>	<b>Std dev <math>\delta^{15}\text{N}</math></b>	<b>%N</b>	<b><math>\delta^{13}\text{C}</math></b>	<b>%C</b>
<b>Zone 3 epiphytes</b>	11	-2.2	1.2	0.6	-29.7	54.4
<b>Zone 4 epiphytes</b>	23	-3.5	1.7	0.6	-29.3	56.6
<b>Zone 5 epiphytes</b>	31	-4.6	2.0	0.6	-29.8	56.8
<b>Zone 3 soils</b>	8	-0.8	0.4	1.7	-26.8	53.4
<b>Zone 4 soils</b>	19	-0.5	0.6	1.8	-26.3	54.6
<b>Zone 5 soils</b>	29	-0.7	0.4	1.8	-25.8	53.7
<b><i>Sphryosperma</i> sp.</b>	6	-5.3	1.3	0.6	-31.0	57.5
<b><i>Elaphoglossum</i> sp. 1</b>	6	-6.6	2.3	0.7	-30.2	51.6
<b><i>Epidendrum</i> sp.</b>	4	-3.9	0.6	1.1	-29.7	60.7
<b><i>Vriesia</i> sp. 1</b>	9	-1.6	1.0	0.6	-28.2	55.0
<b><i>Disterigma</i> sp.</b>	6	-6.1	0.2	0.4	-32.1	59.4
<b><i>Maxillaria</i> sp. 1</b>	6	-3.8	1.6	0.8	-30.7	58.5
<b><i>Maxillaria</i> sp. 2</b>	3	-4.4	1.0	0.7	-31.9	64.4
<b><i>Vriesia</i> sp. 2</b>	9	-2.8	1.0	0.6	-28.9	55.5
<b><i>Elaphoglossum</i> sp. 2</b>	6	-6.0	1.7	0.5	-29.3	52.3
<b><i>Pleurothallis</i> sp. 1</b>	9	-3.0	1.0	0.6	-30.7	57.8
<b><i>Pleurothallis</i> sp. 2</b>	7	-2.9	0.6	0.8	-29.3	55.2

Table 5.2. Average nitrogen and carbon stable isotopic and elemental composition of canopy plants and soils in the Wara catchment. Zones are as defined in Johansson (1974). Also shown is the number of each type of sample as well standard deviation of the  $\delta^{15}\text{N}$  values for each type of sample (for identification of significant differences).

	<b>Wara <math>\delta^{15}\text{N}</math> (‰) <math>\pm</math> standard deviation</b>	<b>Killa <math>\delta^{15}\text{N}</math> (‰) <math>\pm</math> standard deviation</b>	<b>Wara <math>\delta^{13}\text{C}</math> (‰) <math>\pm</math> standard deviation</b>	<b>Killa <math>\delta^{13}\text{C}</math> (‰) <math>\pm</math> standard deviation</b>
<b>Epiphytes (bromeliads and orchids)</b>	-3.8 $\pm$ 2.0	n/a	-29.6 $\pm$ 1.8	n/a
<b>Woody epiphyte stems and vines</b>	-3.1 $\pm$ 2.3	n/a	-31.5 $\pm$ 2.0	n/a
<b>Canopy soils</b>	-0.7 $\pm$ 0.5	n/a	-26.1 $\pm$ 0.7	n/a
<b>O horizon soils</b>	-0.4 $\pm$ 0.1	0.0 $\pm$ 0.4	-28.2 $\pm$ 0.1	-30.2 $\pm$ 1.7
<b>A horizon soils</b>	1.6 $\pm$ 1.2	2.6 $\pm$ 0.3	-27.9 $\pm$ 0.9	-27.0 $\pm$ 0.1
<b>Mineral soils</b>	0.9 $\pm$ 2.1	3.2 $\pm$ 0.7	-27.5 $\pm$ 1.1	-26.5 $\pm$ 1.0
<b>Tree leaves</b>	-1.9 $\pm$ 1.7	n/a	-28.2 $\pm$ 1.9	n/a
<b>Leaf litter</b>	-3.1 $\pm$ 0.7	-0.1 $\pm$ 1.5	-26.6 $\pm$ 1.3	-30.3 $\pm$ 1.4
<b>Shrubs and other small plants</b>	-2.9 $\pm$ 1.2	1.0 $\pm$ 1.1	-33.2 $\pm$ 1.4	-28.4 $\pm$ 6.3
<b>Aquatic/ riparian plants</b>	-1.0 $\pm$ 1.5	1.0 $\pm$ 1.6	-38.3 $\pm$ 2.7	-39.4 $\pm$ 2.8
<b>TDN in rain or throughfall</b>	3.6 $\pm$ 3.0	4.0 $\pm$ 5.0		
<b>Stream POM</b>	-0.5 $\pm$ 0.4	0.5 $\pm$ 1.4		
<b>Stream TDN</b>	2.7 $\pm$ 1.9	1.3 $\pm$ 3.2		
<b>Stream <math>\text{NO}_3^-</math></b>	1.4 $\pm$ 0.5	1.4 $\pm$ 0.6		

Table 5.3.  $\delta^{15}\text{N}$  and  $\delta^{13}\text{C}$  of various fractions in the pristine (“Wara”) and deforested (“Killa”) sites. n/a = not applicable.

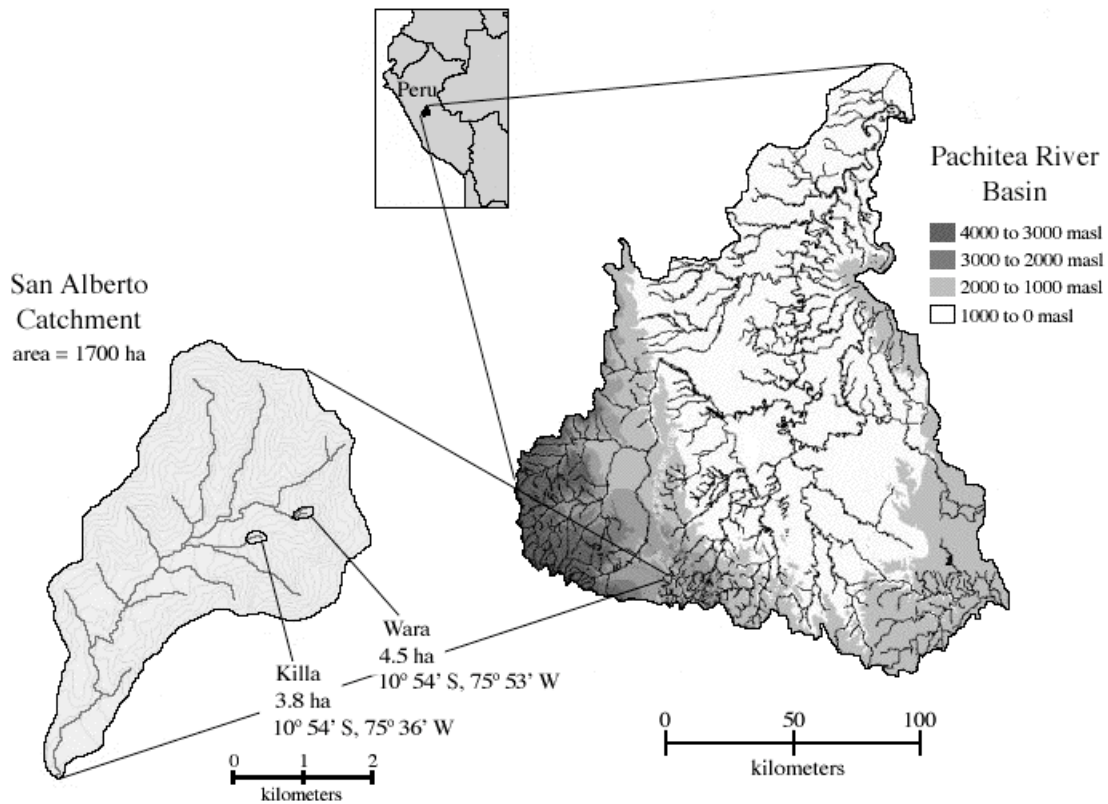


Figure 5.1. Map of the study area. The location of the two study catchments (Wara and Killa) is shown within the San Alberto catchment, located in the Pachitea River Basin of the Peruvian Amazon.

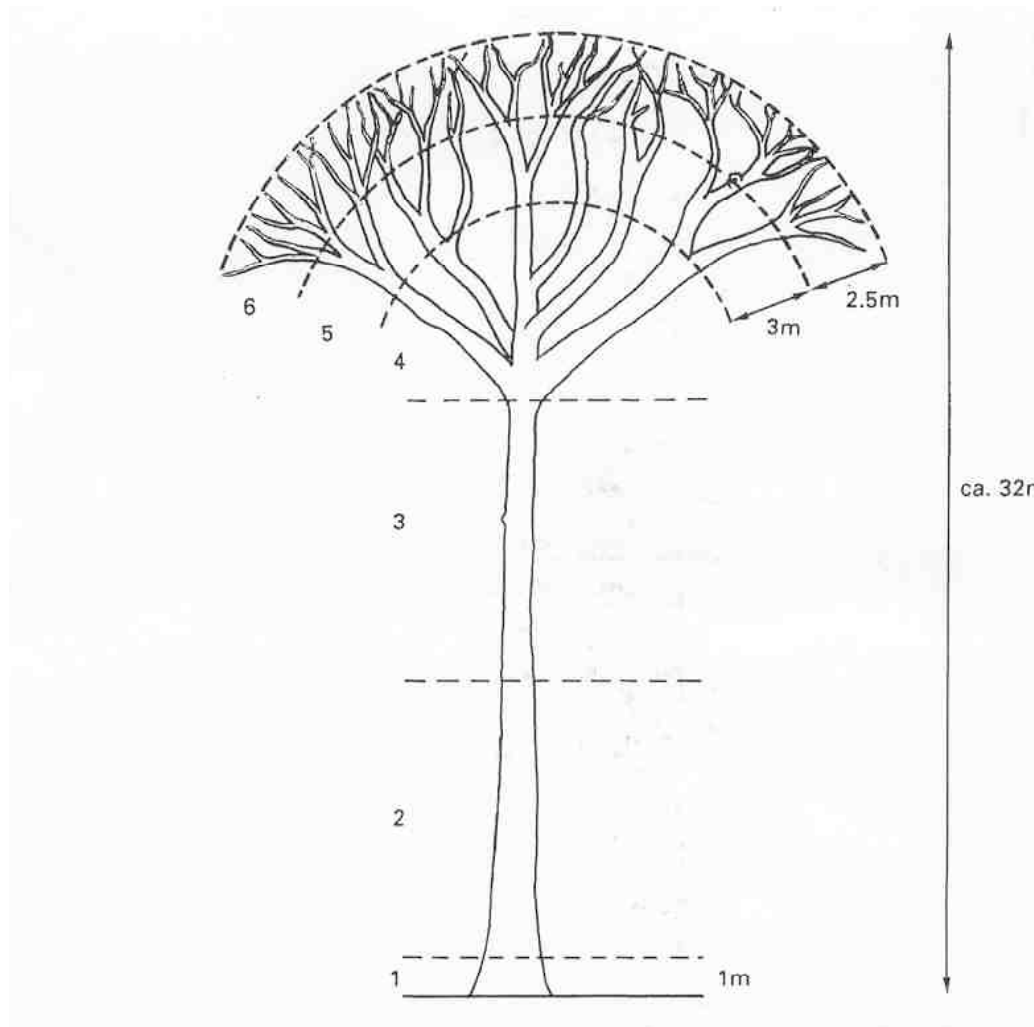


Figure 5.2. Canopy zonation scheme of Johansson (1974).

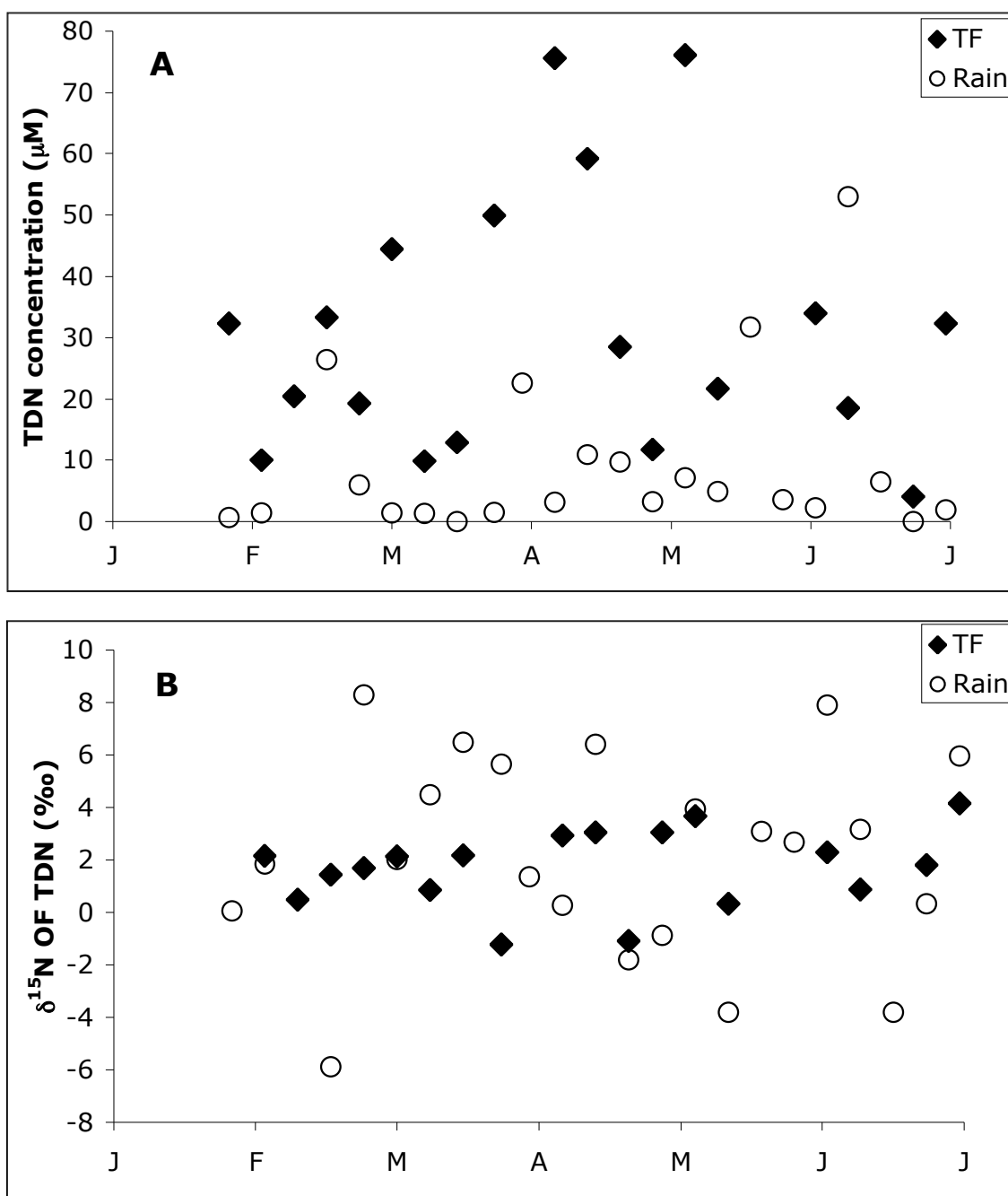


Figure 5.3. Concentration (in  $\mu\text{M}$ ) and  $\delta^{15}\text{N}$  (‰) of TDN in rain and throughfall (TF) collected in the Parque Nacional Yanachaga Chemillen.

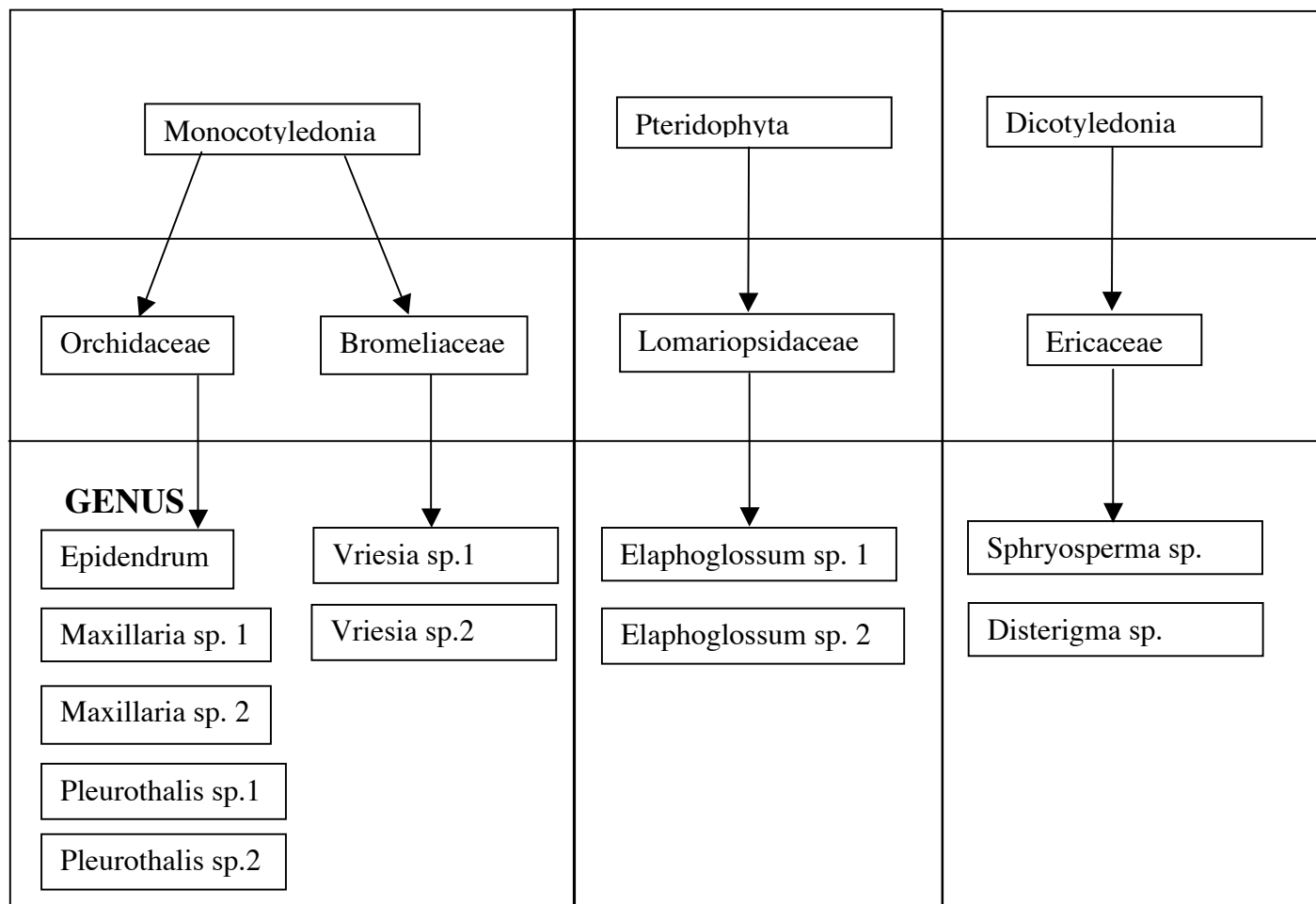


Figure 5.4. Classification scheme of the epiphytes sampled in this study.

<b>A</b>	<b>Dicotyledonia</b>	<b>Monocotyledonia</b>
<b>Monocotyledonia</b>	0.000	
<b>Pteridophyta</b>	0.420	0.000

<b>B</b>	<b>Ericaceae</b>	<b>Lomaridopsidaceae</b>	<b>Orchidaceae</b>
<b>Bromeliaceae</b>	0.000	0.000	0.001
<b>Ericaceae</b>		0.395	0.000
<b>Lomaridopsidaceae</b>			0.000

<b>C</b>	<i>Elaphoglossum</i>	<i>Epidendrum</i>	<i>Maxillaria</i>	<i>Pleurothalis</i>	<i>Sphyrosperma</i>	<i>Vriesia</i>
<i>Disterigma</i>	0.761	0.012	0.002	0.000	0.296	0.000
<i>Elaphoglossum</i>		0.004	0.007	0.000	0.297	0.000
<i>Epidendrum</i>			0.809	0.073	0.075	0.009
<i>Maxillaria</i>				0.054	0.111	0.004
<i>Pleurothalis</i>					0.012	0.036
<i>Sphyrosperma</i>						0.003

Figure 5.5. Results (as  $p$  values) of two-tailed  $t$  tests to determine significant differences in  $\delta^{15}\text{N}$  between different categories of vascular epiphytes sampled in this study. Differences between classes are shown in (A), between families in (B), and between genera in (C). Values below  $p = 0.05$  are highlighted in red.



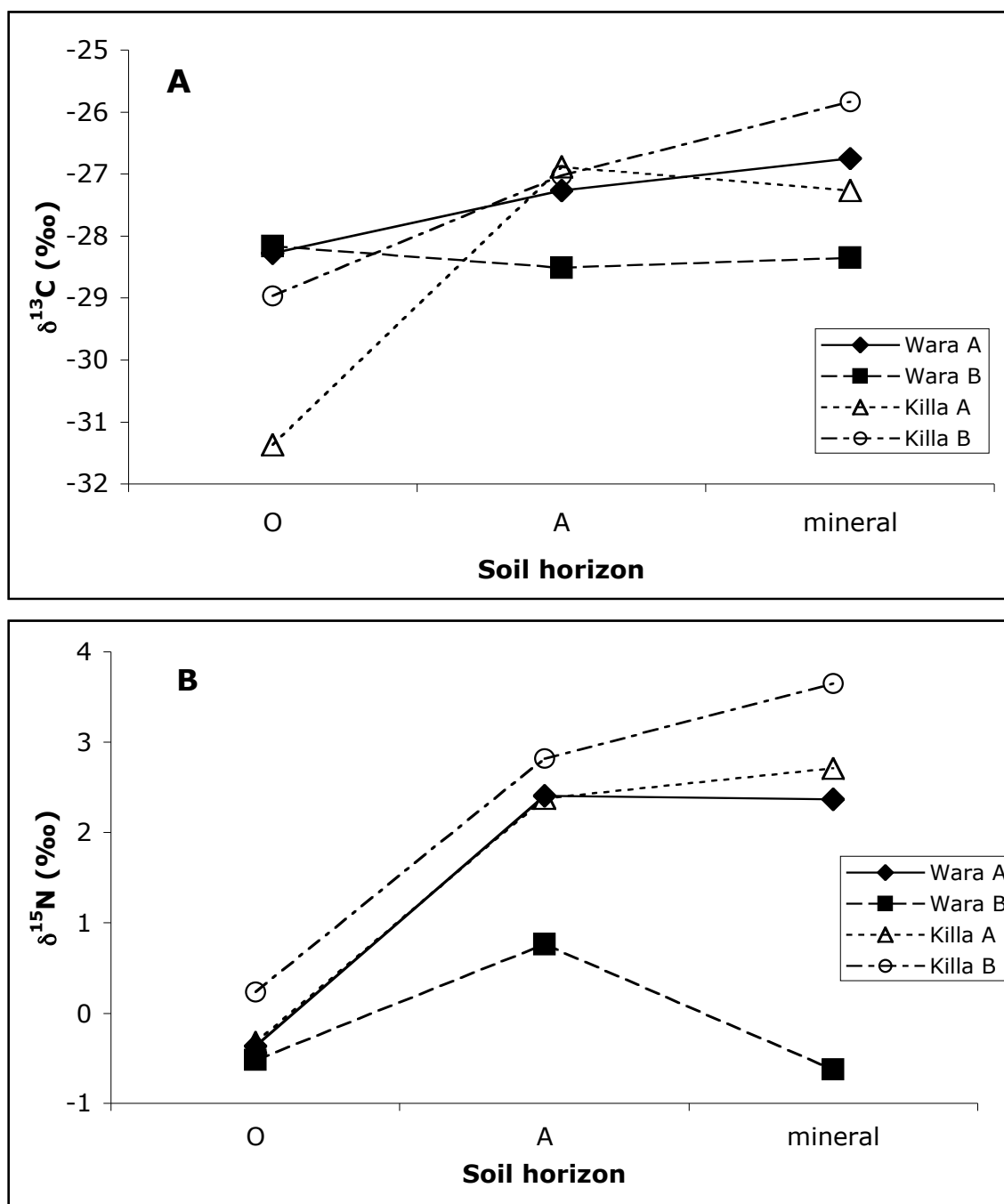


Figure 5.6. Carbon (A) and nitrogen (B) isotopic composition of soil horizons in 2 different plots each in the pristine (Wara) and deforested (Killa) sites.

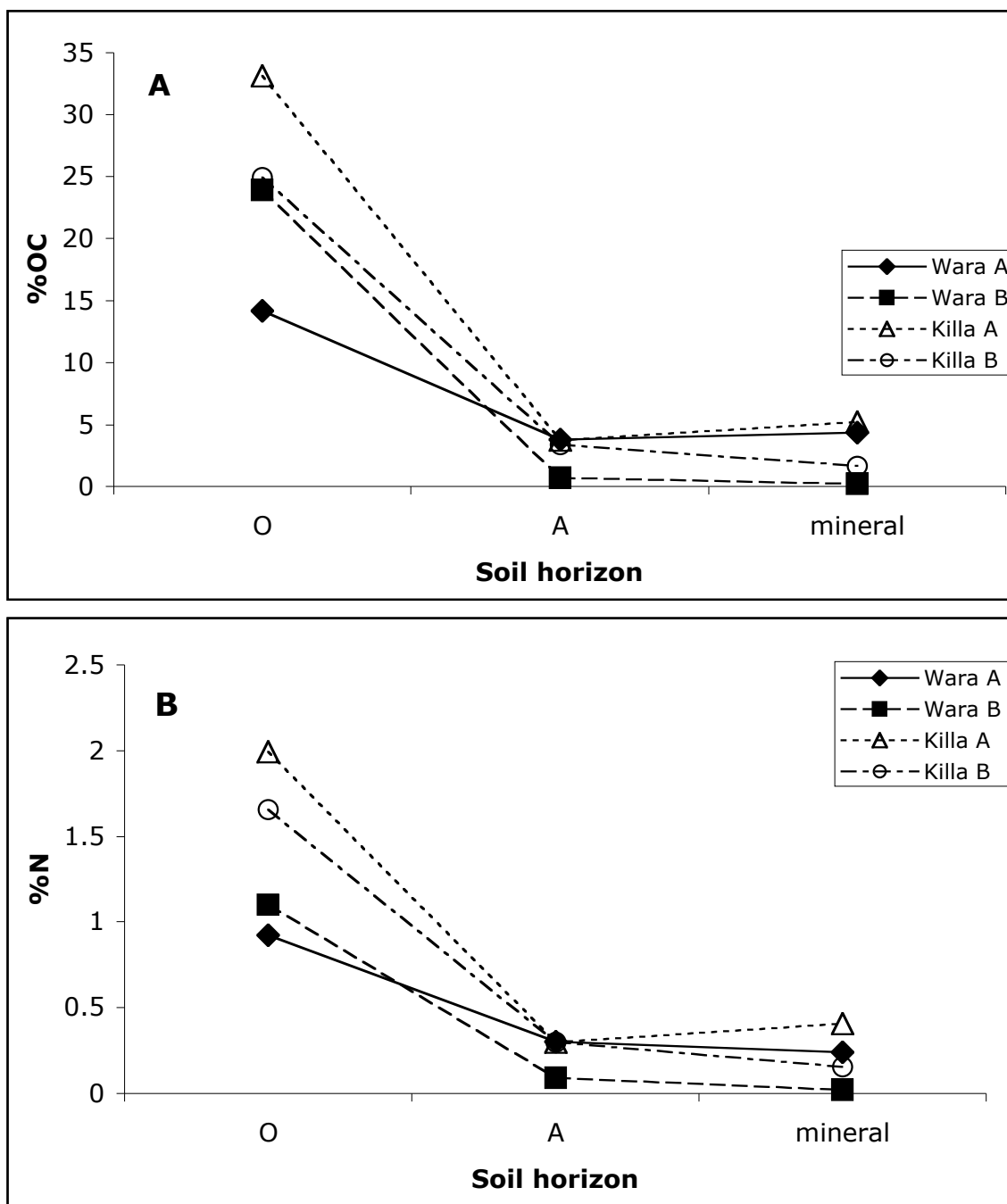


Figure 5.7. Percent by weight of carbon (A) and nitrogen (B) of soil horizons in 2 different plots each in the pristine (Wara) and deforested (Killa) sites.

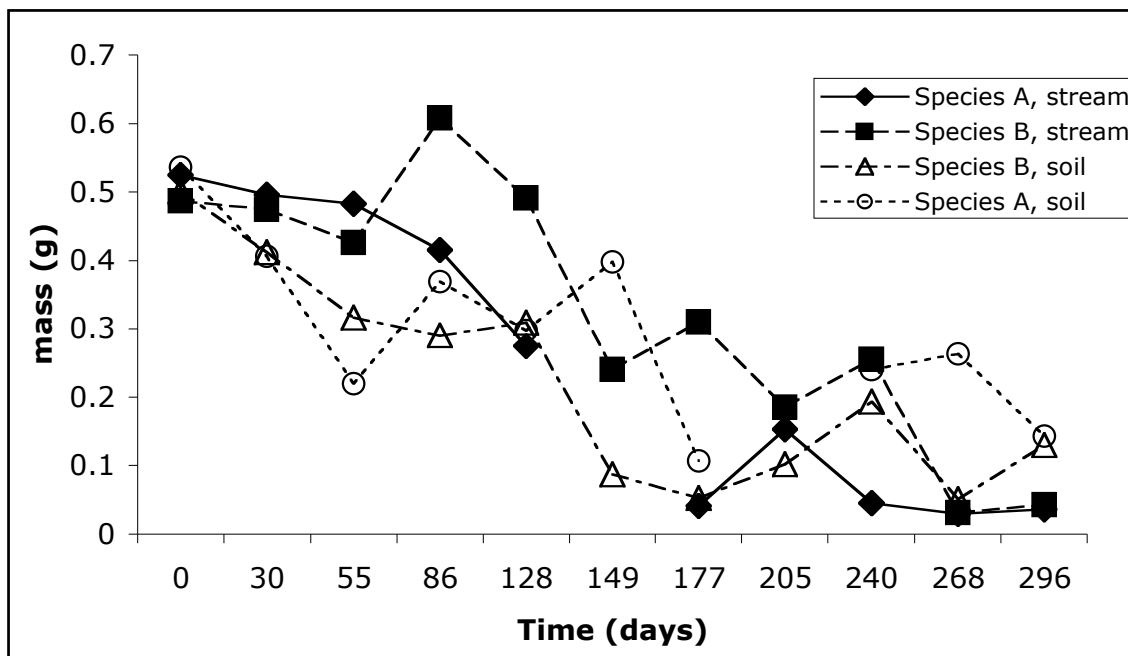


Figure 5.8. Mass of leaf litter – two different species in two treatments – remaining as a function of time in the leaf litter decomposition experiment.

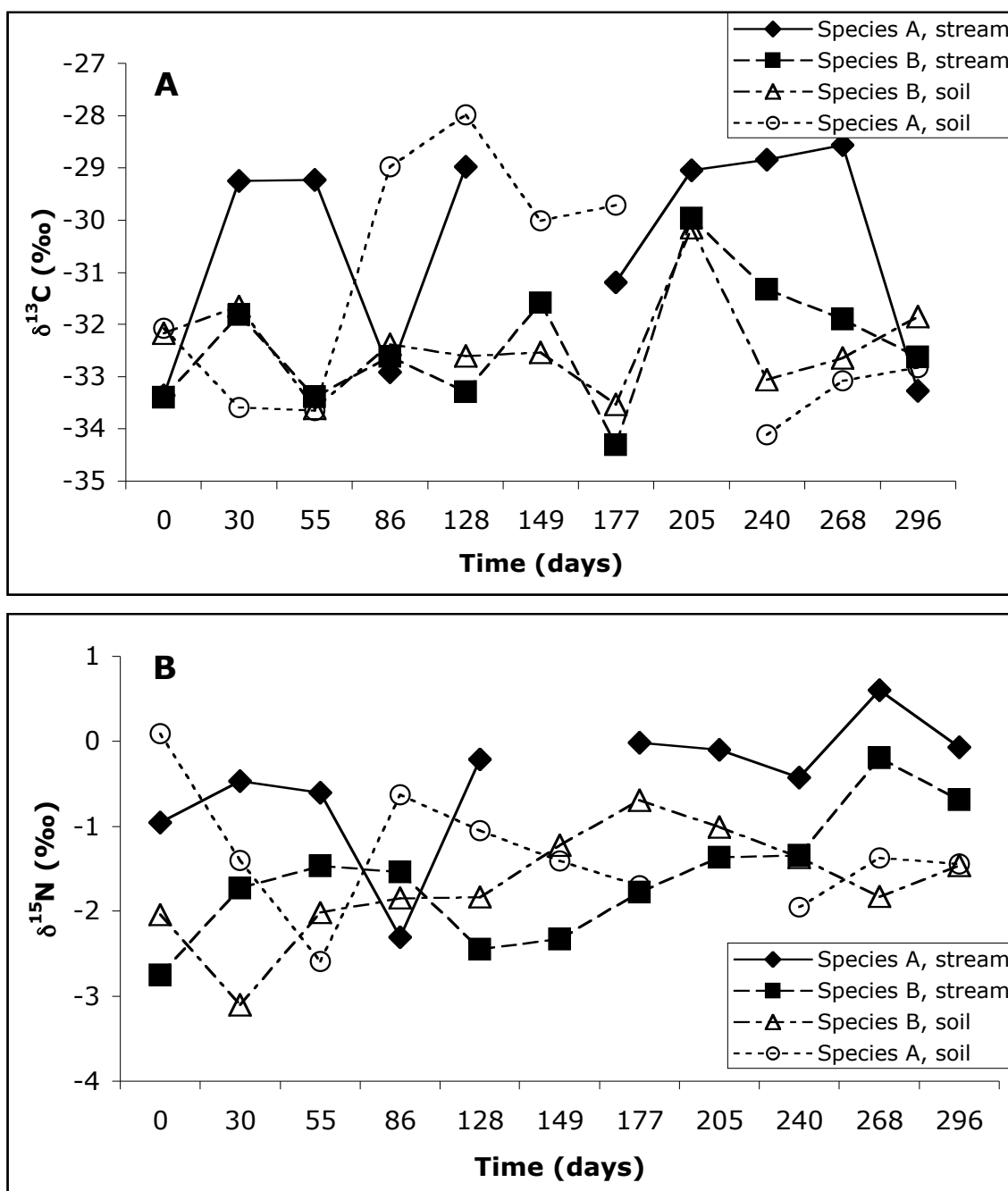


Figure 5.9. Carbon and nitrogen isotopic composition ( $\delta^{13}\text{C}$  and  $\delta^{15}\text{N}$ ) of leaf litter as it decomposes.

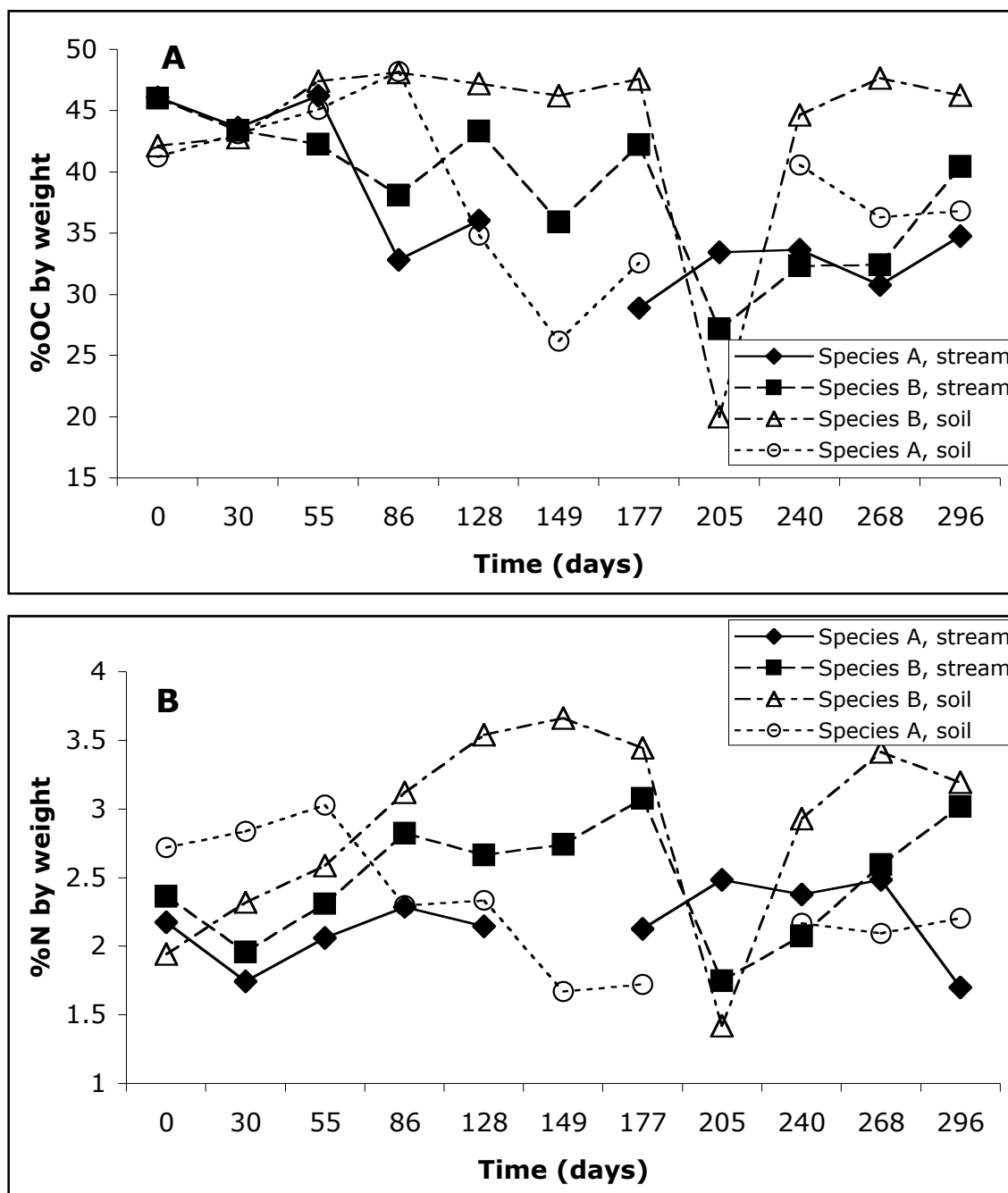


Figure 5.10. Weight percent of OC and N as a function of time in leaf litter as it decomposes.

## **Chapter 6: Nitrogen transformations in soils and streams of the Amazon headwaters of Peru: Evidence from a series of $^{15}\text{N}$ tracer addition experiments**

### **ABSTRACT**

The Andean headwaters influence many of the physical and biogeochemical properties of the Amazon River, but the factors that control the export of biologically important elements from catchments to streams and rivers in the Andes are not defined. In particular, the composition of nitrogen (N) exported from these pristine systems is quite different from that found in North American and other anthropogenically-impacted systems. We conducted a series of nitrogen-15 ( $^{15}\text{N}$ ) tracer injection studies ( $^{15}\text{NH}_4^+$ ,  $^{15}\text{NO}_3^-$ ,  $^{15}\text{N}$ -glycine) in the soils and stream of a small cloudforest catchment located at about 2500 meters above sea level in the Andes Mountains of Peru. Inorganic N export from these systems via streams is low, but low concentrations do not appear to result from high reactivity of dissolved inorganic N (DIN) in the stream. In fact, measured rates of nitrification and uptake of dissolved N onto fine particulate matter were low. However, microbes and fine roots in riparian soils had high demand for added DIN. Added glycine was incorporated into soil organic matter (SOM), either by uptake or sorption, and mineralized to  $\text{NO}_3^-$ , but DON was not absorbed directly by plant roots. Low inorganic N deposition in these forests along with high demand for inorganic N in riparian soils explains the low ambient stream DIN concentrations.

## INTRODUCTION

The eastern Andes are the source of more than 80% of water and sediments to the Amazon River (Gibbs 1967), but it is not known how these headwaters control organic matter fluxes to the mainstem Amazon. Headwater streams can exert major control over the nitrogen (N) cycle and budget of large rivers (Peterson et al. 2001). One example of this control is the Mississippi River basin, where excessive N fertilizer use in the upper basin is implicated in eutrophication at the river mouth (Turner and Rabalais 1991). Although the Amazon is the largest source of organic carbon (C) to the oceans (Richey et al. 1980), little is known about how the concentration and composition of organic matter (OM) is controlled by the Andean headwaters (McClain et al. 1995).

Hydrologic N exports from small streams draining South American montane forests are dominated by dissolved organic N (Perakis and Hedin 2001, Saunders and McClain in press), while similar ecosystems in industrialized areas are often dominated by dissolved inorganic N (DIN), especially nitrate ( $\text{NO}_3^-$ ) (Perakis and Hedin 2002). In Chapter 5 of this dissertation, we explored the hypothesis that these low stream DIN levels were caused by extremely low levels of inorganic N deposition. Rapid removal of DIN from soil and groundwater was observed during baseflow, and greater transfer of DIN to the stream occurred during storm events in the same watershed (Saunders and McClain in press). Similarly, strong and rapid retention of  $^{15}\text{N}$ -labeled  $\text{NO}_3^-$  and  $\text{NH}_4^+$  in was observed in cloudforest soils of Southern Chile. (Perakis and Hedin 2001).

Natural abundance stable isotope content is a useful indicator of N cycling in forests and streams (Brandes et al. 1996, Ostrom et al. 2002, Peterson and Fry 1987). However, additions of isotopically-labeled N compounds can elucidate pathways that might otherwise not have a large difference in  $\delta^{15}\text{N}$  signatures between source and sink (Fry et al. 1995, Bedard-Haughn et al. 2003, Mutchler et al. 2004). Nitrogen-15 additions

have helped characterize N cycling in streams (Hamilton et al. 2001; Merriam et al. 2002; Mulholland et al. 2000, 2004; Peterson et al. 1997). Studies conducted in areas where DIN export is high, such as in the eastern United States (Mulholland et al. 2000, 2004) indicate that high  $\text{NO}_3^-$  export levels can be attributed to high nitrification and low denitrification rates in the stream itself. Few studies have been conducted in either pristine or tropical streams. A  $^{15}\text{NH}_4^+$  addition in a Puerto Rico stream showed that nitrification rates were high in the stream, and that in-stream nitrification could explain high dissolved  $\text{NO}_3^-$  concentrations (Merriam et al. 2002). Uptake by biota and epilimnion were much greater sinks than nitrification for added  $^{15}\text{NH}_4^+$  in a pristine stream in the Alaskan Arctic (Peterson et al. 1997), and autotrophic uptake was dominant during the summer months (Wollheim et al. 1999).

Tracer-level additions of  $^{15}\text{N}$  can help determine the fates, paths, and rates of N transformations in soils (Davidson et al. 1991, Barraclough 1995, Nadelhoffer and Fry 1995, Näsholm et al. 1998). This technique has been employed in areas that are affected by high DIN deposition rates, where N saturation is a problem (Aber et al. 1989). In European forests, a high demand exists for both  $\text{NH}_4^+$  and  $\text{NO}_3^-$ , and  $\text{NO}_3^-$  is preferentially retained in soils over  $\text{NH}_4^+$ , despite the fact that  $\text{NO}_3^-$  is more likely to be lost in runoff (Buchmann et al. 1996, Providoli et al. 2005). Similarly, in soils of North America, rapid uptake of  $\text{NO}_3^-$  by both plants and soil microbes occurs, despite losses due to high runoff events (Davidson et al. 1992, Strickland et al. 1992, Currie et al. 1999, Nadelhoffer et al. 1999).

The goal of this study is to characterize the N transformations in a first-order stream and adjacent catchment in a tropical montane cloudforest in the Peruvian Andes. We conducted a series of tracer addition experiments to determine the important N



cycling processes that control dissolved and particulate N export in cloudforest catchments in the Peruvian Andean Amazon.

## METHODS

This study was conducted during 2003 and 2004 in a small stream in the Parque Nacional Yanachaga-Chemillen, located near Oxapampa, Peru. All experiments were conducted in the Wara watershed (Figure 5.1). Three stream  $^{15}\text{N}$  tracer injection studies were conducted. An addition of  $^{15}\text{NH}_4\text{Cl}$  was conducted during January of 2003. This was followed by a  $\text{K}^{15}\text{NO}_3$  addition in July of 2004, and a  $^{15}\text{N}$ -glycine addition in August of 2004. The molecular structure of glycine, the smallest amino acid, is shown in Figure 6.1. In each case, the experimental conditions were maintained as similar as possible. Each of the labeled compounds was prepared in a 1.17 mM N solution and dripped into the stream at approximately 1 ml per minute over a time period of several days. The length of each experiment was dictated by the battery life. During the glycine addition experiment, the pump rate was 1.6 ml/minute. All of the chemicals were purchased from Sigma-Aldrich Corporation (Isotech) and were at least 98% enriched in  $^{15}\text{N}$ . The level of added tracer was low enough in not to significantly alter the ambient concentration of  $\text{NH}_4^+$ ,  $\text{NO}_3^-$ , or DON, but the expected isotopic enrichment at the injection site was above 30,000‰ (98 atom%  $^{15}\text{N}$ ).

Dissolved samples were collected during the experiment by filtering a known volume of stream water through 0.2  $\mu\text{m}$  nylon syringe filters into 40 ml amber borosilicate vials containing 40  $\mu\text{l}$  of concentrated sulfuric acid ( $\text{H}_2\text{SO}_4$ ) as a preservative. These bottles were kept in a cool dark place until they could be analyzed at the University of Texas Marine Science Institute (UTMSI). Particulate samples were collected by filtering whole stream water onto precombusted Whatman<sup>TM</sup> GF/F filters. These filters

were dried for 48 hours at 60° at the Andean Amazon Research Station in Oxapampa, then sealed in Petri dishes and kept dry until they could be analyzed at UTMSI. Stream flow was measured at 10-minute intervals with the v-notch weir and pressure transducer maintained by the Andean Amazon Research Station (Saunders and McClain in press).

Three soil tracer addition studies were conducted from July through August, 2004. Three 50 x 50 cm plots were designated in the riparian zone of the Wara stream. Three types of tracer studies were conducted: one with  $^{15}\text{N}$ -glycine, one with  $^{15}\text{NH}_4^+$ , and one with  $^{15}\text{NO}_3^-$ . The same  $^{15}\text{N}$ -enriched chemicals were used for the soil tracer experiment as for the stream experiments. The soil tracer experiment was modeled on the one described in Perakis and Hedin (2001). Nitrogen was applied at a rate of 0.2 kg N/ha, and  $^{15}\text{N}$  tracers were applied in a volume of deionized water equivalent to a 1.6 mm rainfall event. Samples of approximately 100 g of soil were taken 30 minutes before the tracer application, 30 minutes after the tracer application, two days after the tracer application, and then once a week for the next four weeks. Soil samples were transported back to the field station in Oxapampa in sealed Ziploc bags and processed immediately. Fine roots and large inclusions such as pieces of wood, litter, and rocks were picked from each soil sample, and dissolved N was extracted from 40 g (wet weight) of soil by soaking for 1 hour with 100 ml of 0.5 M KCl, then filtering through pre-combusted Whatman GFF glass fiber filters. The extracted soil was dried until constant mass at 60°C in a laboratory oven, and then transported back to UTMSI for measurement of  $\delta^{15}\text{N}$  of SOM. Fine roots were also dried for  $\delta^{15}\text{N}$  analysis. Soil KCl extracts were preserved with 1  $\mu\text{l/ml}$  of  $\text{H}_2\text{SO}_4$  and refrigerated until they could be analyzed for  $\delta^{15}\text{N}$  of  $\text{NO}_3^-$  at UTMSI.

The  $\delta^{15}\text{N}$  of dissolved  $\text{NO}_3^-$  in samples from the stream tracer study was measured using a bacterial denitrifier method (Sigman et al. 2001). Briefly, this method works by

converting dissolved  $\text{NO}_2^-$  and  $\text{NO}_3^-$  to  $\text{N}_2\text{O}$  using denitrifying bacteria. The  $\delta^{15}\text{N}$  of dissolved  $\text{NO}_3^-$  in samples from the soil tracer experiment was determined using the method of McIlvin and Altabet (2005), with modifications for smaller sample volume and lower concentration (Townsend-Small and Brandes, in prep). Nitrous oxide produced from both of these methods was analyzed for  $\delta^{15}\text{N}$  of  $\text{NO}_3^-$  on a gas chromatograph/preconcentrator/isotope ratio mass spectrometer at the University of Texas Marine Science Institute (UTMSI). The  $\delta^{15}\text{N}$  of particulate organic matter (POM) on glass fiber filters, and in fine roots and soil organic matter (SOM) was analyzed on a Carlo Erba 2500 elemental analyzer coupled to the isotope ratio mass spectrometer at UTMSI.

## RESULTS

*$^{15}\text{NH}_4^+$  stream addition*— The maximum  $\delta^{15}\text{N}$  of  $\text{NO}_3^-$  observed during the  $^{15}\text{NH}_4^+$  addition experiment in the stream was 20.8 ‰, from an average pre-tracer level of -2.7‰ (Figure 6.2). The maximum expected increase in  $\delta^{15}\text{N}$  of  $\text{NH}_4^+$  in this experiment, assuming a baseline  $\text{NH}_4^+$  concentration of 1.6  $\mu\text{M}$  (Saunders and McClain in press) and a tracer enrichment of 98 atom‰, is 31,137‰. The maximum increase in  $\delta^{15}\text{N}$  of  $\text{NO}_3^-$  in the  $\text{NH}_4^+$  tracer addition study was observed during the first day of the experiment; in fact,  $\delta^{15}\text{N}$  of  $\text{NO}_3^-$  increased steadily throughout the day (Figure 6.2B). The average  $\delta^{15}\text{N}$  of  $\text{NO}_3^-$  during the following days was 8.4‰ (Figure 6.2A).

The  $\delta^{15}\text{N}$  of POM during the  $\text{NH}_4^+$  addition experiment increased throughout the entire length of the experiment (Figure 6.3), unlike the trend observed for  $\text{NO}_3^-$  isotopes in this study. The average pre-tracer  $\delta^{15}\text{N}$  of POM in the stream was 0.9‰. The

maximum  $\delta^{15}\text{N}$  of POM observed in this study was 32.4‰, and the average for the final day of the experiment was 27.2‰ (Figure 6.3).

*$^{15}\text{NO}_3^-$  stream addition*– During the  $^{15}\text{NO}_3^-$  stream tracer experiment, the  $\delta^{15}\text{N}$  of  $\text{NO}_3^-$  increased to a maximum value of 1120‰ during the second day (Figure 6.4). After this maximum value was observed, the  $\delta^{15}\text{N}$  of  $\text{NO}_3^-$  began to decrease to a value of 380‰ observed just before the pump was turned off (Figure 6.4). The  $\delta^{15}\text{N}$  of  $\text{NO}_3^-$  increased by 56‰ (from 2‰ to 58‰) just 21 minutes after the pump was turned on (Figure 6.4A). After the pump was turned off, the  $\delta^{15}\text{N}$  of  $\text{NO}_3^-$  decreased to near background levels. The average  $\delta^{15}\text{N}$  of  $\text{NO}_3^-$  after the pump was turned off was 15‰ (Figure 6.4A). The standard deviation of the measurement of  $\delta^{15}\text{N}$  of  $\text{NO}_3^-$  was higher than normal for samples with very enriched values. The average standard deviation for the  $\delta^{15}\text{N}$  of  $\text{NO}_3^-$  method described above with non-tracer enriched samples is 0.2‰ or better, but for samples taken during the time when  $^{15}\text{NO}_3^-$  was added to the stream, the standard deviation of measurement ranged from 0.4 to 82.9‰ and the average was 10.9‰.

The  $\delta^{15}\text{N}$  of POM during the  $^{15}\text{NO}_3^-$  stream tracer addition is shown in Figure 6.5. The average  $\delta^{15}\text{N}$  of POM before the pump was turned on was 0.9‰. During the first day of the experiment, the  $\delta^{15}\text{N}$  of POM increased to 13.0‰ in approximately 3 hours, but on the second day the average  $\delta^{15}\text{N}$  of POM was 3.3‰. On the third day of the experiment, the  $\delta^{15}\text{N}$  of POM increased again to an average of 6.6‰ (Figure 6.5B). After the experiment, the  $\delta^{15}\text{N}$  of POM appeared to fluctuate, and the  $\delta^{15}\text{N}$  of POM remained slightly elevated up to nine days after the experiment was terminated (3.8‰, Figure 6.5A).

Reliable stream discharge measurements could not be made in experiments other than the  $^{15}\text{NO}_3^-$  addition experiment due to problems with the pressure transducer. The

$\delta^{15}\text{N}$  of  $\text{NO}_3^-$  and POM are plotted along with stream discharge in Figure 6.6. The initial peak observed in  $\delta^{15}\text{N}$  of  $\text{NO}_3^-$  was concurrent with an increase in stream discharge associated with a heavy rain event (Figure 6.6A). This storm event had the opposite effect on  $\delta^{15}\text{N}$  of POM (Figure 6.6B).

*$^{15}\text{N}$ -glycine stream addition*– The  $\delta^{15}\text{N}$  of  $\text{NO}_3^-$  during the  $^{15}\text{N}$ -glycine stream tracer addition experiment is shown in Figure 6.7. The initial  $\delta^{15}\text{N}$  of  $\text{NO}_3^-$  observed during this experiment was 2.6‰ (Figure 6.7A). During the first day of the experiment, the  $\delta^{15}\text{N}$  of  $\text{NO}_3^-$  increased rapidly to a maximum value of 520‰, and remained more or less constant until the pump was turned off (Figure 6.7B). Once the pump was turned off, the  $\delta^{15}\text{N}$  of  $\text{NO}_3^-$  decreased rapidly to 120‰, and decreased gradually thereafter (Figure 6.7A). The final sample was taken 6 days after the experiment commenced, and the  $\delta^{15}\text{N}$  of  $\text{NO}_3^-$  remained elevated (14.2‰, Figure 6.7A).

The  $\delta^{15}\text{N}$  of POM observed during the  $^{15}\text{N}$ -glycine stream tracer addition experiment is shown in Figure 6.8. Before the experiment, the average  $\delta^{15}\text{N}$  of POM was 1.8‰ (Figure 6.8A). The  $\delta^{15}\text{N}$  of POM did not respond to the tracer addition initially, and in fact decreased slightly, but increased to 10.1‰ by the end of the experiment (Figure 6.8B). After the experiment, the  $\delta^{15}\text{N}$  of POM increased to 13.4‰, and remained elevated over initial values (7.3‰) when the last sample was taken four days later (Figure 6.8A).

*Soil tracer additions*– Soil tracer experiment results are presented in Figures 6.9 through 6.11. In general, roots and SOM responded most to  $\text{NO}_3^-$  additions, then  $\text{NH}_4^+$ , then glycine, indicating that demand for oxidized DIN is greatest in soil plants and microbes. When  $^{15}\text{NO}_3^-$  was added to the soil, initially soil  $\delta^{15}\text{N}$  of soil  $\text{NO}_3^-$  increased dramatically from -5.1‰ to 970‰ (Figure 6.10A), then decreased gradually throughout the remainder of the experiment (Figure 6.9A). There was no initial increase in  $\text{NO}_3^-$

concentration in the  $\text{NO}_3^-$  addition plot, although the tracer did cycle through DIN and PON at a time scale of a week or two (Figure 6.9A and 6.11A). Fine roots and soil OM responded quickly to both  $^{15}\text{NO}_3^-$  and  $^{15}\text{NH}_4^+$  additions, but then the level of tracer in each of these compartments decreased (Figures 6.9 and 6.10 A and B). The  $\delta^{15}\text{N}$  of fine roots seemed to mirror the  $\delta^{15}\text{N}$  of soil  $\text{NO}_3^-$  in the  $^{15}\text{NO}_3^-$  and  $^{15}\text{NH}_4^+$  additions, while in the  $^{15}\text{N}$ -glycine addition, the isotopic composition of soil  $\text{NO}_3^-$  was more closely mirrored by the  $\delta^{15}\text{N}$  of SOM (Figure 6.9).

In the  $^{15}\text{N}$ -glycine addition, an initial increase in  $\delta^{15}\text{N}$  of soil  $\text{NO}_3^-$  was followed by a decrease and then another, more gradual increase in  $\text{NO}_3^-$  (Figure 6.9). Glycine was not initially incorporated directly into either SOM or fine roots (Figure 6.10C). Rather, the added  $^{15}\text{N}$  was incorporated into biomass only after it was remineralized into DIN. In the glycine addition plot, the  $\delta^{15}\text{N}$  of SOM was related to the  $\delta^{15}\text{N}$  of soil  $\text{NO}_3^-$ , while fine roots may have depended on another source of N such as dissolved  $\text{NH}_4^+$ . In the  $^{15}\text{NH}_4^+$  addition, soil  $\text{NO}_3^-$  increased quickly (Figure 6.10B) then decreased and increased again slowly (Figure 6.9B), indicating the possible remineralization of ON into  $\text{NO}_3^-$ . The remineralization of reduced or organic N into  $\text{NO}_3^-$  is supported by  $\text{NO}_3^-$  concentration patterns, which peaked several days after the initial tracer addition in both the  $^{15}\text{NH}_4^+$  and glycine addition plots.

## DISCUSSION

*Stream N transformations*— All three types of N added to the stream exhibited some degree of reactivity, indicating that dissolved N is not transported conservatively in this system. Added  $\text{NH}_4^+$  is both nitrified and taken up onto particles. Fluxes of  $^{15}\text{NO}_3^-$  (analogous to nitrification rate) for this experiment were estimated from the equation of Mulholland et al. (2000):

$$^{15}\text{NO}_3 \text{ flux} = (\Delta\delta^{15}\text{N-NO}_3/1000) \times 0.003663 (Q) ([\text{NO}_3\text{-N}]),$$

where the units of the flux of  $^{15}\text{NO}_3$  are  $\mu\text{g}^{15}\text{N}$  per second. In this equation,  $\Delta\delta^{15}\text{N-NO}_3$  represents the increase in the isotopic composition of  $\text{NO}_3^-$ , 0.003663 represents the ratio of  $^{15}\text{N}/^{14}\text{N}$  in air,  $Q$  represents the stream flow rate in liters per second, and  $[\text{NO}_3\text{-N}]$  represents the nitrate concentration in  $\mu\text{g N}$  per liter. The flux of  $^{15}\text{NO}_3$  (in  $\text{ng}^{15}\text{N}/\text{sec}$ ) for every sampling point in the  $^{15}\text{NH}_4^+$  experiment is shown in Figure 6.12A. Due to mechanical error in the stream weir, I do not have stream discharge measurements or nutrient concentrations for each sampling point, so we used the same estimated values for streamflow and  $\text{NO}_3^-$  concentration for each time point. For the  $^{15}\text{NH}_4^+$  addition experiment, the literature value for streamflow was 1.4 L/sec and  $\text{NO}_3^-$  concentration was 1.7  $\mu\text{M}$  or 23.8  $\mu\text{g/L}$  (Saunders and McClain in press). This assumption limits our calculation in several ways. If the average value of discharge or  $\text{NO}_3^-$  concentration is lower than the actual value, underestimate the flux of  $^{15}\text{NO}_3^-$ , and if the average value is higher than the actual value, my flux calculation is an overestimate. Nonetheless it is a useful calculation to provide rough estimates of the fate of added tracer in this system.

The maximum calculated flux of  $^{15}\text{NO}_3$  observed during the  $^{15}\text{NH}_4^+$  addition experiment was 2.8  $\text{ng}^{15}\text{N}/\text{sec}$ , with a total of about 9.6% of added  $^{15}\text{N}$  being converted to  $\text{NO}_3^-$ , based on average  $\delta^{15}\text{N}$  of  $\text{NO}_3^-$  and  $\text{NO}_3^-$  concentration of 11.9‰ and 23.8 $\mu\text{g/L}$ , respectively. This rate is about 6 times lower than the maximum flux of  $^{15}\text{NO}_3$  observed during a  $^{15}\text{NH}_4^+$  addition experiment ( $\sim 16 \text{ ng}^{15}\text{N}/\text{sec}$ ) in the Walker Branch stream in Tennessee, USA (Mulholland et al. 2000). In that study, nitrification accounted for 23% of added  $^{15}\text{NH}_4^+$  flux (Mulholland et al. 2000). In Upper Ball Creek, North Carolina, USA, the maximum flux of  $^{15}\text{NO}_3$  was about 2.4  $\text{ng}^{15}\text{N}/\text{sec}$ , or 7% of  $^{15}\text{NH}_4^+$  uptake (Tank et al. 2000), very close to our result. Low nitrification rates in Upper Ball Creek were attributed to very low ambient  $\text{NH}_4^+$  concentrations and low quality stream sediments (or

POM with a high C:N ratio), which may explain our observed trend. If nitrifying bacteria in the Wara site are limited by  $\text{NH}_4^+$ , the initial tracer addition may have stimulated nitrification to the high level observed on day 1. Adding  $^{15}\text{NH}_4^+$  to a Puerto Rican stream resulted in high nitrification rates (maximum flux of  $^{15}\text{NO}_3^- \sim 200 \text{ ng}^{15}\text{N}/\text{sec}$ , or more than 50% of the added  $^{15}\text{NH}_4^+$ ), attributed to conditions that are conducive to nitrification such as low light and high water temperatures (Merriam et al. 2002). In the Puerto Rican study, ambient  $\text{NO}_3^-$  concentrations were high ( $129 \text{ } \mu\text{g N}/\text{L}$ ), and  $\text{NH}_4^+$  concentrations were low (from  $2 - 3 \text{ } \mu\text{g N}/\text{L}$ ; Merriam et al. 2002). In general, nitrification rates vary independently, and physical conditions such as temperature, irradiance, and substrate availability drive of this transformation. In our system, the combination of low  $\text{NH}_4^+$  availability, moderate temperatures ( $\sim 10^\circ\text{C}$ ), and low organic carbon availability may have minimized the contribution of nitrification to  $\text{NH}_4^+$  losses.

Similar data for the glycine addition experiment are presented in Figure 6.12B. The same equation for  $^{15}\text{NO}_3^-$  flux was used here, except that the value for  $\Delta\delta^{15}\text{N}-\text{NO}_3^-$  was corrected for the increased rate of addition of the tracer ( $1.6 \text{ ml}/\text{min}$  as opposed to  $1 \text{ ml}/\text{min}$ ). The stream discharge rate was estimated at  $1.5 \text{ L}/\text{sec}$ , and the background concentration of  $\text{NO}_3^-$  was  $0.8 \text{ } \mu\text{M}$ , or  $11.2 \text{ } \mu\text{g}/\text{L}$  (Saunders and McClain in press). The addition of  $^{15}\text{N}$ -glycine caused higher  $^{15}\text{NO}_3^-$  fluxes. The maximum flux observed was  $31.1 \text{ ng}^{15}\text{N}/\text{sec}$ , about 2 times higher than the rate observed during the  $\text{NH}_4^+$  addition in the Walker Branch stream (Mulholland et al. 2000). Our values of  $\delta^{15}\text{N}$  of  $\text{NO}_3^-$  observed during the  $^{15}\text{N}$ -glycine addition indicate that 30% of added  $^{15}\text{N}$  was converted to  $\text{NO}_3^-$ . No other studies have reported the fate of labeled glycine in streams, so comparisons with other ecosystems are impossible. However, since nitrification was higher with glycine than with  $\text{NH}_4^+$ , I hypothesize that microbes in this stream are limited by C availability



and are using glycine as an energy source, supports the idea that nitrification is organic matter limited in Andean cloudforest streams.

The reactivity of dissolved  $\text{NO}_3^-$  is difficult to gauge in this system, because we do not have measurements of the  $\delta^{15}\text{N}$  of other dissolved species, or a measurement of a conservative tracer to assess the impact of dilution. However, the  $\delta^{15}\text{N}$  of  $\text{NO}_3^-$  in the stream varied independently of stream discharge (Figure 6.6A). Several other studies have measured denitrification rates in flowing waters. Denitrification rates were high ( $120 \mu\text{mol m}^{-2} \text{hr}^{-1}$ ) but rapid nitrification and groundwater inputs were sufficient to maintain a high ambient  $\text{NO}_3^-$  concentration during high flows in an agricultural stream in the Midwestern USA (Böhlke et al. 2004). In Walker Branch (Tennessee, USA), denitrification rates were much lower ( $12 \mu\text{mol m}^{-2} \text{hr}^{-1}$ ), but they were sufficient to keep  $\text{NO}_3^-$  concentrations low along with lower nitrification rates than observed in other systems (Mulholland et al. 2004). In the current  $^{15}\text{N}$  tracer addition study, the highest  $\delta^{15}\text{N}$  of  $\text{NO}_3^-$  values occurred during a slight increase in discharge (Figure 6.6A), indicating that during increased baseflow, the main source of water to this system (Saunders and McClain in press), did not dilute the labeled  $\text{NO}_3^-$ . The decrease in  $^{15}\text{NO}_3^-$  later in the experiment could have been due to dilution with  $\text{NO}_3^-$  produced in the stream by nitrification, although nitrification appeared to be minimal in this system. Added  $^{15}\text{NO}_3^-$  may have been converted to  $^{15}\text{NH}_4^+$  (not measured) via dissimilatory nitrate reduction to ammonium (DNRA), which is less common than denitrification in flowing waters, although it can occur in the presence of low levels of labile DOC and high  $\text{NO}_3^-$  availability (Ostrom et al. 2002). Both denitrification and DNRA would likely increase or have a neutral effect on  $\delta^{15}\text{N}$  of remaining  $\text{NO}_3^-$ .

Increases in  $\delta^{15}\text{N}$  of particulate organic matter (POM) in each of the three studies were probably due to uptake by microbes associated with POM (Peterson et al. 1997,

Tank et al. 2000, Merriam et al. 2002) and by sorption (Aufdenkampe et al. 2001). Primary production in small Amazonian streams is low (Quay et al. 1995, McClain and Elsenbeer 2001). Sorption reactions occur preferentially in the presence of reduced N rather than  $\text{NO}_3^-$ , because most minerals and suspended organic material, including humics, are negatively charged. Ammonium may have been taken up onto particles rather than nitrified; at least, more  $^{15}\text{N}$  was incorporated into POM than  $\text{NO}_3^-$  (Figures 6.2 and 6.3). In Puerto Rico, uptake of added  $^{15}\text{NH}_4^+$  onto fine benthic organic matter (FBOM) was more than three times lower than the nitrification rate (Merriam et al. 2002). Likewise, in Upper Ball Creek, where nitrification rates were closest to the present study, nitrification was about six times higher than uptake onto FBOM (Tank et al. 2000). However, in the Walker Branch site, uptake of  $^{15}\text{NH}_4^+$  in FBOM and nitrification were approximately equal (Mulholland et al. 2000). Decomposing leaves were the largest sinks for  $^{15}\text{NH}_4^+$  in the Walker Branch site (Mulholland et al. 2000), but I did not size fractionate my POM samples.

*Soil N transformations*—Nitrate is absorbed rapidly into fine roots (within 30 minutes) and SOM (within 2 days; Figure 6.9A). In contrast, added  $^{15}\text{NH}_4^+$  and  $^{15}\text{N}$ -glycine were incorporated into roots and SOM later in the experiment (Figure 6.9B and C). This result is consistent with other studies showing a high demand for  $\text{NO}_3^-$  in soils and plants (Nadelhoffer et al. 1999, Providoli et al. 2005). However,  $^{15}\text{NO}_3^-$  and  $^{15}\text{NH}_4^+$  were retained more or less equally by biomass in forests in the Chilean Andes, and  $\text{NH}_4^+$  demand was higher than  $\text{NO}_3^-$  demand initially (Perakis and Hedin 2001). Soil nitrification was a significant sink for both  $^{15}\text{NH}_4^+$  and  $^{15}\text{N}$ -glycine in this study, with consistently more  $^{15}\text{N}$  incorporated into soil  $\text{NO}_3^-$  than into fine roots or SOM over the entire experiment (Figure 6.9). These observations suggest that there is a high demand for  $\text{NO}_3^-$  in these forests. Other studies in South American forests have shown high

mineralization and nitrification rates supporting high DIN demand by soil biota (Pérez et al. 1998), and rapid terrestrial uptake may control low DIN exports in these systems (Perakis and Hedin 2001, 2002). We were not able to measure the  $\delta^{15}\text{N}$  of  $\text{NH}_4^+$ , but the presence of nitrification in soils is indicated by the initial peak in  $\delta^{15}\text{N}$  of all measured parameters in the  $\text{NO}_3^-$  addition site, and later peaks (day 20) in the  $\text{NH}_4^+$  and  $^{15}\text{N}$ -glycine addition sites (Figures 6.9 and 6.10). High mineralization rates at the Wara site are indicated by rapid degradation of leaf litter as compared to other forests (Chapter 5, this volume), and rapid litter degradation was linked to high N mineralization rates in tropical systems (Vitousek and Sanford 1986).

Despite evidence for high demand for  $\text{NO}_3^-$  and  $\text{NH}_4^+$ , only a small portion of either tracer was retained in dissolved  $\text{NO}_3^-$ , fine roots or SOM, indicating that denitrification, nitrification or DNRA may be substantial sinks for DIN. All of these processes are higher in tropical than temperate forests (Vitousek and Sanford 1986). DNRA was more than three times higher than denitrification in Puerto Rican soils (Silver et al. 2001). The other N sink we cannot account for is export in baseflow or runoff, which can be high in tropical systems, especially for  $\text{NO}_3^-$ , the most hydrologically mobile N form (Providoli et al. 2005).

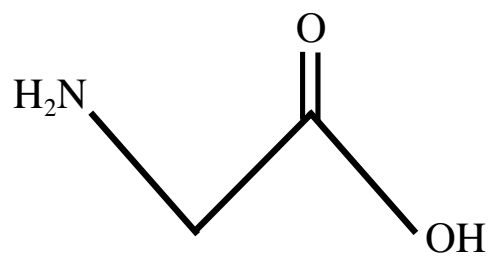
In the Wara stream, nitrification of added  $^{15}\text{N}$ -glycine was higher than that of added  $^{15}\text{NH}_4^+$  (see above). In the soils, however, the differences in  $\delta^{15}\text{N}$  of  $\text{NO}_3^-$  after addition of each tracer are slighter. Initial nitrification of  $^{15}\text{NH}_4^+$  (evidenced by  $\delta^{15}\text{N}$  of  $\text{NO}_3^-$ ) was higher than that of  $^{15}\text{N}$ -glycine, but by mid-experiment (day 15),  $\delta^{15}\text{N}$  of  $\text{NO}_3^-$  was about equal in each plot (Figure 6.9). Similarly, about the same amount of tracer was incorporated into SOM (Figure 6.9). The major difference observed between the  $^{15}\text{NH}_4^+$  and  $^{15}\text{N}$ -glycine additions was the relative amount of tracer incorporated into roots. Plant roots in this system were unresponsive to available amino acids, despite

studies that have shown that uptake of glycine by plants in old-growth boreal forests is similar to uptake of  $\text{NH}_4^+$  (Näsholm et al. 1998), and others that have used  $^{15}\text{N}$ -glycine to label plants for food web studies (Unsicker et al. 2005). The slight increase in  $\delta^{15}\text{N}$  of fine roots observed here after the addition of  $^{15}\text{N}$ -glycine is likely due to mineralization and/or nitrification (Figure 6.9).

## CONCLUSIONS

This is a preliminary study and measurements of conservative tracers, isotopic composition of other dissolved N components, and accurate streamflow measurements are necessary to definitively calculate N transformation rates. However, this information on the relative rates of N cycling in streams and soils of the tropical Andes suggest some preliminary conclusions about mechanisms controlling low DIN exports from the system. High demand for  $\text{NH}_4^+$  and  $\text{NO}_3^-$  in riparian soils leads to low export of DIN to the stream. Nitrate and  $\text{NH}_4^+$  concentrations decrease in waters from upland to riparian zone to the stream (Saunders and McClain in press), and this study shows rapid uptake of these N species in soils. Similarly, in a small stream in the Brazilian Amazon, DIN was derived from in-stream remineralization, and most DIN in groundwater was removed at the riparian zone, although that site had a well-defined, suboxic riparian zone where  $\text{NO}_3^-$  was replaced by  $\text{NH}_4^+$ , and it also had a much gentler relief (Brandes et al. 1996). In-stream N cycling processes in this study were dwarfed by addition of baseflow, and nitrification in the stream appeared to be limited by labile organic C, as indicated by the  $^{15}\text{N}$ -glycine addition experiment. The low DIN levels found in Andean cloud forest ecosystems appear to be controlled by several factors: (1), low inputs of DIN from the riparian zone and in precipitation; (2), limitation of microbially mediated N cycling by organic C availability; (3), low DIN uptake rates in the stream; and (4), removal of

reduced N compounds from stream waters by sorption. Increased inorganic N deposition to the western Andes due to deforestation and industrialization, may cause increased DIN exports from the Amazon headwaters to downstream regions.



glycine  
 $\text{C}_2\text{H}_5\text{NO}_2$   
75.1 g/mol

Figure 6.1. Molecular structure, formula, and weight of glycine.

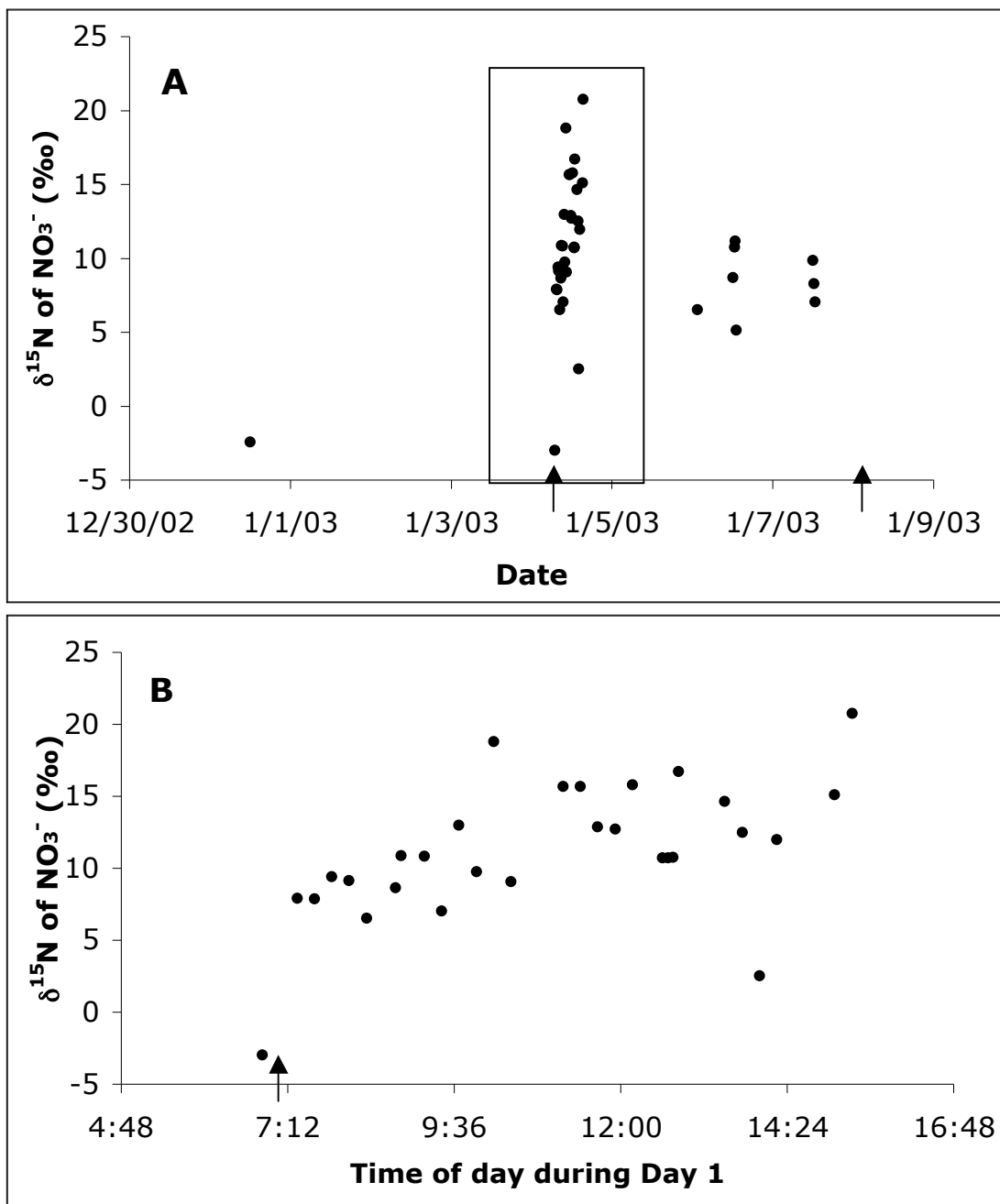


Figure 6.2. Isotopic composition ( $\delta^{15}\text{N}$ ) of dissolved  $\text{NO}_3^-$  in stream water sampled during the  $^{15}\text{NH}_4^+$  tracer injection experiment. A:  $\delta^{15}\text{N}$  of  $\text{NO}_3^-$  for the entire experiment. Arrows represent the starting and stopping of the pump, and the box represents the time shown in (B). B:  $\delta^{15}\text{N}$  of  $\text{NO}_3^-$  observed only during the first day of the experiment. Arrow represents the time when the pump was turned on.

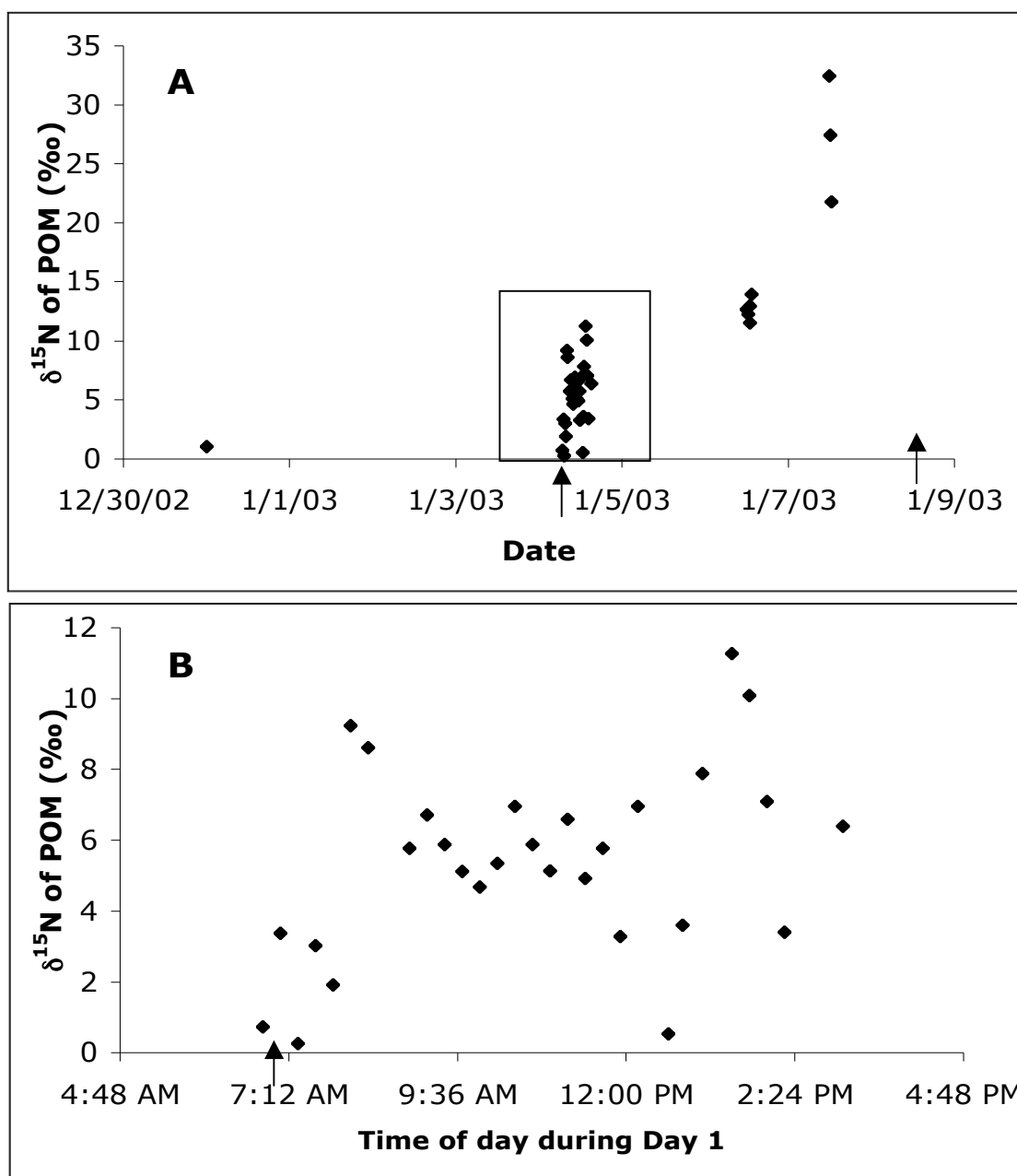


Figure 6.3. Isotopic composition ( $\delta^{15}\text{N}$ ) of suspended POM in stream water sampled during the  $^{15}\text{NH}_4^+$  tracer injection experiment in January of 2003. A:  $\delta^{15}\text{N}$  of POM for the entire experiment. Arrows represent the starting and stopping of the pump, and the box represents the time shown in (B). B:  $\delta^{15}\text{N}$  of POM observed only during the first day of the experiment. Arrow represents the time when the pump was turned on.



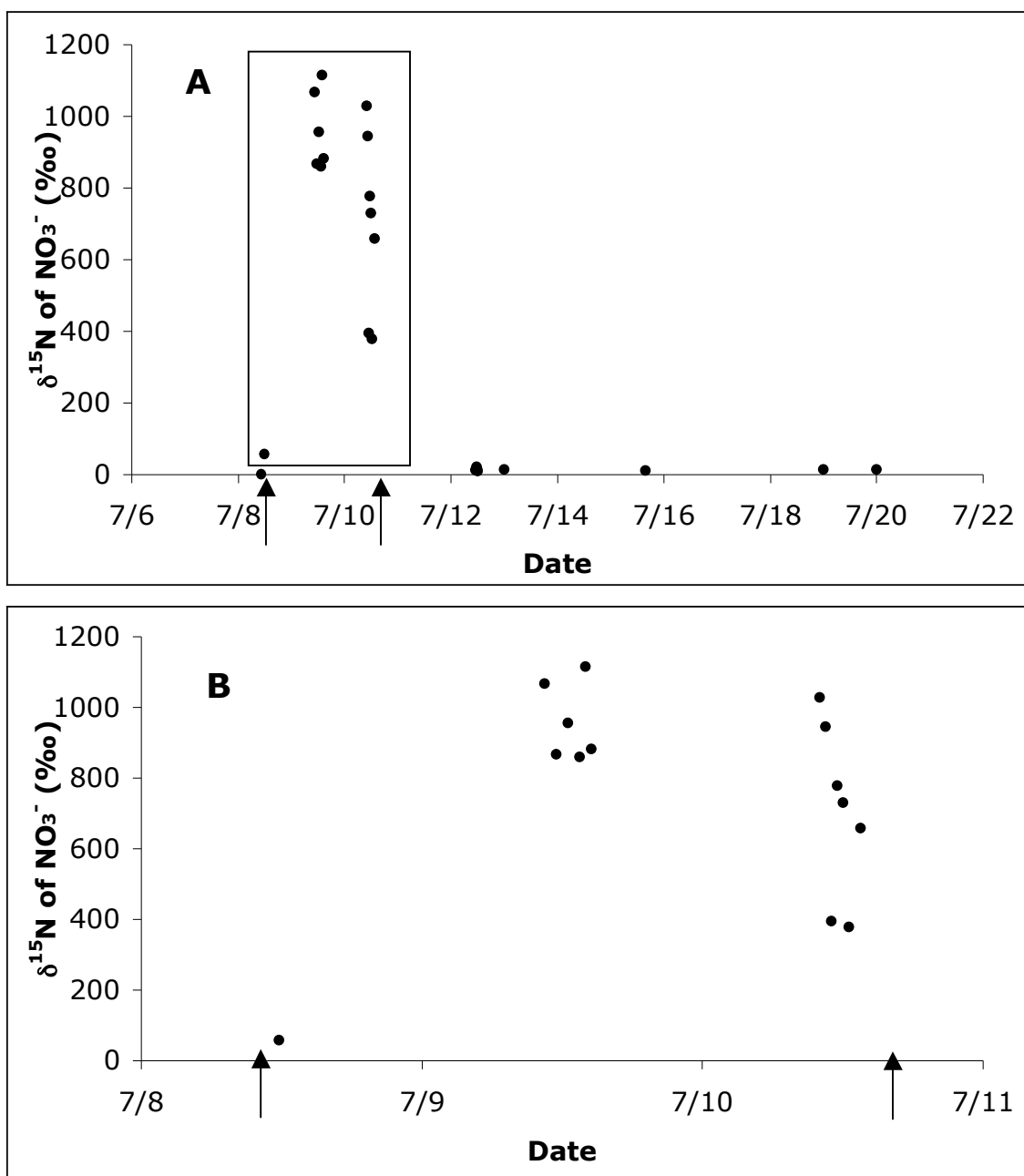


Figure 6.4. Isotopic composition ( $\delta^{15}\text{N}$ ) of  $\text{NO}_3^-$  in stream water sampled during the  $^{15}\text{NO}_3^-$  tracer injection experiment in July of 2004. A:  $\delta^{15}\text{N}$  of  $\text{NO}_3^-$  for the entire experiment. Arrows represent the starting and stopping of the pump, and the box represents the time shown in (B). B:  $\delta^{15}\text{N}$  of  $\text{NO}_3^-$  observed only when the pump was turned on.

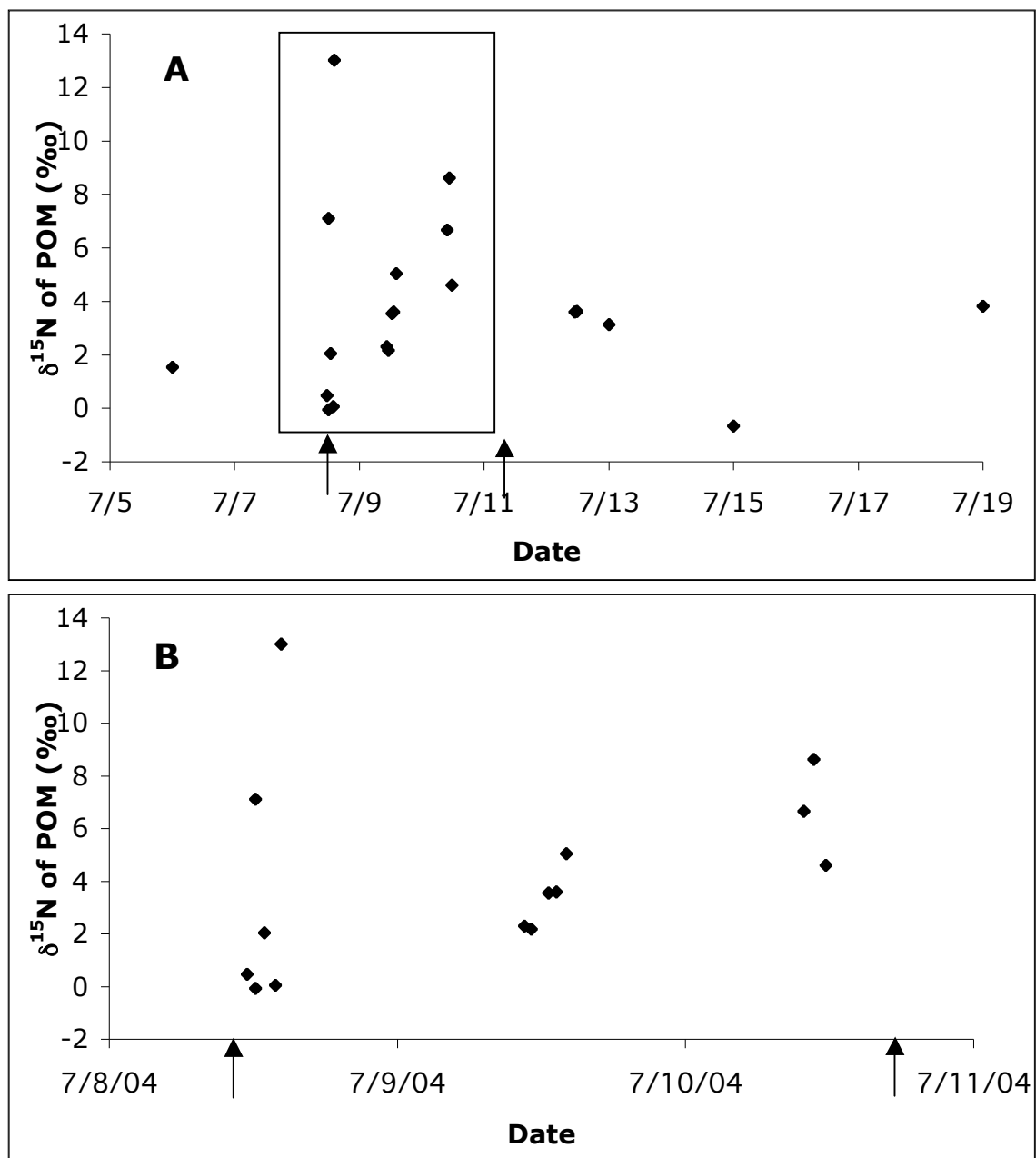


Figure 6.5. Isotopic composition ( $\delta^{15}\text{N}$ ) of POM in stream water sampled during the  $^{15}\text{NO}_3^-$  tracer injection experiment in July of 2004. A:  $\delta^{15}\text{N}$  of POM for the entire experiment. Arrows represent the starting and stopping of the pump, and the box represents the time shown in (B). B:  $\delta^{15}\text{N}$  of POM observed only when the pump was turned on.

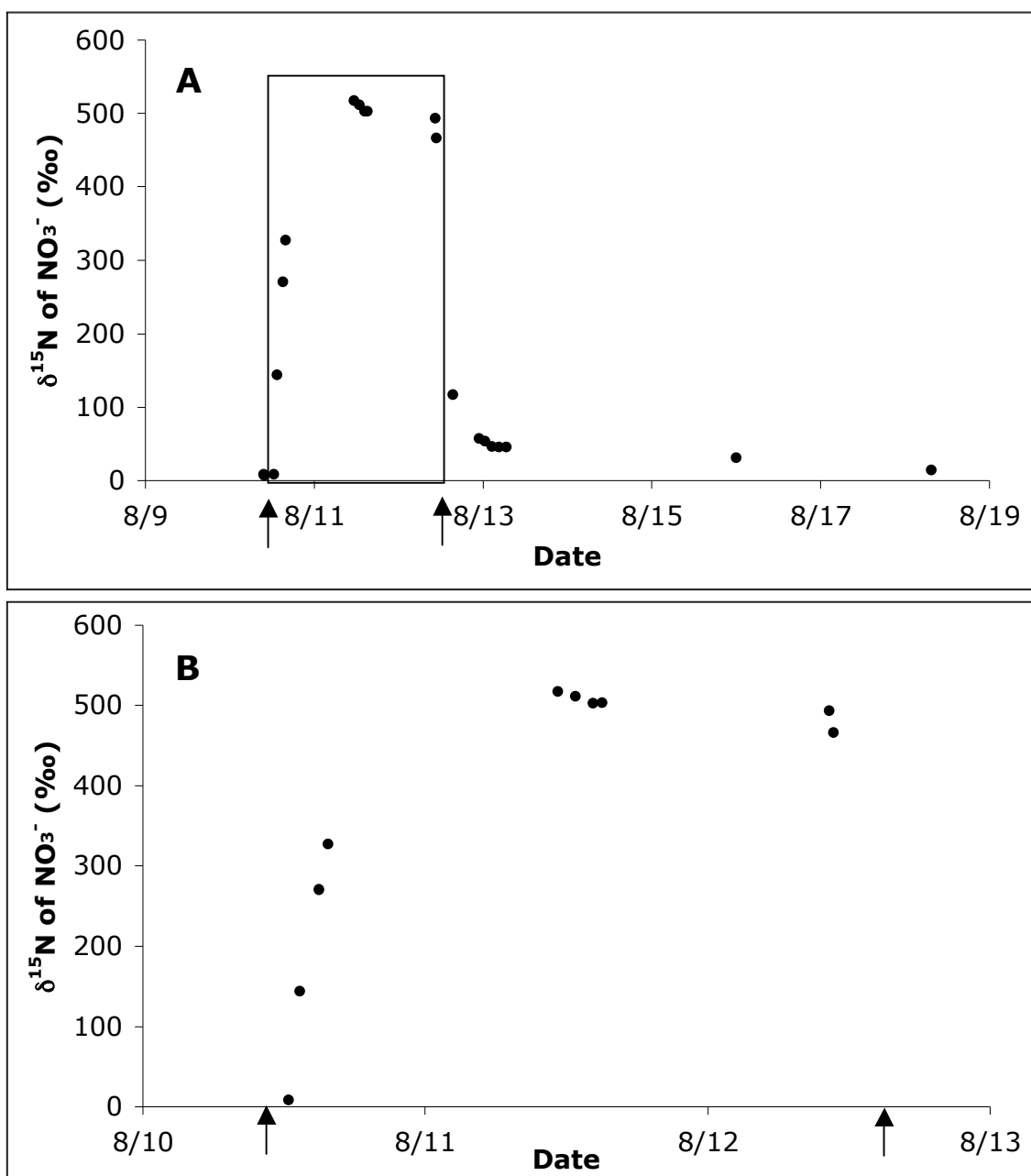


Figure 6.7. Isotopic composition ( $\delta^{15}\text{N}$ ) of  $\text{NO}_3^-$  in stream water sampled during the  $^{15}\text{N}$ -glycine tracer injection experiment in August of 2004. A:  $\delta^{15}\text{N}$  of  $\text{NO}_3^-$  for the entire experiment. Arrows represent the starting and stopping of the pump, and the box represents the time shown in (B). B:  $\delta^{15}\text{N}$  of  $\text{NO}_3^-$  observed only when the pump was turned on.

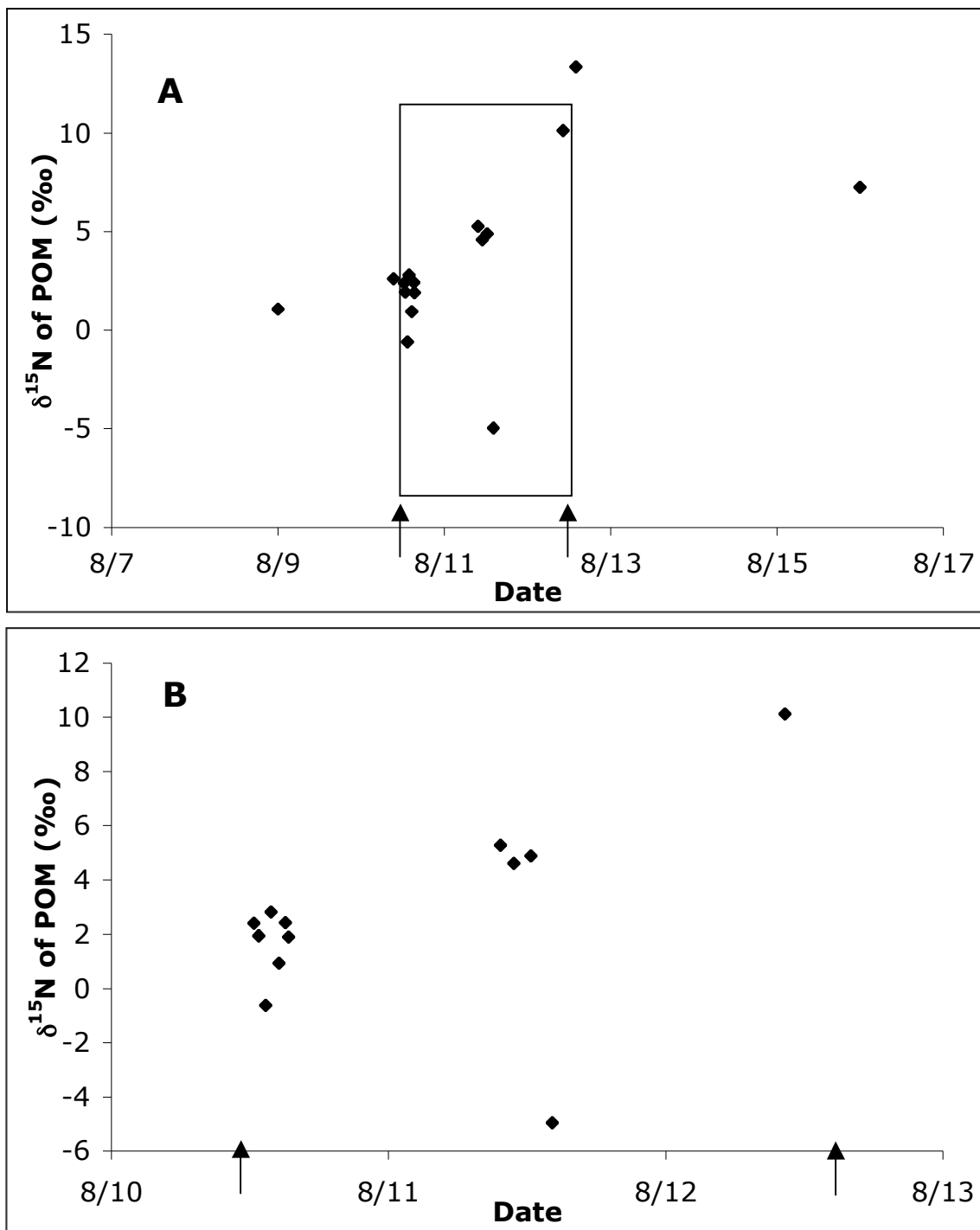


Figure 6.8. Isotopic composition ( $\delta^{15}\text{N}$ ) of POM in stream water sampled during the  $^{15}\text{N}$ -glycine tracer injection experiment in August of 2004. A:  $\delta^{15}\text{N}$  of POM for the entire experiment. Arrows represent the starting and stopping of the pump, and the box represents the time shown in (B). B:  $\delta^{15}\text{N}$  of POM observed only when the pump was turned on.

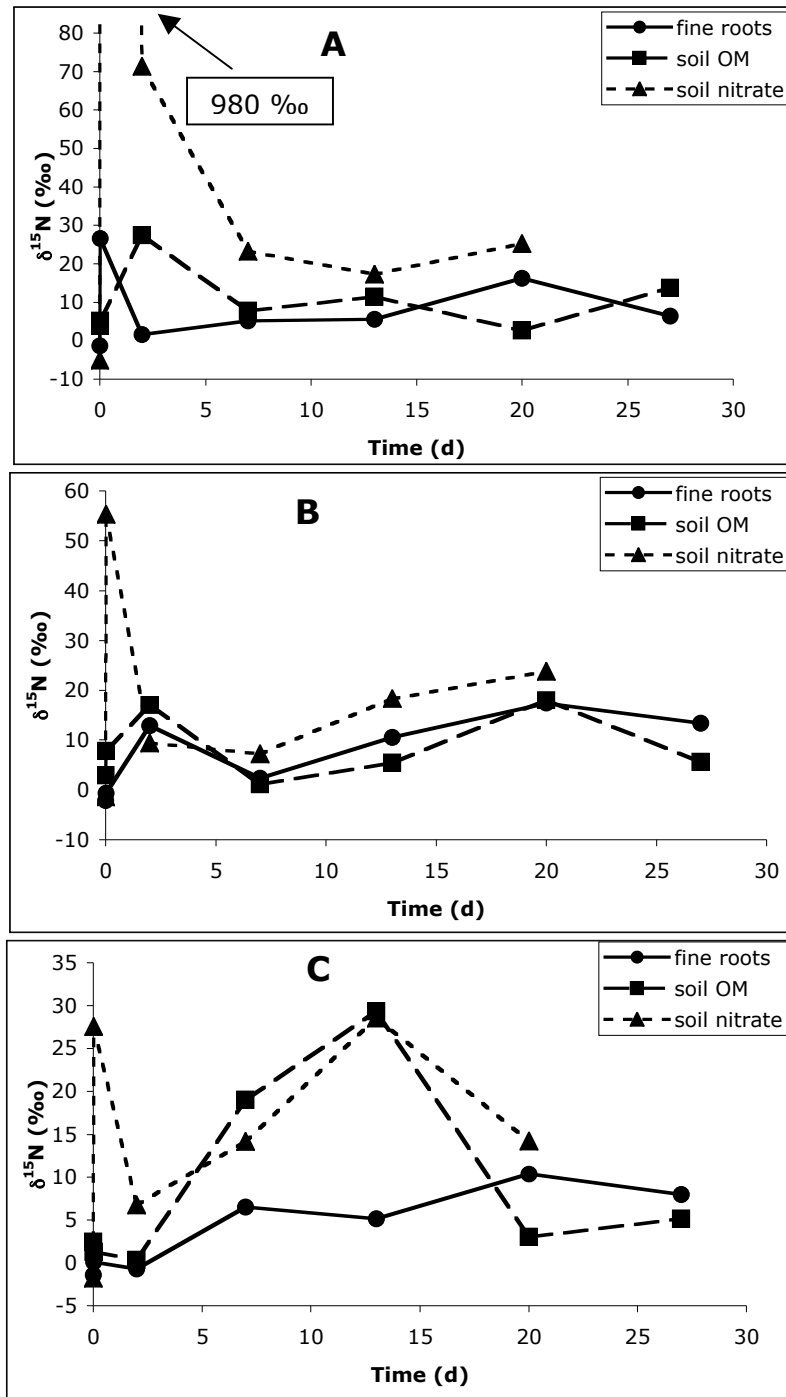


Figure 6.9.  $\delta^{15}\text{N}$  of soil  $\text{NO}_3^-$ , soil OM, and fine roots during three different  $^{15}\text{N}$  tracer addition experiments in the Wara experimental forest. A =  $^{15}\text{NO}_3^-$  addition; B =  $^{15}\text{NH}_4^+$  addition; C =  $^{15}\text{N}$ -glycine addition

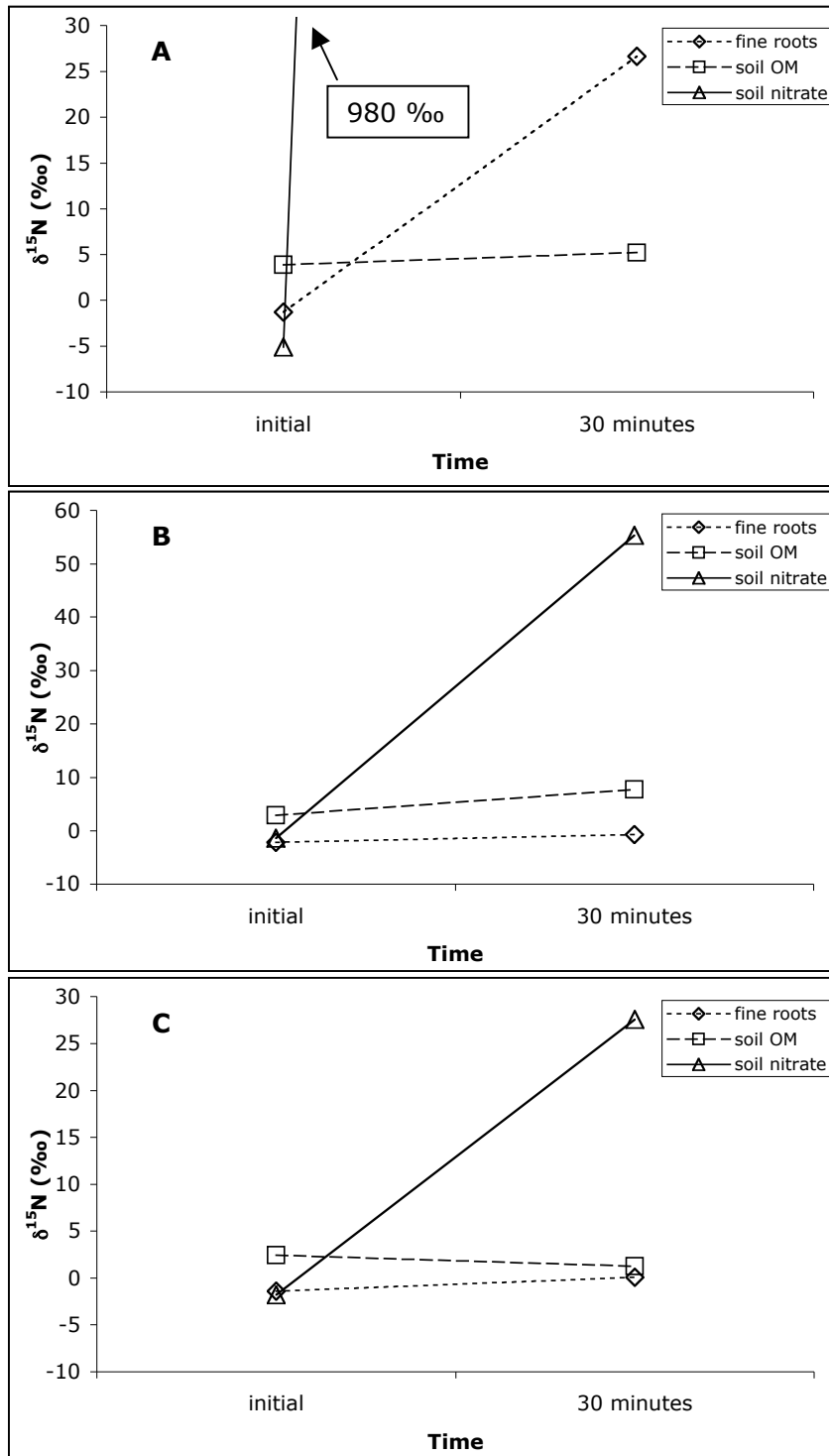


Figure 6.10  $\delta^{15}\text{N}$  of fine roots, soil OM, and soil  $\text{NO}_3^-$  observed for the first 30 minutes of the soil tracer experiments. A =  $^{15}\text{NO}_3^-$  addition experiment; B =  $^{15}\text{NH}_4^+$  addition experiment; C =  $^{15}\text{N}$ -glycine experiment.

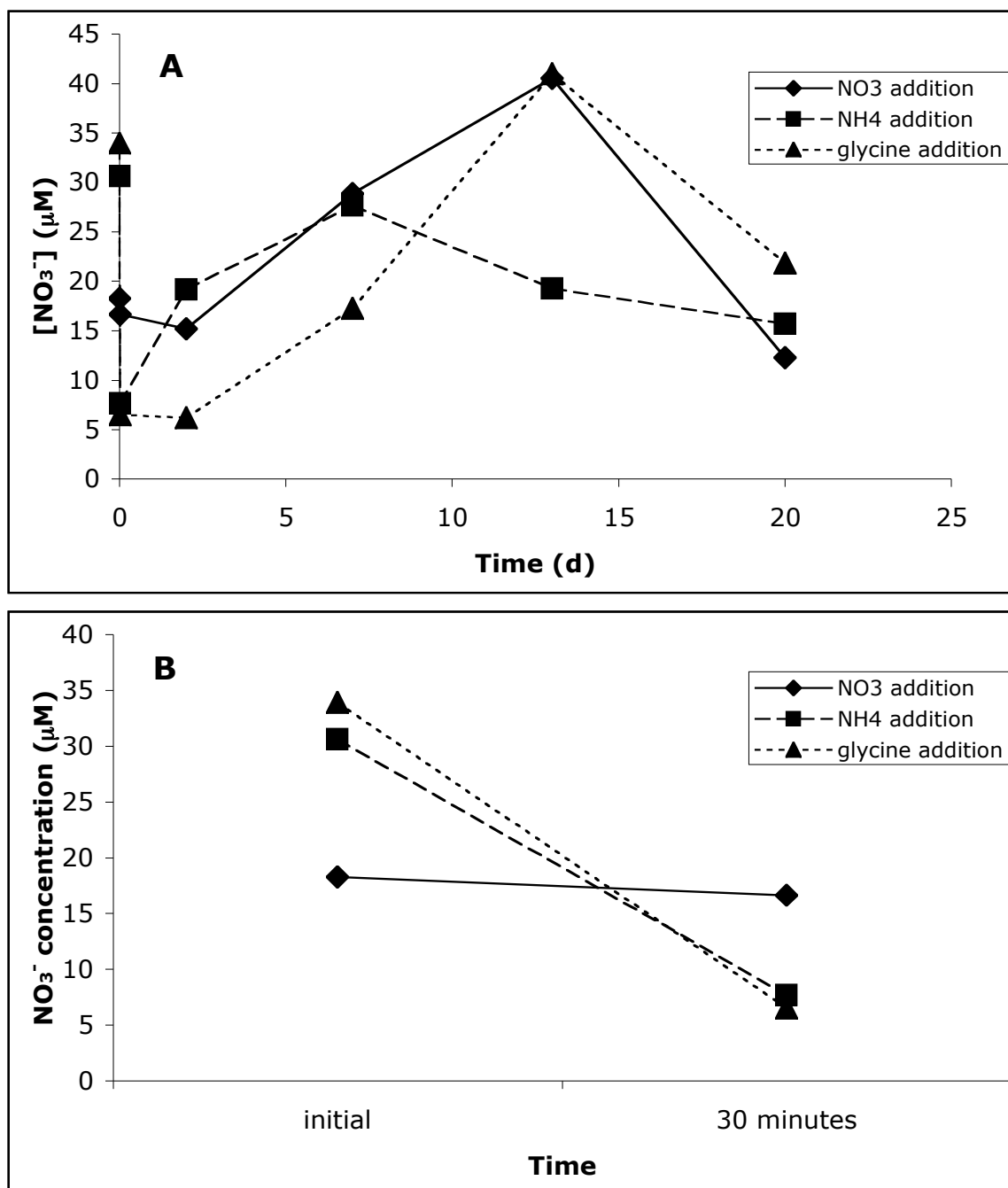


Figure 6.11. Soil dissolved  $\text{NO}_3^-$  concentrations observed during the soil tracer experiments. Data from all three experimental plots are shown. A: Nitrate concentrations over the entire experiment. B: Initial and  $t = 30 \text{ min}$   $\text{NO}_3^-$  concentrations.

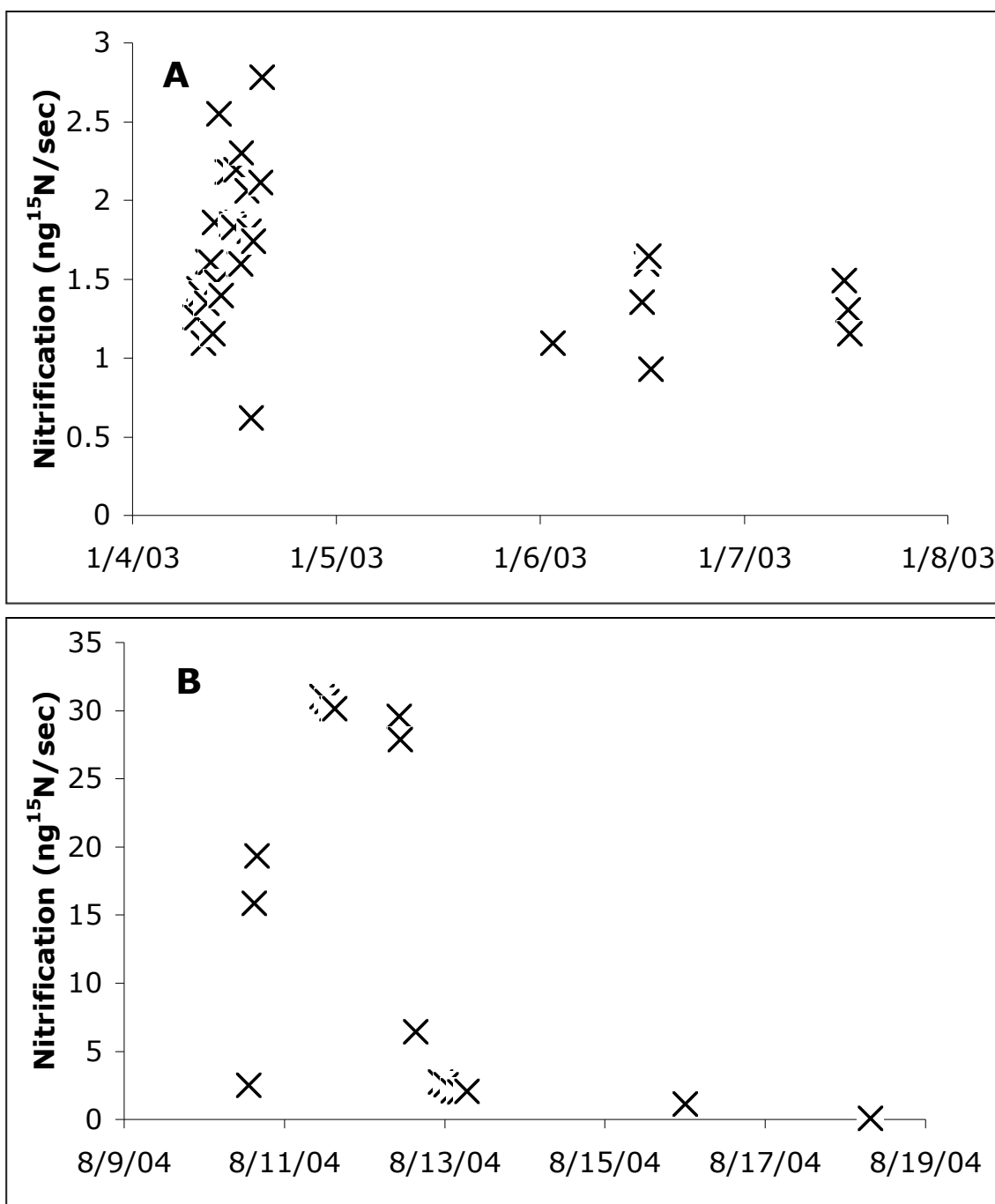


Figure 6.12. Nitrification rates calculated for specific time points in the stream  $^{15}\text{NH}_4^+$  addition experiment (A) and the  $^{15}\text{N}$ -glycine addition experiment (B). Values calculated using the equation of Mulholland et al. (2000).



## References

- Aalto, R., L. Maurice-Bourgoin, T. Dunne, D.R. Montgomery, C.A. Nittrouer, and J.L. Guyot. 2003. Episodic sediment accumulation on Amazonian floodplains influenced by El Niño/Southern Oscillation. *Nature* 425: 493-497.
- Aalto, R., T. Dunne, and J.L. Guyot. 2006. Geomorphic controls and Andean denudation rates. *J. Geol.* 114: 85-99.
- Aber, J.D., and J.M. Melillo. 1991. *Terrestrial Ecosystems*. 429 pp. Saunders College Publishing.
- Aber, J.D., K.J. Nadelhoffer, P. Steudler, and J.M. Melillo. 1989. Nitrogen saturation in northern forest ecosystems. *BioScience* 39: 378-386.
- Amundson R., A.T. Austin, E.A.G. Schuur, K. Yoo, V. Matzek, C. Kendall, A. Uebersax, D. Brenner, and W.T. Baisden. 2003. Global patterns of the isotopic composition of soil and plant nitrogen. *Global Biogeochem. Cy.* 17: doi: 10.1029/2002GB001903.
- Asbury, C.E., W.H. McDowell, R. Trinidad-Pizarro, and S. Berrios. 1994. Solute deposition from cloud water to the canopy of a Puerto Rican montane forest. *Atm. Env.* 28: 1773-1780.
- Aufdenkampe, A.K., J.I. Hedges, J.E. Richey, A.V. Krusche, and C.A. Llerena. 2001. Sorptive fractionation of dissolved organic nitrogen and amino acids onto fine sediments within the Amazon Basin. *Limnol. Oceanogr.* 46: 1921-1935.
- Avissar, R., and D. Werth. 2005. Global hydroclimatological teleconnections resulting from tropical deforestation. *J. Hydrometeorol.* 6: 134-145.
- Barraclough, D. 1995. <sup>15</sup>N isotope dilution techniques to study soil nitrogen transformations and plant uptake. *Nut. Cy. Agroecosyst.* 42: 185-192.
- Batjes, N.H. 1996. Total carbon and nitrogen in the soils of the world. *Eur. J. Soil. Sci.* 47: 151-163.
- Bedard-Haughn, A., J.W. van Groenigen, and C. van Kessel. 2003. Tracing <sup>15</sup>N through landscapes: potential uses and precautions. *J. Hydrol.* 272: 175-190.
- Bellanger, B., S. Huon, F. Velasquez, V. Vallès, C. Girardin, and A. Mariotti. 2004. Monitoring soil organic carbon erosion with  $\delta^{13}\text{C}$  and  $\delta^{15}\text{N}$  on experimental field plots in the Venezuelan Andes. *Catena* 58: 125-150.

- Benzing, D.H. 1998. Vulnerabilities of tropical forests to climate change: the significance of resident epiphytes. *Climate Change* 39: 519-540.
- Bernardes, M.C., L.A. Martinelli, A.V. Krusche, J. Gudelman, M. Moreira, R.L. Victoria, J.P.B.H. Ometto, M.V.R. Ballester, A.K. Aufdenkampe, J.E. Richey, and J.I. Hedges. 2004. Riverine organic matter composition as a function of land use changes, southwest Amazon. *Ecol. Appl.* 14: S263-S279.
- Bird, M.I., S.G. Haberle, and A.R. Chivas. 1994. The effect of altitude on the carbon-isotope composition of forest and grassland soils from Papua New Guinea. *Global Biogeochem. Cy.* 8: 13-22.
- Blair, N.E., E.L. Leithold, and R.C. Aller. 2004. From bedrock to burial: the evolution of particulate organic carbon across coupled watershed-continental margin systems. *Mar. Chem.* 92: 141-156.
- Böhlke, J.K., J.W. Harvey, and M.A. Voytek. 2004. Reach-scale isotope tracer experiment to quantify denitrification and related processes in a nitrate-rich stream, mid-continent United States. *Limnol. Oceanogr.* 49: 821-838.
- Brandes, J.A., and A.H. Devol. 2002. A global marine fixed nitrogen budget: Implications for Holocene nitrogen cycling. *Global Biogeochem. Cy.* 16: doi:10.1029/2001GB001856.
- Brandes, J.A., M.E. McClain, and T.P. Pimentel. 1996. <sup>15</sup>N evidence for the origin and cycling of inorganic nitrogen in a small Amazonian catchment. *Biogeochemistry* 34: 45-56.
- Bronk, D.A., M.W. Lomas, P.M. Glibert, K.J. Schukert, and M.P. Sanderson. 2000. Total dissolved nitrogen analysis: comparisons between the persulfate, UV, and high temperature oxidation methods. *Mar. Chem.* 69: 163-178.
- Brooks, J.R., L.B. Flanagan, N. Buchmann, and J.R. Ehleringer. 1997. Carbon isotope composition of boreal plants: functional grouping of life forms. *Oecologia* 110: 301-311.
- Buchmann, N., G. Gebauer, and E.-D. Schulze. 1996. Partitioning of <sup>15</sup>N-labeled ammonium and nitrate among soil, litter, below- and above-ground biomass of trees and understory in a 15-year-old *Picea abies* plantation. *Biogeochemistry* 33: 1-23.
- Burdige, D.J. 2005. Burial of terrestrial organic matter in marine sediments: A re-assessment. *Global Biogeochem. Cy.* 19: doi: 10.1029/2004GB002368.

- Bussmann, R.W. 2001. Epiphyte diversity in a tropical Andean forest – Reserva Biologica San Francisco, Zamora-Chinchipe, Ecuador. *Ecotropica* 7: 43-59.
- Chagnon, F.J.F., and R.L. Bras. 2005. Contemporary climate change in the Amazon. *Geophys. Res. Lett.* 32: L13703, doi:10.1029/2005GL022722.
- Cai, D.-L., F.C. Tan, and J.M. Edmond. 1988. Sources and transport of particulate organic carbon in the Amazon River and estuary. *Estuar. Coast. Shelf Sci.* 26: 1-14.
- Catchpole, D. 2004. The ecology of vascular epiphytes on a *Ficus* L. host (Moraceae) in a Peruvian cloud forest. Honours thesis, University of Tasmania, Australia.
- Chang, S.-C., I.-L. Lai, and J.-T. Wu. 2002. Estimation of fog deposition on epiphytic bryophytes in a subtropical montane forest ecosystem in northeastern Taiwan. *Atm. Res.* 64: 159-167.
- Clark, K.L., N.M. Nadkarni, and H.L. Gholz. 1998a. Growth, net production, litter decomposition, and net nitrogen accumulation by epiphytic bryophytes in a tropical montane forest. *Biotropica* 30: 12-23.
- Clark, K.L., N.M. Nadkarni, D. Schaefer, and H.L. Gholz. 1998b. Cloud water and precipitation chemistry in a tropical montane cloud forest, Monteverde, Costa Rica. *Atm. Env.* 32: 1595-1603.
- Clark, K.L., N.M. Nadkarni, and H.L. Gholz. 2005. Retention of inorganic nitrogen by epiphytic bryophytes in a tropical montane forest. *Biotropica* 37: 328-336.
- Cole, J.J., and N.F. Caraco. 2001. Carbon in catchments: connecting terrestrial carbon losses with aquatic metabolism. *Mar. Freshwater Res.* 52: 101-110.
- Cornell, S.E., T.D. Jickells, J.N. Cape, A.P. Rowland, and R.A. Duce. 2003. Organic nitrogen deposition on land and coastal environments: a review of methods and data. *Atm. Env.* 37: 2173-2191.
- Coûteaux M.M., L. Sarmiento, P. Bottner, D. Acevedo, and J.M. Thiéry. 2002. Decomposition of standard plant material along an altitudinal transect (65-3968 m) in the tropical Andes. *Soil Biol. Biochem.* 34: 69-78.
- Coyne, A., P. Seyler, H. Etcheber, M. Meybeck, and D. Orange. 2005. Spatial and seasonal dynamics of total suspended sediment and organic carbon species in the Congo River. *Global Biogeochem. Cy.* 19: doi: 10.1029/2004GB002335.
- Coxson, D.S. 1991. Nutrient release from epiphytic bryophytes in tropical montane rain-forest (Guadeloupe). *Can. J. Bot.* 69: 2122-2129.

- Coxson, D.S., and N.M. Nadkarni. 1995. Ecological roles of epiphytes in nutrient cycles of forest ecosystems. *In* Lowman and Nadkarni (eds) *Forest Canopies*. Academic Press, San Diego, Calif. pp. 495-543.
- Currie, W.S., K.J. Nadelhoffer, and J.D. Aber. 1999. Soil detrital processes controlling the movement of  $^{15}\text{N}$  tracers to forest vegetation. *Ecol. Appl.* 9: 87-102.
- Dadson, S., N. Hovius, S. Pegg, W.B. Dade, M.J. Horng, and H. Chen. 2005. Hyperpycnal river flows from an active mountain belt. *J. Geophys. Res.* 110: F04016, doi: 10.1029/2004JF000244.
- Davidson, E.A., S.C. Hart, C.A. Shanks, and M.K. Firestone. 1991. Measuring gross nitrogen mineralization, immobilization, and nitrification by  $^{15}\text{N}$  isotopic pool dilution in intact soil cores. *J. Soil Sci.* 21: 773-778.
- Davidson, E.A., S.C. Hart, and M.K. Firestone. 1992. Internal cycling of nitrate in soils of a mature coniferous forest. *Ecology* 73: 1148-1156.
- Devol, A.H., B.R. Forsberg, J.E. Richey, and T.P. Pimentel. 1995. Seasonal variation in chemical distribution in the Amazon (Solimões) River: A multiyear time series. *Global Biogeochem. Cy.* 9: 307-328.
- Devol, A.H. and J.I. Hedges. 2001. Organic matter and nutrients in the mainstem Amazon River, p. 275-306. *In* M.E. McClain, R.L. Victoria, and J.E. Richey [eds], *The biogeochemistry of the Amazon Basin*. Oxford University Press.
- Diaz, M., A. Haag-Kerwer, R. Wingfield, E. Ball, E. Olivares, T.E.E. Grams, H. Zeigler, and U. Lüttge. 1996. Relationships between carbon and hydrogen isotope ratios and nitrogen levels in leaves of *Clusia* species and two other Clusiaceae genera at various sites and different altitudes in Venezuela. *Trees* 10: 351-358.
- Druffel, E.R.M., J.E. Bauer, and S. Griffin. 2005. Input of particulate organic and dissolved inorganic carbon from the Amazon to the Atlantic Ocean. *Geochem. Geophys. Geosys.* 6: doi: 10.1029/2004GC000842.
- Dunne, T., L.A.K. Mertes, R.H. Meade, J.E. Richey, and B.R. Forsberg. 1998. Exchanges of sediment between the flood plain and channel of the Amazon River in Brazil. *Geol. Soc. Am. Bull.* 110: 450-467.
- Ehleringer, J.R., N. Buchmann, and L.B. Flanagan. 2000. Carbon isotope ratios in belowground carbon cycle processes. *Ecol. Appl.* 10: 412-422.

- Farnsworth, K.L., and J.D. Milliman. 2003. Effects of climatic and anthropogenic change on small mountainous rivers: the Salinas River example. *Global Planet. Change* 39: 53-64.
- Faure, G. 1986. *Principles of isotope geology*, 2<sup>nd</sup> edition. 608 pp. Wiley.
- Fogel, M.L., and L.A. Cifuentes. 1993. Isotope fractionation during primary production, p 73-98. *In* M.H. Engel and S.A. Macko [eds.], *Organic geochemistry: Principles and applications*. Plenum Press.
- Fry, B., D.E. Jones, G.W. Kling, R.B. McKane, K.J. Nadelhoffer, and B.J. Peterson. 1995. Adding <sup>15</sup>N tracers to ecosystem experiments. *In*: *Stable isotopes in the Biosphere* E. Wada, T. Yoneyama, M. Minagawa, T. Ando, and B. Fry [eds.]. pp 171-192. Kyoto University Press.
- Galloway, J.N., J.D. Aber, J.W. Erisman, S.P. Seitzinger, R.W. Howarth, E.B. Cowling, and B.J. Cosby. 2003. The nitrogen cascade. *BioScience* 53: 341-356.
- Gandhi, H., T.N. Wiegner, P.H. Ostrom, L.A. Kaplan, and N.E. Ostrom. 2004. Isotopic (<sup>13</sup>C) analysis of dissolved organic carbon in stream water using an elemental analyzer coupled to a stable isotope ratio mass spectrometer. *Rapid Commun. Mass Spectrom.* 18: 903-906.
- Gibbs, R.J. 1967. The geochemistry of the Amazon River system: Part I. The factors that control the salinity and the composition and concentration of the suspended solids. *Geol. Soc. Am. Bull.* 78: 1203-1232.
- Glauber, A.J. 2001. The effects of landslide disturbance on seasonal cycles of allochthonous inputs to Peruvian Amazonian headwater streams. Master's Thesis, University of Washington, USA.
- Gomez, D. 2000. Composicion floristica en el bosque ribereño de la cuenca alta San Alberto, Oxapampa, Peru. Master's thesis, Universidad Nacional Agraria La Molina, Perú.
- Gomez, D. 2005. Rainfall and cloudwater interception in tropical montane cloud forests and the effect of forest structure. Master's thesis, Florida International University, USA.
- Greenberg, J.P., A.B. Guenther, G. Pétron, C. Wiedinmyer, O. Vega, L.V. Gatti, J. Tota, and G. Fisch. 2004. Biogenic VOC emissions from forested Amazonian landscapes. *Global Change Biol.* 10: 651-662.

- Guenther, A. 1997. Seasonal and spatial variations in natural volatile organic compound emissions. *Ecol. Appl.* 7: 34-45.
- Guyot, J.L., and J.G. Wasson. 1994. Regional pattern of riverine dissolved organic carbon in the Amazon drainage basin of Bolivia. *Limnol. Oceanogr.* 39: 452-458.
- Hamilton, S.K., J.L. Tank, D.F. Raikow, W.M. Wollheim, B.J. Peterson, and J.R. Webster. 2001. Nitrogen uptake and transformation in a Midwestern U.S. stream: a stable isotope enrichment study. *Biogeochemistry* 54: 297-340.
- Hedges, J.I., W.A. Clark, P.D. Quay, J.E. Richey, A.H. Devol, and U. de M. Santos. 1986a. Compositions and fluxes of particulate organic matter in the Amazon River. *Limnol. Oceanogr.* 34: 717-738.
- Hedges, J.I., G.L. Cowie, J.E. Richey, P.D. Quay, R. Benner, M. Strom, and B.R. Forsberg. 1994. Origins and processing of organic matter in the Amazon River as indicated by carbohydrates and amino acids. *Limnol. Oceanogr.* 39: 743-761.
- Hedges, J.I., J.R. Ertel, P.D. Quay, P.M. Grootes, J.E. Richey, A.H. Devol, G.W. Farwell, F.W. Schmidt, and E. Salati. 1986b. Organic carbon-14 in the Amazon River system. *Science* 231: 1129-1131.
- Hedges, J.I., E. Mayorga, E. Tsamakis, M.E. McClain, A. Aufdenkampe, P. Quay, J.E. Richey, R. Benner, S. Opsahl, B. Black, T. Pimentel, J. Quintanilla, and L. Maurice. 2000. Organic matter in Bolivian tributaries of the Amazon River: A comparison to the lower mainstream. *Limnol. Oceanogr.* 45: 1449-1466.
- Hedges, J.I., and J.M. Oades. 1997. Comparative organic geochemistries of soils and marine sediments. *Org. Geochem.* 27: 319-361.
- Hedges, J.I., and J.H. Stern. 1984. Carbon and nitrogen determinations of carbonate-containing solids. *Limnol. Oceanogr.* 29: 657-663.
- Heitz, P., W. Wanek, R. Nadkarni, and N.M. Nadkarni. 2002. Nitrogen-15 natural abundance in a montane cloud forest canopy as an indicator of nitrogen cycling and epiphyte nutrition. *Oecologia* 131: 350-355.
- Hedin, L.O., J.J. Armesto, and A.H. Johnson. 1995. Patterns of nutrient loss from unpolluted, old-growth temperate forests: evaluation of biogeochemical theory. *Ecology* 76: 493-509.
- Heitz, P., W. Wanek, R. Wania, and N.M. Nadkarni. 2002. Nitrogen-15 natural abundance in a montane cloud forest canopy as an indicator of nitrogen cycling and epiphyte nutrition. *Oecologia* 131: 350-355.

- Hobbie, E.A., D.T. Tingey, P.T. Rygielwicz, M.G. Johnson, and D.M. Olszyk. 2002. Contributions of current year photosynthate to fine roots estimated using a  $^{13}\text{C}$ -depleted  $\text{CO}_2$  source. *Plant and Soil* 247: 233-242.
- Holland, E.A., F.J. Dentener, B.H. Braswell, and J.M. Sulzman. 1999. Contemporary and pre-industrial global reactive nitrogen budgets. *Biogeochemistry* 46: 7-43.
- Holloway, J., Dahlgren, R., Hansen, B., & Casey, W. 1998. Contribution of bedrock nitrogen to high nitrate concentrations in stream water. *Nature* 395: 785-788.
- Howarth, R.W., J.R. Fruci, and D. Sherman. 1991. Inputs of sediment and carbon to an estuarine ecosystem: influence of land use. *Ecol. Appl.* 1: 27-39.
- Hultine K.R., and J.D. Marshall. 2000. Altitude trends in conifer leaf morphology and stable carbon isotopic composition. *Oecologia* 123: 32-40.
- Instituto Geologico, Minero y Metalurgico. 1996. Geologia de los Cuadrangulos de Aguaytia, Pano y Pozuzo. Boletín 80 del Instituto Geologico, Minero y Metalurgico. Lima, Peru.
- Ittekkot, V. 1988. Global trends in the nature of organic matter in river suspensions. *Nature* 332: 436-438.
- Johansson, D. 1974. Ecology of vascular epiphytes in West African rain forest. *Acta phytogeographica suecia* 59: 1-136.
- Jones, M.N. 1984. Nitrate reduction by shaking with cadmium: alternative to cadmium columns. *Water Res.* 18: 643-646.
- Junk, W.J. 1985. The Amazon floodplain – a sink or source for organic carbon?, p. 267-283. *In* E.T. Degens, S. Kempe, and R. Herrera [eds.], *Transport of carbon and minerals in major world rivers*. SCOPE.
- Keene, W.C., J.A. Montag, J.R. Maben, M. Southwell, J. Leonard, T.M. Church, J.L. Moody, and J.N. Galloway. 2002. Organic nitrogen in precipitation over Eastern North America. *Atm. Env.* 36: 4529-4540.
- Kelly, D.L., E.V.J. Tanner, E.M.N. Lughadha, and V. Kapos. 1994. Floristics and biogeography of a rain-forest in the Venezuelan Andes. *J. Biogeogr.* 21: 421-440.
- Kitayama, K., and K. Iwamoto. 2001. Patterns of natural  $^{15}\text{N}$  abundance in the leaf-to-soil continuum of tropical rain forests differing in N availability on Mount Kinabalu, Borneo. *Plant and Soil* 229: 203-212.

- Knapp, A.N., D.M. Sigman, and F. Lipshultz. 2005. N isotopic composition of dissolved organic nitrogen and nitrate at the Bermuda Atlantic Time-series Study site. *Global Biogeochem. Cy.* 19: GB1018, doi: 10.1029/2004GB002320.
- Körner, Ch., G.D. Farquhar, and S.C. Wong. 1991. Carbon isotope discrimination by plants follows latitudinal and altitudinal trends. *Oecologia* 88: 30-40.
- Krull, E.S., E.A. Bestland, and W.P. Gates. 2002. Soil organic matter decomposition and turnover in a tropical Ultisol: Evidence from  $\delta^{13}\text{C}$ ,  $\delta^{15}\text{N}$ , and geochemistry. *Radiocarbon* 44: 93-112.
- Krusche, A.V., L.A. Martinelli, R.L. Victoria, M. Bernardes, P.B. de Camargo, M.V. Ballester, and S.E. Trumbore. 2002. Composition of particulate and dissolved organic matter in a disturbed watershed of southeast Brazil (Piracicaba River basin). *Water. Res.* 36: 2743-2752.
- Lajtha, K., and J.D. Marshall. 1994. Sources of variation in the stable isotopic composition of plants, p. 1-21 *In* Lajtha K. and R.H. Michener [eds], *Stable isotopes in ecology and environmental science*. Blackwell.
- Lehmann, M.F., S.M. Bernasconi, A. Barbieri, and J.A. McKenzie. 2002. Preservation of organic matter and alteration of its carbon and nitrogen isotope composition during simulated and in situ early diagenesis. *Geochim. Cosmochim. Acta* 66: 3573-3584.
- Lehmann, M.F., S.M. Bernasconi, J.A. McKenzie, A. Barbieri, M. Simona, and M. Veronesi. 2004. Seasonal variation of the  $\delta^{13}\text{C}$  and  $\delta^{15}\text{N}$  of particulate and dissolved carbon and nitrogen in Lake Lugano: Constraints on biogeochemical cycling in a eutrophic lake. *Limnol. Oceanogr.* 49: 415-429.
- Lesica, P. and R.K. Antibus. 1990. The occurrence of mycorrhizae in vascular epiphytes of two Costa Rican rain forests. *Biotropica* 22: 250-258.
- Lilienfein, J., R.G. Qualls, S.M. Uselman, and S.D. Bridgham. 2004. Adsorption of dissolved organic carbon and nitrogen in soils of a weathering chronosequence. *Soil Sci. Soc. Am. J.* 68: 292-305.
- Lojen, S., E. Spanier, A. Tsemel, T. Katz, N. Eden, and D.L. Angel. 2005.  $\delta^{15}\text{N}$  as a natural tracer of particulate nitrogen effluents released from marine aquaculture. *Mar. Biol.* 148: 87-96.
- Lovett, G.M. 1994. Atmospheric deposition of nutrients and pollutants in North America: an ecological perspective. *Ecol. Appl.* 4: 629-650.



- Ludwig, W., and J.-L. Probst. 1998. River sediment discharge to the oceans: present-day controls and global budgets. *Am. J. Sci.* 298: 265-295.
- Mariotti, A., F. Gadel, P. Giresse, and Kinga-Mouzeo. 1991. Carbon isotope composition and geochemistry of particulate organic matter in the Congo River (Central Africa): Application to the study of Quaternary sediments off the mouth of the river. *Chem. Geol.* 86: 345-357.
- Martinelli, L.A., M.V. Ballester, A.V. Krusche, R.L. Victoria, P.B. de Camargo, M. Bernardes, and J.P.H.B. Ometto. 1999. Landcover changes and  $\delta^{13}\text{C}$  composition of riverine particulate organic matter in the Piracicaba River Basin (southeast region of Brazil). *Limnol. Oceanogr.* 44: 1826-1833.
- Masiello, C.A., and E.R.M. Druffel. 2001. Carbon isotope geochemistry of the Santa Clara River. *Global Biogeochem. Cy.* 15: 407-416.
- Mayorga, E., and A. Aufdenkampe. 2002. Processing of bioactive elements in the Amazon River system, p. 1-24. *In* McClain, M.E. [ed], *The ecohydrology of South American rivers and wetlands*. IAHS Special Publication 6.
- Mayorga, E., A.K. Aufdenkampe, C.A. Masiello, A.V. Krusche, J.I. Hedges, P.D. Quay, J.E. Richey, and T.A. Brown. 2005. Young organic matter as a source of carbon dioxide from Amazonian rivers. *Nature* 436: 538-541.
- McClain, M.E., E.W. Boyer, C.L. Dent, S.E. Gergel, N.B. Grimm, P.M. Groffman, S.C. Hart, J.W. Harvey, C.A. Johnston, E. Mayorga, W.H. McDowell, and G. Pinay. 2003. Biogeochemical hot spots and hot moments at the interface of terrestrial and aquatic ecosystems. *Ecosystems* 6: 301-312.
- McClain, M.E., and H. Elsenbeer. 2001. Terrestrial inputs to Amazon streams and internal biogeochemical processing, p. 185-208. *In* M.E. McClain, R.L. Victoria, and J.E. Richey [eds.], *The Biogeochemistry of the Amazon Basin*. Oxford University Press.
- McClain, M.E., and R.J. Naiman. Mountain lowland linkages and the environment of the Amazon River. In preparation for *BioScience*.
- McClain, M.E., and J.E. Richey. 1996. Regional-scale linkages of terrestrial and lotic ecosystems in the Amazon basin: A conceptual model for organic matter. *Arch. Hydrobiol. Suppl.* 113: 111-125.
- McClain, M.E., J.E. Richey, J.A. Brandes, and T.P. Pimentel. 1997. Dissolved organic matter and terrestrial-lotic linkages in the central Amazon basin of Brazil. *Global Biogeochem. Cy.* 11: 295-311.

- McClain, M.E., J.E. Richey, and R.L. Victoria. 1995. Andean contributions to the biogeochemistry of the Amazon River system. *Bull. Inst. Fr. Études Andines* 24: 425-437.
- McClelland, J.W., and I. Valiela. 1998. Linking nitrogen in estuarine producers to land-derived sources. *Limnol. Oceanogr.* 43: 577-585.
- McDowell, W.H., and C.E. Asbury. 1994. Export of carbon, nitrogen, and major ions from three tropical montane watersheds. *Limnol. Oceanogr.* 39: 111-125.
- McGlynn, B.L., and J.J. McDonnell. 2003. Role of discrete landscape units in controlling catchment dissolved organic carbon dynamics. *Water Resour. Res.* 39: doi: 10.1029/2002WR001525.
- McIlvin, M.R., and M.A. Altabet. 2005. Chemical conversion of nitrate and nitrite to nitrous oxide for nitrogen and oxygen isotopic analysis in freshwater and seawater. *Anal. Chem.* 77: 5589-5595.
- Meade, R.H., T. Dunne, J.E. Richey, U. de M. Santos, and E. Salati. 1985. Storage and remineralization of suspended sediment in the lower Amazon River of Brazil. *Science* 228: 488-490.
- Merriam, J.L., W.H. McDowell, J.L. Tank, W.M. Wollheim, C.L. Crenshaw, and S.L. Johnson. 2000. Characterizing nitrogen dynamics, retention, and transport in a tropical rainforest stream using an *in situ*  $^{15}\text{N}$  addition. *Freshw. Biol.* 47: 143-160.
- Meybeck, M. 1982. Carbon, nitrogen, and phosphorus transport by world rivers. *Am. J. Sci.* 282: 401-450.
- Milliman, J.D. 1995. Sediment discharge to the ocean from small mountainous rivers – The New Guinea example. *Geo.-Mar. Lett.* 15: 3-4.
- Milliman, J.D., and R.H. Meade. 1983. World-wide delivery of river sediment to the oceans. *J. Geol.* 91: 1-21.
- Milliman, J.D., and J.P.M. Syvitski. 1992. Geomorphic/tectonic control of sediment discharge to the ocean: the importance of small mountainous rivers. *J. Geol.* 100: 325-344.
- Morecroft, M.D., F.I. Woodward, and R.H. Marrs. 1992. Altitudinal trends in leaf nutrient contents, leaf size and  $\delta^{13}\text{C}$  of *Alchemilla alpina*. *Funct. Ecol.* 6: 730-740.

- Mulholland, P.J., J.L. Tank, D.M. Sanzone, W.M. Wollheim, B.J. Peterson, J.R. Webster, and J.L. Meyer. 2000. Nitrogen cycling in a forest stream determined by a  $^{15}\text{N}$  tracer addition. *Ecol. Monogr.* 70: 471-493.
- Mulholland, P.J., H.M. Valett, J.R. Webster, S.A. Thomas, L.W. Cooper, S.K. Hamilton, and B.J. Peterson. 2004. Stream denitrification and total nitrate uptake rates measured using a field  $^{15}\text{N}$  tracer addition approach. *Limnol. Oceanogr.* 49: 809-820.
- Mutchler, T., M.J. Sullivan, and B. Fry. 2004. Potential of  $^{14}\text{N}$  isotope enrichment to resolve ambiguities in coastal trophic relationships. *Mar. Ecol. Prog. Ser.* 266: 27-33.
- Nadelhoffer, K.J., M.R. Downs, and B. Fry. 1999. Sinks for  $^{15}\text{N}$ -enriched additions to an oak forest and a red pine plantation. *Ecol. Appl.* 9: 72-86.
- Nadelhoffer, K.J., and B. Fry. 1988. Controls on natural nitrogen-15 and carbon-13 abundances in forest soil organic matter. *Soil Sci. Soc. Am. J.* 52: 1633-1640.
- Nadkarni, N.M., and T.J. Matelson. 1991. Fine litter dynamics within the tree canopy of a tropical cloud forest. *Ecology* 72: 2071-2082.
- Nadkarni, N.M., D. Schaefer, T.J. Matelson, and R. Solano. 2004. Biomass and nutrient pools of canopy and terrestrial components in a primary and a secondary montane cloud forest, Costa Rica. *For. Ecol. Man.* 198: 223-236.
- Näsholm, T., A. Ekblad, A. Nordin, R. Giesler, M. Högberg and P. Högberg. 1998. Boreal forest plants take up organic nitrogen. *Nature* 392: 914-916.
- Neill, C., L.A. Deegan, S.M. Thomas, and C.C. Cerri. 2001. Deforestation for pasture alters nitrogen and phosphorus in small Amazonian streams. *Ecol. Appl.* 11: 1817-1828.
- Noguera, J.L. 2006. Relaciones en la concentración de sedimentos suspendidos en ríos montañosos con el uso de suelos y la descarga total de sedimentos en las cuencas próximas al distrito de Oxapampa-Perú. Master's Thesis. Universidad Nacional Daniel Alcides Carrión, Oxapampa, Peru.
- Neff, J.C., E.A. Holland, F.J. Dentener, W.H. McDowell, and K.M. Russell. 2002. The origin, composition, and rates of organic nitrogen deposition: A missing piece of the nitrogen cycle? *Biogeochem.* 57/58: 99-136.

- Ortiz-Zayas, J.R., W.M. Lewis, Jr., J.F. Saunders III, J.H. McCutchan, Jr., and F.N. Scatena. 2005. Metabolism of a tropical rainforest stream. *J. N. Am. Benthol. Soc.* 24: 769-783.
- Ostrom, N.E., L.O. Hedin, J.C. von Fischer, and G.P. Robertson. 2002. Nitrogen transformations and  $\text{NO}_3^-$  removal at a soil-stream interface: a stable isotope approach. *Ecol. Appl.* 12: 1027-1043.
- Perakis, S.S., and L.O. Hedin. 2001. Fluxes and fates of nitrogen in soil of an unpolluted old-growth temperate forest, Southern Chile. *Ecology* 82: 2245-2260.
- Perakis, S. & Hedin, L. 2002. Nitrogen loss from unpolluted South American forests mainly via dissolved organic compounds. *Nature* 415: 416-419.
- Pérez, C.A., L.O. Hedin, and J.J. Armesto. 1998. Nitrogen mineralization in two unpolluted old-growth forests of contrasting biodiversity and dynamics. *Ecosystems* 1: 361-373.
- Peterson, B.J., M. Bahr, and G.W. Kling. 1997. A tracer investigation of nitrogen cycling in a pristine tundra river. *Can. J. Fish. Aquat. Sci.* 54: 2361-2367.
- Peterson, B.J., and B. Fry. 1987. Stable isotopes in ecosystem studies. *Ann Rev. Ecol. Syst.* 18: 293-320.
- Peterson, B.J., W.M. Wollheim, P.J. Mullholland, J.R. Webster, J.L. Meyer, J.L. Tank, E. Martí, W.B. Bowden, H.M. Valett, A.E. Hershey, W.H. McDowell, W.K. Dodds, S.K. Hamilton, S. Gregory, and D.D. Morrall. 2001. Control of nitrogen export from watersheds by headwater streams. *Science* 292: 86-90.
- Poole, G.C. 2002. Fluvial landscape ecology: addressing uniqueness within the river discontinuum. *Freshw. Biol.* 47: 641-660.
- Providoli, I., H. Bugmann, R. Siegwolf, N. Buchmann, and P. Schleppi. 2005. Flow of deposited inorganic N in two Gleysol-dominated mountain catchments traced with  $^{15}\text{NO}_3^-$  and  $^{15}\text{NH}_4^+$ . *Biogeochemistry* 76: 453-475.
- Quay, P.D., D.O. Wilbur, J.E. Richey, A.H. Devol, R. Benner, and B.R. Forsberg. 1995. The  $^{18}\text{O}:^{16}\text{O}$  of dissolved oxygen in rivers and lakes in the Amazon Basin: Determining the ratio of respiration to photosynthesis rates in freshwaters. *Limnol. Oceanogr.* 40: 718-729.
- Quay, P.D., D.O. Wilbur, J.E. Richey, J.I. Hedges, A.H. Devol, and R. Victoria. 1992. Carbon cycling in the Amazon River: Implications from the  $^{13}\text{C}$  compositions of particles and solutes. *Limnol. Oceanogr.* 37: 857-871.

- Raymond, P.A., and J.E. Bauer. 2001. Riverine export of aged terrestrial organic matter to the North Atlantic Ocean. *Nature* 409: 497-500.
- Restrepo, J.D., B. Kjerfve, M. Hermelin, and J.C. Restrepo. 2006. Factors controlling sediment yield in a major South American drainage basin: the Magdalena River, Colombia. 2006. *J. Hydrol.* 316: 213-232.
- Reynolds, B.C., and M.D. Hunter. 2004. Nutrient cycling. *In* Lowman and Nadkarni [eds], *Forest Canopies*, 2<sup>nd</sup> edition. Elsevier. pp. 387-396.
- Richey, J.E., J.T. Brock, R.J. Naiman, R.C. Wissmar, and R.F. Stallard. 1980. Organic carbon: oxidation and transport in the Amazon River. *Science* 207: 1348-1351.
- Richey, J.E., J.I. Hedges, A.H. Devol, P.D. Quay, R. Victoria, L. Martinelli, and B.R. Forsberg. 1990. Biogeochemistry of carbon in the Amazon River. *Limnol. Oceanogr.* 35: 352-371.
- Richey, J.E., J.M. Melack, A.K. Aufdenkampe, V.M. Ballester, and L.L. Hess. 2002. Outgassing from Amazonian rivers and wetlands as a large tropical source of atmospheric CO<sub>2</sub>. *Nature* 416: 617-620.
- Richey, J.E., R.L. Victoria, E. Salati, and B.R. Forsberg. 1991. The biogeochemistry of a major river system: the Amazon case study, p. 57-74. *In* E.T. Degens, S. Kempe, and J.E. Richey [eds.], *SCOPE 42: Biogeochemistry of Major World Rivers*. John Wiley & Sons.
- Santiago, L.S., K. Silvera, J.L. Andrade, and T.E. Dawson. 2005. El uso de isótopos estables en biología tropical. *Interciencia* 30: 536-542.
- Saunders, T.J., and M.E. McClain. In press. The N and P biogeochemistry of terrestrial-aquatic flowpaths in a small montane catchment of the Peruvian Amazon. *Hydrol. Processes*.
- Schlesinger, W.H. *Biogeochemistry: an analysis of global change*. 2<sup>nd</sup> ed. Academic Press.
- Seigenthaler, U., and H. Oescheger. 1980. Correlation of <sup>18</sup>O in precipitation with temperature and altitude. *Nature* 285: 314-317.
- Sigman D.M., K.L. Casciotti, M. Andreani, C. Barford, M. Galanter, and J.K. Böhlke. 2001. A bacterial method for the nitrogen isotopic analysis of nitrate in seawater and freshwater. *Anal. Chem.* 73: 4145-4153.
- Silver, W.L., D.J. Herman, and M.K. Firestone. Dissimilatory nitrate reduction to ammonium in upland tropical forest soils. *Ecology* 82: 2410-2416.

- Sioli, H. 1984. The Amazon and its main affluents: Hydrology, morphology of the river courses, and river types, p. 127-165. *In* H. Sioli [ed.], The Amazon. Junk.
- Sparks, J.P., and J. R. Ehleringer. 1997. Leaf carbon isotope discrimination and nitrogen content for riparian trees along elevation transects. *Oecologia* 109: 362-367.
- Stewart, G.R., S. Schmidt, L.L. Handley, M.H. Turnbull, P.D. Erskine, and C.A. Joly. 1995.  $^{15}\text{N}$  natural abundance of vascular rainforest epiphytes: implications for nitrogen source and acquisition. *Plant Cell Env.* 18: 85-90.
- Strickland, T.C., P. Sollins, N. Rudd, and D.S. Schimel. 1992. Rapid stabilization and mobilization of  $^{15}\text{N}$  in forest and range soils. *Soil Biol. Biochem.* 24: 849-855.
- Stuiver, M., and H.A. Polach. 1977. Discussion: Reporting of  $^{14}\text{C}$  data. *Radiocarbon* 19: 355-363.
- Tank, J.L., J.L. Meyer, D.M. Sanzone, P.J. Mulholland, J.R. Webster, B.J. Peterson, and N.E. Leonard. 2000. Analysis of nitrogen cycling in a forest stream during autumn using a  $^{15}\text{N}$  tracer addition. *Limnol. Oceanogr.* 45: 1013-1029.
- Telles, E.C.C., P.B. Camargo, L.A. Martinelli, S.E. Trumbore, E.S. Costa, J. Santos, N. Higuchi, and R.C. Oliveira, Jr. 2003. Influence of soil texture on carbon dynamics and storage potential in tropical forest soils of Amazonia. *Global Biogeochem. Cycles* 17: 1040, doi: 10.1029/2002GB001953.
- Thomas, S.M., C. Neill, L.A. Deegan, A.V. Krusche, V.M. Ballester, and R.L. Victoria. 2004. Influences of land use and stream size on particulate and dissolved materials in a small Amazonian stream network. *Biogeochemistry* 68: 135-151.
- Turner, R.E., and N.N. Rabalais. 1991. Changes in Mississippi River water quality this century: implications for coastal food webs. *BioScience* 41: 140-147.
- Valderrama, J.C. 1989. The simultaneous analysis of total nitrogen and total phosphorus in natural waters. *Mar. Chem.* 10: 109-122.
- van Breemen, N. 2002. Natural organic tendency. *Nature* 415: 381-382.
- Vannote, R.L., G.W. Marshall, K.W. Cummins, J.R. Sedell, and C.E. Cushing. 1980. The river continuum concept. *Can. J. Fish. Aquat. Sci.* 37: 130-137.
- Vera, M., J. Cavalier, and J. Santamaria. 1999. Tree leaf nitrogen and phosphorus reabsorption in a montane forest of the central Andes, Colombia. *Rev. Biol. Trop.* 47: 33-43.

- Vitousek, P.M., and R.L. Sanford, Jr. 1986. Nutrient cycling in moist tropical forest. *Ann. Rev. Ecol. Syst.* 17: 137-167.
- Viviroli, D., and R. Weingartner. 2004. The hydrological significance of mountains: from regional to global scale. *Hydrol. Earth Sys.* 8: 1016-1029.
- Walling, D.E. 1999. Linking land use, erosion, and sediment yields in river basins. *Hydrobiol.* 410: 223-240.
- Wania, R., P. Heitz, and W. Wanek. 2002. Natural  $^{15}\text{N}$  abundance of epiphytes depends on the position within the forest canopy: source signals and isotope fractionation. *Plant Cell Env.* 25: 581-589.
- Weathers, K.C., G.M. Lovett, G.E. Likens, and N.F.M. Caraco. 2000. Cloudwater inputs of nitrogen to forest ecosystems in Southern Chile: Forms, fluxes, and sources. *Ecosystems* 3: 590-595.
- Wedin, D.A., L.L. Tieszen, B. Dewey, and J. Pastor. 1995. Carbon isotope dynamics during grass decomposition and soil organic matter formation. *Ecology* 76: 1381-1392.
- Wollheim, W.M., B.J. Peterson, L.A. Deegan, M. Bahr, J.E. Hobbie, D. Jones, W.B. Bowden, A.E. Hershey, G.W. Kling, and M.C. Miller. 1999. A coupled field and modeling approach for the analysis of nitrogen cycling in streams. *J. N. Am. Benth. Soc.* 18: 199-221.
- Zotz, G., and P. Hietz. 2001. The physiological ecology of vascular epiphytes: current knowledge, open questions. *J. Exp. Bot.* 52: 2067-2078.

## **VITA**

Amy Townsend-Small was born in Seattle, Washington on November 13, 1976, the daughter of Donna Townsend and Richard Small. After graduating from Holliston High School, Holliston, Massachusetts, in 1994, she entered Skidmore College in Saratoga Springs, New York. During the summer of 1996 she attended the University of Massachusetts at Boston. In the spring of 1997 she attended The University of Westminster in London, England. In the fall of 1997 she attended the Semester in Environmental Science at the Marine Biological Laboratory in Woods Hole, Massachusetts. She received a Bachelor of Arts degree with a double major in Biology and English from Skidmore College in 1998. During the subsequent years she worked as a book editor and photography assistant in Boston, Massachusetts. She entered the Graduate School of The University of Texas at Austin in May 2001.

Permanent Address: 32 Highgate Street, Allston, Massachusetts 02134

This dissertation was typed by the author.